ABC Imagem Cardiovascular

Volume 39 | Number 2

April/May/June 2026

Sociedade Brasileira de Cardiologia
ISSN-2675-312X

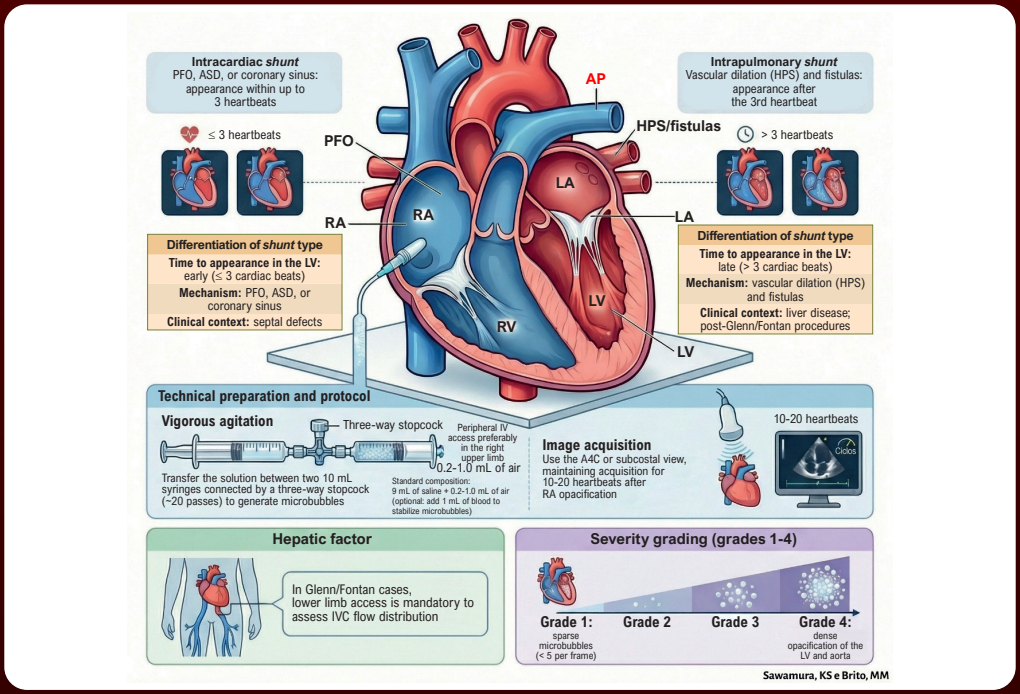

Central Illustration of the article: My Approach to Agitated Saline Contrast Echocardiography in Pediatric Patients

DIC | SBC Sociedade Brasileira de Cardiologia 1943 | ABC Imagem Cardiovascular

Contents

Click on the title to read the article

Departament of Cardiovascular Imaging

President
Adenalva Lima de Souza Beck - DF

Vice President of Echocardiography
Marco Stephan Lofrano Alves - PR

Vice President of Nuclear Cardiology
Adriana Pereira Glavam - RJ

Vice President of Vascular Echography
Marcos Paulo Lacerda Bernardo - RJ

Vice President of Magnetic Resonance Imaging
Gabriela Liberato de Sousa - SP

Vice President of Computed Tomography
Antonio Tito Paladino Filho - SP

Vice President of Congenital Heart Disease and Pediatric Cardiology
Cristiane Nunes Martins - MG

Managing Director
Daniela do Carmo Rassi Frota - GO

Financial Director
Mohamed Hassan Saleh - SP

Journal Editor
Marcelo Dantas Tavares de Melo – PB

Consulting Board

Members
André Luiz Cerqueira de Almeida - BA
Carlos Eduardo Rochitte - SP
Marcelo Luiz Campos Vieira - SP
Samira Saady Morhy - SP
Silvio Henrique Barberato - PR

Scientific Committee

Coordinator
Marco Stephan Lofrano Alves - PR

Members
Adriana Pereira Glavam - RJ
Marcos Paulo Lacerda Bernardo - RJ
Gabriela Liberato de Sousa - SP
Antonio Tito Paladino Filho - SP
Cristiane Nunes Martins - MG

Echocardiography Certification Committee

Coordinator
Rafael Modesto Fernandes - BA

Adult Echo Members
Alex dos Santos Félix - RJ
Angele Azevedo Alves Mattoso - BA
Arthur Cortez Gonçalves - MG
Eliza de Almeida Gripp - RJ
Gracielly Rodrigues de Barros - ES
Liria Maria Lima da Silva - SP
Marcio Mendes Pereira - MA
Renato de Aguiar Hortegal - SP
Vitoria Regia Beserra Barbosa Ximenes - PI

Congenital Echo Members
Danielle Lopes Rocha - ES
Flavia Engers Salles Benites - MS
Halsted Alarcao Gomes Pereira Da Silva - SP
Maria Elisa Martini Albretch - SP

Seniors
Glaucia Maria Penha Tavares - SP
José Aldo Ribeiro Teodoro -SP
Marcelo Iorio Garcia - RJ
Márcio Miranda Brito - TO
Tatiane Mascarenhas Santiago Emerich - ES

Social Media Committee

Coordinator
Bruna Olandoski Erbano - PR
Alex dos Santos Félix - RJ

Members
Kelvin Henrique Vilalva - SP
Claudia Cosentino Gallafrio - SP
Karen Saori Shiraishi Sawamura - SP

Professional Defense and Institutional Relations Committee

Coordinator
Andrea de Andrade Vilela - SP

Members
Antonio Tito Paladino Filho - SP
Daniela do Carmo Rassi Frota - GO
Gracielly Rodrigues de Barros - ES
Isabel Cristina Britto Guimarães - BA
Simone Nascimento dos Santos - DF

Committee of Education and Accreditation

Coordinator
Edgar Bezerra de Lira Filho - SP

Members
Andrea de Andrade Vilela - SP
Daniela do Carmo Rassi Frota - GO
Edgar Daminello - SP
José Luiz Barros Pena - MG
Marcos Paulo Lacerda Bernardo - RJ
Sandra Nívea Dos Reis Saraiva Falcão - CE

Intersociety Committee

Coordinator
Silvio Henrique Barberato - PR

Members
Marcelo Luiz Campos Vieira - SP

Delegado DIC SISIAC
Ivan Romero Rivera - AL

DIC Youth Committee

Coordinator
Alexandre Costa Souza - BA

Members
Marcus Vinicius Silva Freire De Carvalho - BA
Camila Martins Ferreira – DF
Fernanda Maria Franco Castro - MG
Lucas Feldman Paz de Lima - RJ
Luiz Otavio de Arruda Santos - SP
Marina Albanez Albuquerque de Medeiros - PE

DIC Woman Committee

Coordinator
Marly Maria Uellendahl Lopes - SP

Members
Karen Saori Shiraishi Sawamura - SP
Simone Nascimento dos Santos - DF
Simone Cristina Soares Brandão - PE
Mônica Luiza de Alcantara - RJ
Marina Albanez Albuquerque de Medeiros - PE
Samira Saady Morhy - SP

ABC Imagem Cardiovascular

Volume 39, Nº 2, April/May/June 2026

Indexing: SciELO (Scientific Electronic Library Online), Lilacs (Latin American and Caribbean Health Sciences Literature), Latindex (Regional Cooperative Online Information System for Scholarly Journals from Latin America, the Caribbean, Spain and Portugal) and DOAJ (Directory of Open Access Journals)

Address: Av. Marechal Câmara, 160 – 3º andar – Sala 330
20020-907 • Centro • Rio de Janeiro, RJ • Brazil
Phone.: (21) 3478-2700
E-mail: abcimaging@cardiol.br
https://www.abcimaging.org/

Commercial Department
Phone: (11) 3411-5500
E-mail: comercialsp@cardiol.br

Editorial Production
SBC – Scientific Department

Graphic Design and Diagramming
SBC – Scientific Department

Cardiac Amyloidosis: Is It Truly a Hypertrophic Phenotype Cardiomyopathy?

Tonnison de Oliveira Silva[1,2]

Escola Bahiana de Medicina e Saúde Pública,[1] *Salvador, BA – Brazil*
Hospital Cardio Pulmonar, IDOR, Rede D'or,[2] *Salvador, BA – Brazil*

Cardiac amyloidosis is a classic example of an infiltrative disease whose predominant phenotype is characterized by a hypertrophic pattern of myocardial involvement.[1,2] The most relevant studies—both those focused on the development of disease-modifying therapies and cohorts evaluating diagnostic tools—have used increased ventricular wall thickness as a key criterion for suspecting cardiac amyloidosis.[1-6] Based on this concept, several diagnostic algorithms have proposed ventricular wall thickening as one of the major red flags for investigating amyloid cardiomyopathy.[1,2]

However, increased ventricular wall thickness does not appear to be a universal requirement for diagnosis. Emerging evidence suggests that both Immunoglobulin Light Chain Amyloidosis (AL) and Transthyretin Amyloidosis (ATTR) amyloidosis can be diagnosed, including through noninvasive methods, even in the absence of the classic hypertrophic phenotype.

Devesa *et al.,* reported a cohort of patients with Heart Failure with Preserved Ejection Fraction (ejection fraction > 50%) and no increased ventricular wall thickness. In this series, the prevalence of ATTR was approximately 5%. Three patients (5%) were identified with ATTR among 58 individuals; all had the wild-type form, were older than 75 years, and had a maximum wall thickness of 11 mm.[7]

In another retrospective study including 98 patients with a diagnosis of cardiac amyloidosis, participants were divided into two groups: those with increased wall thickness (defined as ≥ 12 mm) and those without (< 12 mm). Wall thickness was defined as the mean of interventricular septal and inferolateral wall measurements. Of the total cohort, nine patients (9%) did not exhibit increased wall thickness (< 12 mm), with a mean value of 10 mm. All cases corresponded to AL amyloidosis.[8]

Muller SA *et al.*, in investigating the etiology of patients with Heart Failure (HF) and extracardiac red flags suggestive of amyloidosis, analyzed a sample of 114 patients with cardiac amyloidosis. Of these, 12 (11%) did not exhibit increased wall thickness (< 12 mm), although they met other diagnostic criteria, including positive technetium-labeled pyrophosphate scintigraphy.[9]

In a large cohort of patients with cardiac amyloidosis, 1,845 individuals were evaluated between 2006 and 2024. It was observed that 13% of AL cases and approximately 7% of ATTR cases had normal or only mildly increased left ventricular wall thickness (≤ 12 mm). Notably, women tended to have lower ventricular wall thickness. Furthermore, within the subgroup with wall thickness ≤ 12 mm, approximately 70% demonstrated increased relative wall thickness (relative wall thickness [RWT] > 0.42), consistent with concentric remodeling.[10]

Case reports further illustrate this clinical scenario. In a recent publication in the European Heart Journal (2024), a 69-year-old man with heart failure and a rare pathogenic variant in the transthyretin protein (TTR) gene (p.Tyr78Phe) was described. In this case, bone scintigraphy showed no tracer uptake, and echocardiography did not reveal increased wall thickness.[11]

Thus, the absence of ventricular wall thickening does not exclude cardiac amyloidosis, whether AL or ATTR. Amyloid disease begins long before overt hypertrophy becomes manifest, and its absence may reflect early disease stages—although this is only one of several possible explanations. Interstitial infiltration by misfolded amyloid fibrils, associated with extracellular space expansion, proteotoxicity, disruption of myocardial architecture, inflammation, and fibrosis, may result in diastolic dysfunction, atrial enlargement, and heart failure with preserved ejection fraction, even before significant increases in ventricular wall thickness become apparent on echocardiography.[12,13] Moreover, a dichotomous diagnostic approach based solely on absolute cutoff values (≥ 12 mm versus < 12 mm), without considering intra- and interobserver variability, anthropometric differences, and sex-related factors, may contribute to underdiagnosis. This is particularly relevant in individuals with smaller body surface area and in women, in whom absolute ventricular wall thickness tends to be lower.[11] When echocardiography is used exclusively as a screening tool based on isolated septal and posterior wall measurements in search of values > 12 mm, its diagnostic potential may be underutilized. Echocardiographic assessment allows evaluation not only of wall thickness, but also of concentric remodeling patterns, ventricular mass, chamber dimensions, diastolic function, and myocardial strain. These parameters should be interpreted in an integrated manner in the presence of clinical suspicion of cardiac amyloidosis.[1,2]

Clinical scenarios involving rare genetic variants with atypical phenotypic presentations further reinforce that excessive reliance on the classic morphologic phenotype may delay disease recognition.[11]

Keywords

Amyloidosis without hypertrophy; cardiac amyloidosis; hypertrophic phenotype

Mailing Address: Tonnison de Oliveira Silva •
Escola Bahiana de Medicina e Saúde Pública. Rua Dom João VI. Postal code: 40285-001. Brotas, Salvador, BA – Brazil
E-mail: tonnisonsilva@hotmail.com

DOI: https://doi.org/10.36660/abcimg.20260058i

The presentation of cardiac amyloidosis without ventricular wall thickening should not be regarded merely as an anecdotal exception, but rather as a potential representation of earlier stages of disease, lower infiltrative burden, sex-related differences, or limitations of isolated morphologic criteria.[7-11]

This discussion does not seek to deny the hypertrophic phenotype as the most characteristic presentation of amyloid cardiomyopathy, but rather to acknowledge that it is not universal. Alternative morphological presentations need to be better understood and possibly incorporated into clinical reasoning and diagnostic workflows. This perspective can be crucial for raising early diagnostic suspicion, preventing the disease from remaining undetected until more advanced and severe stages.

References

1. Kittleson MM, Ruberg FL, Ambardekar AV, Brannagan TH, Cheng RK, Clarke JO, et al. 2023 ACC Expert Consensus Decision Pathway on Comprehensive Multidisciplinary Care for the Patient with Cardiac Amyloidosis: A Report of the American College of Cardiology Solution Set Oversight Committee. J Am Coll Cardiol. 2023;81(11):1076-126. doi: 10.1016/j.jacc.2022.11.022.
2. Kittleson MM, Maurer MS, Ambardekar AV, Bullock-Palmer RP, Chang PP, Eisen HJ, et al. Cardiac Amyloidosis: Evolving Diagnosis and Management: A Scientific Statement from the American Heart Association. Circulation. 2020;142(1):e7-e22. doi: 10.1161/CIR.0000000000000792.
3. Gillmore JD, Maurer MS, Falk RH, Merlini G, Damy T, Dispenzieri A, et al. Nonbiopsy Diagnosis of Cardiac Transthyretin Amyloidosis. Circulation. 2016;133(24):2404-12. doi: 10.1161/CIRCULATIONAHA.116.021612.
4. Maurer MS, Schwartz JH, Gundapaneni B, Elliott PM, Merlini G, Waddington-Cruz M, et al. Tafamidis Treatment for Patients with Transthyretin Amyloid Cardiomyopathy. N Engl J Med. 2018;379(11):1007-16. doi: 10.1056/NEJMoa1805689.
5. Gillmore JD, Judge DP, Cappelli F, Fontana M, Garcia-Pavia P, Gibbs S, et al. Efficacy and Safety of Acoramidis in Transthyretin Amyloid Cardiomyopathy. N Engl J Med. 2024;390(2):132-42. doi: 10.1056/NEJMoa2305434.
6. Fontana M, Berk JL, Gillmore JD, Witteles RM, Grogan M, Drachman B, et al. Vutrisiran in Patients with Transthyretin Amyloidosis with Cardiomyopathy. N Engl J Med. 2025;392(1):33-44. doi: 10.1056/NEJMoa2409134.
7. Devesa A, Blasco AC, Lázaro AMP, Askari E, Lapeña G, Talavera SG, et al. Prevalence of Transthyretin Amyloidosis in Patients with Heart Failure and no Left Ventricular Hypertrophy. ESC Heart Fail. 2021;8(4):2856-65. doi: 10.1002/ehf2.13360.
8. Nagy D, Révész K, Peskó G, Varga G, Horváth L, Farkas P, et al. Cardiac Amyloidosis with Normal Wall Thickness: Prevalence, Clinical Characteristics and Outcome in a Retrospective Analysis. Biomedicines. 2022;10(7):1765. doi: 10.3390/biomedicines10071765.
9. Muller SA, Achten A, van der Meer MG, Zwetsloot PP, Sanders-van Wijk S, van der Harst P, et al. Absence of an Increased Wall Thickness does Not Rule Out Cardiac Amyloidosis. Amyloid. 2024;31(3):244-6. doi: 10.1080/13506129.2024.2348681.
10. El Helou MC, Finet JE, Kassab J, El Dahdah J, Rubio AC, Kanta A, et al. Left Ventricular Wall Thickness and Derived Parameters in Cardiac Amyloidosis. Prog Cardiovasc Dis. 2026;94:30-9. doi: 10.1016/j.pcad.2025.11.002.
11. Beard E, Bouleti C, Alos B. First Case of Symptomatic Transthyretin Cardiac Amyloidosis with Rare Tyr78Phe Variant, Normal Left Ventricular Wall Thickness, and no Cardiac Uptake on Scintigraphy. Eur Heart J. 2024;45(24):2170. doi: 10.1093/eurheartj/ehae120.
12. Fontana M, Pica S, Reant P, Abdel-Gadir A, Treibel TA, Banypersad SM, et al. Prognostic Value of Late Gadolinium Enhancement Cardiovascular Magnetic Resonance in Cardiac Amyloidosis. Circulation. 2015;132(16):1570-9. doi: 10.1161/CIRCULATIONAHA.115.016567.
13. Fontana M, Ioannou A, Cuddy S, Dorbala S, Masri A, Moon JC, et al. The Last Decade in Cardiac Amyloidosis: Advances in Understanding Pathophysiology, Diagnosis and Quantification, Prognosis, Treatment Strategies, and Monitoring Response. JACC Cardiovasc Imaging. 2025;18(4):478-99. doi: 10.1016/j.jcmg.2024.10.011.

Chemotherapy-Induced Cardiotoxicity in the Pediatric Population: What Are the Unique Aspects of Cardiovascular Imaging Follow-Up?

Jéssica Laureano Martins,[1] *Maria do Carmo Menezes Bezerra Duarte,*[2] *Fabiana Gomes Aragão Magalhães Feitosa,*[3] *Maria Verônica Câmara dos Santos*[4,5]

Universidade Federal da Paraíba, [1] *João Pessoa, PB – Brazil*
Instituto de Medicina Integral Professor Fernando Figueira, [2] *Recife, PE – Brazil*
UPE, Hospital Universitário Oswaldo Cruz, [3] *Recife, PE – Brazil*
AC Camargo Cancer Center,[4] *São Paulo, SP – Brazil*
Hospital Santa Marcelina,[5] *São Paulo, SP – Brazil*

Cancer remains among the leading public health challenges in Brazil and worldwide. For the three-year period from 2026 to 2028, the Brazilian National Cancer Institute (INCA) estimates that there will be approximately 781,000 new cancer cases per year in Brazil. In the child and adolescent group, an estimated 7,560 new cases are expected annually.[1]

Advances in the treatment of pediatric cancer have significantly increased survival rates in recent decades, exceeding 80% at 5 years, provided that it is diagnosed early and treated in referral centers. In this scenario, cardiovascular disease has become the leading non-oncological cause of morbidity and mortality among childhood and adolescent cancer survivors, with an estimated risk 5 to 6 times higher than what is observed in the general population.[2]

Cardiotoxicity associated with antineoplastic therapy is defined as cardiovascular changes identified through clinical manifestations, biomarkers, or imaging methods, during or after treatment (months or decades), provided that other etiologies are excluded. The clinical spectrum is broad and ranges from subclinical changes to heart failure, arrhythmias, systemic and pulmonary hypertension, pericarditis, valvular heart disease, thromboembolic events, and myocardial ischemia.[3-5]

The risk of cardiotoxicity is associated with isolated or combined exposure to chemotherapeutic agents (anthracyclines, alkylating agents, antimetabolites, tyrosine kinase inhibitors, among others); mediastinal, cervical, and neuraxial radiotherapy; immunotherapies; CAR T-cell therapy; and hematopoietic stem cell transplantation.[3-5] Regardless of the cumulative doses of chemotherapeutic agents, genetic polymorphisms can influence drug metabolism and, consequently, individual vulnerability.[3,5]

In the pediatric population, the impact is potentially more significant due to myocardial immaturity, interference with cardiac growth during physical development, and the increased risk of progressive myocardial remodeling, especially given the comorbidities inherent to aging.[3,5]

Pediatric cardio-oncology is not merely an adaptation of established recommendations for adults, but rather a field with unique biological, epidemiological, and diagnostic features that directly impact screening and cardiovascular follow-up of these patients.

Surveillance strategies must be more sensitive, individualized, and longitudinally structured. Accordingly, multimodal cardiovascular imaging plays a central role in early detection of cardiotoxicity and patient follow-up, allowing timely cardioprotective and/or therapeutic interventions.[6,7]

In this context, international consensus recommends echocardiography as the primary essential technique for cardiological assessment before, during, and after cancer treatment. The two-dimensional method has been validated, although the three-dimensional method is considered the most sensitive for evaluating ventricular systolic function, compared with magnetic resonance imaging, which is the gold standard in myocardial functional assessment.[6,7]

Systolic dysfunction, especially asymptomatic (subclinical), is the most frequent complication in the follow-up of patients with cancer. In addition, early recognition of diastolic dysfunction may be predictive of contractile changes, restrictive changes, and loss of ventricular mass.[6,7]

Cardiotoxicity is defined on echocardiography during treatment when there is a 10 percentage point drop in left ventricular ejection fraction (LVEF) and/or a ≥ 15% relative drop in left ventricular global longitudinal strain (LVGLS) compared to baseline, or values below the normal cutoff points.[6,7] Several studies have shown the sensitivity of left ventricular myocardial strain analysis using speckle tracking in the early detection of dysfunction, where the percentage drop precedes the decrease in LVEF. After treatment, values below the cutoff points for LVEF and/or LVGLS should be used as reference for the diagnosis of ventricular systolic dysfunction.

In a 2020 retrospective study in France, Wolf et al. evaluated 79 pediatric patients treated with anthracyclines for acute leukemia and Hodgkin lymphoma over a 10-year period and observed that 28% presented with abnormal LVGLS, despite preserved LVEF.[8] Another retrospective study conducted in Germany in 2024 by Rique et al. evaluated 38 children with acute leukemia treated with anthracyclines and detected LVGLS alterations in 28.9% of cases.[9] In Brazil, a study in this population evaluated the frequency of cardiotoxicity in 45 children and

Keywords

Cardiotoxicity; Echocardiography; Drug Therapy; Neoplasms; Child

Mailing Address: Jéssica Laureano Martins •
Universidade Federal da Paraíba. Cidade Universitária, s/n. Postal code: 58051-900. Castelo Branco, João Pessoa, PB – Brazil
E-mail: jessicalaureanom@gmail.com

DOI: https://doi.org/10.36660/abcimg.20260044i

adolescents with cancer (75.5% with hematological neoplasia). Echocardiographic alterations were identified in 42.2% of patients undergoing chemotherapy, with a marked reduction in LVGLS, even in the absence of a decrease in LVEF. These findings reinforce the relevance of more sensitive imaging methods in early detection of myocardial dysfunction.[10]

Special considerations for the pediatric population[6,7]

- **Baseline echocardiographic examination:** Should be performed before the start of potentially cardiotoxic therapy to assess myocardial anatomy and function, as a comparative baseline for subsequent assessments. If it is not possible to perform the examination at this stage, normal cutoff values should be considered when echocardiographic assessment becomes feasible.
- **Echocardiographic assessment during treatment:** Should be performed during the week preceding the infusion of potentially cardiotoxic chemotherapy, avoiding the subsequent 2 weeks due to the hypermetabolic state. For comparison between examinations, the patient should be hemodynamically similar to the baseline.
- **LVEF:** LVEF varies depending on preload and afterload, may remain normal during treatment, and does not define subclinical injury; therefore, it should not be used in isolation to define cardiotoxicity. The biplanar Simpson method is recommended, and the normal value in the pediatric population is ≥ 55%.
- **LVGLS:** LVGLS is currently the most sensitive marker of subclinical myocardial dysfunction and should be systematically assessed before, during, and after the end of treatment. Serial follow-up should ideally be performed with the same equipment/software and examiner. This technique allows for the early identification of myocardial damage, even in the presence of preserved LVEF. The cutoff point for normality in cardio-oncology is −18.0%. Values between −16% and −17.0% are considered signs of subclinical impairment, supporting the initiation of a cardioprotective medication strategy.
- **Linear and volumetric echocardiographic measurements:** Should be adjusted for body surface area and interpreted using Z-scores.
- **Diastolic function:** Should be part of the routine (E/A, E/e', indexed left atrial volume). Changes in heart rate can precede systolic dysfunction, especially with high cumulative chemotherapy exposure. Consider limitations due to the influence of preload, afterload, and heart rate. Left atrial strain has been gradually incorporated into diastolic functional analysis.
- **Right ventricle:** Systolic function should be assessed using classic parameters (Fractional Area Change [FAC], Tricuspid Annular Plane Systolic Excursion [TAPSE], tricuspid S') and right ventricular free wall strain.
- **Echocardiographic assessment during complications:** Findings should be considered as a snapshot in time. After the situation has been resolved, schedule a new evaluation to document functional status and continue with individualized follow-up.
- **Vascular ultrasound:** Plays a complementary role in evaluating signs of peripheral thrombosis and endothelial injury, especially of the carotid arteries, since signs of early atherosclerosis are part of survivor assessment.
- **Cardiac magnetic resonance imaging**: Recommended when there is diagnostic uncertainty, inadequate echocardiographic window, or suspicion of myocardial fibrosis, as well as for assessment of the pericardium and intracardiac or adjacent masses. In pediatrics, its routine use is limited due to the need for sedation, availability, and cost.

The pediatric perspective in cardio-oncology presents particular challenges, given that cardiotoxicity related to cancer treatment is not limited to an acute event, but represents a dynamic process that can interfere with myocardial growth and maturation over time. The vulnerability of the developing heart, associated with early exposure to potentially cardiotoxic therapies, confers a prolonged risk of progressive myocardial dysfunction. In this context, the use of more sensitive, reproducible, and integrated cardiovascular imaging strategies becomes fundamental. The multimodal approach, with emphasis on echocardiography (and cardiac magnetic resonance imaging in selected situations), increases diagnostic accuracy and contributes to better risk stratification. Additionally, structured longitudinal follow-up, with interpretation based on clinical individualization, is essential for adequate follow-up of these patients.

Finally, the incorporation of genetic, clinical, and therapeutic factors into risk models, coupled with continuous imaging monitoring, represents a promising perspective for precision medicine, with the goal of reducing cardiovascular morbidity and mortality and improving the quality of life of pediatric cancer survivors.

References

1. Instituto Nacional de Câncer José Alencar Gomes da Silva. Estimativa 2026-2028: Incidência de Câncer no Brasil. Rio de Janeiro: INCA; 2025.
2. Ryan TD, Bates JE, Kinahan KE, Leger KJ, Mulrooney DA, Narayan HK, et al. Cardiovascular Toxicity in Patients Treated for Childhood Cancer: A Scientific Statement from the American Heart Association. Circulation. 2025;151(15):e926-43. doi: 10.1161/CIR.0000000000001308.
3. Lyon AR, López-Fernández T, Couch LS, Asteggiano R, Aznar MC, Bergler-Klein J, et al. 2022 ESC Guidelines on Cardio-Oncology Developed in Collaboration with the European Hematology Association (EHA), the European Society for Therapeutic Radiology and Oncology (ESTRO) and the International Cardio-Oncology Society (IC-OS). Eur Heart J. 2022;43(41):4229-361. doi: 10.1093/eurheartj/ehac244.
4. Hajjar LA, Costa IBSS, Lopes MACQ, Hoff PMG, Diz MDPE, Fonseca SMR, et al. Brazilian Cardio-Oncology Guideline - 2020. Arq Bras Cardiol. 2020;115(5):1006-43. doi: 10.36660/abc.20201006.

5. Seber A, Miachon AS, Tanaka AC, Castro AMS, Carvalho AC, Petrilli AS, et al. First Guidelines on Pediatric Cardio-Oncology from the Brazilian Society of Cardiology. Arq Bras Cardiol. 2013;100(5 Suppl 1):1-68. doi: 10.5935/abc.2013S005.

6. Melo MDT, Paiva MG, Santos MVC, Rochitte CE, Moreira VM, Saleh MH, et al. Brazilian Position Statement on the Use Of Multimodality Imaging in Cardio-Oncology - 2021. Arq Bras Cardiol. 2021;117(4):845-909. doi: 10.36660/abc.20200266.

7. Mertens L, Singh G, Armenian S, Chen MH, Dorfman AL, Garg R, et al. Multimodality Imaging for Cardiac Surveillance of Cancer Treatment in Children: Recommendations from the American Society of Echocardiography. J Am Soc Echocardiogr. 2023;36(12):1227-53. doi: 10.1016/j.echo.2023.09.009.

8. Wolf CM, Reiner B, Kühn A, Hager A, Müller J, Meierhofer C, et al. Subclinical Cardiac Dysfunction in Childhood Cancer Survivors on 10-Years Follow-Up Correlates with Cumulative Anthracycline Dose and is Best Detected by Cardiopulmonary Exercise Testing, Circulating Serum Biomarker, Speckle Tracking Echocardiography, and Tissue Doppler Imaging. Front Pediatr. 2020;8:123. doi: 10.3389/fped.2020.00123.

9. Rique A, Cautela J, Thuny F, Michel G, Ovaert C, El Louali F. Left Ventricular Longitudinal Strain Abnormalities in Childhood Exposure to Anthracycline Chemotherapy. Children. 2024;11(3):378. doi: 10.3390/children11030378.

10. Martins JL, Feitosa FGAM, Santos MVC, Menezes TMGAL, Sena AD, Rodrigues EPL, et al. Early Detection of Cardiotoxicity in Pediatric and Adolescent Patients with Cancer Treated with Anthracyclines in Northeastern Brazil. Hematol Transfus Cell Ther. 2026;48(2):106255. doi: 10.1016/j.htct.2026.106255.

Elevated Lipoprotein(a) in Patients Without Comorbidities: Which Imaging Tests Should be Ordered?

Eduardo Gomes Lima,[1,2] *Leticia Neves Solon Carvalho,*[1,3] *Tatiane Mascarenhas Santiago Emerich,*[1,4] *Eduardo Ferreira Amorim,*[1] *Fabiana Hanna Rached*[1,5]

Instituto do Coração do Hospital das Clínicas da Faculdade de Medicina da USP (InCor-HCFMUSP),[1] *São Paulo, SP – Brazil*
Hospital 9 de Julho - Rede Américas,[2] *São Paulo, SP – Brazil*
Hospital de Messejana Dr. Carlos Alberto Studart Gomes,[3] *Fortaleza, CE – Brazil*
Centrocor,[4] *Vitória – ES, Brazil*
Hospital Israelita Albert Einstein,[5] *São Paulo, SP – Brazil*

The incorporation of lipoprotein(a) [Lp(a)] into contemporary cardiovascular risk assessment has introduced a practical question that is increasingly common in clinical practice: when faced with an elevated result, how should risk be reclassified and what management should be adopted, given that current guidelines recommend measuring Lp(a) at least once in adulthood and recognize it as a risk-modifying factor.[1,2] However, the cardiovascular risk estimation proposed by these same guidelines — based on prognostic scores such as Predicting Risk of Cardiovascular Disease EVENTs - atherosclerotic cardiovascular disease (PREVENT-ASCVD), developed in 2023 by the American Heart Association — does not, *a priori*, account for the impact of elevated Lp(a) levels in its calculation.[2] This creates a clinical scenario that is both concrete and challenging: the possibility that an asymptomatic patient, without traditional risk factors, may carry a biologically relevant risk factor that the score simply does not "see." Thus arises the central question: what should be done when Lp(a) is elevated? In particular, should cardiovascular imaging be used to refine risk stratification?

A reasonable answer to these important questions requires an analysis of the biology and evidence that have propelled Lp(a) to its newly acquired prominence in the field of primary prevention in cardiology. Lp(a) is a particle similar to low-density lipoprotein (LDL), composed by an apolipoprotein B-100 molecule covalently bound to apolipoprotein(a), with levels predominantly determined by the *LPA* gene and relative stability throughout life.[2,3] Its association with atherosclerotic cardiovascular disease is supported by epidemiological, genetic, and Mendelian randomization evidence, giving the particle a status stronger than that of a simple associative marker.[2,3] Data from 450,000 patients demonstrate a strong linear correlation between elevated Lp(a) levels and atherosclerotic disease, with an approximate 11% increase in relative risk for every 50 nmol/L.[4]

Keywords

Lipoprotein(a); Primary Prevention; Atherosclerosis.

Mailing Address: Eduardo Gomes Lima •
Universidade de São Paulo, Instituto do Coração. Av Dr Enéas de C Aguiar, 44. Postal code: 05403-000. São Paulo, SP – Brazil
E-mail: eduglima@yahoo.com.br

DOI: https://doi.org/10.36660/abcimg.20260053i

In addition to its atherogenic properties related to its LDL-like core, lipoprotein(a) [Lp(a)] carries oxidized phospholipids and acts through multiple inflammatory, thrombotic, and pro-calcifying pathways. For this reason, Lp(a) not only contributes to overall cardiovascular risk but also serves as an independent factor for the development and progression of calcific aortic stenosis.[5] This process occurs through the osteogenic differentiation of valvular interstitial cells, resulting in the mineral deposition of hydroxyapatite.[6] Lp(a) levels above 35 mg/dL have been identified as independent predictors of increased calcification activity, assessed by Positron emission tomgraphy — computer tomography (PET-CT) — and are also associated with accelerated hemodynamic progression on echocardiography, greater need for aortic valve replacement, and increased mortality.[7]

As previously discussed, the incorporation of Lp(a) into contemporary cardiovascular risk assessment has introduced a practical dilemma: what should be done when elevated values are detected that traditional scores, such as PREVENT-ASCVD, fail to capture? This growing body of evidence has ultimately repositioned Lp(a) measurement within clinical guidelines. The 2026 American College of Cardiology / American Heart Association (ACC/AHA) guideline recommends measuring Lp(a) in all adults at least once in their lifetime for cardiovascular risk assessment.[2] The 2025 Brazilian Guideline on Dyslipidemias and Atherosclerosis Prevention further recognizes that Lp(a) levels ≥50 mg/dL or ≥125 nmol/L act as risk enhancers, potentially reclassifying a patient from low to intermediate risk or from intermediate to high risk.[1] At very high levels (Lp(a) >180 mg/dL or >390 nmol/L), the patient should be considered high risk.

Once it is acknowledged that Lp(a) modifies risk interpretation, the next step is to clarify how to proceed when elevated values are identified in individuals reclassified based on this parameter. In the context of primary prevention, the Brazilian guideline also supports the use of imaging methods for early detection of subclinical atherosclerosis in selected individuals with elevated Lp(a).[1]

A reflection is warranted on the evolution of imaging methods which, in addition to becoming more accessible, are now capable of detecting atherosclerosis at its earliest stages. This early detection through tomographic or ultrasound-based techniques, combined with the ability to adjust therapy intensity based on imaging findings, creates a scenario in which documenting plaque fundamentally

changes the direction of treatment. In this context, the coronary artery calcium (CAC) score plays a central role in most asymptomatic patients, including those without extreme Lp(a) values. The reason is not only its extensive validation in primary prevention, but also the nature of the question it answers: if Lp(a) raises the suspicion of underestimated biological risk, CAC reveals whether this vulnerability has already manifested as subclinical coronary atherosclerosis. In other words, Lp(a) indicates predisposition, while CAC reveals its current anatomical expression.[8,9] It is probability versus the reality of risk.

This link between Lp(a) and CAC is not merely conceptual, but also clinical and prognostic. In a recent meta-analysis involving more than 40,000 individuals, elevated Lp(a) levels were associated with a higher prevalence of CAC greater than zero and with greater CAC progression over time, with a particularly relevant signal in asymptomatic populations.[10] This reinforces that when Lp(a) modifies risk interpretation, CAC serves as a coherent marker of the subclinical manifestation of a biologically more atherogenic phenotype.[10]

In an analysis of asymptomatic individuals from MESA and the Dallas Heart Study, Mehta and colleagues demonstrated that elevated Lp(a) and CAC are independent markers of risk for cardiovascular events.[8] More importantly, the combination of both elevated markers identified a particularly high-risk phenotype: participants with Lp(a) ≥50 mg/dL and CAC ≥100 had a 10-year cumulative incidence of atherosclerotic events exceeding 20%, approaching levels typically observed in secondary prevention populations.[8] Among individuals with CAC = 0, on the other hand, elevated Lp(a) remained associated with relative risk, but absolute event rates were much lower in the short and medium term.[8,9] Bhatia and colleagues[9] expanded this understanding in a multicenter cohort of more than 11,000 participants without known atherosclerotic disease. Lp(a) >50 mg/dL and CAC >0 remained independently associated with events, reinforcing the notion of complementarity between biomarker information and imaging findings. However, the highest risk was concentrated in the strata with higher CAC scores, especially when elevated Lp(a) coexisted with CAC ≥300.[9]

The value of CAC, therefore, is not only prognostic but also decisional. A score of zero can reduce the urgency of pharmacologic escalation in patients who are truly low risk, whereas scores ≥100 shift the patient into a category in which intensifying preventive therapy becomes much more compelling.[4,5] At higher strata, such as CAC ≥300, the risk burden approaches that observed in secondary-prevention populations, reinforcing the need for more aggressive LDL-cholesterol reduction targets.[2,9] In addition, in carefully selected patients with low bleeding risk, higher CAC values may help identify individuals who are likely to derive net benefit from the initiation of antiplatelet therapy in a primary-prevention setting.[11]

It is precisely here that tomographic imaging distinguishes itself from other modalities. Coronary CT angiography can identify non-calcified plaque and provide more detailed anatomical characterization, which is physiopathologically appealing – especially because the biology of Lp(a) is not limited to calcified disease. Even so, its routine use as a first-line test in asymptomatic individuals with elevated Lp(a) appears excessive in most cases: it involves greater complexity, iodinated contrast, higher cost, and often yields findings whose incremental therapeutic impact is less clear than the pragmatic value of CAC. In high-risk cardiovascular patients, however, some expert statements consider the use of coronary CT angiography for risk re-stratification in asymptomatic individuals.[12]

The use of carotid ultrasound to identify atherosclerotic plaques has also been shown to be associated with elevated Lp(a) levels and may imply up to a four-fold higher risk of cardiovascular events when plaque is present in individuals with Lp(a) ≥30 mg/dL, compared with those with Lp(a) <30 mg/dL and no plaques.[13] Thus, because this method is more affordable and accessible, it may serve as an alternative to CAC for risk prediction. However, unlike CAC – which not only identifies the presence or absence of disease but also quantifies plaque burden in a numerical and continuous manner – ultrasound documents plaque and estimates the severity of obstruction. This difference in the nature of the methods explains the preference for CAC as a predictor of cardiovascular events, especially myocardial infarction.

This does not mean turning CAC into a universal test for all individuals with elevated Lp(a). The marker should never be interpreted in isolation from the clinical context. Age, family history of premature atherosclerotic disease, the magnitude of Lp(a) elevation, concomitant LDL-cholesterol levels, the presence of other risk-enhancing factors, and – above all – the likelihood that the result will meaningfully change management must all be considered. It is also reasonable to acknowledge that very high Lp(a) levels, especially when accompanied by a strong family history or other signs of atherosclerotic susceptibility, may lower the threshold for investigation and therapeutic intensification, even when clinical scores appear reassuring. Still, in asymptomatic patients without significant comorbidities and without extreme Lp(a) values, CAC seems to offer the best balance between diagnostic parsimony and clinical utility.

Despite the strong correlation between elevated Lp(a) and calcific aortic stenosis, there are currently no recommendations for routine echocardiographic screening in asymptomatic patients. Patients with a diagnosis of aortic stenosis, however, should have Lp(a) measured, as this may benefit family members through cascade screening.[2,13,14]

In summary, as is natural with the introduction of new paradigms, the universal recommendation to measure Lp(a) has expanded our ability to recognize cardiovascular risk, but it has also generated uncertainties along the way: how should we act when the factor that modifies clinical interpretation is not incorporated into the score that guides the initial decision? In this context, it is important to remember that identifying established atherosclerosis is not a prerequisite for action: even in the absence of imaging, the adoption of healthy lifestyle habits has been shown to substantially reduce cardiovascular risk, reinforcing the central role of lifestyle as an immediate tool for primary prevention. Imaging, in turn, should not be viewed as technological excess, but rather as an instrument of clinical precision and therapeutic individualization. Among the available methods, the CAC

score emerges as a rational strategy to refine risk in most asymptomatic individuals without comorbidities and with elevated Lp(a), especially when the question is whether subclinical atherosclerotic burden is already sufficient to warrant intensification of treatment targets and to support patient engagement in prevention and consequent reduction of cardiovascular event risk.

If Lp(a) measurement introduced a new element in risk prediction within the realm of serum biomarkers, imaging – through its ability to detect nascent, established, or unstable disease – refines this prediction by guiding the intensity of the therapeutic approach. Until new prediction methods using genomics or proteomics are validated, the best way to position ourselves in relation to cardiovascular risk is by observing the presence of disease and its progression as a continuum. In this regard, plaque detection, its location, and its quantification remain the most useful markers for guiding therapeutic decision-making.

References

1. Rached FH, Miname MH, Rocha VZ, Zimerman A, Cesena FHY, Sposito AC, et al. Brazilian Guideline on Dyslipidemias and Prevention of Atherosclerosis - 2025. Arq Bras Cardiol. 2025;122(9):e20250640. doi: 10.36660/abc.20250640.
2. Blumenthal RS, Morris PB, Gaudino M, Johnson HM, Anderson TS, Bittner VA, et al. 2026 ACC/AHA/AACVPR/ABC/ACPM/ADA/AGS/APhA/ASPC/NLA/PCNA Guideline on the Management of Dyslipidemia: A Report of the American College of Cardiology/American Heart Association Joint Committee on Clinical Practice Guidelines. J Am Coll Cardiol. 2026:S0735-1097(25)10254-4. doi: 10.1016/j.jacc.2025.11.016.
3. Bess C, Mehta A, Joshi PH. All We Need to Know about Lipoprotein(a). Prog Cardiovasc Dis. 2024;84:27-33. doi: 10.1016/j.pcad.2024.05.007.
4. Patel AP, Wang M, Pirruccello JP, Ellinor PT, Ng K, Kathiresan S, et al. Lp(a) (Lipoprotein[a]) Concentrations and Incident Atherosclerotic Cardiovascular Disease: New Insights from a Large National Biobank. Arterioscler Thromb Vasc Biol. 2021;41(1):465-74. doi: 10.1161/ATVBAHA.120.315291.
5. Pantelidis P, Oikonomou E, Lampsas S, Zakynthinos GE, Lysandrou A, Kalogeras K, et al. Lipoprotein(a) and Calcific Aortic Valve Disease Initiation and Progression: A Systematic Review and Meta-Analysis. Cardiovasc Res. 2023;119(8):1641-55. doi: 10.1093/cvr/cvad062.
6. Yu B, Hafiane A, Thanassoulis G, Ott L, Filwood N, Cerruti M, et al. Lipoprotein(a) Induces Human Aortic Valve Interstitial Cell Calcification. JACC Basic Transl Sci. 2017;2(4):358-71. doi: 10.1016/j.jacbts.2017.03.015.
7. Zheng KH, Tsimikas S, Pawade T, Kroon J, Jenkins WSA, Doris MK, et al. Lipoprotein(a) and Oxidized Phospholipids Promote Valve Calcification in Patients with Aortic Stenosis. J Am Coll Cardiol. 2019;73(17):2150-62. doi: 10.1016/j.jacc.2019.01.070.
8. Mehta A, Vasquez N, Ayers CR, Patel J, Hooda A, Khera A, et al. Independent Association of Lipoprotein(a) and Coronary Artery Calcification with Atherosclerotic Cardiovascular Risk. J Am Coll Cardiol. 2022;79(8):757-68. doi: 10.1016/j.jacc.2021.11.058.
9. Bhatia HS, Fan Y, Dharmavaram G, Razavi AC, Tsai MY, Ramsis M, et al. Use of Coronary Artery Calcium Scoring in Individuals with Elevated Lipoprotein(a): A Multicohort Study. J Am Coll Cardiol. 2026:S0735-1097(26)05437-9. doi: 10.1016/j.jacc.2026.02.5067.
10. Qiu Y, Hao W, Guo Y, Guo Q, Zhang Y, Liu X, et al. The Association of Lipoprotein (a) with Coronary Artery Calcification: A Systematic Review and Meta-Analysis. Atherosclerosis. 2024;388:117405. doi: 10.1016/j.atherosclerosis.2023.117405.
11. Doshi A, Gandhi H, Patel KN, Majmundar M, Doshi R. Aspirin for Primary Prevention in Patients with Elevated Coronary Artery Calcium Score: A Systematic Review of Current Evidences. Am J Cardiol. 2024;220:9-15. doi: 10.1016/j.amjcard.2024.03.021.
12. Winchester DE, Maron DJ, Blankstein R, Chang IC, Kirtane AJ, Kwong RY, et al. ACC/AHA/ASE/ASNC/ASPC/HFSA/HRS/SCAI/SCCT/SCMR/STS 2023 Multimodality Appropriate Use Criteria for the Detection and Risk Assessment of Chronic Coronary Disease. J Am Coll Cardiol. 2023;81(25):2445-67. doi: 10.1016/j.jacc.2023.03.410.
13. Qi Y, Duan Y, Deng Q, Yang N, Sun J, Li J, et al. Independent Relationship of Lipoprotein(a) and Carotid Atherosclerosis with Long-Term Risk of Cardiovascular Disease. J Am Heart Assoc. 2024;13(9):e033488. doi: 10.1161/JAHA.123.033488.
14. Cegla J, Neely RDG, France M, Ferns G, Byrne CD, Halcox J, et al. HEART UK Consensus Statement on Lipoprotein(a): A Call to Action. Atherosclerosis. 2019;291:62-70. doi: 10.1016/j.atherosclerosis.2019.10.011.

Original Article

Impact of Isometric Exercise on Left Ventricular Mechanics Assessed by Global Longitudinal Strain and Myocardial Work in Healthy Adults

Marcio Mendes Pereira,[1] *Maria Estefania Bosco Otto,*[2,3] *Juliana Lins da Paz Portela*[1]

UDI Hospital/Rede D'or São Luiz,[1] *São Luis, MA – Brazil*
Universidade de Brasília,[2] *Brasília, DF – Brazil*
DF Star,[3] *Brasília, DF – Brazil*

Abstract

Background: **Traditional volumetric parameters have limitations in detecting subtle left ventricular (LV) systolic dysfunction. Global longitudinal strain (GLS) and myocardial work (MW) allow a more sensitive assessment of ventricular mechanics.**

Objectives: **To evaluate changes in GLS and MW indices during isometric handgrip exercise compared with resting conditions.**

Methods: **A total of 30 healthy individuals (29.3 ± 6.1 years; 50% male) were included in the sample. Echocardiography was performed at rest and during handgrip exercise (30%-40% of maximal strength). GLS, LV ejection fraction (LVEF), and MW indices were assessed: i) global work index (GWI), ii) global constructive work (GCW), iii) global wasted work (GWW), and iv) global work efficiency (GWE). Comparisons were performed using paired tests. Statistical significance was set at $p < 0.05$.**

Results: **Handgrip exercise increased both systolic blood pressure (115 ± 16 vs 133 ± 18 mmHg; $p < 0.0001$) and diastolic blood pressure (69 ± 9 vs 79 ± 13 mmHg; $p = 0.0002$), without significant changes in LVEF (64.8% vs 64.4%; $p = 0.62$). A decrease in GLS was observed (20.38% ± 2.57% vs 19.60% ± 2.52%; $p = 0.028$), along with increases in GWI (+244 mmHg%; $p = 0.0002$), GCW (+313 mmHg%; $p < 0.0001$), and GWW (+52 mmHg%; $p = 0.0008$) as well as a decrease in GWE (94.8% ± 1.8% vs 93.6% ± 2.5%; $p = 0.022$).**

Conclusions: **Handgrip exercise induces measurable ventricular mechanical changes in healthy individuals, reflecting a physiological response to acute pressure overload.**

Keywords: **Exercise; Echocardiography; Left Ventricular Dysfunction.**

Introduction

Assessment of left ventricular (LV) systolic function is central to contemporary echocardiography. Although LV ejection fraction (LVEF) is widely used, its dependence on ventricular geometry and loading conditions limits the detection of subclinical myocardial dysfunction.[1] In this context, more sensitive techniques, such as speckle-tracking echocardiography (STE) and global longitudinal strain (GLS), have expanded the ability to assess myocardial mechanical performance.

GLS, which is obtained by STE, quantifies shortening of LV subendocardial fibers and provides a sensitive measure of myocardial contractility.[2] GLS is an early marker of ventricular dysfunction with established prognostic value and is often altered before changes in LVEF become apparent.[3] However, its sensitivity to variations in loading conditions, including preload and afterload, limits its isolated interpretation, which has justified the development of methods capable of integrating myocardial deformation into the hemodynamic context.

Myocardial work (MW) integrates myocardial deformation with the noninvasively estimated systolic pressure gradient through pressure-strain curves, allowing a more comprehensive assessment of LV mechanics under different loading conditions.[4] These indices show good correlation with invasive measures of ventricular performance and lower afterload dependence compared with strain alone, thereby expanding their clinical applicability.[4-7]

Isometric handgrip exercise is a simple, safe, and reproducible method for inducing cardiovascular stress, promoting an acute increase in systolic blood pressure (BP) and afterload.[6,9] Classic studies demonstrated that individuals with preserved ventricular reserve increase systolic work, whereas patients with ventricular dysfunction exhibit adverse hemodynamic responses, including

Mailing Address: Marcio Mendes Pereira •
UDI Hospital. AV. Prof. Carlos Cunha, 2000. Postal code: 65076-820. Jaracti, São Luis, MA – Brazil
E-mail: marciomp50@hotmail.com
Manuscript received March 24, 2026, revised manuscript April 6, 2026, accepted April 15, 2026
Editor responsible for the review: Marcelo Tavares

DOI: https://doi.org/10.36660/abcimg.20260036i

Central Illustration: Impact of Isometric Exercise on Left Ventricular Mechanics Assessed by Global Longitudinal Strain and Myocardial Work in Healthy Adults

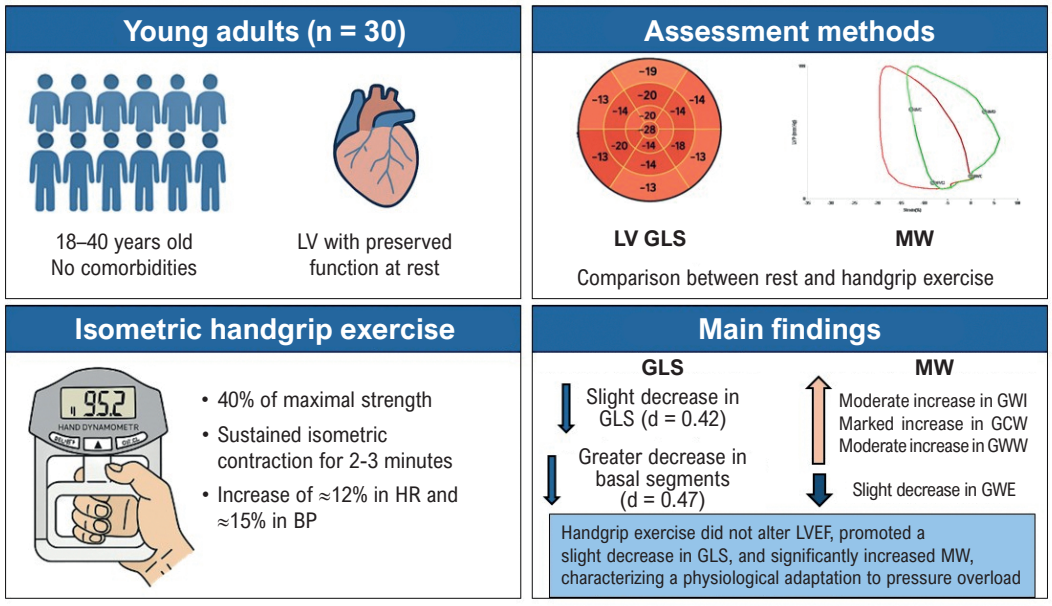

Arq Bras Cardiol: Imagem cardiovasc. 2026;39(2):e20260036

BP: blood pressure; GCW: global constructive work; GLS: global longitudinal strain; GWE: global work efficiency; GWI: global work index; GWW: global wasted work; HR: heart rate; LV: left ventricle; LVEF: LV ejection fraction; MW: myocardial work.

increased end-diastolic pressure and decreased MW efficiency.[9,10] More recent echocardiographic protocols have confirmed that handgrip exercise reproduces controlled hemodynamic stress and enables sensitive assessment of ventricular mechanical adaptations, including increased global work index (GWI) and a slight decrease in global work efficiency (GWE).[7,11]

This study evaluated, in healthy young adults, changes in GLS and MW indices during isometric handgrip exercise compared with resting conditions, aiming to characterize the physiological LV response to acute pressure overload.

Methods

Study design and population

This was a prospective, cross-sectional study that included healthy young adults (18-40 years) undergoing echocardiographic evaluation at rest and during isometric handgrip exercise. Individuals with preserved myocardial function and no clinical comorbidities were included. Participants with significant structural heart disease, arrhythmias, limiting musculoskeletal disorders, or contraindications to stress echocardiography were excluded.

Sample size calculation was based on normative MW values described by Olsen et al.,[5] using GWI as the primary outcome and considering a paired design (rest vs handgrip exercise). A conservative increase of 150 mmHg% in GWI was adopted, with an estimated standard deviation of differences of 240 mmHg%, based on data from Cebrowska et al.[12] Considering a significance level of 5% and statistical power of 80%, the formula for paired mean comparisons indicated a minimum requirement of 21 individuals. To increase the precision of estimates and analytical robustness, 30 participants were included in the final sample.

Echocardiographic acquisition and analysis

Transthoracic echocardiography was performed using the Vivid™ E95 Ultrasound System (GE Vingmed Ultrasound AS, Horten, Norway), equipped with a 3.5-MHz MS5 sector transducer. Standard 2D images were acquired over three cardiac cycles, synchronized to the QRS complex, and stored in digital format for offline analysis using EchoPAC™ software (version 206; GE Vingmed Ultrasound AS, Horten, Norway), according to the recommendations of the American Society of Echocardiography.[13]

LVEF was obtained using the biplane Simpson method. Diastolic function was assessed according to current guidelines. GLS was analyzed using STE with standard apical views.

MW assessment

MW indices (i.e., GWI, global constructive work [GCW], global wasted work [GWW], and GWE) were automatically calculated from pressure-strain curves. For this purpose, brachial BP measured at the time of the examination was used.

Handgrip exercise protocol

The handgrip protocol consisted of sustained isometric contraction at 40% of maximal voluntary strength, previously determined by dynamometry. The effort was maintained for 2-3 minutes, with echocardiographic image acquisition performed between the second and third minutes.

Statistical analysis

Comparisons between resting and handgrip conditions were performed using paired tests according to data distribution. Statistical significance was set at $p < 0.05$. Effect size was calculated to estimate the magnitude of the observed differences.

Ethical considerations

The study was approved by the local human research ethics committee, and all participants provided written informed consent.

Results

A total of 30 healthy individuals were evaluated, 50% of whom were male, with a mean age of 29.3 ± 6.1 years, and all completed the isometric handgrip exercise protocol. Overall clinical characteristics demonstrated mean values consistent with the studied age range. During handgrip exercise, significant increases were observed in systolic BP (115 mmHg vs 133 mmHg; $p < 0.0001$), diastolic BP (69 mmHg vs 79 mmHg; $p = 0.0002$), and heart rate (72 bpm vs 81 bpm; $p < 0.0001$), characterizing the typical hemodynamic response to isometric effort (Table 1).

Structural echocardiographic measurements demonstrated ventricular dimensions and LV mass within normal ranges, without relevant morphological abnormalities. Global systolic function remained preserved throughout the protocol, with no changes in LVEF between rest and stress conditions (64.8% vs 64.4%; $p = 0.6163$). Diastolic function parameters also remained stable, with a mild decrease in lateral e' velocity (16.4 cm/s vs 14.9 cm/s; $p = 0.0123$), without relevant changes in the functional pattern (Table 2).

In the GLS analysis, a slight absolute decrease was observed during handgrip exercise (20.3% vs 19.6%; $p = 0.0283$), with a small effect size (Cohen's $d = 0.42$). The decrease was more evident in basal segments, also with a small effect size ($d = 0.47$), whereas mid and apical segments showed minimal variations and very small effect sizes ($d = 0.11$ and 0.16, respectively), without statistical significance (Table 3).

Regarding MW, there was a significant increase in GWI (1,810 mmHg% vs 2,054 mmHg%; $p = 0.0002$), with a moderate effect size ($d = 0.77$), and in GCW (2,172 mmHg% vs 2,486 mmHg%; $p < 0.0001$), which showed a large effect size ($d = 1.05$), representing the greatest magnitude among the evaluated parameters. GWW also increased, with a moderate effect size ($d = 0.68$). GWE showed a slight decrease, with a small effect size ($d = 0.44$).

Segmental MW analysis demonstrated increases in basal segments (1,719 mmHg% vs 1,959 mmHg%; $p = 0.0003$) and mid segments (1,655 mmHg% vs 2,047 mmHg%; $p = 0.0001$), with moderate effect sizes ($d = 0.81$ and 0.72, respectively), whereas apical segments showed no significant variation. These results are presented in detail in Table 3.

Figure 1 graphically summarizes the distribution of the main evaluated parameters. LVEF remained stable, GLS showed a slight decrease, and consistent increases were observed in GWI, GCW, and GWW, accompanied by a mild decrease in GWE.

Discussion

The present study contributes by demonstrating the integrated LV response to isometric handgrip stress in healthy individuals through the combination of GLS and MW indices. Our findings show that acute afterload increase promotes a consistent rise in BP, preservation of LVEF, a slight decrease in GLS, and increased MW indices as well as increased GWW and a mild decrease in GWE (Central Illustration). These results expand the understanding of the physiological myocardial adaptation to pressure stress and reinforce the value of a multiparametric approach for identifying changes not detectable by LVEF alone.

The consistent increase in systolic and diastolic BP during handgrip exercise confirms the role of this maneuver as a reproducible hemodynamic stressor, in agreement with the classic findings of Helfant et al.[8] and Kivowitz et al.,[9] who described the physiological mechanisms underlying

Table 1 – Clinical characteristics of the study population

Variable	n	Mean ± SD	Minimum	Maximum
Weight, kg	30	72.3 ± 12.8	55	100
Height, cm	30	167.2 ± 9.1	150	184
Body surface area, m^2	30	1.81 ± 0.19	1.51	2.21
Resting systolic BP, mmHg	30	115.3 ± 16.2	87	146
Resting diastolic BP, mmHg	30	69.0 ± 9.5	53	90
Systolic BP during handgrip exercise, mmHg*	30	133.4 ± 18.4	95	172
Diastolic BP during handgrip exercise, mmHg*	30	79.5 ± 13.5	51	110
Resting HR, bpm	30	72.0 ± 11.9	53	111
HR during handgrip exercise, bpm*	30	81.7 ± 10.0	60	100

**p < 0.05 compared with rest. Source: Prepared by the authors (2025). BP: blood pressure; HR: heart rate; SD: standard deviation.*

the pressor response to isometric effort. These authors demonstrated that increased sympathetic tone and peripheral vascular resistance are the main determinants of BP increase, whereas HR shows only a modest increase, a pattern also observed in the present investigation. More recent studies, such as that by Samuel et al.,[14] further support the usefulness of handgrip exercise as a practical, accessible alternative to more complex dynamic stress protocols, especially in the assessment of subtle changes in ventricular performance.

The stability of LVEF both at rest and during stress highlights the limitation of volumetric parameters in detecting subtle contractile changes induced by loading variations, corroborating observations by Thomas et al.[15] and Clemmensen et al.[16] They demonstrated that LVEF may remain unchanged despite relevant modifications in systolic mechanics, which underscores the need for more sensitive tools such as GLS and MW.

The slight decrease in GLS during handgrip exercise represents an expected physiological finding. This behavior, described by Flachskampf and Chandrashekar,[4] reflects the sensitivity of strain to afterload changes. The greater decrease in basal segments reinforces the regional heterogeneity of the mechanical response, as suggested by Thomas et al.[15] These regions exhibit higher wall stress and depend more directly on longitudinal shortening, making them more susceptible to acute pressure overload. The relative stability of mid and apical segments suggests preservation of overall contractile reserve in healthy individuals.

MW indices provided relevant complementary information. The significant increase in GWI and GCW during handgrip exercise is consistent with the physiological increase in mechanical energy required to overcome the greater systolic load. Studies by Zhu et al.[2] and Caminiti et al.[7] demonstrated similar behavior both in healthy individuals and in populations with hypertension or coronary artery disease, reinforcing the sensitivity of the pressure-strain model in quantifying contractile adjustments in response to acute stimuli.

The increase in GWW represents another physiologically consistent finding. In scenarios of acute afterload increase, as described by Russell et al.[17] and summarized by Flachskampf and Chandrashekar,[4] part of the energy generated by the myocardium is expected not to be converted into useful work because of temporal dyssynchrony between tension generation and effective fiber shortening. This mechanism contributes to the slight decrease in GWE, which nevertheless remained within the physiological range. The observed values are consistent with normative limits previously described by Olsen et al.,[5] reinforcing the validity of these findings in a healthy population.

Segmental LV analysis revealed an additional aspect of the physiological adaptation to isometric stress. During handgrip exercise, a decrease in GLS was observed in basal segments, accompanied by increased MW in these same regions, a pattern also observed in mid segments. This dissociation between lower deformation and greater MW suggests a physiological adjustment to acute afterload increase, in which reduced longitudinal shortening is compensated

Table 2 – Echocardiographic characteristics of the sample (n = 30)

Parameter	Média ± DP	Mín-Máx
Cardiac structure		
LV end-diastolic diameter, cm	4.75 ± 0.44	3.90-5.60
LV end-systolic diameter, cm	2.96 ± 0.48	2.00-4.90
Posterior wall thickness, cm	0.80 ± 0.09	0.70-1.00
Interventricular septal thickness, cm	0.80 ± 0.10	0.70-1.10
LV mass index, g/m^2	72.16 ± 15.67	46.80-110.40
Indexed left atrial volume, mL/m^2	24.70 ± 6.34	14-40
Systolic function – rest		
End-diastolic volume, mL	84.47 ± 23.29	42-142
End-systolic volume, mL	29.87 ± 9.31	10-55
Stroke volume, mL	54.60 ± 15.21	31-87
Ejection fraction, %	64.80% ± 4.07%	60-76
Systolic function – handgrip exercise		
End-diastolic volume, mL#	87.70 ± 23.71	47-146
End-systolic volume, mL#	31.53 ± 11.05	14-62
Stroke volume, mL#	56.17 ± 13.67	31-84
Ejection fraction, %#	64.47% ± 4.15%	58-74
Diastolic function – rest		
E-wave velocity, cm/s	86.40 ± 21.89	58-141
Medial e', cm/s	11.75 ± 2.39	7-17
Lateral e', cm/s	16.45 ± 3.92	10-27
E/e' ratio	6.27 ± 1.70	3.45-10.67
Diastolic function – handgrip exercise		
E-wave velocity, cm/s#	84.33 ± 18.99	45-145
Medial e', cm/s#	11.23 ± 2.06	7-15
Lateral e', cm/s*	14.97 ± 2.92	10-20
E/e' ratio#	6.63 ± 1.55	3.85-10.70

*#p > 0.05 compared with rest. *p < 0.05 compared with rest. Source: Prepared by the authors (2025). LV: left ventricle; Max: maximum; Min: minimum; SD: standard deviation.*

Table 3 – Strain and MW parameters (rest vs handgrip exercise)

Parameter	Rest	Handgrip Exercise	Δ	p-value	Cohen's d
GLS, %	20.38 ± 2.57	19.60 ± 2.52	−0.78	0.0283	0.42
Basal segment strain, %	18.41 ± 2.93	17.30 ± 2.38	−1.12	0.0208	0.47
Mid segment strain, %	20.35 ± 2.21	20.15 ± 2.62	−0.20	0.5455	0.11
Apical segment strain, %	24.07 ± 3.61	23.52 ± 3.66	−0.55	0.3971	0.16
GWI, mmHg%	1.810 ± 322	2.054 ± 403	+244	0.0002	0.77
GCW, mmHg%	2.172 ± 371	2.486 ± 453	+313	< 0.0001	1.05
GWW, mmHg%	108.4 ± 43.9	160.4 ± 75.8	+52.0	0.0008	0.68
GWE, %	94.83 ± 1.76	93.57 ± 2.45	−1.27	0.0224	0.44
Basal segment MW, mmHg%	1.719 ± 346	1.959 ± 283	+240	0.0003	0.81
Mid segment MW, mmHg%	1.655	2.047	+392	0.0001	0.72
Apical segment MW, mmHg%	1.970	2.168	+198	0.0710	0.34

Source: Prepared by the authors (2025). GCW: global constructive work; GLS: global longitudinal strain; GWE: global work efficiency; GWI: global work index; GWW: global wasted work; MW: myocardial work.

by greater mechanical energy generation to maintain overall performance. Taken together, the observed pattern remained aligned with the normal phenotype described by Grandperrin et al.,[18] which underscores that the regional response to stress represents physiological contractile adaptation rather than subclinical dysfunction.

This study has limitations that should be considered. The exclusive inclusion of healthy young adults and the relatively small sample size limit the generalizability of the results to clinical populations. In addition, echocardiographic acquisition during isometric effort may introduce technical variability in image quality. On the other hand, the prospective and standardized design, the homogeneous sample without comorbidities, which allowed physiological characterization with reduced external interference, and the integrated evaluation of GLS and MW are important strengths, increasing sensitivity for detecting subtle changes in ventricular mechanics. The inclusion of effect size analysis also adds interpretative value by allowing assessment of the practical relevance of the observed differences.

Taken together, these findings reinforce the value of handgrip exercise as a practical, safe, and reproducible submaximal stress tool. The integrated GLS and MW approach proved capable of detecting acute physiological modifications not identifiable by traditional methods such as LVEF and may be particularly relevant in contexts requiring assessment of contractile reserve or identification of subclinical dysfunction.

In addition to characterizing the physiological LV response to isometric stress, this study contributes to consolidating the role of GLS and MW as central tools in the contemporary assessment of ventricular mechanics, highlighting handgrip exercise as a valuable strategy for both physiological studies and clinical applications.

Conclusions

Isometric handgrip exercise induced measurable hemodynamic and mechanical changes in healthy individuals, characterized by stable LVEF, a slight decrease in GLS, and significant increases in GWI and GCW as well as increased GWW and a mild decrease in GWE. These findings reflect physiological contractile adaptation to acute pressure overload and reinforce handgrip exercise as a simple, safe, reproducible tool for assessing ventricular mechanics beyond traditional volumetric parameters.

Author Contributions

Conception and design of the research, analysis and interpretation of the data, writing of the manuscript and ritical revision of the manuscript for intellectual content: Pereira MM, Portela JLP, Otto MEB; acquisition of data: Pereira MM, Portela JLP; statistical analysis: Pereira MM.

Potential Conflict of Interest

No potential conflict of interest relevant to this article was reported.

Sources of Funding

There were no external funding sources for this study.

Study Association

This study is not associated with any thesis or dissertation work.

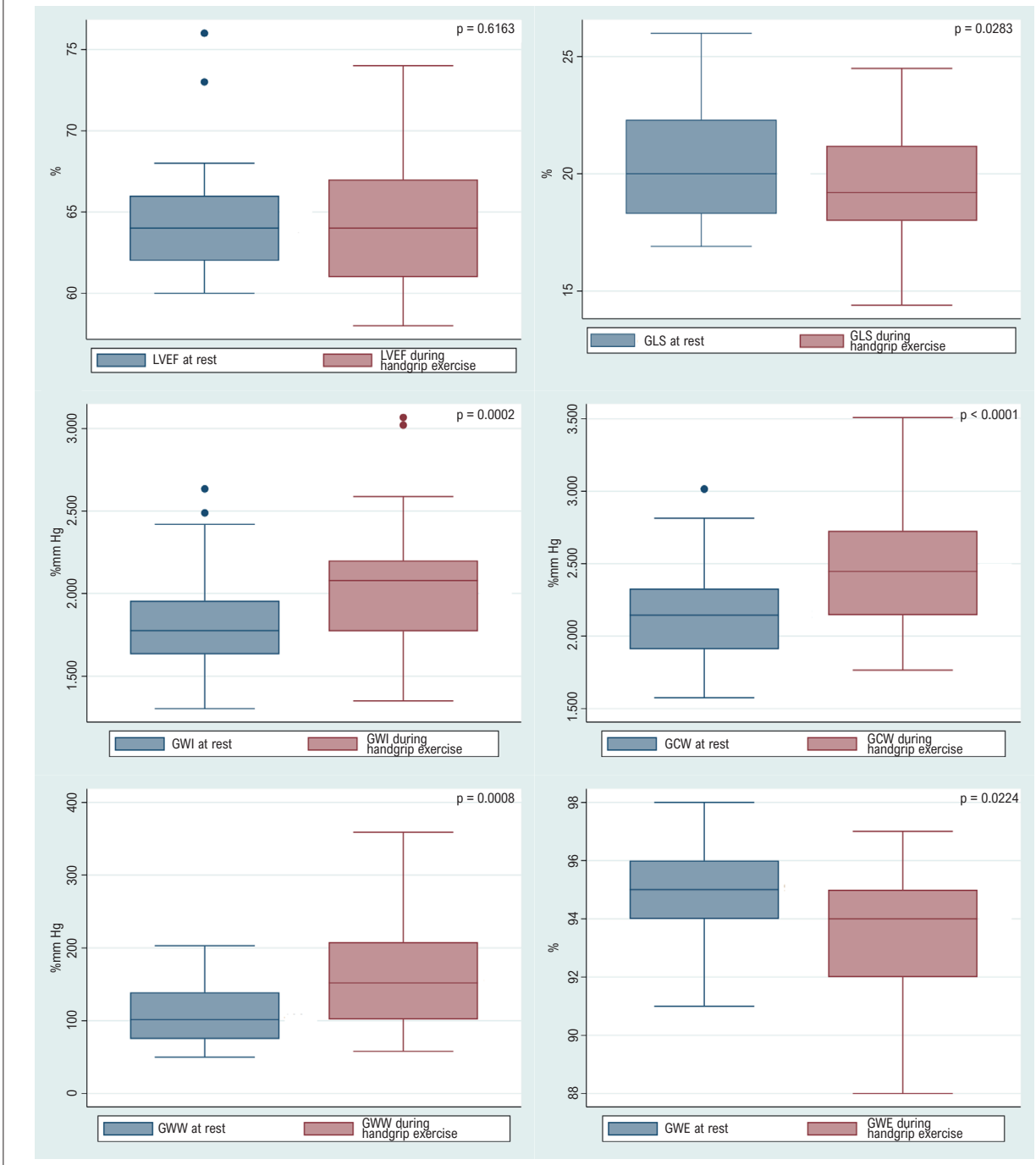

Figure 1 – *Variation in ventricular function, GLS, and MW parameters between rest and handgrip exercise. GCW: global constructive work; GLS: global longitudinal strain; GWE: global work efficiency; GWI: global work index; GWW: global wasted work; LVEF: left ventricular ejection fraction.*

Ethics approval and consent to participate

This study was approved by the Ethics Committee of the Hospital Carlos Macieira under the protocol number 7.784.405. All the procedures in this study were in accordance with the 1975 Helsinki Declaration, updated in 2013. Informed consent was obtained from all participants included in the study.

Use of Artificial Intelligence

The authors did not use any artificial intelligence tools in the development of this work.

Data Availability Statement

The underlying content of the research text is contained within the manuscript.

References

1. Stanton T, Leano R, Marwick TH. Prediction of All-Cause Mortality from Global Longitudinal Speckle Strain: Comparison with Ejection Fraction and Wall Motion Scoring. Circ Cardiovasc Imaging. 2009;2(5):356-64. doi: 10.1161/CIRCIMAGING.109.862334.
2. Zhu H, Guo Y, Wang X, Yang C, Li Y, Meng X, et al. Myocardial Work by Speckle Tracking Echocardiography Accurately Assesses Left Ventricular Function of Coronary Artery Disease Patients. Front Cardiovasc Med. 2021;8:727389. doi: 10.3389/fcvm.2021.727389.
3. Oikonomou EK, Kokkinidis DG, Kampaktsis PN, Amir EA, Marwick TH, Gupta D, et al. Assessment of Prognostic Value of Left Ventricular Global Longitudinal Strain for Early Prediction of Chemotherapy-Induced Cardiotoxicity: A Systematic Review and Meta-Analysis. JAMA Cardiol. 2019;4(10):1007-18. doi: 10.1001/jamacardio.2019.2952.
4. Flachskampf FA, Chandrashekar Y. Myocardial Work and Work Index: Related but Different for Clinical Usage. JACC Cardiovasc Imaging. 2022;15(8):1521-3. doi: 10.1016/j.jcmg.2022.07.001.
5. Olsen FJ, Skaarup KG, Lassen MCH, Johansen ND, Sengeløv M, Jensen GB, et al. Normal Values for Myocardial Work Indices Derived from Pressure-Strain Loop Analyses: From the CCHS. Circ Cardiovasc Imaging. 2022;15(5):e013712. doi: 10.1161/CIRCIMAGING.121.013712.
6. Olsen FJ, Bjerregaard CL, Skaarup KG, Lassen MCH, Johansen ND, Modin D, et al. Impact of Echocardiographic Analyses of Valvular Event Timing on Myocardial Work Indices. Eur Heart J Cardiovasc Imaging. 2023;24(3):314-23. doi: 10.1093/ehjci/jeac171.
7. Caminiti G, Volterrani M, Iellamo F, Marazzi G, D'Antoni V, Calandri C, et al. Acute Changes in Myocardial Work during Isometric Exercise in Hypertensive Patients with Ischemic Heart Disease: A Case-Control Study. J Clin Med. 2024;13(19):5955. doi: 10.3390/jcm13195955.
8. Helfant RH, De Villa MA, Meister SG. Effect of Sustained Isometric Handgrip Exercise on Left Ventricular Performance. Circulation. 1971;44(6):982-93. doi: 10.1161/01.cir.44.6.982.
9. Kivowitz C, Parmley WW, Donoso R, Marcus H, Ganz W, Swan HJ. Effects of Isometric Exercise on Cardiac Performance. The Grip Test. Circulation. 1971;44(6):994-1002. doi: 10.1161/01.cir.44.6.994.
10. Fisher ML, Nutter DO, Jacobs W, Schlant RC. Haemodynamic Responses to Isometric Exercise (Handgrip) in Patients with Heart Disease. Br Heart J. 1973;35(4):422-32. doi: 10.1136/hrt.35.4.422.
11. Samuel TJ, Beaudry R, Haykowsky MJ, Sarma S, Park S, Dombrowsky T, et al. Isometric Handgrip Echocardiography: A Noninvasive Stress Test to Assess Left Ventricular Diastolic Function. Clin Cardiol. 2017;40(12):1247-55. doi: 10.1002/clc.22818.
12. Cebrowska K, Mińczykowski A, Krauze T, Guzik P, Szczepanik A, Wykrętowicz A. The Pressure-Strain Work Indices in Response to Isometric Handgrip Exercise. Kardiol Pol. 2021;79(4):455-7. doi: 10.33963/KP.15912.
13. Lang RM, Badano LP, Mor-Avi V, Afilalo J, Armstrong A, Ernande L, et al. Recommendations for Cardiac Chamber Quantification by Echocardiography in Adults: An Update from the American Society of Echocardiography and the European Association of Cardiovascular Imaging. J Am Soc Echocardiogr. 2015;28(1):1-39.e14. doi: 10.1016/j.echo.2014.10.003.
14. Samuel TJ, Haykowsky MJF, Sarma S, Nelson MD. Diastolic Stress Testing: Have You Considered Isometric Handgrip Echocardiography? JACC Cardiovasc Imaging. 2019;12(10):2095-7. doi: 10.1016/j.jcmg.2019.07.023.
15. Thomas JD, Edvardsen T, Abraham T, Appadurai V, Badano L, Banchs J, et al. Clinical Applications of Strain Echocardiography: A Clinical Consensus Statement from the American Society of Echocardiography Developed in Collaboration with the European Association of Cardiovascular Imaging of the European Society of Cardiology. J Am Soc Echocardiogr. 2025;38(11):985-1020. doi: 10.1016/j.echo.2025.07.007.
16. Clemmensen TS, Eiskjær H, Mikkelsen F, Granstam SO, Flachskampf FA, Sørensen J, et al. Left Ventricular Pressure-Strain-Derived Myocardial Work at Rest and during Exercise in Patients with Cardiac Amyloidosis. J Am Soc Echocardiogr. 2020;33(5):573-82. doi: 10.1016/j.echo.2019.11.018.
17. Russell K, Eriksen M, Aaberge L, Wilhelmsen N, Skulstad H, Gjesdal O, et al. Assessment of Wasted Myocardial Work: A Novel Method to Quantify Energy Loss Due to Uncoordinated Left Ventricular Contractions. Am J Physiol Heart Circ Physiol. 2013;305(7):H996-1003. doi: 10.1152/ajpheart.00191.2013.
18. Grandperrin A, Schnell F, Donal E, Galli E, Hedon C, Cazorla O, et al. Specific Alterations of Regional Myocardial Work in Strength-Trained Athletes Using Anabolic Androgenic Steroids Compared to Athletes with Genetic Hypertrophic Cardiomyopathy. J Sport Health Sci. 2023;12(4):477-85. doi: 10.1016/j.jshs.2022.07.004.

Myocardial Work During Isometric Exercise: From Physiology to Clinical Practice

Rodrigo Bellio de Mattos Barretto,[1] *Carlos Eduardo Suaide Silva*[2]

Universidade de São Paulo, Instituto do Coração,[1] *São Paulo, SP – Brazil*

Diagnósticos da América AS,[2] *Barueri, SP – Brazil*

Short Editorial related to the article: Impact of Isometric Exercise on Left Ventricular Mechanics Assessed by Global Longitudinal Strain and Myocardial Work in Healthy Adults

Assessment of left ventricular function by echocardiography has advanced remarkably in its ability to characterize aspects that extend beyond traditional measures of volume and ejection fraction (EF). Among these advances, the evaluation of contractility through two-dimensional strain analysis has gained particular prominence. Technological developments now allow this measure to be adjusted for afterload through myocardial work (MW), providing greater potential to identify subtle changes in ventricular function.[1]

Isometric exercise represents a strategy to increase afterload through handgrip, proving particularly useful in echocardiography because it enables the identification of functional changes in different clinical settings, including coronary artery disease, assessment of diastolic function, hypertension, athletes, and even atrial functional mitral regurgitation.[2-6]

The study presented adds important evidence by demonstrating how isometric handgrip stress can reveal subtle physiological adaptations in left ventricular mechanics among healthy adults. As reported by the authors, handgrip increased systolic blood pressure without changing left ventricular EF (64.8% vs. 64.4%), reinforcing the limitations of EF as an isolated marker of systolic performance, a finding that was expected.

The integration of global longitudinal strain (GLS) with blood pressure measurements, translated into MW, provided a more comprehensive understanding of changes in ventricular function when comparing data obtained at rest with those recorded during isometric exercise. The slight reduction in GLS observed during exercise was compensated for by the increased MW load imposed on the left ventricle, as evidenced by the increase in total and constructive MW. These findings support the greater myocardial oxygen consumption (VO_2) required under these conditions, as reflected by the observed values. Conversely, an increase in wasted MW and a consequent reduction in cardiac efficiency were also identified, illustrating the complexity of mechanical efficiency under pressure overload.

Another relevant aspect is that abnormalities in the basal segments of the left ventricle were primarily responsible for the reduction in GLS during exercise and also contributed to the greater increase in MW. These segments are known to be more susceptible to loading conditions and play a greater role in longitudinal deformation mechanics. In contrast, apical segments, despite containing a proportionally greater amount of longitudinal fibers, are less influenced by the load induced by handgrip because of their geometric arrangement. This type of regional characterization has important implications for populations with hypertension, early-stage cardiomyopathies, or exposure to cardiotoxic agents, scenarios in which the sensitivity of MW may provide a diagnostic advantage.

This study reinforces the use of isometric exercise as a feasible maneuver capable of clearly demonstrating physiological changes and expanding the understanding of cardiovascular phenomena when analyzed through MW. At a time when echocardiography seeks accessible methods to assess contractile reserve and detect subclinical dysfunction, handgrip emerges as a practical and physiologically informative alternative.

This opens a broad field of investigation regarding its application in different clinical settings aimed at the early recognition of abnormalities, a topic that has already been explored in prior research.[7,8] Nevertheless, this enthusiasm must still be supported by evidence demonstrating its clinical value, endorsed by guidelines, expert consensus documents, and, above all, its association with clinical outcomes.

In summary, this study represents a robust, necessary contribution to contemporary echocardiography. By integrating myocardial deformation findings, loading conditions, and mechanical efficiency, it establishes MW as a central component of advanced functional assessment, not only by refining the interpretation of systolic performance beyond EF but also by measurably expanding our ability to recognize subclinical dysfunction and guide clinical decision-making with greater precision. It therefore represents an important step toward a more comprehensive and integrated echocardiographic approach, one that is increasingly necessary in contemporary clinical practice.

Keywords

Global Longitudinal Strain; Stress Echocardiography

Mailing Address: Rodrigo B. M. Barretto •
Universidade de São Paulo, Instituto do Coração. Av. Eneas Carneiro Aquiar, 44. Postal Code: 05403-000. São Paulo, SP – Brazil
E-mail: barretto.rodrigo@terra.com.br

DOI: https://doi.org/10.36660/abcimg.20260073i

References

1. Helfant RH, De Villa MA, Meister SG. Effect of Sustained Isometric Handgrip Exercise on Left Ventricular Performance. Circulation. 1971;44(6):982-93. doi: 10.1161/01.cir.44.6.982.
2. Afridi I, Main ML, Parrish DL, Kizilbash A, Levine BD, Grayburn PA. Usefulness of Isometric Hand Grip Exercise in Detecting Coronary Artery Disease during Dobutamine Atropine Stress Echocardiography in Patients with Either Stable Angina Pectoris or Another Type of Positive Stress Test. Am J Cardiol. 1998;82(5):564-8. doi: 10.1016/s0002-9149(98)00398-1.
3. Cauwenberghs N, Cornelissen V, Christle JW, Hedman K, Myers J, Haddad F, et al. Impact of Age, Sex and Heart Rate Variability on the Acute Cardiovascular Response to Isometric Handgrip Exercise. J Hum Hypertens. 2021;35(1):55-64. doi: 10.1038/s41371-020-0311-y.
4. Freitas APTG, Massoni NM, Barretto RBM. Left Ventricular Longitudinal Strain Echocardiogram and Handgrip: A Useful Tool for Detecting Ischemia in the Emergency Room. Arq Bras Cardiol: Imagem Cardiovasc. 2021;34(4):eabc238. doi: 10.47593/2675-312X/20213404eabc238.
5. Samuel TJ, Beaudry R, Haykowsky MJ, Sarma S, Park S, Dombrowsky T, et al. Isometric Handgrip Echocardiography: A Noninvasive Stress Test to Assess Left Ventricular Diastolic Function. Clin Cardiol. 2017;40(12):1247-55. doi: 10.1002/clc.22818.
6. Spieker M, Sidabras J, Lagarden H, Christian L, Angendohr S, Zweck E, et al. Prevalence and Prognostic Impact of Dynamic Atrial Functional Mitral Regurgitation Assessed by Isometric Handgrip Exercise. Eur Heart J Cardiovasc Imaging. 2024;25(5):589-98. doi: 10.1093/ehjci/jead336.
7. Caminiti G, Volterrani M, Iellamo F, Marazzi G, D'Antoni V, Calandri C, et al. Acute Changes in Myocardial Work during Isometric Exercise in Hypertensive Patients with Ischemic Heart Disease: A Case-Control Study. J Clin Med. 2024;13(19):5955. doi: 10.3390/jcm13195955.
8. Cebrowska K, Mińczykowski A, Krauze T, Guzik P, Szczepanik A, Wykrętowicz A. The Pressure-Strain Work Indices in Response to Isometric Handgrip Exercise. Kardiol Pol. 2021;79(4):455-7. doi: 10.33963/KP.15912.

Concordance Between Echocardiographic Left Ventricular Ejection Fraction by Simpson's Method, Global Longitudinal Strain, and Cardiac Magnetic Resonance

Álvaro Herrera-Escandón,[1,2] Juan Pablo Morales-Grisales,[1] Sebastián Ayala-Zapata,[1] Stephany Barbosa-Balaguera,[3] Álvaro José Muriel-Ruiz,[1] Juan Felipe Bravo-Rueda,[2] José Eduardo Citelli-Ramírez,[1,2] Luis Fernando Osío-Jimenez,[2] Luis Miguel Benitez-Gómez,[2] Carlos Javier Ramírez-Estupiñán[2]

Universidad del Valle, Departamento de Medicina Interna, Sección de Cardiología,[1] Cali – Colombia

Clínica Imbanaco, Servicio de Cardiología,[2] Cali – Colombia

Clínica Colsanitas S.A., Clínica Sebastián de Belalcázar, Servicio de Cardiología,[3] Cali – Colombia

Abstract

Background: **Left ventricular ejection fraction (LVEF) measured by echocardiography is a widely used parameter in clinical practice for the assessment of ventricular function. More recently, global longitudinal strain (GLS) has emerged as a complementary method, as has the assessment of LVEF by cardiac magnetic resonance (CMR). However, regional evidence evaluating the concordance among these three techniques remains limited.**

Objectives: **To assess the concordance between echocardiographic and CMR measurements in patients treated at a cardiovascular clinic in the city of Cali, Colombia.**

Methods: **This cross-sectional, analytical, descriptive study included 35 patients with confirmed or suspected heart disease, in whom all three methods were performed consecutively. Concordance was evaluated using Lin's concordance correlation coefficient (CCC), Bland-Altman plots for LVEF, and linear and quadratic weighted κ coefficients for agreement between LVEF classifications.**

Results: **The mean age was 58 years, and 60% of participants were male. The most common comorbidities were hypertension (22%) and dyslipidemia (11%). The mean LVEF was 59% by Simpson's method and 57.7% by CMR, while the mean GLS was −17.7%. Concordance was as follows: Simpson's LVEF vs. CMR (CCC, 0.831; 95%CI, 0.609-0.932); GLS vs. CMR-derived LVEF (CCC, 0.751; 95%CI, 0.419-0.903); and Simpson's LVEF vs. GLS (CCC, 0.891; 95%CI, 0.721-0.957).**

Conclusions: **Both Simpson's method and GLS are valid tools for estimating systolic function. CMR remains the reference standard.**

Keywords: **Stroke Volume; Echocardiography; Magnetic Resonance Spectroscopy.**

Introduction

Left ventricular ejection fraction (LVEF) is the principal parameter of systolic function and one of the most widely used metrics in clinical practice. It serves as a key prognostic marker in heart failure, myocardial infarction, valvular disease, and in the risk stratification of multiple cardiovascular conditions.[1] Throughout the history of medicine, a number of approaches have been used to quantify systolic function, ranging from heart rate and pulse pressure to conventional radiography and nuclear imaging techniques. Notably, LVEF reflects ventricular ejection (stroke volume) rather than directly measuring myocardial contractility.[2] Traditionally, LVEF is quantified using 2D echocardiography with the biplane Simpson's method, which has demonstrated broad clinical utility despite inherent limitations, including operator dependence, variability in acoustic window quality, and reliance on geometric assumptions.[3]

In recent years, the assessment of ventricular function using speckle-tracking echocardiography (STE), particularly global longitudinal strain (GLS), has emerged as a robust and complementary technique for evaluating global left ventricle (LV) function, with greater sensitivity for detecting subclinical dysfunction. In addition to providing independent prognostic information, GLS shows strong correlations with LVEF and with parameters derived from reference imaging modalities such as cardiac magnetic resonance (CMR).[3]

CMR is considered the reference standard for the assessment of ventricular volumes, mass, and function due to its high accuracy and reproducibility. However, its high

Mailing Address: Stephany Barbosa Balaguera •
Universidad del Valle. Calle 13 # 100-00. Postal code: 760042. Cali – Colombia
E-mail: sb.balaguera@hotmail.com
Manuscript received November 27, 2025, revised manuscript February 22, 2026, accepted April 8, 2026
Editor responsible for the review: Marcelo Tavares

DOI: https://doi.org/10.36660/abcimg.20250102i

Central Illustration: Concordance Between Echocardiographic Left Ventricular Ejection Fraction by Simpson's Method, Global Longitudinal Strain, and Cardiac Magnetic Resonance

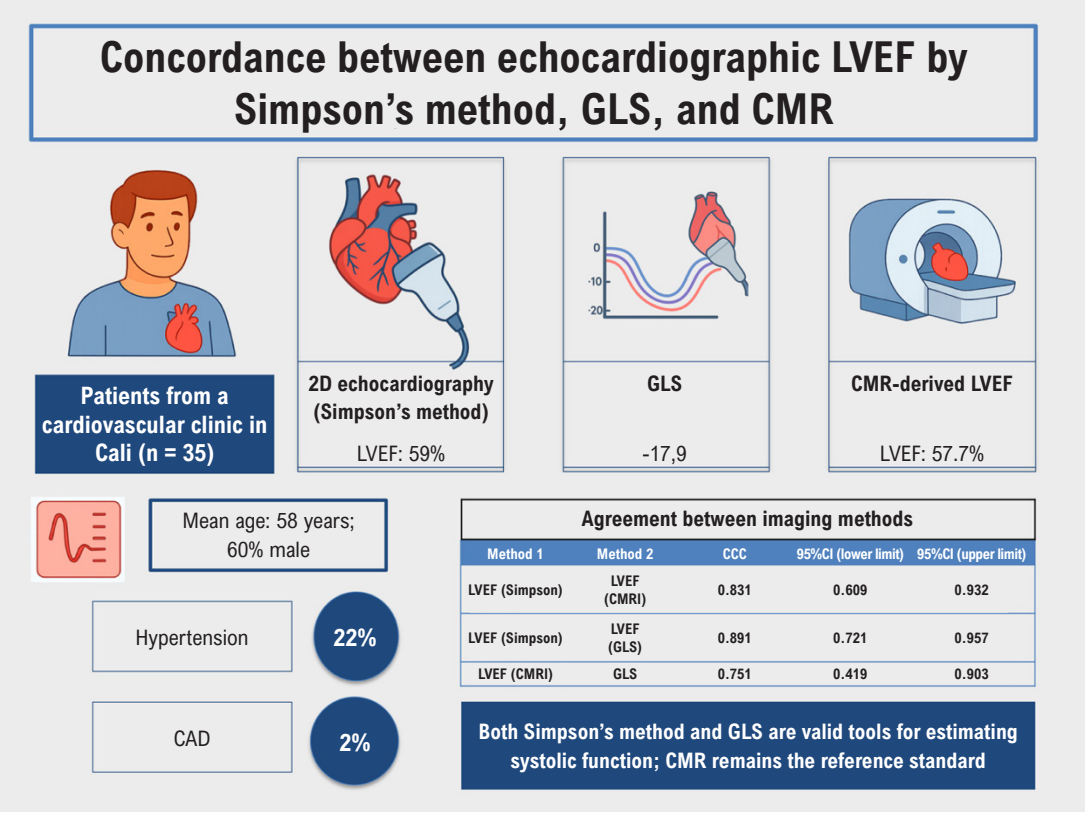

Arq Bras Cardiol: Imagem cardiovasc. 2026;39(2):e20250102

Concordance Between Echocardiographic Left Ventricular Ejection Fraction by Simpson's Method, Global Longitudinal Strain, and Cardiac Magnetic Resonance CAD: coronary artery disease; CCC: Lin's concordance correlation coefficient; CMR: cardiac magnetic resonance; GLS: global longitudinal strain; LVEF: left ventricular ejection fraction.

cost, limited availability, and restricted accessibility in middle-income countries limit its routine use. Consequently, validating echocardiographic methods against CMR within local clinical settings is essential, particularly given that echocardiography remains the cornerstone of cardiovascular diagnosis.[1]

In Colombia, cardiovascular centers have progressively incorporated advanced imaging techniques. However, regional evidence evaluating the concordance between Simpson-derived LVEF, ventricular strain parameters, and CMR-derived LVEF remains limited. Generating local data may improve diagnostic accuracy and support more effective therapeutic decision-making in patients with prevalent cardiovascular diseases.

Therefore, the present study aims to evaluate the agreement between echocardiographic LVEF obtained using the biplane Simpson method and automated volumetric analysis, and CMR-derived LVEF. Additionally, the study explores the relationship between GLS measurements and CMR-based assessment of systolic function in patients treated at a cardiovascular clinic in the city of Cali, Colombia.

Methods

Study design and population

A descriptive, analytical, cross-sectional study was conducted, including 35 patients referred for CMR for morphological assessment. Each patient also underwent a comprehensive transthoracic echocardiographic examination, including strain analysis and the determination of ventricular volumes and ejection fraction, performed within the same evaluation period.

Because of the exploratory nature of this study, the sample size was determined by convenience and included all consecutive patients who met the inclusion criteria and had complete echocardiographic and CMR data available within the predefined time frame.

The study population comprised patients aged ≥ 18 years with a confirmed diagnosis or suspected heart disease, who underwent both a complete echocardiogram and CMR within a 24-hour interval, with all required data available for analysis.

Clinical and demographic assessment

A demographic and clinical evaluation was performed, including patient characteristics, indications for imaging, and final diagnostic outcomes.

Echocardiographic assessment

Echocardiographic analyses were conducted in the echocardiography laboratory of a level IV cardiovascular clinic by cardiologists specialized in echocardiography. Imaging was performed using Philips EPIQ and Affiniti 70C systems and analyzed using the TomTec platform.

Images were acquired in three standard apical views (two-, three-, and four-chamber) to enable reconstruction of the 17-segment LV model. GLS was obtained by using 2D STE following automated endocardial border detection, with manual adjustments when necessary. GLS was calculated as the average peak systolic longitudinal strain across all 17 LV segments.

LV end-diastolic and end-systolic volumes were automatically calculated by the software based on endocardial border delineation from the apical views. LVEF was subsequently derived from these volumetric measurements according to standard echocardiographic principles. Although GLS and volumetric LVEF were obtained during the same acquisition, they represent independent measurements of myocardial deformation and ventricular volume.

The echocardiographic operator was blinded to the CMR results. Additional variables from the final echocardiographic report were also recorded.

CMR

CMR-derived strain analysis was not performed. During the study period, feature-tracking CMR strain analysis was not routinely available at our institution and therefore could not be systematically incorporated into the study protocol.

Statistical analysis

Statistical analyses were performed using RStudio version 2025.09.2+418. The normality of continuous variables was assessed using the Shapiro-Wilk test. Normally distributed variables are presented as mean ± standard deviation, whereas non-normally distributed variables are reported as median and interquartile range. Categorical variables are expressed as absolute and relative frequencies.

Agreement between LVEF measurements obtained by different imaging modalities was evaluated using Lin's concordance correlation coefficient (CCC) and Bland-Altman analysis for continuous values. Agreement between categorical classifications of LVEF severity was assessed using linear and quadratic weighted κ coefficients.

All concordance estimates are reported with 95%CIs, and a two-sided p-value < 0.05 was considered statistically significant.

Results

A total of 35 patients were included in the clinical, echocardiographic, and CMR analyses. Table 1 summarizes the demographic characteristics of the study population, the main cardiovascular conditions, and relevant paraclinical findings. Figure 1 presents the clinical indications for CMR, with dilated cardiomyopathy being the most frequent indication (29%).

Table 1 – Characteristics of the study population

Demographic and clinical data	
Variables	**Value**
Age, years (IQR)	58 (41-62.5)
Male sex, n (%)	21 (60.0)
Hypertension, n (%)	8 (22.9)
T2DM, n (%)	2 (5.7)
Dyslipidemia, n (%)	4 (11.4)
Smoking history, n (%)	3 (8.6)
Significant CAD, n (%)	1 (2.9)
MINOCA, n (%)	1 (2.9)
Myocarditis, n (%)	3 (8.6)
Laboratory data	
Variables	**Value**
Troponin, pg/mL (IQR)	0.44 (0.13-36.12)
NT-proBNP, pg/mL (IQR)	4,371 (362-5,717)

CAD: coronary artery disease; IQR: interquartile range; MINOCA: myocardial infarction with non-obstructive coronary arteries; NT-proBNP: N-terminal pro-B-type natriuretic peptide; T2DM: type 2 diabetes mellitus.

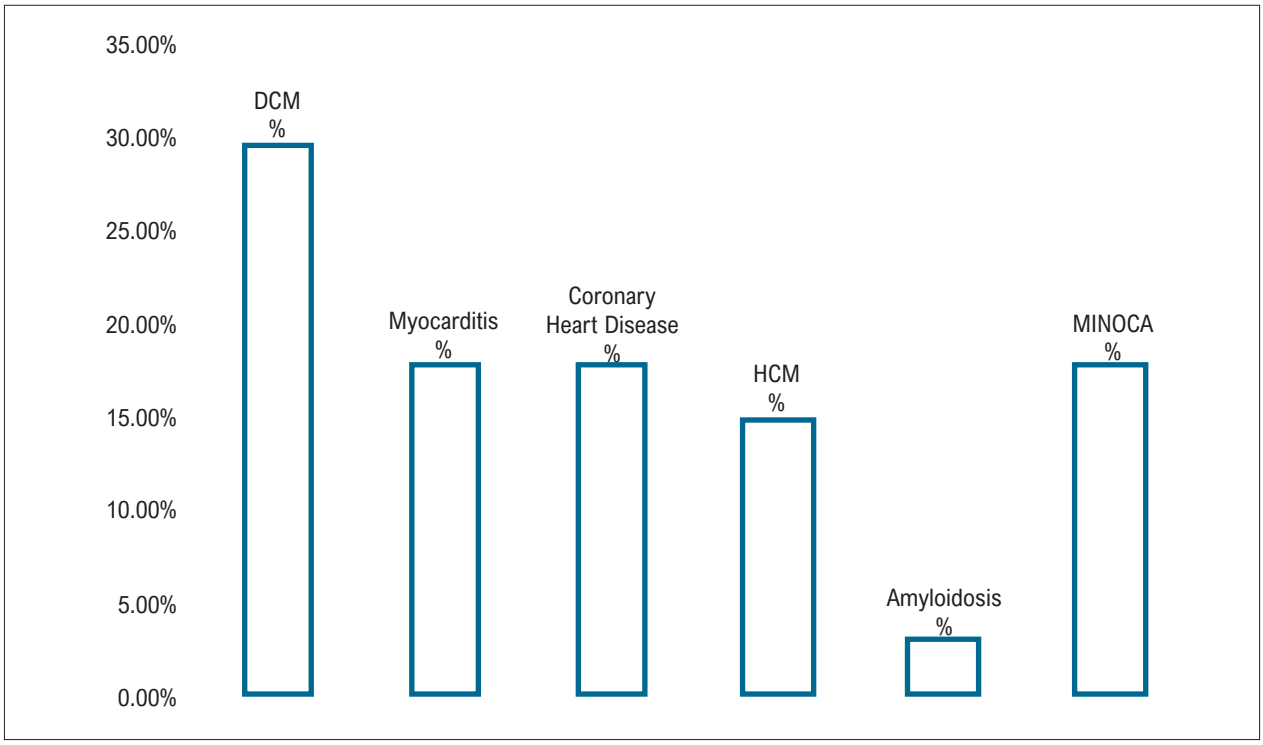

Figure 1 – *Distribution of clinical indications for CMR in the study population. CHD: coronary heart disease; DCM: dilated cardiomyopathy; HCM: hypertrophic cardiomyopathy; MINOCA: myocardial infarction with non-obstructive coronary arteries.*

Table 2 summarizes the overall echocardiographic findings. The mean interventricular septal and inferoposterior wall thicknesses were 10.1 mm and 9.6 mm, respectively. Table 2 also reports the mean and median values of key echocardiographic parameters, including ventricular dimensions in systole and diastole, as well as indices of diastolic function. In addition, the average systolic function assessed by each method evaluated in this study is presented.

In the analysis of agreement for continuous values, substantial concordance was observed among the three methods. The highest concordance was found between Simpson-derived LVEF and GLS (Table 3). Bland-Altman analysis demonstrated no evidence of systematic bias between methods. The comparison between Simpson-derived LVEF and CMR showed a minimal mean difference (MD) with acceptable limits of agreement. Similarly, GLS showed no clinically relevant systematic overestimation or underestimation when compared with CMR (Graph 1; Graph 2; Graph 3).

Regarding the categorical classification of systolic function severity, agreement was good across all comparisons (Table 4).

Central Illustration summarizes the key findings of the study.

Discussion

The assessment of LVEF remains one of the most widely used approaches for evaluating systolic function in clinical practice. Despite its central role in diagnosis and therapeutic decision-making across multiple cardiovascular conditions, the available techniques for measuring LVEF have inherent limitations that may reduce sensitivity and reproducibility.[4]

CMR is the most accurate method for measuring LVEF and is therefore considered the reference standard for comparison with other imaging modalities. Previous studies have shown that 3D echocardiography demonstrates the lowest bias when compared with CMR.[2,4] In contrast, 2D echocardiographic methods have been associated with variability of up to ± 15% relative to CMR and have been shown to misclassify approximately 9.3% of patients with cardiotoxicity identified by CMR. In the MATCH study, differences exceeding 10% between 2D and 3D LVEF measurements were observed when compared with CMR, with variability influenced by female sex and body mass index > 35 kg/m^2.[5]

In the search for methods with lower variability, myocardial strain has emerged as a robust tool for evaluating global LV function. Strain imaging has demonstrated clinical utility in the detection of subclinical dysfunction in heart failure, cardiomyopathies, valvular disease, and chemotherapy-related cardiotoxicity.[6,7] GLS also provides independent prognostic information, including mortality risk, even in cases where LVEF has limited discriminatory capacity.

In the present study, agreement among the three noninvasive methods for assessing systolic function (Simpson biplane LVEF, GLS, and CMR-derived LVEF) was good, both for continuous values and for categorical classification. According to the criteria proposed by Altman et.,[8] the concordance between Simpson-derived LVEF and GLS (CCC, 0.891), as well as between Simpson-derived LVEF and CMR (CCC, 0.831), can be considered excellent (> 0.8). In contrast, the agreement between GLS and CMR-derived LVEF (CCC, 0.751), although slightly lower, still represents good concordance.

Table 2 – Echocardiographic, strain-derived, and CMR data

Variables	Value
Echocardiographic measurements	
LVEF by Simpson, %	59 (50-61)
LV end-diastolic volume, mL	107 (42-245)
LV end-systolic volume, mL	57 (18-185)
LV end-diastolic diameter, mm	49 (37-74)
LV end-systolic diameter, mm	34 (24-65)
Septal wall thickness, mm	10 (9-10)
Posterior wall thickness, mm	
Indexed LA volume, mL/m^2	43 (19-111)
E/A ratio	1.2 (0.9-1.5)
E/e′ ratio	9 (6-17)
TAPSE, mm	22.4 ± 3.0
Segmental wall-motion abnormalities, n (%)	12 (34.3)
Strain-derived measurements	
GLS, %	−17.9 (−20.4 a −15.0)
LVEF (2D STE automated volumetric analysis), %	58.8 (21.1-73.6)
LV end-diastolic volume, mL	90.5 (53-245)
LV end-systolic volume, mL	44.8 (14-193)
CMR measurements	
LVEF by CMR, %	57.7 (47-65)
LV end-diastolic volume, mL	151.5 (89-421)
LV end-systolic volume, mL	63 (29-320)
LGE, n (%)	7 (20.0)
Myocardial edema (T2), n (%)	3 (8.6)
Pericardial effusion, n (%)	3 (8.6)

CMR: cardiac magnetic resonance; GLS: global longitudinal strain; LA: left atrium; LGE: late gadolinium enhancement; LV: left ventricle; LVEF: left ventricular ejection fraction; STE: speckle-tracking echocardiography; TAPSE: tricuspid annular plane systolic excursion.

Table 3 – Agreement between imaging methods

Method 1	Method 2	CCC	95%CI (lower limit)	95%CI (upper limit)
LVEF (Simpson)	LVEF (CMR)	0.831	0.609	0.932
LVEF (Simpson)	LVEF (GLS-derived)	0.891	0.721	0.957
LVEF (CMR)	GLS	0.751	0.419	0.903

CCC: Lin's concordance correlation coefficient; CMR: cardiac magnetic resonance; GLS: global longitudinal strain; LVEF: left ventricular ejection fraction.

Bland-Altman analysis further supports these findings. The comparison between Simpson-derived LVEF and CMR demonstrated a minimal MD (−0.07), suggesting near equivalence, albeit with relatively wide limits of agreement, reflecting interindividual variability. In contrast, GLS tended to slightly underestimate LVEF compared with CMR (MD, −1.64), with even wider limits of agreement. These findings suggest that, although GLS may underestimate LVEF relative to CMR, it maintains a strong relationship with conventional 2D measurements, supporting its role

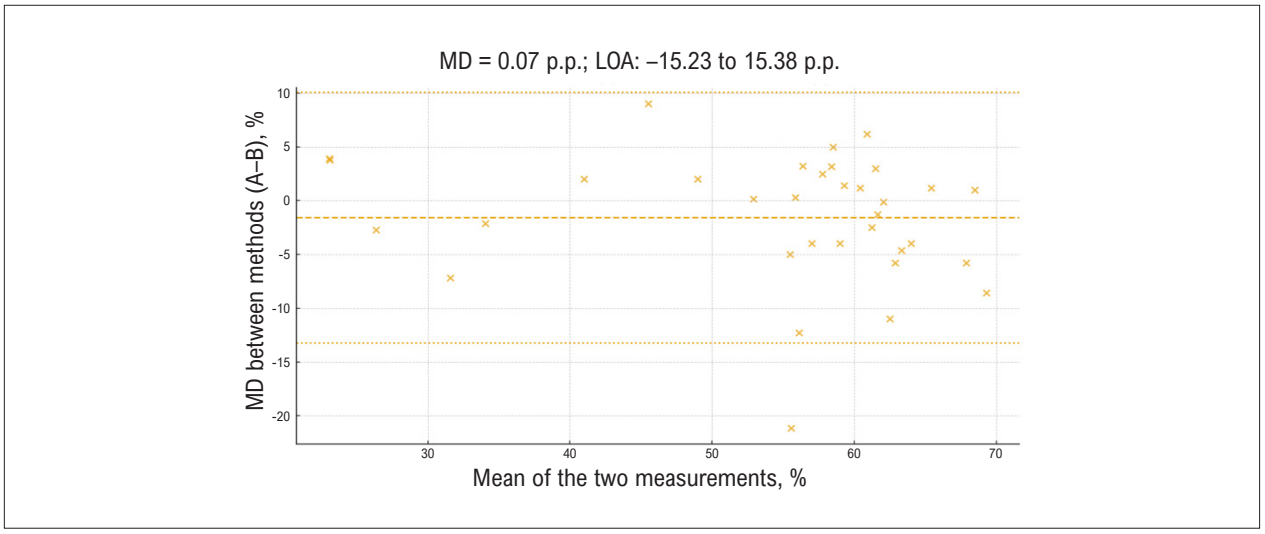

Graph 1 – *MD between LVEF measured by Simpson's method and CMR-derived LVEF. CMR: cardiac magnetic resonance; MD: mean difference; LOA: limits of agreement; LVEF: left ventricular ejection fraction.*

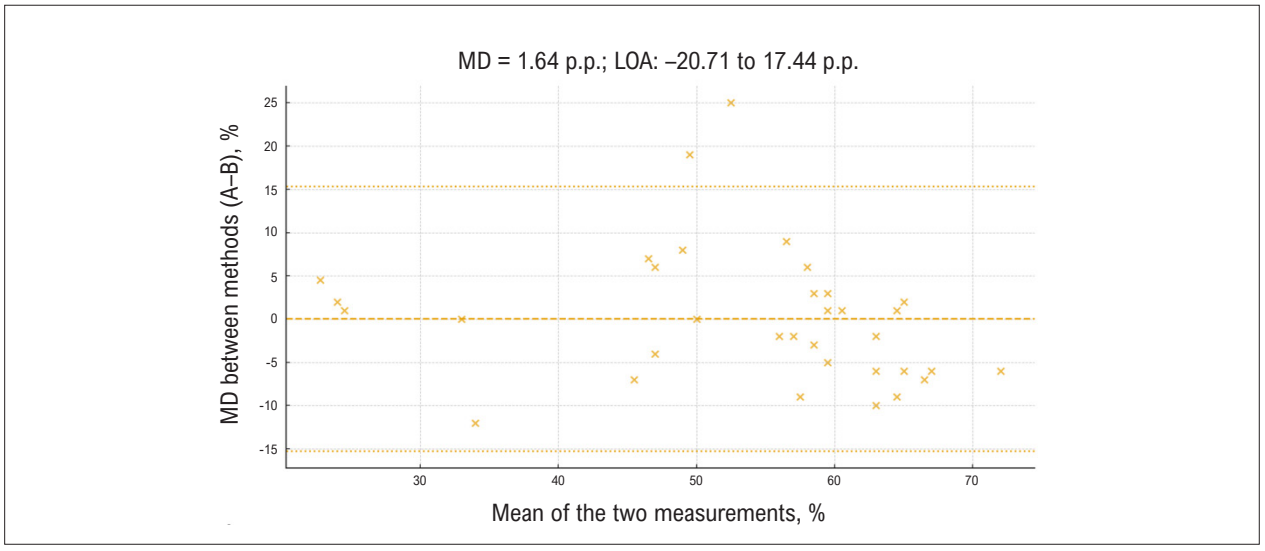

Graph 2 – *MD between GLS-derived LVEF (2D STE automated volumetric analysis) and CMR-derived LVEF. CMR: cardiac magnetic resonance; GLS: global longitudinal strain; LOA: limits of agreement; LVEF: left ventricular ejection fraction; MD: mean difference; STE: speckle-tracking echocardiography.*

as a complementary parameter rather than a substitute for volumetric assessment.

From a clinical perspective, where categorical LVEF thresholds guide diagnosis, treatment, and intervention, agreement was nearly perfect when assessed using quadratic weighted κ. Both Simpson-derived LVEF (κ = 0.808) and GLS-derived classification (κ = 0.862) showed excellent concordance with CMR, which indicates all three methods allow consistent classification of ventricular dysfunction severity.

Our findings are consistent with previous studies demonstrating good agreement between echocardiographic and CMR-derived LVEF, particularly when standardized acquisition protocols and high-quality imaging are used. However, the Bland-Altman analysis revealed relatively wide limits of agreement (approximately ± 15-20 p.p.), which may be clinically significant at the individual level. Such variability is particularly relevant when LVEF thresholds are used to guide therapeutic decisions, including eligibility for device therapy or initiation of specific pharmacological treatments. These observations reinforce the importance of interpreting LVEF within a broader clinical and imaging context rather than in isolation.

Study limitations

This study has several limitations. The relatively small sample size reduces statistical power and increases uncertainty

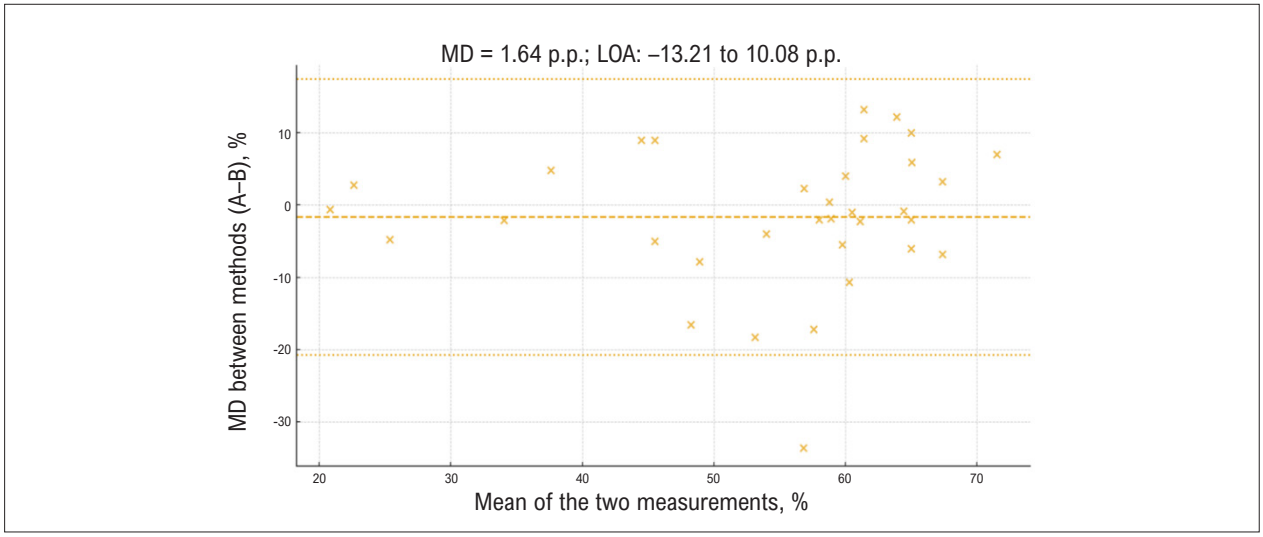

Graph 3 – *MD between LVEF measured by Simpson's method and GLS-derived LVEF (2D STE automated volumetric analysis). GLS: global longitudinal strain; LOA: limits of agreement; LVEF: left ventricular ejection fraction; MD: mean difference; STE: speckle-tracking echocardiography.*

Table 4 – Agreement between methods for categorical classification of LVEF

A) Simpson vs CMR					
LVEF (Simpson)	**Normal**	**Mild**	**Moderate**	**Severe**	**Total**
Normal	21	1	1	0	23
Mild	3	4	0	0	7
Moderate	0	0	1	0	1
Severe	0	0	1	3	4
Total	24	5	3	3	35
Quadratic weighted κ: 0.808					
95%CI: 0.743-0.874					
B) GLS vs CMR					
LVEF (GLS-derived)	**Normal**	**Mild**	**Moderate**	**Severe**	**Total**
Normal	23	2	1	0	26
Mild	1	2	0	0	3
Moderate	0	1	2	0	3
Severe	0	0	0	3	3
Total	24	5	3	3	35
Quadratic weighted κ: 0.862					
95%CI: 0.812-0.912					

CMR: cardiac magnetic resonance; GLS: global longitudinal strain; LVEF: left ventricular ejection fraction.

around concordance estimates, as reflected in the width of confidence intervals. In addition, the single-center design may limit external validity and generalizability. Therefore, the results should be interpreted as exploratory and hypothesis-generating. Larger, prospective, multicenter studies are needed to confirm the reproducibility and external applicability of these findings.

Another important limitation is the clinical heterogeneity of the study population, which included patients with diverse cardiovascular conditions. Variations in myocardial geometry,

regional wall-motion abnormalities, and tissue characteristics may influence agreement between echocardiographic and CMR measurements and may partly explain the observed variability.

Furthermore, 3D echocardiography was not included in this study. Given that 3D echocardiography has been shown to improve agreement with CMR-derived ventricular volumes and LVEF, future studies incorporating this modality may provide additional insight into the interchangeability of noninvasive imaging techniques.

Overall, these findings indicate that both Simpson's method and GLS are valid tools for estimating systolic function. GLS represents a promising complementary parameter, particularly useful for detecting subclinical dysfunction and subtle longitudinal changes. However, it should not replace volumetric assessment of LVEF. While automated volumetric analysis using 2D STE software showed good agreement with Simpson-derived LVEF, volumetric quantification remains essential in clinical scenarios requiring precision. CMR continues to be the reference standard, particularly when accurate quantification or detailed tissue characterization is required.

Conclusions

Both Simpson's method and GLS are valid tools for the assessment of systolic function, whereas CMR remains the reference standard. GLS represents a valuable complementary parameter for evaluating LVEF, particularly for the detection of subtle or subclinical dysfunction; however, it should not be considered a substitute for volumetric LVEF measurement. Further studies are warranted to compare the diagnostic performance of imaging modalities used in clinical practice for the assessment of LV systolic function.

Author Contributions

Conception and design of the research: Herrera-Escandón A, Ayala-Zapata S, Muriel-Ruiz AJ, Citelli-Ramírez JE, Osío-Jimenez LF, Benitez-Gómez LM, Ramírez-Estupiñán CJ; acquisition of data: Herrera-Escandón A, Bravo-Rueda JF, Citelli-Ramírez JE, Osío-Jimenez LF, Benitez-Gómez LM, Ramírez-Estupiñán CJ; analysis and interpretation of the data: Morales Grisales JP, Barbosa Balaguera S, Muriel-Ruiz AJ, Citelli-Ramírez JE, Osío-Jimenez LF, Ramírez-Estupiñán CJ; statistical analysis: Ayala-Zapata S; writing of the manuscript: Herrera-Escandón A, Morales Grisales JP, Ayala-Zapata S, Barbosa Balaguera S, Muriel-Ruiz AJ, Bravo-Rueda JF, Benitez-Gómez LM, Ramírez-Estupiñán CJ; Critical revision of the manuscript for intellectual content: Herrera-Escandón A, Ayala-Zapata S, Barbosa Balaguera S.

Potential Conflict of Interest

No potential conflict of interest relevant to this article was reported.

Sources of Funding

There were no external funding sources for this study.

Study Association

This study is not associated with any thesis or dissertation work.

Ethics Approval and Consent to Participate

This article does not contain any studies with human participants or animals performed by any of the authors.

Use of Artificial Intelligence

During the preparation of this work, the author(s) used ChatGPT to create images included in the Central Illustration. After using this tool/service, the author(s) reviewed and edited the content as needed and take full responsibility for the content of the published article.

Availability of Research Data

All datasets supporting the results of this study are available upon request from the corresponding author.

References

1. Rosano GMC, Teerlink JR, Kinugawa K, Bayes-Genis A, Chioncel O, Fang J, et al. The use of Left Ventricular Ejection Fraction in the Diagnosis and Management of Heart Failure. A Clinical Consensus Statement of the Heart Failure Association (HFA) of the ESC, the Heart Failure Society of America (HFSA), and the Japanese Heart Failure Society (JHFS). Eur J Heart Fail. 2025;27(7):1174-87. doi: 10.1002/ejhf.3646.
2. Konstam MA, Abboud FM. Ejection Fraction: Misunderstood and Overrated (Changing the Paradigm in Categorizing Heart Failure). Circulation. 2017;135(8):717-9. doi: 10.1161/CIRCULATIONAHA.116.025795.
3. Lang RM, Badano LP, Mor-Avi V, Afilalo J, Armstrong A, Ernande L, et al. Recommendations for Cardiac Chamber Quantification by Echocardiography in Adults: An Update from the American Society of Echocardiography and the European Association of Cardiovascular Imaging. J Am Soc Echocardiogr. 2015;28(1):1-39.e14. doi: 10.1016/j.echo.2014.10.003.
4. Nazir MS, Okafor J, Murphy T, Andres MS, Ramalingham S, Rosen SD, et al. Echocardiography versus Cardiac MRI for Measurement of Left Ventricular Ejection Fraction in Individuals with Cancer and Suspected Cardiotoxicity. Radiol Cardiothorac Imaging. 2024;6(1):e230048. doi: 10.1148/ryct.230048.
5. Wenzel JP, Albrecht JN, Toprak B, Petersen E, Nikorowitsch J, Cavus E, et al. Head-to-Head Comparison of Cardiac Magnetic Resonance Imaging and Transthoracic Echocardiography in the General Population (MATCH). Clin Res Cardiol. 2025. doi: 10.1007/s00392-025-02660-1.
6. Thomas JD, Edvardsen T, Abraham T, Appadurai V, Badano L, Banchs J, et al. Clinical Applications of Strain Echocardiography: A Clinical Consensus Statement from the American Society of Echocardiography Developed in Collaboration with the European Association of Cardiovascular Imaging of the European Society of Cardiology. J Am Soc Echocardiogr. 2025;38(11):985-1020. doi: 10.1016/j.echo.2025.07.007.

7. Marwick TH, Gillebert TC, Aurigemma G, Chirinos J, Derumeaux G, Galderisi M, et al. Recommendations on the Use of Echocardiography in Adult Hypertension: A Report from the European Association of Cardiovascular Imaging (EACVI) and the American Society of Echocardiography (ASE)†. Eur Heart J Cardiovasc Imaging. 2015;16(6):577-605. doi: 10.1093/ehjci/jev076.

8. Altman DG. Practical Statistics for Medical Research. London: Chapman and Hall; 1991.

Beyond Ejection Fraction: Integrating Myocardial Strain and Cardiac Magnetic Resonance into the Contemporary Assessment of Left Ventricular Function

Marly Uellendahl[1,2]

Universidade Federal de São Paulo (UNIFESP),[1] *São Paulo, SP – Brazil*

DASA – Diagnósticos da América S.A.,[2] *São Paulo, SP – Brazil*

Short Editorial related to the article: Concordance Between Echocardiographic Left Ventricular Ejection Fraction by Simpson's Method, Global Longitudinal Strain, and Cardiac Magnetic Resonance

The assessment of left ventricular function is undergoing a profound transformation. For decades, left ventricular ejection fraction (LVEF) has occupied a central role in clinical practice, guiding diagnosis, risk stratification, and therapeutic decision-making across a broad spectrum of cardiovascular diseases. Its extensive clinical validation, ease of acquisition, and reproducibility have established two-dimensional echocardiography as the first-line modality for evaluating left ventricular systolic function.[1,2]

However, advances in cardiovascular imaging have demonstrated that myocardial function cannot be fully characterized by a single volumetric parameter. Although LVEF remains a robust marker of global left ventricular performance, its dependence on loading conditions and its limited sensitivity for detecting early contractile abnormalities underscore the need for a more comprehensive functional assessment.

In this context, the incorporation of myocardial deformation imaging through global longitudinal strain (GLS) represents one of the most significant advances in echocardiography over the past two decades. By directly quantifying the deformation of longitudinal myocardial fibers, which are predominantly located within the subendocardial layer, GLS enables the detection of myocardial dysfunction before reductions in LVEF become apparent.[3] Consequently, its use enhances diagnostic sensitivity, improves risk stratification, and provides incremental prognostic information across a wide range of cardiovascular diseases.

Concurrently, cardiac magnetic resonance (CMR) has become the reference standard for the quantification of ventricular volumes and systolic function owing to its high accuracy, excellent spatial resolution, superior reproducibility, and independence from the acoustic window limitations inherent to echocardiography.[4] Furthermore, its unique ability to characterize myocardial tissue has substantially expanded our understanding of the pathophysiological mechanisms underlying cardiovascular diseases, strengthening its role in the multimodality assessment of cardiac structure and function.

This technological evolution has fundamentally reshaped the paradigm of cardiovascular imaging. The contemporary objective is no longer to identify a single marker capable of summarizing the complexity of ventricular function, but rather to integrate complementary information obtained from different imaging modalities, each reflecting distinct aspects of myocardial mechanics. From this perspective, LVEF, GLS, and CMR should not be viewed as competing techniques; instead, they provide complementary information that, when interpreted together, allows a more accurate and comprehensive evaluation of ventricular performance.

It is within this framework that the study published in this issue of the journal should be interpreted. By evaluating the agreement between LVEF measured by the Simpson biplane method, GLS, and ventricular function assessed by CMR, the authors address a clinically relevant question: to what extent can different imaging modalities be considered equivalent for the assessment of left ventricular function?

More importantly than simply comparing diagnostic techniques, the study highlights an aspect that is often overlooked in the literature: the distinction between correlation and agreement. In method-comparison studies, a high correlation coefficient does not necessarily imply clinical equivalence. Accordingly, the authors should be commended for their methodological approach, which includes Lin's concordance correlation coefficient, Bland–Altman analysis, and weighted kappa statistics, all of which provide a more robust assessment of agreement between different imaging techniques.[5]

The results demonstrated good agreement between LVEF measured by two-dimensional echocardiography and that obtained by CMR, as well as substantial agreement between GLS-derived parameters and CMR-based functional assessment. In addition, strong agreement was observed between measurements obtained using the Simpson biplane method and those derived from myocardial deformation analysis, reinforcing both the robustness of conventional echocardiography and the incremental value of strain imaging in the characterization of ventricular function.

Perhaps the study's most important contribution, however, lies not in demonstrating high statistical agreement among the different methods, but rather in showing that

Keywords

Stroke Volume; Left Ventricular Dysfunction; Magnetic Resonance Imaging

Mailing Address: Marly Uellendahl •
UNIFESP. Alameda Vale da Mantiqueira, 204. Postal Code: 06532-016. Santana de Parnaíba, SP – Brazil
E-mail: mauellendahl@gmail.com

DOI: https://doi.org/10.36660/abcimg.20260087i

statistical agreement should not be interpreted as clinical interchangeability. Although concordance coefficients were high, Bland–Altman analyses revealed relatively wide limits of agreement between the imaging modalities. This finding has important practical implications, particularly when therapeutic decisions rely on specific LVEF thresholds or when small serial changes may influence the interpretation of disease progression in patients with heart failure.

Likewise, the study reinforces a concept that has become increasingly well established in the literature: GLS should not be regarded as a substitute for LVEF. Rather, these parameters reflect distinct physiological dimensions of ventricular function and respond to different mechanisms of myocardial adaptation. Whereas LVEF primarily represents the global volumetric performance of the left ventricle, GLS directly quantifies the longitudinal deformation of subendocardial fibers, which are often affected during the earliest stages of several cardiovascular diseases.[3] The integrated interpretation of these parameters provides a more comprehensive and biologically meaningful characterization of ventricular function than either measurement alone.

From this perspective, the growing interest in strain imaging should not be interpreted as an attempt to replace LVEF, but rather as the incorporation of a functional biomarker that complements its interpretation. This concept is particularly relevant in clinical settings in which LVEF remains preserved despite the presence of early myocardial abnormalities, including cancer therapy-related cardiotoxicity, valvular heart disease, infiltrative cardiomyopathies, and heart failure with preserved ejection fraction. The integration of these complementary parameters enhances diagnostic sensitivity and contributes to more refined risk stratification.

Another noteworthy aspect of this study is its pragmatic design. By including patients with a broad spectrum of cardiovascular conditions, the investigators reproduced the heterogeneity routinely encountered in clinical practice. Although this diversity may increase variability among imaging methods, it also strengthens the external validity of the findings, making them more representative of the challenges faced by cardiovascular imaging specialists in daily practice.

Naturally, several limitations should be acknowledged. The relatively small sample size, single-center design, absence of three-dimensional echocardiography, and lack of feature-tracking strain analysis by CMR partially limit the generalizability of the results. Nevertheless, these limitations do not diminish the study's scientific relevance. On the contrary, they highlight the need for larger multicenter investigations capable of integrating different imaging modalities into more comprehensive models of functional assessment and clinical validation.

The future of cardiovascular imaging will likely not be defined by the replacement of one modality with another. Rather, true progress lies in the integration of complementary information that more faithfully reflects the complexity of ventricular mechanics. Echocardiography, myocardial deformation imaging, and CMR should be regarded as synergistic tools, each providing unique insights that contribute to a more comprehensive characterization of myocardial structure, function, and pathophysiology.

Rather than debating which imaging modality should occupy the central role in the assessment of left ventricular function, contemporary cardiology increasingly recognizes that no single biomarker can fully capture the complexity of myocardial performance. The future of cardiovascular imaging lies in the rational integration of complementary diagnostic modalities, leveraging the strengths of each technique to provide a more accurate, individualized, and clinically meaningful evaluation.

From this perspective, the study discussed in this issue reinforces a paradigm that is becoming firmly established in clinical practice: LVEF remains indispensable; GLS provides important incremental value; and CMR continues to represent the reference standard for ventricular quantification. The integration of these complementary tools, rather than the replacement of one with another, represents the natural path toward a truly contemporary assessment of left ventricular function.

References

1. Herrera-Escandón A, Morales-Grisales JP, Ayala-Zapata S, Barbosa-Balaguera S, Muriel-Ruiz AJ, Bravo-Rueda JF, et al. Concordância Entre a Fração de Ejeção do Ventrículo Esquerdo por Ecocardiografia pelo Método de Simpson, o Strain Longitudinal Global e a Ressonância Magnética Cardíaca. Arq Bras Cardiol: Imagem Cardiovasc. 2026;39(2):e20250102. doi: 10.36660/abcimg.20250102.

2. Lang RM, Badano LP, Mor-Avi V, Afilalo J, Armstrong A, Ernande L, et al. Recommendations for Cardiac Chamber Quantification by Echocardiography in Adults: An Update from the American Society of Echocardiography and the European Association of Cardiovascular Imaging. J Am Soc Echocardiogr. 2015;28(1):1-39.e14. doi: 10.1016/j.echo.2014.10.003.

3. Smiseth OA, Torp H, Opdahl A, Haugaa KH, Urheim S. Myocardial Strain Imaging: How Useful Is It In Clinical Decision Making? Eur Heart J. 2016;37(15):1196-207. doi: 10.1093/eurheartj/ehv529.

4. Kramer CM, Barkhausen J, Bucciarelli-Ducci C, Flamm SD, Kim RJ, Nagel E. Standardized Cardiovascular Magnetic Resonance Imaging (CMR) Protocols: 2020 Update. J Cardiovasc Magn Reson. 2020;22(1):17. doi: 10.1186/s12968-020-00607-1.

5. Bland JM, Altman DG. Statistical Methods for Assessing Agreement between Two Methods of Clinical Measurement. Lancet. 1986;1(8476):307-10.

Major Depressive Disorder and Quality of Life in Patients With Coronary Artery Disease Assessed by Myocardial Perfusion Imaging

Guilherme Gonçais Lopes Almeida,[1] Gustavo B. Barbirato,[1] Valéria de Queiroz Pagnin,[1] Daniel Pagnin,[1] Cláudio Tinoco Mesquita[1,2,3,4]

Universidade Federal Fluminense,[1] Niterói, RJ – Brazil
Hospital Pró-Cardíaco,[2] Rio de Janeiro, RJ – Brazil
Hospital Samaritano,[3] Rio de Janeiro, RJ – Brazil
Americas Medical City,[4] Rio de Janeiro, RJ – Brazil

Abstract

Background: Major depressive disorder (MDD) may negatively influence cardiovascular prognosis, increasing the morbidity and mortality of patients with coronary artery disease (CAD). Thus, the psychometric assessment of these individuals may contribute to understanding how mental health impacts the pathophysiology of myocardial ischemia.

Objective: To evaluate the prevalence of MDD in patients with CAD undergoing stress and rest myocardial perfusion imaging (MPI) using the psychometric instrument Patient Health Questionnaire-9 (PHQ-9). As secondary objectives, to correlate quality of life (QoL) data obtained using the 12-Item Short Form Survey (SF-12) and Positive and Negative Affect Schedule (PANAS) instruments with the presence or absence of myocardial ischemia detected by MPI.

Methods: The SF-12, PHQ-9, and PANAS questionnaires were administered to 120 consecutive patients referred for MPI for CAD evaluation. The prevalence of MDD was assessed, and the results were correlated with MPI findings and QoL scale scores.

Results: A high prevalence of MDD was identified (58 cases; 48.3%), with no association with risk factors, age, or MPI findings. A significant rate of suicidal ideation was observed among the evaluated patients (15 cases; 12.5%), in addition to reduced QoL in 88.3% of patients (n = 106), with scores below 50 on the physical SF-12, and in 65% (n = 78), with scores below 50 on the mental SF-12, indicating poor perceived mental health.

Conclusion: These findings reinforce the need for a multidisciplinary approach in the management of patients with suspected CAD, including systematic mental health assessment, given the opportunities to improve outcomes during patient interactions with the health care system.

Keywords: Major Depressive Disorder; Quality of Life; Myocardial Ischemia.

Introduction

Coronary artery disease (CAD) is the leading cause of death and disability in the United States and in developed Western countries. Approximately every 40 seconds, an individual experiences an acute myocardial infarction (AMI), with an estimated 720,000 new acute coronary events occurring annually.[1] In 2021, CAD remained the leading cause of death worldwide, accounting for approximately 9.44 million deaths.[2] In Brazil, 2021 data demonstrated an age-standardized CAD mortality rate of 67.1 per 100,000 inhabitants.[3]

Major depressive disorder (MDD) is associated with significant levels of disability and suffering for both patients and their families,[4] and its appropriate treatment may contribute to restoring quality of life (QoL) and promoting well-being.[5]

Studies conducted in different care settings involving patients with CAD have demonstrated that fewer than half of individuals diagnosed with mental disorders had been previously identified and, among those diagnosed, only a proportion received specialized treatment with a psychiatrist or psychotherapy.[6]

MDD is a multifactorial condition capable of causing relevant physiological alterations. In myocardial perfusion imaging (MPI), some studies suggest the presence of reversible perfusion defects in patients with MDD, which may indicate episodes of transient myocardial ischemia.[7]

This study was based on the hypothesis that correlations exist between MDD symptoms and the main parameters obtained from stress and rest MPI. The primary objective

Mailing Address: Guilherme Gonçais •
Universidade Federal Fluminense. Av Marquês do Paraná, 303. Postal code: 24220-900. Centro, Niterói, RJ – Brazil
E-mail: guilhermegoncais@id.uff.br
Manuscript received April 6, 2025, revised manuscript April 6, 2026, accepted April 25, 2026
Editor responsible for the review: Marcelo Tavares

DOI: https://doi.org/10.36660/abcimg.20260048i

Central Illustration: Major Depressive Disorder and Quality of Life in Patients With Coronary Artery Disease Assessed by Myocardial Perfusion Imaging

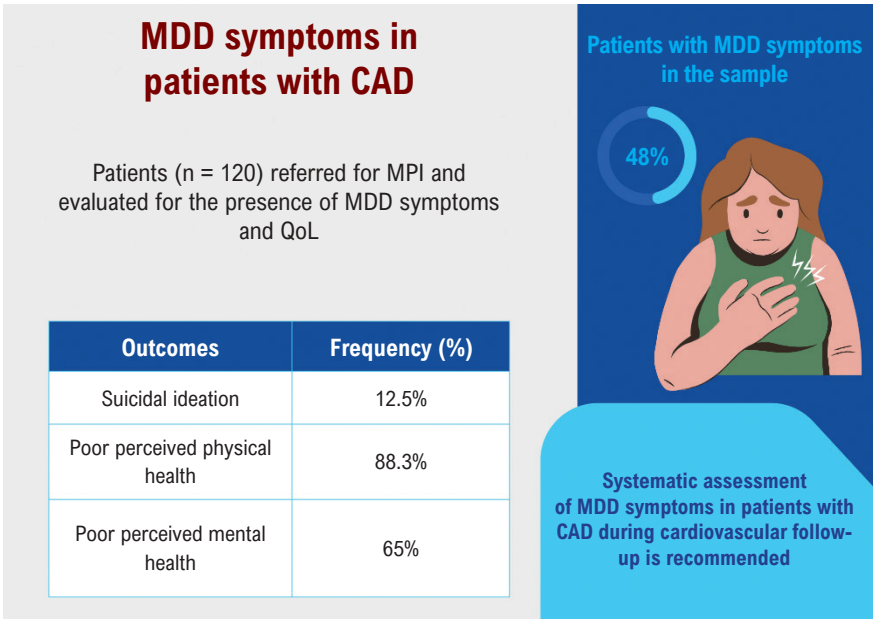

Arq Bras Cardiol: Imagem cardiovasc. 2026;39(2):e20260048

Major Depressive Disorder and Quality of Life in Patients With Coronary Artery Disease Assessed by Myocardial Perfusion Imaging. CAD: coronary artery disease; MDD: major depressive disorder; MPI: myocardial perfusion imaging; QoL: quality of life.

was to identify the prevalence of MDD in patients referred for cardiovascular evaluation at a federal university hospital through the application of validated psychometric instruments. Additionally, the study aimed to evaluate the prevalence of MDD symptoms using the Patient Health Questionnaire-9 (PHQ-9) in individuals undergoing stress and rest MPI as well as to correlate these symptoms with QoL scores obtained using the 12-Item Short Form Survey (SF-12) and Positive and Negative Affect Schedule (PANAS) instruments, according to the presence or absence of myocardial ischemia.

Associations between MDD symptoms and the main parameters obtained from stress and rest MPI were also investigated to provide an integrated understanding of the interaction between mental health, QoL, and cardiac perfusion abnormalities in this population.

Methods

Study design and population

This was a cross-sectional, observational, prospective analysis based on a primary quantitative database derived from a study conducted at a federal university hospital. Data were collected through structured interviews with closed-ended questions and the application of 3 instruments validated for use nationwide.

The sample was obtained by convenience sampling and included 120 consecutive adult patients undergoing MPI for CAD investigation at the university hospital. Data collection was performed between December 2018 and January 2019.

Information regarding sex, age, and history of systemic arterial hypertension, diabetes mellitus, obesity, dyslipidemia, family history of CAD, menopause, AMI, coronary artery bypass graft surgery, angioplasty with stent implantation, stroke, chronic kidney disease, aortic aneurysm, and vascular disease was collected from medical records.

Data regarding mental health assessment instruments, including SF-12, PHQ-9, and PANAS, as well as parameters obtained from MPI, were also collected. Statistical analysis sought to correlate MPI findings, such as the presence of ischemia, left ventricular ejection fraction (LVEF), and ventricular volumes, with MDD symptoms assessed using psychometric questionnaires.

The study complied with current ethical requirements and was approved by a human research ethics committee under CAAE 89721625.0.0000.5243.

Psychiatric and QoL assessment

The PHQ-9,[8] PANAS,[9] and SF-12[10] scales were used to assess psychiatric symptoms. PHQ-9 was employed to evaluate MDD symptoms, whereas PANAS and SF-12 were used to assess QoL and emotional aspects.

PHQ-9

PHQ-9 is used for MDD diagnosis and symptom severity stratification.[11] The instrument contains nine questions based on the diagnostic criteria of the Diagnostic and Statistical Manual of Mental Disorders, fifth edition.

Each item includes the following response options: "not at all," "less than 1 week," "1 week or more," and "nearly every day," corresponding to scores of 0, 1, 2, and 3, respectively. The total score ranges from 0 to 27 points and is classified as follows: i) absence of MDD (0-4 points); ii) mild MDD (5-9 points); iii) moderate MDD (10-14 points); iv) moderately severe MDD (15-19 points); and v) severe MDD (20-27 points).

PANAS

PANAS evaluates two dimensions of individuals' emotional state: positive affect and negative affect.[12] The instrument consists of 20 items distributed across two subscales with 10 questions each, one focused on positive emotions and the other on negative emotions.

Responses range from 1 ("very rarely or never") to 5 ("very frequently or always"). Results were calculated using the application recommended by the investigators responsible for validation of the instrument. Final scores range from 10 to 50 points, with higher values indicating greater intensity of positive or negative emotions.

12-Item Short Form Health Survey

SF-12 is a shortened version translated and validated into Portuguese from the 36-Item Short Form Survey (SF-36).[10] It is a more objective instrument for assessing health-related QoL.

SF-12 consists of 12 items distributed across eight domains grouped into two main components: i) the physical component, which includes functional capacity, physical aspects, pain, and general health status; and ii) the mental component, related to mental health, emotional aspects, social aspects, and vitality.

SF-12 has a final score ranging from 0 to 100, in which 0 represents the worst general health status and 100 the best health status. It demonstrates performance similar to that of SF-36 in the assessment of health-related QoL and is widely documented medical literature, both in its original English version and in versions validated for different languages.

MPI acquisition and analysis

MPI examinations were performed using a single-detector gamma camera (Millenium MPR, GE HealthCare) equipped with a low-energy, high-resolution collimator. Tomographic images were acquired by single-photon emission computed tomography (SPECT), electrocardiogram-gated, using 64 projections and a 64 × 64 matrix.

After acquisition, images were reconstructed by filtered back projection using a Butterworth filter and processed using the e-Soft software, including the Cedars-Sinai and Emory Cardiac Toolbox packages. Global and segmental contractility analysis, as well as LVEF assessment, were performed by gated SPECT. The adopted myocardial segmentation model consisted of 17 segments.

The analyzed MPI variables included the presence of ischemia, defined as an area of radiotracer hypouptake on post-stress images with normalization on rest images, and the presence of fibrosis, defined as an area of persistent hypouptake on both post-stress and rest images. Post-stress and rest LVEF, as well as ventricular volumes under both conditions, were also evaluated.

Statistical analysis

Descriptive analysis was presented in tables, with categorical variables expressed as absolute and relative frequencies (%), and numerical variables presented using appropriate measures of central tendency and dispersion.

Inferential analysis included the following methods: the relationship between numerical MPI parameters and PHQ-9, SF-12, and PANAS scale scores, as well as other numerical variables, was evaluated using Spearman's correlation coefficient. Associations involving categorical variables were analyzed using the Mann-Whitney or Kruskal-Wallis tests. Comparisons between the presence of ischemia on MPI and numerical variables were performed using the Mann-Whitney *U* test, whereas associations with categorical variables were assessed using the chi-square test.

Data distribution normality was verified using the Shapiro-Wilk test and graphical inspection of histograms. Statistical analyses were performed using IBM SPSS Statistics for Windows, version 26 (IBM Corp., Armonk, N.Y., USA). Statistical significance was set at 5%.

The analyzed numerical variables did not demonstrate a normal (Gaussian) distribution, as shown by the Shapiro-Wilk test and graphical evaluation of histograms. Therefore, data were summarized using median and interquartile range (Q1-Q3), corresponding to the central 50% of observations between the first and third quartiles. The interquartile range was used as the measure of dispersion associated with the median, analogous to the use of standard deviation in relation to the mean.

Results

The overall profile of the 120 patients included in the study was described using numerical and categorical variables in the total sample. Numerical variables were presented using appropriate measures of central tendency and dispersion, whereas categorical variables were expressed as absolute and relative frequencies (%).

Table 1 presents the characterization of the analyzed demographic and clinical variables, including median, interquartile range (Q1-Q3), and statistical analysis of differences between groups classified according to PHQ-9 results. No statistically significant differences were observed among the analyzed variables when comparing patients with moderate/severe MDD and those with minimal/mild MDD.

Patients had a median age of 62 years and were predominantly female. Arterial hypertension was the most frequent comorbidity, identified in 82% of the sample. Among

Table 1 – Demographic and clinical characteristics of patients according to PHQ-9 results

Variable	Moderately severe/Severe MDD (n and %)	Minimal/Moderate MDD (n and %)	p-value
Age (years) – median (Q1-Q3)	61 (55-66)	63 (58-66)	0.290
Male sex	21 (36.2%)	25 (40.3%)	0.640
Female sex	37 (63.8%)	37 (59.7%)	0.640
Family income (R$) – median (Q1-Q3)	890 (784-1,700)	1,474 (818-2,000)	0.062
Hypertension	38 (80.9%)	44 (83.0%)	0.780
DM	20 (43.5%)	15 (28.3%)	0.120
Smoking	7 (14.9%)	6 (9.6%)	0.420
Obesity	14 (29.8%)	8 (15.1%)	0.070
Dyslipidemia	21 (44.7%)	20 (37.7%)	0.370
FH	23 (48.9%)	18 (39.1%)	0.090
Menopause	25 (53.2%)	23 (43.4%)	0.420
Previous CAD	12 (25.5%)	15 (32.6%)	0.520
AMI	8 (17.0%)	9 (17.0%)	0.960
CABG	4 (8.5%)	5 (9.4%)	0.580
PTCA	6 (12.8%)	10 (21.3%)	0.190
CABG or PTCA	10 (21.3%)	14 (26.4%)	0.550

AMI: acute myocardial infarction; CABG: coronary artery bypass graft surgery; CAD: coronary artery disease; DM: diabetes mellitus; FH: Coronary artery disease family history; MDD: major depressive disorder; PHQ-9: Patient Health Questionnaire-9; PTCA: percutaneous transluminal coronary angioplasty.

women, 48 were postmenopausal, and 44% of participants were smokers or had a history of tobacco use.

MDD was identified in a substantial number of patients: 58 individuals (48%) presented moderately severe/severe MDD. Among these patients, 15 (12.5%) reported suicidal ideation.

Correlation analysis was performed between MPI parameters, age, and scores from the PHQ-9, PANAS, and SF-12 instruments. Table 2 presents Spearman's correlation coefficient (r), the respective p values, and the number of cases included in each analysis involving MPI parameters, age, and psychometric scale scores.

No correlation was observed between post-stress LVEF and PHQ-9, PANAS, and SF-12 scores. Although patients demonstrated poor perceived physical and mental health, there was no direct relationship between these findings and the severity of MPI results.

A significant inverse correlation was observed between resting end-diastolic volume (REDV) and age ($r = -0.225$; $p = 0.013$; $n = 120$), indicating that older age was associated with lower REDV values in the analyzed sample. No statistically significant correlations, at the 5% level, were identified between the remaining MPI parameters and PHQ-9, SF-12, and PANAS scale scores.

Table 3 presents the description of MPI parameters according to score classifications as well as the respective p values obtained from statistical tests. MPI variables were expressed as median and interquartile range (Q1-Q3) and compared using the Mann-Whitney test when two groups were present and the Kruskal-Wallis test when 3 or more groups were analyzed.

When analyzing the relationship between PHQ-9 scores and MPI parameters, no statistically significant correlations were identified.

Table 4 presents the distribution of PHQ-9 and SF-12 score classifications according to the presence or absence of ischemia on MPI as well as the respective p values obtained from statistical tests. Score classifications were expressed as absolute (n) and relative (%) frequencies and compared using the chi-square test.

No statistically significant association at the 5% level was observed between PHQ-9 and SF-12 score classifications and the presence of ischemia on MPI.

Discussion

The present study demonstrated a finding of high clinical relevance: 48% of patients referred for evaluation by MPI presented symptoms compatible with moderate to severe MDD according to the PHQ-9 score. Because of the high prevalence of MDD symptoms observed in the studied population, we believe that systematic assessment of these symptoms in patients referred for CAD investigation is essential, allowing early detection and appropriate management of this condition (Central Illustration).

Table 2 – Correlation between MPI parameters, age, and PHQ-9, SF-12, and PANAS scores

Variable	Parameter	Post-stress LVEF	Rest LVEF	Post-stress EDV	Rest EDV	Post-stress ESV	Rest ESV
Age (years)	r	0.097	0.069	−0.171	−0.225	−0.134	−0.126
	p	0.29	0.46	0.061	0.013	0.14	0.17
	n	120	120	120	120	120	120
PHQ-9 score (depression)	r	0.118	0.109	0.06	0.021	−0.054	−0.048
	p	0.20	0.24	0.51	0.82	0.58	0.60
	n	120	120	120	120	120	120
SF-12 PCS score	r	−0.003	−0.084	−0.039	0.074	0.001	0.075
	p	0.98	0.36	0.67	0.42	0.99	0.42
	n	120	120	120	120	120	120
SF-12 MCS score	r	0.034	0.064	−0.034	−0.020	−0.026	−0.047
	p	0.71	0.49	0.71	0.83	0.78	0.61
	n	120	120	120	120	120	120
Positive PANAS score	r	−0.033	−0.114	0.076	0.041	0.053	0.121
	p	0.72	0.22	0.41	0.65	0.56	0.19
	n	119	119	119	119	119	119
Negative PANAS score	r	−0.093	−0.121	0.160	0.082	0.100	0.090
	p	0.31	0.19	0.08	0.38	0.28	0.33
	n	119	119	119	119	119	119

EDV: end-diastolic volume; ESV: end-systolic volume; LVEF: left ventricular ejection fraction; MCS: Mental Component Summary; MPI: myocardial perfusion imaging; PANAS: Positive and Negative Affect Schedule; PCS: Physical Component Summary; PHQ-9: Patient Health Questionnaire-9; SF-12: 12-Item Short Form Health Survey.

Despite the high prevalence of MDD symptoms, no correlations were identified between MDD scores, QoL indices, and parameters obtained from MPI. No association was observed between MPI abnormalities and greater burden of MDD symptoms. Therefore, MPI did not prove to be an effective marker of cardiovascular severity in patients with MDD symptoms.

When comparing our results with Brazilian population-based data, the prevalence of moderately severe/severe MDD found in our sample (48%) was substantially higher than that reported in large national studies. In an epidemiological survey involving 49,658 Brazilian adults[3] and based on PHQ-9, only 10.5% of individuals presented clinically relevant MDD, defined by a score ≥ 10, a significantly lower value than that identified in our clinical population.

Furthermore, although the population-based study demonstrated an unfavorable impact of MDD on cardiovascular health, reducing by 27% the likelihood of an individual presenting favorable cardiovascular health (odds ratio, 0.73; 95%CI, 0.62-0.86), no prevalence of MDD as high as that observed in our health care setting was identified. These contrasts suggest that patients with suspected or established CAD treated in an outpatient public health care setting present greater emotional and psychological burden, possibly influenced by factors such as recurrent chest pain, fear of future cardiovascular events, functional limitation, and uncertainty regarding prognosis.[13]

In addition, pathophysiological mechanisms related to the interaction between chronic inflammation, oxidative stress, and neuroendocrine activation in ischemic disease may contribute to this scenario.[14] Thus, the nearly 4-fold higher prevalence of moderately severe/severe MDD observed in our cohort reinforces the hypothesis that individuals with CAD constitute a group with high psychosocial vulnerability, requiring systematic screening and integrated cardiometabolic and mental health management strategies.

Several studies have described physiological mechanisms supporting the relationship between MDD and cardiovascular disease. Activation of the hypothalamic-pituitary-adrenal axis in individuals with MDD promotes increased glucocorticoid secretion, associated with peripheral insulin resistance, hyperglycemia, and elevated blood pressure, all recognized cardiovascular risk factors.[15]

Increased glucocorticoid levels are also associated with greater secretion of proinflammatory interleukins, such as interleukin-6 and tumor necrosis factor-alpha. This exacerbated inflammatory response is associated with the risk

Table 3 – Ventricular function variables obtained by MPI and their comparison according to PHQ-9 score classification

Variable	PHQ-9 classification (MDD)	n	Median	IQR	p-value
Post-stress LVEF	Minimal	32	65	52-76	0.47
	Mild/Moderate	53	63	51-73	
	Moderately severe/Severe	35	68	58-75	
Rest LVEF	Minimal	32	61	53-75	0.80
	Mild/Moderate	53	67	55-76	
	Moderately severe/Severe	35	69	60-75	
Post-stress EDV	Minimal	32	55	41-78	0.20
	Mild/Moderate	53	65	52-90	
	Moderately severe/Severe	35	62	51-77	
Rest EDV	Minimal	32	63	46-100	0.86
	Mild/Moderate	53	67	49-85	
	Moderately severe/Severe	35	66	55-85	
Post-stress ESV	Minimal	32	19	10-37	0.52
	Mild/Moderate	53	26	14-38	
	Moderately severe/Severe	35	19	13-30	
Rest ESV	Minimal	32	27	11-48	0.99
	Mild/Moderate	53	23	13-37	
	Moderately severe/Severe	35	19	14-34	

EDV: end-diastolic volume; ESV: end-systolic volume; IQR: interquartile range; LVEF: left ventricular ejection fraction; MDD: major depressive disorder; MPI: myocardial perfusion imaging; PHQ-9: Patient Health Questionnaire-9.

Table 4 – Distribution of PHQ-9 and SF-12 scores according to the presence or absence of ischemia on MPI

Variable	Classification	With ischemia, n (%)	Without ischemia, n (%)	p-value
PHQ-9 Classification (MDD)	Minimal	16 (27.1%)	16 (26.2%)	0.99
	Mild/Moderate	26 (44.1%)	27 (44.3%)	
	Moderately severe/Severe	17 (28.8%)	18 (29.5%)	
Suicidal ideation	Yes	6 (10.2%)	9 (14.8%)	0.44
	No	53 (89.8%)	52 (85.2%)	
SF-12 PCS score > 50 points	Yes	4 (6.8%)	10 (16.4%)	0.10
	No	55 (93.2%)	51 (83.6%)	
SF-12 MCS score > 50 points	Yes	22 (37.3%)	20 (32.8%)	0.60
	No	37 (62.7%)	41 (67.2%)	

MCS: Mental Component Summary; MDD: major depressive disorder; MPI: myocardial perfusion imaging; PCS: Physical Component Summary; PHQ-9: Patient Health Questionnaire-9; SF-12: 12-Item Short Form Health Survey.

of atherosclerosis and alterations in neurotransmitter release, which may contribute to worsening of MDD symptoms.[16] In addition, a possible imbalance of the autonomic nervous system in patients with MDD could favor sympathetic hyperactivity, altering cardiac contractility and increasing susceptibility to arrhythmia development.[16]

Studies using MPI in patients with MDD demonstrated that this population presents greater susceptibility to emotionally induced myocardial ischemia, evidencing myocardial perfusion abnormalities in these individuals.[17]

The analyzed population also demonstrated poor overall perception of physical health. As observed in the physical

component of the SF-12, 106 individuals (88.3%) presented scores below 50. Patients with MDD and CAD may present greater physical limitation, lower functional capacity, and higher prevalence of fatigue and low energy levels.[18]

Furthermore, 78 individuals (65%) presented poor perceived mental health, defined by scores below 50 in the mental component of the SF-12. Patients with this perception tend to present greater emotional and physical impact related to CAD,[19] which may result in greater limitation of daily activities, poorer treatment adherence, and lower engagement in cardiovascular rehabilitation programs.[20]

The 2025 European Society of Cardiology Clinical Consensus Statement on mental health and cardiovascular disease[21] reinforces that systematic assessment of MDD and other mental disorders should be incorporated into the routine care of patients with cardiovascular disease. The document recommends the use of validated tools, such as the Patient Health Questionnaire-2 and PHQ-9, for initial screening after cardiovascular events or in the presence of clinical suspicion, considering the high prevalence of these conditions and their negative prognostic impact.

In our study, a particularly high prevalence of moderately severe/severe MDD was observed among patients referred for MPI (48%), in addition to a substantial rate of suicidal ideation (12.5%), without association with clinical, demographic, or functional variables. In light of the ESC recommendations, our findings reinforce the urgent need to routinely incorporate structured mental health screening into cardiovascular care pathways, considering that psychological distress may be present even in the absence of traditional clinical markers, thereby requiring proactive strategies for identification and intervention aimed at risk reduction, improvement of QoL, and potential modification of clinical outcomes.[21]

Among the limitations of this study, the use of a convenience sample composed of patients referred for evaluation at a university hospital should be highlighted, which may have contributed to a greater burden of comorbidities in the analyzed population. Additionally, patients were evaluated during a period preceding the COVID-19 pandemic, a condition that in several studies was associated with worsening of mental health-related disorders.[22]

Conclusion

This study demonstrated a high prevalence of moderately severe/severe MDD in patients referred for cardiovascular evaluation by MPI. These patients should be identified early and receive follow-up and specific mental health guidance. The implementation of structured protocols for systematic screening of mental disorders in the context of cardiovascular evaluation may represent a relevant strategy for reducing cardiovascular risk, improving QoL, and potentially modifying the clinical outcomes of these individuals.

Author Contributions

Conception and design of the research: Gonçais G, Barbirato GB, Pagnin D, Pagnin VQ, Mesquita CT; acquisition of data: Barbirato GB; analysis and interpretation of the data and writing of the manuscript: Gonçais G, Pagnin VQ, Mesquita CT; statistical analysis: Gonçais G, Pagnin D; critical revision of the manuscript for intellectual content: Pagnin D, Pagnin VQ, Mesquita CT.

Potential Conflict of Interest

No potential conflict of interest relevant to this article was reported.

Sources of Funding

There were no external funding sources for this study.

Study Association

This article is part of the thesis of master submitted by Almeida GG, from Universidade Federal Fluminense.

Ethics Approval and Consent to Participate

This study was approved by the Ethics Committee of the CEP-UFF (Universidade Federal Fluminense) under the protocol number 7.768.804. All the procedures in this study were in accordance with the 1975 Helsinki Declaration, updated in 2013.

Use of Artificial Intelligence

The authors did not use any artificial intelligence tools in the development of this work.

Availability of Research Data

The underlying content of the research text is contained within the manuscript.

References

1. Martin SS, Aday AW, Allen NB, Almarzooq ZI, Anderson CAM, Arora P, et al. 2025 Heart Disease and Stroke Statistics: A Report of US and Global Data from the American Heart Association. Circulation. 2025;151(8):e41-e660. doi: 10.1161/CIR.0000000000001303.
2. GBD 2021 Causes of Death Collaborators. Global Burden of 288 Causes of Death and Life Expectancy Decomposition in 204 Countries and Territories and 811 Subnational Locations, 1990-2021: A Systematic Analysis for the Global Burden of Disease Study 2021. Lancet. 2024;403(10440):2100-32. doi: 10.1016/S0140-6736(24)00367-2.
3. Bousquet-Santos K, Chen R, Kubzansky LD. A Sad Heart: Depression and Favorable Cardiovascular Health in Brazil. Prev Med. 2021;142:106378. doi: 10.1016/j.ypmed.2020.106378.
4. Groch MW, Erwin WD. SPECT in the Year 2000: Basic Principles. J Nucl Med Technol. 2000;28(4):233-44.
5. Habert J, Katzman MA, Oluboka OJ, McIntyre RS, McIntosh D, MacQueen GM, et al. Functional Recovery in Major Depressive Disorder: Focus on Early Optimized Treatment. Prim Care Companion CNS Disord. 2016;18(5). doi: 10.4088/PCC.15r01926.

6. Peltzer S, Müller H, Köstler U, Schulz-Nieswandt F, Jessen F, Albus C, et al. Detection and Treatment of Mental Disorders in Patients with Coronary Heart Disease (MenDis-CHD): A Cross-Sectional Study. PLoS One. 2020;15(12):e0243800. doi: 10.1371/journal.pone.0243800.

7. Jiang W, Babyak MA, Rozanski A, Sherwood A, O'Connor CM, Waugh RA, et al. Depression and Increased Myocardial Ischemic Activity in Patients with Ischemic Heart Disease. Am Heart J. 2003;146(1):55-61. doi: 10.1016/S0002-8703(03)00152-2.

8. Osório FL, Mendes AV, Crippa JA, Loureiro SR. Study of the Discriminative Validity of the PHQ-9 and PHQ-2 in a Sample of Brazilian Women in the Context of Primary Health Care. Perspect Psychiatr Care. 2009;45(3):216-27. doi: 10.1111/j.1744-6163.2009.00224.x.

9. Zanon C, Bastianello MR, Pacico JC, Hutz CS. Desenvolvimento e Validação de uma Escala de Afetos Positivos e Negativos. Psico-USF. 2013;18(2):193-202. doi: 10.1590/S1413-82712013000200003.

10. Ciconelli RM. Tradução para o Português e Validação do Questionário Genérico de Avaliação de Qualidade de Vida "Medical Outcomes Study 36-Item Short-Form Health Survey (SF-36)" [Thesis]. São Paulo: Universidade Federal de São Paulo, Escola Paulista de Medicina; 1997.

11. Kroenke K, Spitzer RL, Williams JB. The PHQ-9: Validity of a Brief Depression Severity Measure. J Gen Intern Med. 2001;16(9):606-13. doi: 10.1046/j.1525-1497.2001.016009606.x.

12. Watson D, Clark LA, Tellegen A. Development and Validation of Brief Measures of Positive and Negative Affect: The PANAS Scales. J Pers Soc Psychol. 1988;54(6):1063-70. doi: 10.1037//0022-3514.54.6.1063.

13. Hanna MR, Caspi A, Houts RM, Moffitt TE, Torvik FA. Co-Occurrence between Mental Disorders and Physical Diseases: A Study of Nationwide Primary-Care Medical Records. Psychol Med. 2024;54(15):4274-86. doi: 10.1017/S0033291724002575.

14. D'Oria R, Schipani R, Leonardini A, Natalicchio A, Perrini S, Cignarelli A, et al. The Role of Oxidative Stress in Cardiac Disease: From Physiological Response to Injury Factor. Oxid Med Cell Longev. 2020;2020:5732956. doi: 10.1155/2020/5732956.

15. Warriach ZI, Patel S, Khan F, Ferrer GF. Association of Depression with Cardiovascular Diseases. Cureus. 2022;14(6):e26296. doi: 10.7759/cureus.26296.

16. Huang L, Zhang L, Liu C, Xu Q, Qiu K. Interaction and Mechanisms of Depression and Cardiovascular Disease: A Mini-Review. PeerJ. 2025;13:e20148. doi: 10.7717/peerj.20148.

17. Burg MM, Meadows J, Shimbo D, Davidson KW, Schwartz JE, Soufer R. Confluence of Depression and Acute Psychological Stress among Patients with Stable Coronary Heart Disease: Effects on Myocardial Perfusion. J Am Heart Assoc. 2014;3(6):e000898. doi: 10.1161/JAHA.114.000898.

18. Kohlmann S, Gierk B, Murray AM, Scholl A, Lehmann M, Löwe B. Base Rates of Depressive Symptoms in Patients with Coronary Heart Disease: An Individual Symptom Analysis. PLoS One. 2016;11(5):e0156167. doi: 10.1371/journal.pone.0156167.

19. Kunschitz E, Friedrich O, Schöppl C, Maitz J, Sipötz J. Illness Perception Patterns in Patients with Coronary Artery Disease. Psychol Health Med. 2017;22(8):940-6. doi: 10.1080/13548506.2016.1271439.

20. Bueno H, Deaton C, Farrero M, Forsyth F, Braunschweig F, Buccheri S, et al. 2025 ESC Clinical Consensus Statement on Mental Health and Cardiovascular Disease: Developed Under the Auspices of the ESC Clinical Practice Guidelines Committee. Eur Heart J. 2025;46(41):4156-225. doi: 10.1093/eurheartj/ehaf191.

21. Sun Y, Wu Y, Fan S, Dal Santo T, Li L, Jiang X, et al. Comparison of Mental Health Symptoms Before and during the Covid-19 Pandemic: Evidence from a Systematic Review and Meta-Analysis of 134 Cohorts. BMJ. 2023;380:e074224. doi: 10.1136/bmj-2022-074224.

Beyond Imaging: The Silent Impact of Depression on Coronary Artery Disease

Priscila Cestari Quagliato[1]

Hospital e Maternidade São Luiz Campinas,[1] *Campinas, SP – Brazil*

Short editorial related to the article: Major Depressive Disorder and Quality of Life in Patients With Coronary Artery Disease Assessed by Myocardial Perfusion Imaging

Coronary artery disease (CAD) remains the leading cause of global morbidity and mortality, and its intersection with mental health has received prominent attention in contemporary cardiology discussions. In 2025, the European Society of Cardiology published a guideline specifically addressing the multidirectional association between mental health and cardiovascular disease.[1] Key issues were highlighted, including healthcare professionals' limited awareness regarding the prevalence of mental disorders and their direct impacts on cardiovascular health, as well as inadequate recognition of severe mental illness and the stigmas associated with these conditions.

Mental disorders play a detrimental role in cardiovascular prevention, affecting treatment adherence and management of acute decompensations. The overlapping symptoms of the two conditions and the difficulties in monitoring chronic disease negatively impact patient prognosis.[2]

A recent study conducted at a Brazilian federal university hospital revealed an alarming scenario: among 120 patients undergoing myocardial perfusion imaging, 48.3% presented symptoms consistent with moderately severe to severe depression, and 12.5% reported suicidal ideation. This prevalence is almost five times higher than that observed in the general Brazilian population,[3] reinforcing these patients' psychosocial vulnerability. The study did not demonstrate a statistically significant association between the severity of depressive symptoms and the presence of ischemia detected by conventional myocardial perfusion imaging, suggesting that psychological distress may be independent of immediate anatomical severity.

This apparent lack of association further complicates the clinical scenario. Although previous studies, such as the one by Fotopoulos et al.,[4] have attempted to correlate perfusion findings with depression and anxiety, outpatient settings have shown that traditional risk factors for CAD also predispose to mental disorders in a bidirectional cycle. For example, obesity and smoking are closely linked to depressive symptoms through reward mechanisms and chronic inflammation. The impact on quality of life is drastic, with 88.3% of patients reporting poor perception of their physical health.[5]

Symptoms such as frustration, sadness, anxiety, sleep disturbances, and intense fear of death have been reported as post-myocardial infarction experiences; however, persistent or disabling distress may also indicate an associated psychiatric disorder. [6]

Studies such as the one by Barbirato et al.[7] have demonstrated that mental stress testing can induce myocardial perfusion defects in up to 40% of asymptomatic patients, highlighting the complexity of the neuro-humoral mechanisms linking the mind to the heart. Given the shortage of mental health specialists in Brazil (with only 6.69 psychiatrists per 100,000 inhabitants and an uneven geographical distribution),[8] it is imperative that the diagnosis and initial management of mental health disorders be integrated into the routine practice of primary care physicians and cardiologists.

In this context, the formation of a multidisciplinary cardiology and mental health team is strongly recommended, operating analogously to the well-established heart team for highly complex cases.[9] A stepwise implementation of this multidisciplinary team following the ACTIVE principles has been proposed for team development (Figure 1). The acronym stands for Acknowledge, Check, (use validated) Tools, Implement, Venture, and Evaluate, thereby allowing better process control and adaptation to the realities of individual health settings.

The implementation of brief, validated screening tools, such as the PHQ-2 or PHQ-9, as part of routine cardiological assessment, represents a "golden opportunity." These measures enable early interventions and a truly patient-centered approach. In conclusion, modern cardiology requires us to look beyond. Ignoring the heart–mind connection results in incomplete care. Clinical practice must evolve to incorporate structured mental health screening, thereby ensuring better clinical outcomes and quality of life for patients.

Keywords

Coronary Artery Disease; Depression; Mental Health; Cardiology

Mailing Address: Priscila Cestari Quagliato •
Hospital e Maternidade São Luiz Campinas. Av. Andrade Neves, 863. Postal Code: 13070-000. Campinas, SP – Brazil
E-mail: cestari.fpriscila@gmail.com

DOI: https://doi.org/10.36660/abcimg.20260074i

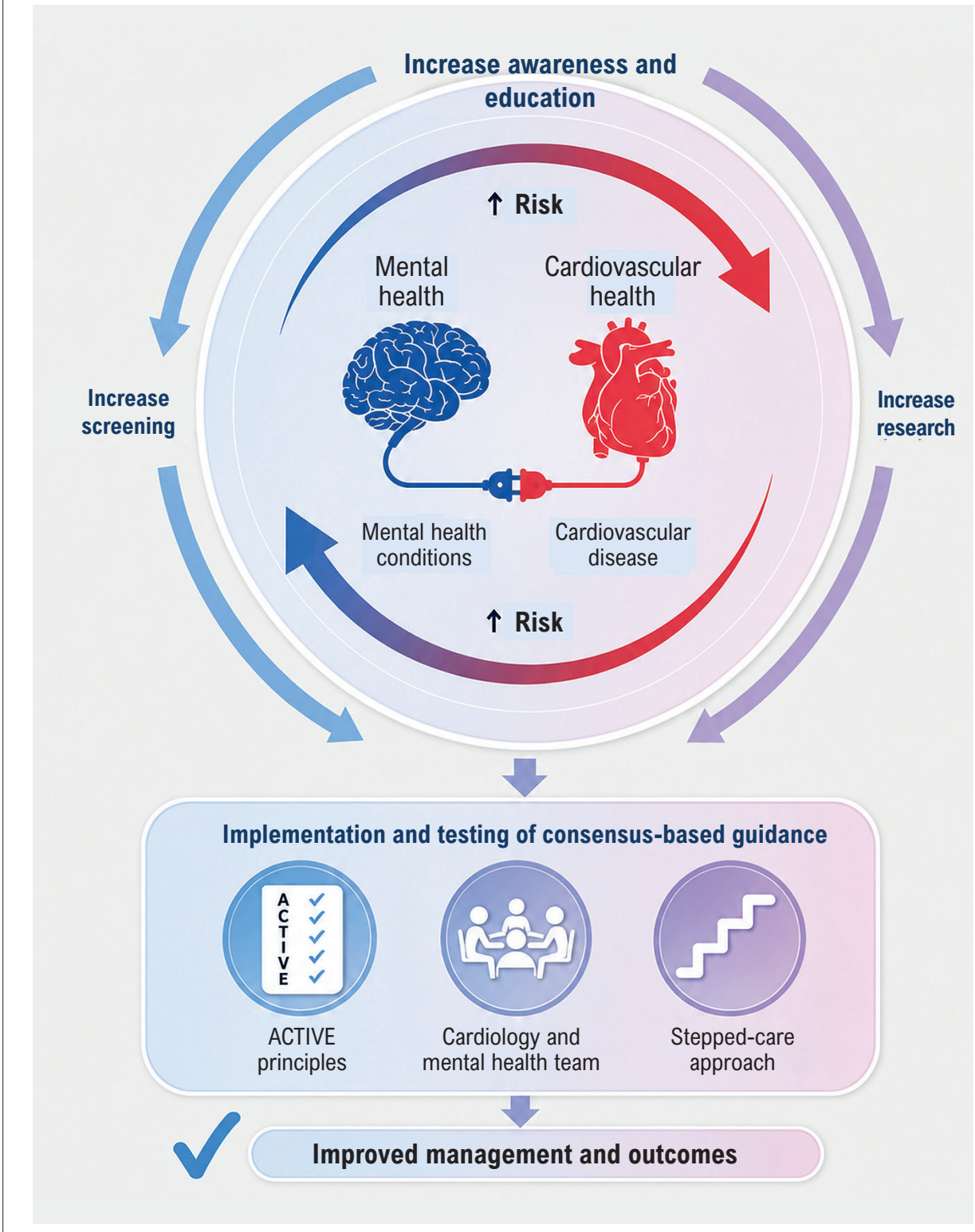

Figure 1 – *The multidirectional cycle between cardiovascular disease and mental health and the suggested ACTIVE (Acknowledge, Check, [use validated] Tools, Implement, Venture, Evaluate) principles for implementing multidisciplinary teams. Adapted from the 2025 ESC Clinical Consensus Statement on mental health and cardiovascular disease: developed under the auspices of the ESC Clinical Practice Guidelines Committee. European Heart Journal.*[1]

References

1 Bueno H, Deaton C, Farrero M, Forsyth F, Braunschweig F, Buccheri S, et al. 2025 ESC Clinical Consensus Statement on mental Health and Cardiovascular Disease: Developed Under the Auspices of the ESC Clinical Practice Guidelines Committee. Eur Heart J. 2025;46(41):4156-225. doi: 10.1093/eurheartj/ehaf191.

2 Heiberg IH, Jacobsen BK, Balteskard L, Bramness JG, Naess Ø, Ystrom E, et al. Undiagnosed Cardiovascular Disease Prior to Cardiovascular Death in Individuals with Severe Mental Illness. Acta Psychiatr Scand. 2019;139(6):558-71. doi: 10.1111/acps.13017.

3 Bousquet-Santos K, Chen R, Kubzansky LD. A Sad Heart: Depression and Favorable Cardiovascular Health in Brazil. Prev Med. 2021;142:106378. doi: 10.1016/j.ypmed.2020.106378.

4 Fotopoulos A, Petrikis P, Iakovou I, Papadopoulos A, Sakelariou K, Gkika E, et al. The Impact of Depression and Anxiety in Prognosis of Patients Undergoing Myocardial Perfusion Imaging with 99mTc Tetrofosmin SPECT for Evaluation of Possible Myocardial Ischemia. Nucl Med Rev Cent East Eur. 2020;23(2):58-62. doi: 10.5603/NMR.a2020.0014.

5 Milaneschi Y, Lamers F, Peyrot WJ, Baune BT, Breen G, Dehghan A, et al. Genetic Association of Major Depression with Atypical Features and Obesity-Related Immunometabolic Dysregulations. JAMA Psychiatry. 2017;74(12):1214-25. doi: 10.1001/jamapsychiatry.2017.3016.

6 Levine GN, Carney RM, Cohen BE, Dunn SL, Gaffey AE, Kronish IM, et al. Post-Myocardial Infarction Psychological Distress: A Scientific Statement from the American Heart Association. Circulation. 2025;152(16):e298-e310. doi: 10.1161/CIR.0000000000001381.

7 Barbirato GB, Félix R, Azevedo JC, Corrêa PL, Nóbrega AC, Coimbra A, et al. Prevalence of Induced Ischemia by Mental Distress. Arq Bras Cardiol. 2010;94(3):301-7. doi: 10.1590/s0066-782x2010000300007.

8 Instituto Nacional de Psiquiatria do Desenvolvimento para Crianças e Adolescentes. Dados sobre a distribuição de psiquiatras no Brasil [Internet]. São Paulo: INPD; 2025 [cited 2026 May 13]. Available from: https://inpd.org.br.

9 Bäck M, Antoniou S, Butler T, Dendale P, Greco A, Hansen D, et al. A Multidisciplinary Approach to Reduce the Burden of Cardiovascular Disease, with Special Reference to the Allied Professionals' Perspective: A Clinical Consensus Statement by the European Society of Cardiology Task Force on Allied Professionals with Contributions from the Association of Cardiovascular Nursing and Allied Professions, the Association for Acute CardioVascular Care, the European Association of Percutaneous Cardiovascular Interventions, the European Association of Preventive Cardiology, the European Heart Rhythm Association, and the Heart Failure Association of the European Society of Cardiology. Eur J Cardiovasc Nurs. 2026;25(2):219-24. doi: 10.1093/eurjcn/zvaf165.

Anabolic-Androgenic Steroids and Acute Myocardial Infarction in Young Adults: A Literature Review Based on a Case Series

Fabiana Rocha Botelho de Oliveira,[1] Danielli Oliveira de Costa Lino,[1] Germano Freire Bezerra Filho,[2] Bruno Cavalcante Linhares,[2] Leonardo Brito De Souza,[2] Luiz Filipe Torres de Alencar,[2] Matheus Rolim Santa Cruz,[2] Mateus Paiva Marques Feitosa[2]

Hospital de Messejana,[1] Fortaleza, CE – Brazil
Universidade de Fortaleza,[2] Fortaleza, CE – Brazil

Abstract

Background: **The use of anabolic-androgenic steroids (AAS) has increased substantially, especially among young adults seeking aesthetic enhancement and improved physical performance. Scientific evidence demonstrates a significant association between the abuse of these substances and severe cardiovascular events, including acute myocardial infarction (AMI), often occurring in individuals without traditional cardiovascular risk factors.**

Objective: **To describe the adverse effects of AAS on the cardiovascular system and the main pathophysiological mechanisms involved in the development of AMI through the analysis of a clinical case series combined with a review of medical literature.**

Methods: **A systematic literature review was conducted using the PubMed and SciELO databases, complemented by the analysis of three clinical cases. Demographic variables and characteristics related to AAS use, including duration of exposure and route of administration, were evaluated, with emphasis on the pathophysiological mechanisms associated with AMI.**

Results: **Analysis of the clinical cases identified different mechanisms related to AMI, including coronary thrombosis, atherosclerosis with plaque rupture, and spontaneous coronary artery dissection. The literature review also identified other relevant mechanisms, such as coronary vasospasm and toxic myocarditis. A predominance of male patients was observed, with the highest incidence occurring among individuals aged 20-40 years, and testosterone esters were the most frequently used AAS.**

Conclusions: **AAS abuse represents a major threat to cardiovascular health and is associated with AMI through multiple pathophysiological mechanisms. These findings reinforce the need for public awareness as well as the development of preventive strategies and clinical guidelines aimed at managing this emerging condition.**

Keywords: **Anabolic Androgenic Steroids; Myocardial Infarction; Atherosclerosis; Myocarditis.**

Introduction

Through Resolution No. 2,333/2023, the Brazilian Federal Council of Medicine (CFM for short, in Portuguese) prohibited the prescription of anabolic-androgenic steroids (AAS) for aesthetic purposes, muscle mass gain, and physical performance enhancement. In Brazil, however, the prevalence of AAS use may reach 31.6% in specific groups, such as physical education students and gym instructors.[1] Worldwide, the prevalence of nonmedical use of such substances is estimated at 4%-5% among men.[2]

Mailing Address: **Fabiana Rocha Botelho de Oliveira**
Universidade de Fortaleza. Av. Washington Soares, 1321. Postal code: 60811-905. Fortaleza, CE – Brazil
E-mail: germanofbfilho@hotmail.com
Manuscript received April 6, 2026, revised manuscript April 6, 2026, accepted April 20, 2026
Editor responsible for the review: Marcelo Tavares

DOI: https://doi.org/10.36660/abcimg.20260049i

The use of AAS is associated with muscle hypertrophy, increased energy reserves, and virilizing effects, promoting aesthetic improvement and enhanced physical performance; thus, they are widely used by high-performance athletes.[1] However, excessive use is associated with important cardiovascular adverse effects, contributing to increased morbidity and mortality. The main reported complications include dyslipidemia, hypertension, coagulopathies, cardiomyopathies, arrhythmias, and acute myocardial infarction (AMI), whose occurrence may be explained by different pathophysiological mechanisms (Central Illustration).

Over the last decade, there has been an increase in the number of young AAS users without traditional cardiovascular risk factors who developed acute coronary syndrome (ACS) as the main clinical outcome.[4] This scenario reinforces the hypothesis that AAS may act as triggering substances for coronary events in differents pathways (Figure 1), representing a potential public health problem.

Understanding this topic is essential to reduce the underreporting of AMI cases associated with the use of AAS

Central Illustration: Anabolic-Androgenic Steroids and Acute Myocardial Infarction in Young Adults: A Literature Review Based on a Case Series

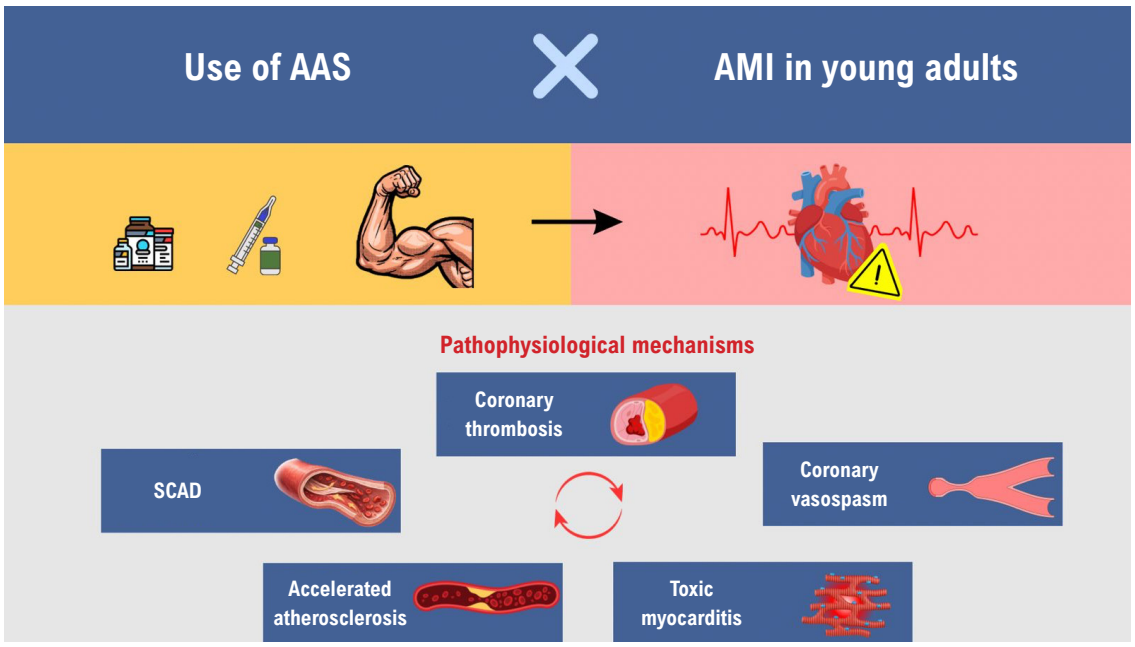

Arq Bras Cardiol: Imagem cardiovasc. 2026;39(2):e20260049

Anabolic-Androgenic Steroids and Acute Myocardial Infarction in Young Adults: A Literature Review Based on a Case Series. AMI: acute myocardial infarction; AAS: anabolic-androgenic steroids; SCAD: spontaneous coronary artery dissection.

and to enable more appropriate diagnostic, therapeutic, and preventive strategies. Therefore, the aim of this study was to review the cardiovascular alterations associated with inappropriate AAS use, with emphasis on the different pathophysiological mechanisms involved in AMI and other cardiac complications, based on a literature review and analysis of a clinical case series.

Methods

For this study, data were collected from the PubMed and SciELO databases. Articles published between 1990 and 2024, in English and Portuguese, involving studies conducted in humans, were included. The search strategy used the following keywords: "myocardial infarction," "anabolic steroids," "atherosclerosis," "atherosclerotic plaque erosion," "coronary vasospasm," "MINOCA," and "toxic myocarditis." Duplicate articles or those that did not contribute in a relevant and up-to-date manner to the objectives of the study were excluded.

In addition to the literature review, three clinical cases were selected through the analysis of hospital electronic medical records. Inclusion criteria comprised patients without previous comorbidities, with a history of current use of AAS, and who presented with an acute myocardial event requiring coronary angiography during hospitalization. Patients with preexisting cardiovascular comorbidities and those older than 50 years were excluded.

The selected patients signed an informed consent form provided after invitation to participate in the study. Confidentiality of the collected information was ensured by the researchers; data were used exclusively to fulfill the objectives of the present study, in accordance with the ethical principles established by Resolution No. 466/12 of the Brazilian National Health Council, linked to the Ministry of Health.

Results

AAS are synthetic substances structurally similar to testosterone and may be administered orally, topically, or by injection.[5] Testosterone exerts androgenic functions related to the development and maintenance of male sexual characteristics as well as anabolic functions, such as skeletal muscle and bone tissue growth.[6]

Excessive use of these compounds is associated with a prothrombotic state, hypertension, left ventricular hypertrophy, alterations in lipid metabolism, increased visceral fat, dyslipidemia, premature atherosclerosis, coronary vasospasm, and endothelial dysfunction, increasing the risk of myocardial ischemia (Figure 2).[4,7,8]

Despite the associated risks, users frequently administer doses 10-100 times higher than therapeutic levels and often combine different types of AAS simultaneously or cyclically to enhance aesthetic and physical performance effects.[9]

Evidence-based clinical cases: mechanisms of acute myocardial infarction in patients using anabolic-androgenic steroids

Anabolic-Androgenic Steroids use and Acute myocardial infarction associated with coronary thrombotic events

Case 1: Acute myocardial infarction caused by a coronary thrombotic event in a young patient using anabolic-androgenic steroids

A 32-year-old male patient without previous comorbidities, who had been using injectable Deca-Durabolin® for the previous 3 months, presented to the emergency department with typical chest pain associated with ST-segment elevation (STE). Coronary angiography demonstrated a negative image in the middle third of the right coronary artery (RCA), with a high thrombotic burden and embolization to the right posterior descending branch and the right posterior ventricular branch (Figure 3, Panel A).

Thrombus aspiration was performed, with removal of a small amount of thrombus, followed by balloon angioplasty of the right posterior ventricular artery. Distal flow (TIMI I) and residual thrombus image persisted. Intracoronary tirofiban administration was selected, along with oral dual antiplatelet therapy using aspirin and prasugrel, in addition to full anticoagulation with heparin. Subsequently, repeat evaluation with intravascular imaging using intravascular ultrasound (IVUS) was scheduled after 5 days of clinical therapy to determine the mechanism of AMI.

After clinical treatment, a significant reduction in thrombotic burden was observed, associated with improvement in distal flow (TIMI III). Intravascular IVUS assessment (Figure 3, Panel B) demonstrated the absence of atherosclerotic plaque and residual thrombus as well as an adequate luminal area. The patient was discharged 2 days after the second cardiac catheterization. Transthoracic echocardiography (TTE) showed a left ventricular (LV) ejection fraction (LVEF) of 50% and inferior wall hypokinesia. Anticoagulant therapy with rivaroxaban was prescribed at hospital discharge.

The relationship between AAS use and increased thrombotic risk has been investigated since 1988, when the first report of sudden death in a young user of these substances was described.[10] During the use of AAS, alterations occur in the primary, secondary, and tertiary phases of hemostasis, which favors thrombus formation. The prothrombotic state observed in these patients is related to increased platelet adhesion and aggregation resulting from enzymatic and glycoprotein imbalances involved in the coagulation cascade, potentially leading to AMI, stroke, and pulmonary embolism.[11]

Chang et al.[10] demonstrated increased levels of coagulation factors II, V, VIII, IX, X, and XII, associated with greater prothrombin production and mild alterations in fibrinogen levels. Factors VIII and IX participate in the formation of the tenase complex, whereas factors V and X compose the prothrombinase complex, both essential for thrombin generation and fibrin formation. Conversely, some studies also observed increased levels of coagulation inhibitors, such as antithrombin, protein C, protein S, and tissue factor pathway inhibitor, which reduce thrombus formation.

Regarding fibrinolysis, a reduction in plasminogen activator inhibitor-1 has been described, associated with increased tissue plasminogen activator and plasminogen levels, favoring fibrin clot degradation.[8,10]

Other prothrombotic factors have also been described, including elevated serum homocysteine levels, increased thromboxane A2 (a potent platelet aggregator), accelerated erythropoiesis with consequent increased blood viscosity, and reduced prostacyclin levels, an important inhibitor of platelet aggregation.[12]

In the HAARLEM study, involving 100 men using AAS, increased levels of factors II, IX, and XI were observed, in addition to increased levels of protein S and D-dimer, which suggests maintenance of coagulation pathway activity.[8] Therefore, the exact effects of AAS on the hemostatic system remain controversial, which reinforces the need for more robust studies and better clarification of the involved pathophysiological mechanisms.

Anabolic-Androgenic Steroids use and Acute myocardial infarction associated with accelerated atherosclerosis

Case 2: Anabolic-androgenic steroids and accelerated atherosclerosis

A 38-year-old male patient without previous comorbidities, who had been using Deca-Durabolin® for the previous 6 months, presented to the emergency department with typical chest pain, electrocardiogram (ECG) showing STE, and nonsustained ventricular tachycardia. Coronary angiography demonstrated total occlusion in the proximal third of the circumflex artery (Cx), involving bifurcation with the left marginal artery (LMA) with an acute appearance, in addition to total occlusion of the proximal third of the RCA with a chronic appearance, 80% obstruction in the middle third of the left anterior descending artery (LAD) , and a 70% lesion in the third diagonal branch (Figures 4 and 5).

Percutaneous coronary intervention with drug-eluting stent implantation at the Cx/LMA bifurcation was performed. Dual antiplatelet therapy with aspirin and clopidogrel was initiated, in addition to high-intensity statin therapy and heart failure treatment, considering that TTE demonstrated LV inferior wall akinesia, anterolateral and lateral LV wall hypokinesia, and diastolic dysfunction with an ejection fraction of 39%. Before hospital discharge, angioplasty of the residual LAD lesion with drug-eluting stent implantation was performed.

Atherosclerosis is a chronic cardiometabolic disease characterized by lipid accumulation within the vascular wall, promoting endothelial inflammation. Its pathophysiological process begins with oxidation of low-density lipoprotein (LDL) by macrophages within the vascular intima, resulting in foam cell formation, fatty streaks, and subsequently atheromatous plaques. This process triggers oxidative imbalance, with excessive production of free radicals and activation of inflammatory cytokines responsible for the progression of atheromatosis.[11]

The biochemical mechanism through which AAS contribute to the development of atherosclerosis remains controversial. According to Baggish et al., doses greater than 1,000 mg/week increase levels of apolipoprotein B, the main component of LDL. In addition, AAS increase the expression of endothelial adhesion molecules, facilitating LDL migration into the vascular intima.[13]

An increased LDL/high-density lipoprotein (HDL) ratio is also observed due to enhanced HDL catabolism mediated by hepatic lipase, whose levels are elevated in AAS users.[14] These lipid alterations are related not only to isolated substance use but mainly to duration of use, administered dose, and route of administration. Parenterally administered AAS, because they bypass first-pass hepatic metabolism, tend to have less adverse impact on the lipid profile.[15,16]

Additionally, reduced levels of apolipoprotein A1, a molecule involved in reverse cholesterol transport and lipid removal from the vascular wall, have been described.[14]

Interestingly, AAS appear to reduce the levels of lipoprotein(a) [Lp(a)], a cardiovascular risk marker with a strong genetic component. Users of danazol demonstrated decreased serum levels of Lp(a), which suggests possible distinct effects of AAS on lipid metabolism and require further clarification.[17]

The CRISP CT study evaluated coronary inflammation through the perivascular fat attenuation index (FAI), even in the absence of atherosclerotic plaques. AAS users presented higher perivascular FAI values, which suggests coronary perivascular inflammation even in individuals with lower body fat percentage. This finding may be related to blockade of mature adipocyte differentiation induced by AAS, characterizing these individuals as a risk group for atherosclerotic events regardless of body composition control.[18,19]

Anabolic-Androgenic Steroids use and Acute myocardial infarction associated with nonobstructive coronary arteries

Case 3: Myocardial infarction with nonobstructive coronary arteries caused by spontaneous coronary artery dissection

A 34-year-old male patient without previous comorbidities, who had been using Durateston® for the previous 4 months, presented to the emergency department with complete right hemiplegia and aphasia. Noncontrast cranial computed tomography demonstrated hypodensity in the territory of the middle cerebral artery (MCA), a finding compatible with ischemic stroke.

During etiological investigation of the stroke, cranial and cervical vessel computed tomography angiography demonstrated occlusion of the left MCA. TTE revealed apical LV dyskinesia associated with the presence of a mobile intracavitary thrombus measuring 41 mm × 23 mm. Therefore, the stroke was attributed to a cardioembolic mechanism.

However, due to the presence of ventricular dyskinesia, coronary angiography was performed and demonstrated contrast subtraction involving the middle and distal thirds of the LAD. The coronary arteries did not present significant obstructive lesions, and findings compatible with type 1 spontaneous coronary artery dissection (SCAD) affecting the middle and distal LAD segments were identified. Complementary intravascular imaging was not performed. The patient was discharged on clopidogrel and apixaban. TTE demonstrated an LVEF of 50%, associated with apical LV dyskinesia.

In 2020, the updated European Society of Cardiology guidelines redefined myocardial infarction with nonobstructive coronary arteries (MINOCA) as myocardial infarction of ischemic etiology in the absence of coronary stenosis greater than 50% caused by obstructive atherosclerotic disease on angiography, therefore excluding nonischemic causes previously included in the concept.[20]

Thus, patients presenting with clinical findings suggestive of AMI, alterations in biomarkers of acute myocardial injury, ECG abnormalities with or without STE, and echocardiographic findings compatible with myocardial ischemia, but without significant obstructive coronary disease on angiography, should be investigated for MINOCA.

Among the pathophysiological mechanisms associated with MINOCA, SCAD, which is frequently underdiagnosed, stands out. SCAD is defined as a nontraumatic, noniatrogenic, nonatherosclerotic separation of the layers of the coronary artery, resulting in false lumen formation.[21]

Two main pathophysiological mechanisms have been proposed: rupture of the intimal layer with communication between the subintimal space and the true lumen, and formation of intramural hematoma secondary to rupture of microvessels within the medial layer, leading to arterial compression, reduced coronary flow, ischemia, and AMI.[22]

The etiology of SCAD has not yet been fully clarified, but it is known to involve genetic predisposition associated with precipitating factors, such as physical or emotional stress, illicit drug use, stimulants, and hormonal alterations. Cases associated with AAS use are rare; however, cardiocirculatory stress induced by these substances (e.g., hypertension, atherosclerosis, and coronary vasospasm), associated with intense physical exercise, may favor the occurrence of SCAD.[23]

SCAD predominantly affects young or middle-aged women, generally between 45-53 years of age, frequently in the absence of classic atherosclerotic risk factors. It may occur in nulliparous, pregnant, postpartum, and postmenopausal women.[24] Evidence suggests that cyclic hormonal alterations exert greater influence on SCAD than absolute serum levels of estrogen and progesterone.[25] However, conclusive studies regarding the direct role of AAS in this context are still lacking.

Within the pathophysiological spectrum of ACS associated with use of AAS, coronary vasospasm also deserves attention. Inappropriate use of such substances promotes sympathetic hyperactivation, vasoconstriction, and increased blood pressure (BP). Coronary vasospasm is directly related to vascular smooth muscle hyperreactivity, resulting in abnormal contraction of smooth muscle cells and disturbance of coronary vasomotor tone. Vasospasm is

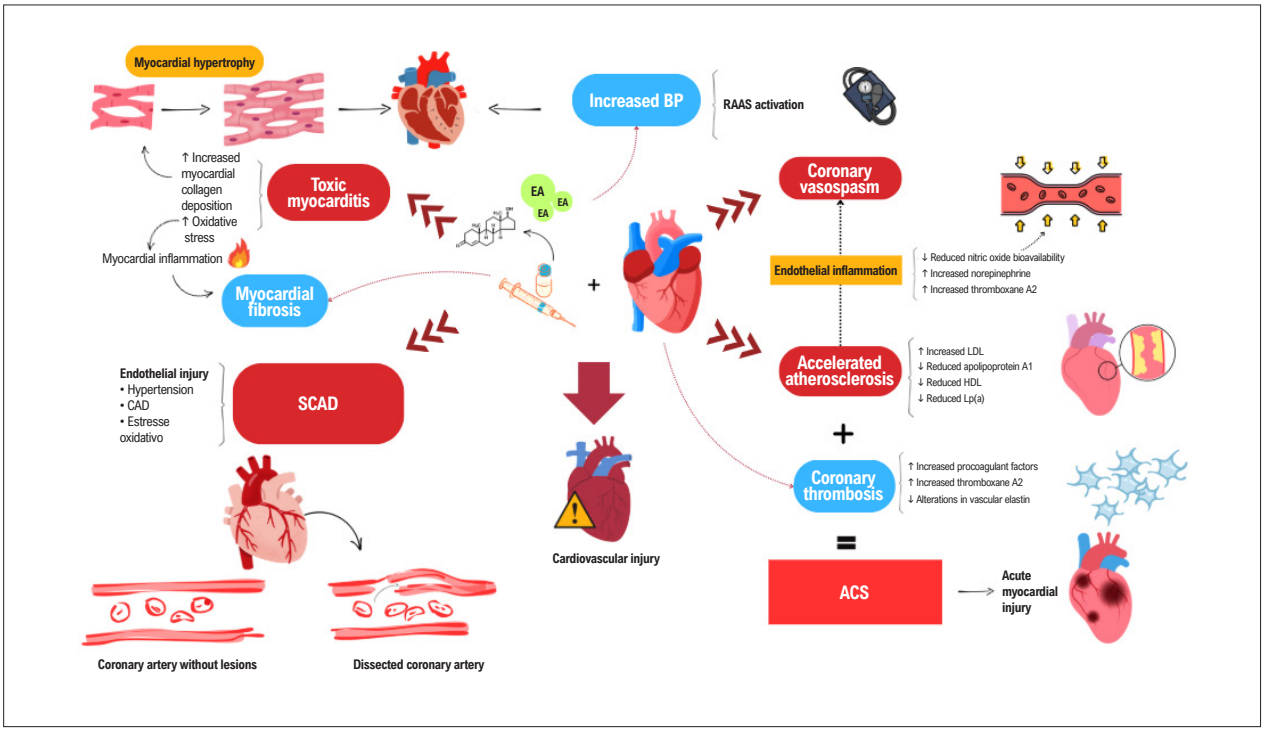

Figure 1 – *Cardiovascular adverse effects of anabolic-androgenic steroids. Source: Adapted from Fadah et al.[12] ACS: acute coronary syndrome; BP: blood pressure; CAD: coronary artery disease; HDL: high-density lipoprotein; LDL: low-density lipoprotein; Lp(a): lipoprotein(a); RAAS: renin-angiotensin-aldosterone system; SCAD: spontaneous coronary artery dissection.*

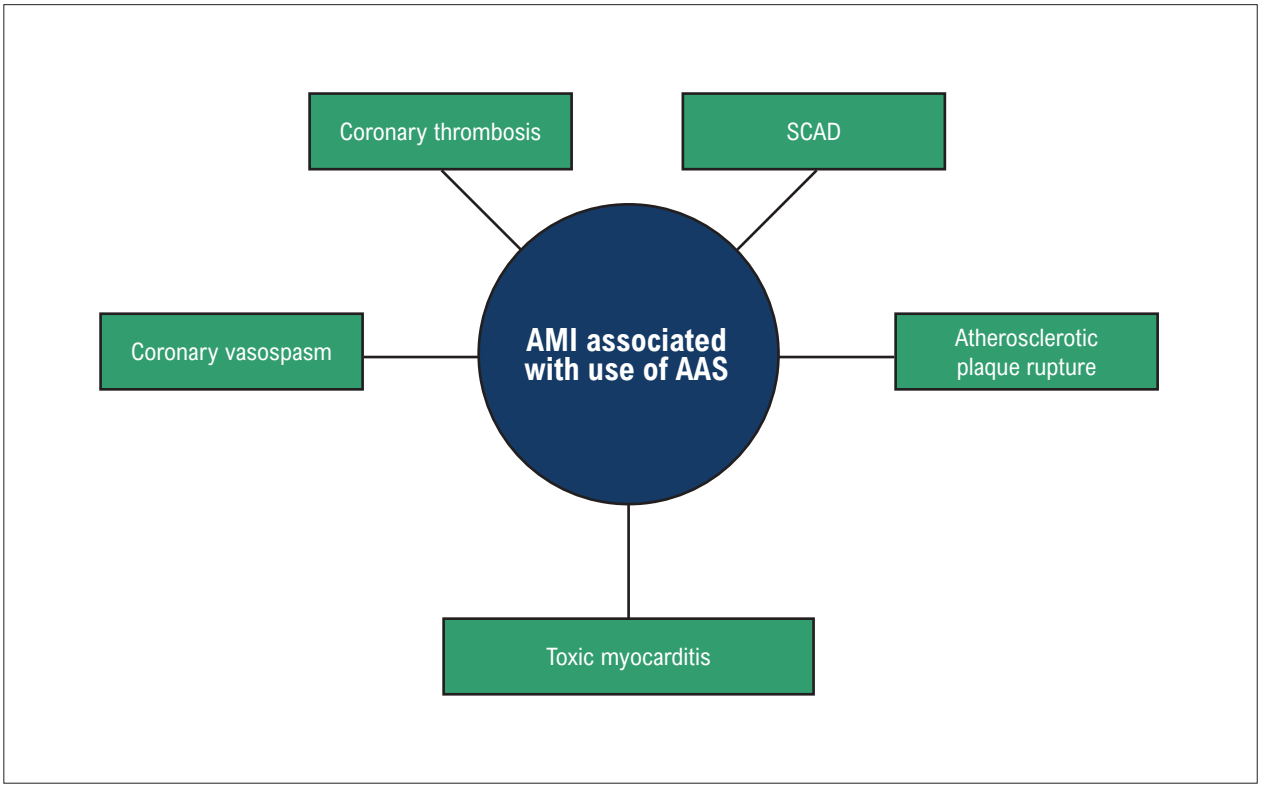

Figure 2 – *Pathophysiological mechanisms of AAS associated with AMI. Source: Author's personal archive. AAS: anabolic-androgenic steroids; AMI: acute myocardial infarction; SCAD: spontaneous coronary artery dissection.*

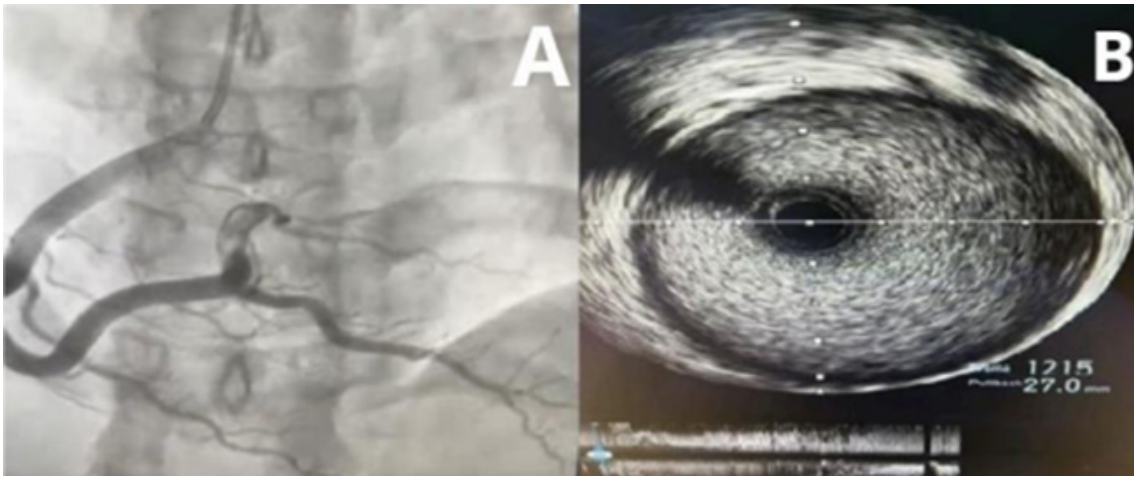

Figure 3 – *A) Coronary angiography in the right anterior oblique projection demonstrating a negative image suggestive of thrombus in the right posterior ventricular artery. B) Intravascular ultrasound performed at the site of the thrombotic image after 5 days of antithrombotic therapy, demonstrating intact endothelium, absence of atherosclerotic plaque, and adequate luminal area. Source: Author's personal archive.*

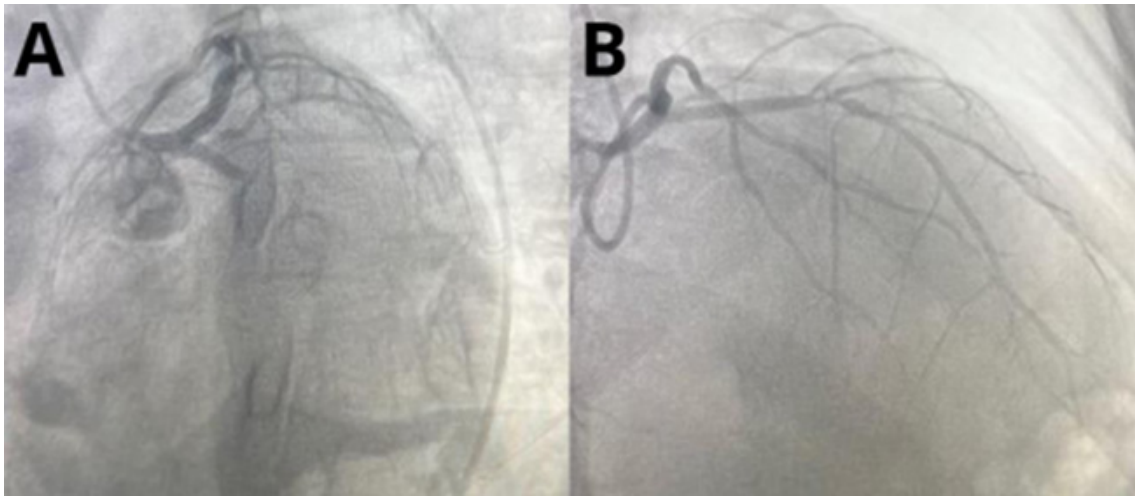

Figure 4 – *A) Coronary angiography in the left anterior oblique caudal projection demonstrating total occlusion in the middle third of the Cx. B) Coronary angiography in the right anterior oblique cranial projection demonstrating total occlusion of the Cx associated with significant lesions in the middle third of the LAD and in the third diagonal branch. Cx: circumflex artery; LAD: left anterior descending artery. Source: Author's personal archive.*

defined as intense vasoconstriction (> 90%) of an epicardial coronary artery, with significant impairment of blood flow and potential development of myocardial ischemia.[25,26]

Vasospasm may occur spontaneously or due to vascular hyperreactivity in response to endogenous and exogenous substances. Testosterone is known to induce abnormal vascular response to norepinephrine by inhibiting its reuptake and favoring coronary vasospasm.[27]

Thus, AAS contribute to loss of coronary vasodilatory mechanisms and promote increased levels of vasoconstrictive substances, such as endothelin-1, norepinephrine, thromboxane, and angiotensin II.[7,11,15]

Associated with this process, AAS act as precursors of endothelial injury through alterations in the lipid profile, chronic vascular inflammation, and acceleration of atherosclerosis. This mechanism represents an important pathway of direct injury to the coronary endothelium, creating a favorable substrate for coronary spasm associated with sympathetic hyperreactivity. Consequently, vascular hypercontractility occurs due to imbalance between

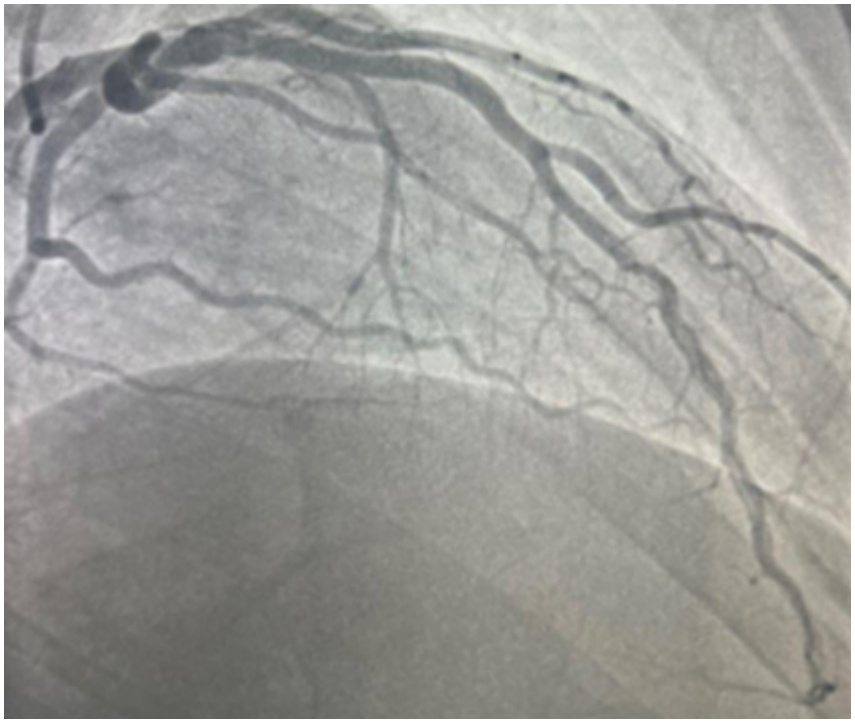

Figure 5 – *Coronary angiography in the right cranial posteroanterior projection demonstrating contrast subtraction involving the middle and distal thirds of the LAD, compatible with type 1 angiographic pattern of spontaneous coronary artery dissection. LAD: left anterior descending artery. Source: Author's personal archive.*

vasodilatory and vasoconstrictive substances, culminating in acute myocardial injury.[15]

In the cardiac catheterization laboratory, diagnosis of coronary vasospasm may be challenging, since the spasm may have resolved spontaneously or after nitrate administration in the emergency department. Provocative testing with intracoronary acetylcholine has diagnostic value; however, its use in clinical practice is limited due to low availability and the risk of ventricular arrhythmias associated with the procedure.

Anabolic-androgenic steroids and myocarditis

A systematic review with meta-analysis demonstrated that approximately 34.5% of MINOCA cases may present an associated diagnosis of myocarditis.[27] Myocarditis is defined as an inflammatory disease of myocardium, with endomyocardial biopsy considered the diagnostic gold standard. Toxic myocarditis corresponds to a subgroup of secondary etiologies related to exposure to heavy metals, radiation, and drugs, including alcohol, amphetamines, and AAS.

AAS promote alterations in cardiac size, mass, geometry, and function.[9] These modifications may mimic hypertrophic cardiomyopathy, with increased interventricular septal and LV posterior wall thickness.[28] Cardiac hypertrophy represents a multifactorial response resulting from direct effects on cardiomyocytes associated with hemodynamic and metabolic alterations.[28]

Montisci et al.[29] conducted an autopsy study involving four athletes using AAS and identified myocardial fibrosis, myofibrillar destruction, and eosinophilic infiltration within cardiac tissue. AAS induce pathological cardiac hypertrophy through modulation of gene transcription, acting directly on RNA and regulating protein synthesis via androgen receptors located in the nuclei of cardiomyocytes.[12] In addition, alterations involving enzymes, ionic flow, and the myocardial interstitial matrix may also occur.

In an experimental study involving rats exposed to AAS associated with physical exercise, Carmo et al.[30] demonstrated increased type III collagen production related to interstitial alterations and myocardial fibrosis, associated with greater activation of the renin-angiotensin-aldosterone system (RAAS).

Angiotensin II is the main biologically active component of the RAAS and plays an important role in regulating BP, plasma volume, and sympathetic activity.[31] Studies demonstrate that cardiac angiotensin II production may occur independently of the systemic endocrine system.[31] This substance promotes cardiomyocyte hypertrophy and fibroblast proliferation, stimulating collagen and fibronectin synthesis while reducing the activity of enzymes responsible for collagen degradation.[30] Angiotensin II AT1 receptors show markedly increased expression in AAS users.[12]

Another relevant aspect is the structural similarity between AAS and aldosterone, a mineralocorticoid hormone produced in the adrenal cortex. Aldosterone also contributes to increased collagen deposition within the cardiovascular matrix, promoting the development of myocardial fibrosis.[12,32]

In addition to these mechanisms, alterations in enzymatic reactions, intracellular ion transport (especially calcium), excessive free radical production, and release of proinflammatory cytokines may occur.[33] These phenomena favor cellular apoptosis and mitochondrial dysfunction, leading to loss of structural integrity of cardiomyocytes and modification of contractile proteins. Associated with disruption of calcium homeostasis, these alterations contribute to the development of myocardial fibrosis and cardiac hypertrophy.[12]

Activation of the renin-angiotensin-aldosterone axis through the direct action of angiotensin II and aldosterone promotes increased blood volume.[12] This effect, associated with sympathetic hyperactivity and maintenance of increased levels of norepinephrine, favors elevation of mean BP and increases the risk of hypertension and hemodynamic overload.[33]

Several studies demonstrate that AAS users present increased left ventricular mass index, reduced LVEF, impaired left ventricular diastolic function, and elevated BP levels. Abdullah et al.[35] demonstrated, through echocardiographic evaluation of current and former AAS users, the presence of biventricular cardiomyopathy associated with reduced right ventricular function.[12]

Structural alterations in cardiomyocytes also promote modifications in cardiac action potential, creating a substrate for arrhythmias and increasing the risk of sudden death in this patient population.

Sobreira Filho et al.[36] reported a case of toxic myocarditis initially mimicking non-ST-segment elevation ACS in a 30-year-old patient using testosterone enanthate, trenbolone acetate, and boldenone. Coronary angiography did not demonstrate obstructive coronary lesions; however, ventriculography revealed severe and diffuse hypokinesia of the inferior, apical, and septal walls, a finding later confirmed by TTE, associated with reduced LVEF to 43%. Cardiac magnetic resonance imaging was essential to differentiate the nonischemic fibrosis pattern and establish a more accurate diagnosis (Figure 6, Panels A and B).[36]

Toxic myocarditis involves multiple pathophysiological mechanisms, including autoimmune reactions, exposure to cardiotoxic agents, and acute infectious processes.[37] Among the associated chemical agents, AAS stand out because of increased production of proinflammatory mediators induced by the testosterone present in many of these compounds.[38]

According to Cooper,[38] exposure to cardiotoxic agents such as AAS may induce alterations in cellular metabolism, excessive production of reactive oxygen species, and mitochondrial dysfunction, culminating in cellular necrosis or apoptosis. In addition, an immune-mediated inflammatory response characterized by infiltration of T lymphocytes and macrophages into myocardial tissue may occur, associated with release of proinflammatory cytokines (e.g., interleukin-1, tumor necrosis factor alpha, and interleukin-6), which further potentiates cardiac muscle damage.[39]

Discussion

Chronic use of AAS at supraphysiological doses is associated with several severe adverse effects capable of significantly compromising users' cardiovascular health.

In the present case series, all patients were young men between 20-40 years of age, without previous comorbidities and with a history of AAS use. Each case illustrates different pathophysiological mechanisms related to the cardiovascular toxicity of these substances, including coronary thrombosis, accelerated atherosclerosis with plaque rupture, SCAD, and

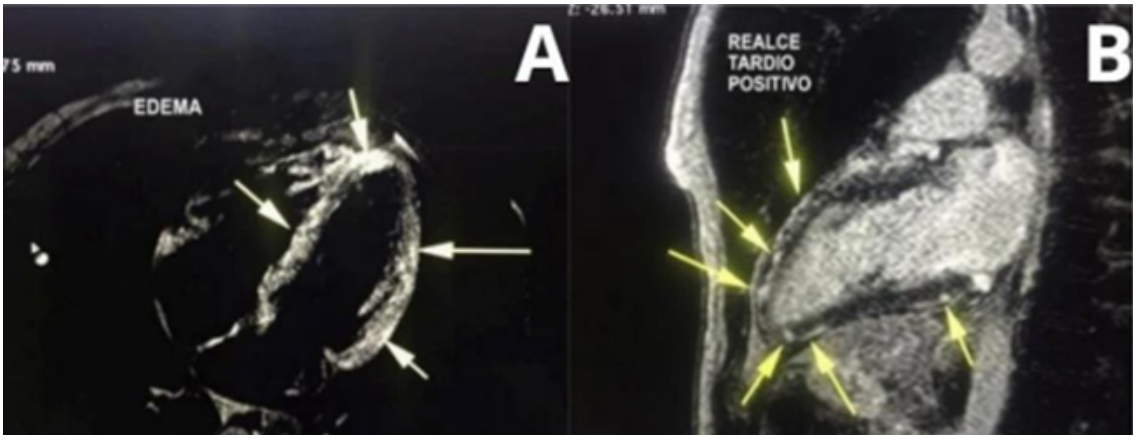

Figure 6 – *A) Triple IR T2-weighted T2 sequence in the four-chamber view demonstrating hyperintense areas suggestive of myocardial edema. B) Late gadolinium enhancement sequence in the two-chamber view demonstrating hyperintense areas with a mesoepicardial nonischemic pattern suggestive of myocardial fibrosis and/or necrosis. Source: Author's personal archive.*

toxic myocarditis. Predominant use of injectable testosterone esters was observed.

Although the analyzed sample was exclusively male, the progressive increase in AAS use among young women should also be highlighted, mainly motivated by the pursuit of improved athletic performance and body aesthetics. Studies demonstrate prevalence rates of up to 16.8% among female bodybuilders, 4.4% among athletes or resistance-training practitioners, and 1.4% in the general female population.[40]

Despite the cardiovascular deleterious effects already widely described in the literature, increasing abusive and indiscriminate use of these substances has been observed among recreational users, frequently without adequate medical supervision and without full awareness of the associated potential risks. The medical community should remain attentive to the possible cardiovascular repercussions associated with AAS, seeking to expand knowledge on this topic in order to improve diagnostic, therapeutic, and preventive strategies.

In addition, discontinuation of AAS frequently requires a multidisciplinary approach, considering the occurrence of rebound effects and the association with psychiatric comorbidities, such as anxiety disorder and body dysmorphic disorder, often aggravated by social pressure related to pursuit of the ideal body.

Over recent decades, a marked increase has been observed in reports of AMI among young patients using AAS. However, additional studies are still needed to strengthen the causal association between use of these substances and the different pathophysiological mechanisms involved in the development of ACS, considering the possible influence of concomitant predisposing factors.

Furthermore, studies evaluating specific substances individually are needed, since concomitant use of multiple AAS makes individualized analysis of the cardiovascular effects of each compound difficult.

Conclusion

As briefly summarized in Central Illustration, it was possible to review the main mechanisms related to AMI in young patients using AAS, including coronary thrombotic events, accelerated atherosclerosis, MINOCA, and toxic myocarditis.

These findings reinforce that indiscriminate use of these substances represents an important public health problem, especially among young adults without traditional cardiovascular risk factors. Therefore, despite the prohibition established by the CFM, strengthening awareness and prevention strategies involving healthcare professionals, the general population, and media outlets remains essential in order to reduce the cardiovascular impacts associated with abusive use of AAS.

Author Contributions

Conception and design of the research and critical revision of the manuscript for intellectual content: Oliveira FRB, Lino DOC, Feitosa MPM; acquisition of data: Oliveira FRB, Feitosa MPM; analysis and interpretation of the data: Oliveira FRB, Bezerra Filho GF, Linhares BC, Feitosa MPM; writing of the manuscript: Oliveira FRB, Bezerra Filho GF, Linhares BC, Souza LB, Alencar LFT, Cruz MRSC, Feitosa MPM; preparation of the images included in the article: Bezerra Filho GF, Linhares BC, Souza LB, Alencar LFT, Cruz MRSC.

Potential Conflict of Interest

No potential conflict of interest relevant to this article was reported.

Sources of Funding

There were no external funding sources for this study.

Study Association

This article is part of the thesis of master submitted by Fabiana Rocha Botelho de Oliveira, from Hospital de Messejana.

Ethics Approval and Consent to Participate

This article does not contain any studies with human participants or animals performed by any of the authors.

Use of Artificial Intelligence

During the preparation of this work, the authors used ChatGPT to improve the grammar and semantics of the text and Open Evidence to facilitate the search for articles related to the proposed topic, assisting in the development of the final manuscript.

Availability of Research Data

The underlying content of the research text is contained within the manuscript.

References

1. Abrahin OSC, Souza NSF, Sousa EC, Moreira JKR, Nascimento VC. Prevalence of the Use of Anabolic Androgenic Steroids by Physical Education Students and Teachers Who Work in Health Clubs. Rev Bras Med Esporte. 2013;19(1):27-30. doi: 10.1590/S1517-86922013000100005.
2. Smit DL, Hon O, Venhuis BJ, den Heijer M, Ronde W. Baseline Characteristics of the HAARLEM Study: 100 Male Amateur Athletes Using Anabolic Androgenic Steroids. Scand J Med Sci Sports. 2020;30(3):531-9. doi: 10.1111/sms.13592.
3. Perry JC, Schuetz TM, Memon MD, Faiz S, Cancarevic I. Anabolic Steroids and Cardiovascular Outcomes: The Controversy. Cureus. 2020;12(7):e9333. doi: 10.7759/cureus.9333.
4. Baggish AL, Weiner RB, Kanayama G, Hudson JI, Lu MT, Hoffmann U, et al. Cardiovascular Toxicity of Illicit Anabolic-Androgenic Steroid Use. Circulation. 2017;135(21):1991-2002. doi: 10.1161/CIRCULATIONAHA.116.026945.

5. Kicman AT. Pharmacology of Anabolic Steroids. Br J Pharmacol. 2008;154(3):502-21. doi: 10.1038/bjp.2008.165.

6. Corona G, Rastrelli G, Vignozzi L, Maggi M. Emerging Medication for the Treatment of Male Hypogonadism. Expert Opin Emerg Drugs. 2012;17(2):239-59. doi: 10.1517/14728214.2012.683411.

7. Beltrame JF, Crea F, Kaski JC, Ogawa H, Ong P, Sechtem U, et al. The Who, What, Why, When, How and Where of Vasospastic Angina. Circ J. 2016;80(2):289-98. doi: 10.1253/circj.CJ-15-1202.

8. Camilleri E, Smit DL, van Rein N, Le Cessie S, de Hon O, den Heijer M, et al. Coagulation Profiles during and after Anabolic Androgenic Steroid Use: Data from the HAARLEM Study. Res Pract Thromb Haemost. 2023;7(7):102215. doi: 10.1016/j.rpth.2023.102215.

9. Carmo EC, Fernandes T, Oliveira EM. Anabolic Steroids: From the Athlete to Cardiacapthy Patient. Rev Educ Fís/UEM. 2012;23(2)307-18. doi: 10.4025/reveducfis.v23i2.12462.

10. Chang S, Münster AB, Gram J, Sidelmann JJ. Anabolic Androgenic Steroid Abuse: The Effects on Thrombosis Risk, Coagulation, and Fibrinolysis. Semin Thromb Hemost. 2018;44(8):734-46. doi: 10.1055/s-0038-1670639.

11. Christou GA, Christou KA, Nikas DN, Goudevenos JA. Acute Myocardial Infarction in a Young Bodybuilder Taking Anabolic Androgenic Steroids: A Case Report and Critical Review of the Literature. Eur J Prev Cardiol. 2016;23(16):1785-96. doi: 10.1177/2047487316651341.

12. Fadah K, Gopi G, Lingireddy A, Blumer V, Dewald T, Mentz RJ. Anabolic Androgenic Steroids and Cardiomyopathy: An Update. Front Cardiovasc Med. 2023;10:1214374. doi: 10.3389/fcvm.2023.1214374.

13. Death AK, McGrath KC, Sader MA, Nakhla S, Jessup W, Handelsman DJ, et al. Dihydrotestosterone Promotes Vascular Cell Adhesion Molecule-1 Expression in Male Human Endothelial Cells Via a Nuclear Factor-kappaB-Dependent Pathway. Endocrinology. 2004;145(4):1889-97. doi: 10.1210/en.2003-0789.

14. Hartgens F, Rietjens G, Keizer HA, Kuipers H, Wolffenbuttel BH. Effects of Androgenic-Anabolic Steroids on Apolipoproteins and Lipoprotein (a). Br J Sports Med. 2004;38(3):253-9. doi: 10.1136/bjsm.2003.000199.

15. Severo CB, Ribeiro JP, Umpierre D, Da Silveira AD, Padilha MC, De Aquino FR Neto, et al. Increased Atherothrombotic Markers and Endothelial Dysfunction in Steroid Users. Eur J Prev Cardiol. 2013;20(2):195-201. doi: 10.1177/2047487312437062.

16. Dukewich M, Stolz AA. Anabolic Steroid-Associated Liver Injury. Clin Liver Dis. 2024;23(1):e0196. doi: 10.1097/CLD.0000000000000196.

17. Crook D, Sidhu M, Seed M, O'Donnell M, Stevenson JC. Lipoprotein Lp(a) Levels are Reduced by Danazol, an Anabolic Steroid. Atherosclerosis. 1992;92(1):41-7. doi: 10.1016/0021-9150(92)90008-5.

18. Oikonomou EK, Marwan M, Desai MY, Mancio J, Alashi A, Centeno EH, et al. Non-Invasive Detection of Coronary Inflammation Using Computed Tomography and Prediction of Residual Cardiovascular Risk (the CRISP CT Study): A Post-Hoc Analysis of Prospective Outcome Data. Lancet. 2018;392(10151):929-39. doi: 10.1016/S0140-6736(18)31114-0.

19. Souza FR, Rochitte CE, Silva DC, Sampaio B, Passarelli M, Santos MRD, et al. Coronary Inflammation by Computed Tomography Pericoronary Fat Attenuation and Increased Cytokines in Young Male Anabolic Androgenic Steroid Users. Arq Bras Cardiol. 2023;120(11):e20220822. doi: 10.36660/abc.20220822.

20. Occhipinti G, Bucciarelli-Ducci C, Capodanno D. Diagnostic Pathways in Myocardial Infarction with Non-Obstructive Coronary Artery Disease (MINOCA). Eur Heart J Acute Cardiovasc Care. 2021;10(7):813-22. doi: 10.1093/ehjacc/zuab049.

21. Basso C, Morgagni GL, Thiene G. Spontaneous Coronary Artery Dissection: A Neglected Cause of Acute Myocardial Ischaemia and Sudden Death. Heart. 1996;75(5):451-4. doi: 10.1136/hrt.75.5.451.

22. Heidari A, Sabzi F, Faraji R. Spontaneous Coronary Artery Dissection in Anabolic Steroid Misuse. Ann Card Anaesth. 2018;21(1):103-4. doi: 10.4103/aca.ACA_161_17.

23. Hayes SN, Tweet MS, Adlam D, Kim ESH, Gulati R, Price JE, et al. Spontaneous Coronary Artery Dissection: JACC State-of-the-Art Review. J Am Coll Cardiol. 2020;76(8):961-84. doi: 10.1016/j.jacc.2020.05.084.

24. Kim ESH. Spontaneous Coronary-Artery Dissection. N Engl J Med. 2020;383(24):2358-70. doi: 10.1056/NEJMra2001524.

25. Tamis-Holland JE, Jneid H, Reynolds HR, Agewall S, Brilakis ES, Brown TM, et al. Contemporary Diagnosis and Management of Patients with Myocardial Infarction in the Absence of Obstructive Coronary Artery Disease: A Scientific Statement from the American Heart Association. Circulation. 2019;139(18):e891-e908. doi: 10.1161/CIR.0000000000000670.

26. Carbone A, D'Andrea A, Riegler L, Scarafile R, Pezzullo E, Martone F, et al. Cardiac Damage in Athlete's Heart: When the "Supernormal" Heart Fails! World J Cardiol. 2017;9(6):470-80. doi: 10.4330/wjc.v9.i6.470.

27. Hausvater A, Smilowitz NR, Li B, Redel-Traub G, Quien M, Qian Y, et al. Myocarditis in Relation to Angiographic Findings in Patients with Provisional Diagnoses of MINOCA. JACC Cardiovasc Imaging. 2020;13(9):1906-13. doi: 10.1016/j.jcmg.2020.02.037.

28. Adami PE, Koutlianos N, Baggish A, Bermon S, Cavarretta E, Deligiannis A, et al. Cardiovascular Effects of Doping Substances, Commonly Prescribed Medications and Ergogenic Aids in Relation to Sports: A Position Statement of the Sport Cardiology and Exercise Nucleus of the European Association of Preventive Cardiology. Eur J Prev Cardiol. 2022;29(3):559-75. doi: 10.1093/eurjpc/zwab198.

29. Montisci M, El Mazloum R, Cecchetto G, Terranova C, Ferrara SD, Thiene G, et al. Anabolic Androgenic Steroids Abuse and Cardiac Death in Athletes: Morphological and Toxicological Findings in Four Fatal Cases. Forensic Sci Int. 2012;217(1-3):e13-8. doi: 10.1016/j.forsciint.2011.10.032.

30. Carmo EC, Rosa KT, Koike DC, Fernandes T, Silva ND Jr, Mattos KC, et al. Association Between Anabolic Steroids and Aerobic Physical Training Leads to Cardiac Morphological Alterations and Loss of Ventricular Function in Rats. Rev Bras Med Esporte. 2011;17(2):137-41. doi: 10.1590/S1517-86922011000200014 .

31. Oigman W, Neves MFT. Sistema Renina-Angiotensina e Hipertrofia Ventricular Esquerda. Rev Bras Hipertens. 2000;7(3):261-7.

32. Santos MA, Oliveira CV, Silva AS. Adverse Cardiovascular Effects from the Use of Anabolic-Androgenic Steroids as Ergogenic Resources. Subst Use Misuse. 2014;49(9):1132-7. doi: 10.3109/10826084.2014.903751.

33. Pereira BVM, Nascimento BR. Miocardiopatias tóxicas: álcool, anfetaminas e anabolizantes. Rev Med Minas Gerais. 2013;23(3):358-66.

34. Beutel A, Bergamaschi CT, Campos RR. Effects of Chronic Anabolic Steroid Treatment on Tonic and Reflex Cardiovascular Control in Male Rats. J Steroid Biochem Mol Biol. 2005;93(1):43-8. doi: 10.1016/j.jsbmb.2004.11.003.

35. Abdullah R, Bjørnebekk A, Hauger LE, Hullstein IR, Edvardsen T, Haugaa KH, et al. Severe Biventricular Cardiomyopathy in Both Current and Former Long-Term Users of Anabolic-Androgenic Steroids. Eur J Prev Cardiol. 2024;31(5):599-608. doi: 10.1093/eurjpc/zwad362.

36. Sobreira FM Filho, Lino DOC, Belém LS, Rocha RPS, Lima CJM, Alcântra ACB. Acute Myocarditis in User of Anabolic Hormones Diagnosed by Magnetic Resonance Imaging: A Case Report. ABC Imagem Cardiovasc. 2018;31(3):207-10. doi: 10.5935/2318-8219.20180031.

37. Tschöpe C, Ammirati E, Bozkurt B, Caforio ALP, Cooper LT, Felix SB, et al. Myocarditis and Inflammatory Cardiomyopathy: Current Evidence and Future Directions. Nat Rev Cardiol. 2021;18(3):169-93. doi: 10.1038/s41569-020-00435-x.

38. Cooper LT Jr. Myocarditis. N Engl J Med. 2009;360(15):1526-38. doi: 10.1056/NEJMra0800028.

39. Caforio AL, Pankuweit S, Arbustini E, Basso C, Gimeno-Blanes J, Felix SB, et al. Current State of Knowledge on Aetiology, Diagnosis, Management,

and Therapy of Myocarditis: A Position Statement of the European Society of Cardiology Working Group on Myocardial and Pericardial Diseases. Eur Heart J. 2013;34(33):2636-48. doi: 10.1093/eurheartj/eht210.

40. Piatkowski T, Whiteside B, Robertson J, Henning A, Lau EHY, Dunn M. What is the Prevalence of Anabolic-Androgenic Steroid Use among Women? A Systematic Review. Addiction. 2024;119(12):2088-100. doi: 10.1111/add.16643.

A New Frontier in Cardiovascular Prevention: Beyond Prohibition, Clinical Management of Anabolic Steroid Users

Fabio Roston,[1] Alexandre Aby Azar Ribeiro,[1] Naiara Caroline Makiniks,[1] Luiz Felipe Branco Ribeiro,[1] Liliana Ludwing Ziegler[1]

Hospital Norte Paranaense (HONPAR),[1] Arapongas, PR – Brazil

Short Editorial related to the article: Anabolic-Androgenic Steroids and Acute Myocardial Infarction in Young Adults: A Literature Review Based on a Case Series

The traditional approach to Anabolic-Androgenic Steroid (AAS) use has been largely driven by prohibition and stigma. However, with prevalence rates reaching as high as 31.6% in specific populations in Brazil,[1] it has become imperative for the medical community to shift its paradigm: moving from a reactive response to acute events toward a strategic, vigilant, and proactive approach to AAS users. The current challenge is not merely to discourage use, but to identify subclinical cardiovascular disease at an early stage in young individuals who, despite an appearance of robust health, may harbor potentially fatal substrates for Acute Myocardial Infarction (AMI).

Subclinical Diagnosis: The Role of Advanced Echocardiography

Conventional cardiac assessment often fails to detect early damage, as Left Ventricular Ejection Fraction (LVEF) may remain within normal limits despite established myocardial injury. The literature highlights that AAS users exhibit alterations in cardiac geometry and function, including pathological hypertrophy, diastolic dysfunction, and biventricular impairment.[2,3]

In this setting, echocardiography incorporating advanced measurements such as myocardial strain has emerged as an essential diagnostic tool. Although LVEF may remain preserved during the early stages, myocardial deformation (strain) analysis enables the detection of incipient systolic dysfunction resulting from fibrosis and myofibrillar destruction caused by the direct toxic effects of androgens. Recent studies have demonstrated that both current and former AAS users may exhibit persistent biventricular cardiomyopathy,[4] reinforcing the need for continuous monitoring.

Unmasking Occult Dysfunction: Exercise Stress Echocardiography with Global Longitudinal Strain

If resting evaluation is already insufficient to detect early cardiomyopathy in AAS users, exercise stress echocardiography (performed on a treadmill or cycle ergometer) adds a critical diagnostic dimension by assessing contractile reserve and hemodynamic response under conditions that mimic the physiological demands of resistance training and competitive athletic activity. Unlike pharmacologic stress testing, exercise-based stress reproduces the real-world conditions under which these individuals frequently develop symptoms — atypical chest pain, disproportionate dyspnea, presyncope, or unexplained declines in performance — and, in this context, abnormalities concealed at rest often become evident.[5]

The integration of exercise myocardial strain imaging (global and regional longitudinal deformation acquired at peak exercise or immediately during recovery) represents a major advancement in this evaluation. In healthy hearts, a progressively increased Global Longitudinal Strain (GLS) is expected during exercise, reflecting preserved contractile reserve. In AAS users, even when resting LVEF and GLS remain within normal ranges, attenuation or reversal of the expected GLS augmentation under stress is frequently observed, along with regional heterogeneity — findings consistent with subclinical interstitial fibrosis, microvascular ischemia, and early exhaustion of myocardial reserve.

This pattern is particularly valuable for three reasons. First, it provides an early functional marker of androgen-induced cardiomyopathy, capable of identifying the transition from adaptive hypertrophy to pathological remodeling before overt clinical manifestations develop. Second, it allows for arrhythmogenic risk stratification, as regions exhibiting abnormal strain during exercise often correspond to electrically unstable substrates — a critical consideration in a population with an elevated incidence of sudden cardiac death. Third, it offers an objective and reproducible endpoint for longitudinal follow-up, enabling assessment of reversibility after AAS discontinuation and evaluation of therapeutic response to interventions such as Renin-Angiotensin-Aldosterone System (RAAS) blockade and intensive lipid-lowering therapy.

In clinical practice, stress echocardiography with GLS should be considered for symptomatic users, individuals with borderline abnormalities on resting studies (GLS at the lower limit of normal, concentric hypertrophy, or early diastolic dysfunction), and as a pre-participation screening tool for strength athletes with a current or prior history of AAS use. The combination of functional capacity data, blood pressure response to exercise, electrocardiographic findings, and regional myocardial deformation under stress

Keywords

Myocardial Infarction; Anabolic Androgenic Steroids; Cardiomyopathies

Mailing Address: Fabio Roston •
Hospital Norte Paranaense. Rod Pr 218, Km 1. Postal code: 86702-420. Arapongas, PR – Brazil
E-mail: fabioroston7@yahoo.com.br

DOI: https://doi.org/10.36660/abcimg.20260076i

provides a substantially more sensitive risk profile than any single modality alone.

Myocardial Work: Refining the Assessment of Steroid-Induced Cardiotoxicity

One important limitation of GLS is its dependence on afterload. In a population in which systemic hypertension and sustained elevations in systolic blood pressure during exercise are almost the norm — as is often the case among chronic AAS users — a reduction in GLS may underestimate true myocardial injury or, conversely, may reflect hemodynamic status more than underlying myocardial damage. It is precisely within this gap that myocardial work analysis derived from GLS finds its most elegant application.

This method integrates the longitudinal strain curve with an estimated left ventricular pressure curve (derived from noninvasive brachial blood pressure measurements), generating a pressure–strain loop from which four indices are derived: Global Work Index (GWI), Global Constructive Work (GCW) — the energy effectively converted into ventricular ejection — Global Wasted Work (GWW) — energy dissipated through out-of-phase shortening and lengthening — and Global Work Efficiency (GWE). By incorporating afterload into the analysis, these indices provide a functional assessment that is relatively independent of hemodynamic conditions, overcoming one of the major methodological limitations of GLS alone in hypertensive and hypertrophic patients.

Within the specific context of AAS-related cardiotoxicity, this refinement is particularly relevant. Riou and colleagues[6] compared strength athletes using AAS, athletes with Hypertrophic Cardiomyopathy (HCM), and healthy athletic controls. Although both hypertrophic groups demonstrated reduced longitudinal strain, GWE was significantly lower in both AAS users and HCM patients compared with controls (approximately 90% versus 93%). Even more noteworthy was the regional pattern identified: in AAS users, abnormalities in constructive work and efficiency were predominantly localized to the basal septal segments, whereas in HCM, impairment involved both septal and apical segments. This finding provides an additional diagnostic perspective: regional myocardial work mapping may help differentiate androgen-induced toxic hypertrophy from genetically mediated hypertrophy, a clinically critical differential diagnosis in athletes presenting with septal thickening.

From a pathophysiological standpoint, reduced efficiency and increased wasted work reflect segmental dyssynchrony and subclinical interstitial fibrosis resulting from the direct toxic effects of androgens on cardiomyocytes, including myofibrillar destruction, increased collagen synthesis, and electrical remodeling that predisposes individuals to sudden cardiac death.[7] Myocardial work, therefore, represents a marker that integrates functional, mechanical, and potentially prognostic information within a single tool, readily incorporated into resting echocardiographic protocols and, in more advanced centers, into stress echocardiographic evaluations as well.

Accordingly, incorporating myocardial work analysis into the assessment of AAS users should be viewed as a natural refinement step of strain-based evaluation: it adds pathophysiological specificity, reduces the confounding influence of afterload, and provides regional information that may guide differential diagnosis and, potentially, therapeutic monitoring. It should be emphasized, however, that myocardial work remains a promising and physiologically elegant tool, but it has not yet been fully established as a dominant clinical marker.

Myocardial work assessment through strain imaging — both at rest and during stress testing — represents a promising yet still evolving area of investigation in the characterization of the cardiac effects of AASs. Significant gaps remain regarding the establishment of population-specific reference values, the definition of prognostically validated cutoff points, the reversibility of abnormalities following cessation of AAS use, and the impact of therapeutic interventions on myocardial deformation over time. Advancing this field will require robust multicenter longitudinal studies capable of validating the clinical applicability of the method and supporting structured protocols for prevention, early diagnosis, prognostic improvement, and therapeutic monitoring in this unique patient population.

Active Detection of Atherosclerosis: Coronary CT Angiography

The notion that young AAS users are free from atherosclerosis is a dangerous myth. AAS accelerates atherosclerosis through profound disruption of lipid metabolism, increasing Low-Density Lipoprotein (LDL) cholesterol via hepatic lipase activity while simultaneously reducing High-Density Lipoprotein (HDL) cholesterol.[2] Even more concerning is the presence of perivascular inflammation, which may occur even in individuals with very low body fat percentages.[8]

Coronary CT Angiography (CCTA) should be considered as part of an active screening strategy for coronary artery disease in these patients. The CRISP-CT study demonstrated that the Fat Attenuation Index (FAI) measured on CCTA can detect coronary inflammation even before the development of obstructive plaques. Given that AAS users exhibit increased perivascular inflammation and endothelial oxidative stress,[8] CCTA provides substantially more precise risk stratification than traditional clinical risk scores, enabling early identification of patients at risk for plaque rupture or endothelial erosion.

Aggressive Treatment and Therapeutic Alliance

Once risk has been identified, management of comorbidities should be aggressive and multifactorial. Intervention cannot be limited solely to discontinuation of AAS use, which often requires support from a multidisciplinary team due to body image disturbances and anxiety-related disorders. Clinical management should include:

- Rigorous Lipid Control: Use of high-intensity statin therapy to mitigate accelerated atherosclerosis and endothelial dysfunction.

- Hypertension and RAAS Management: AAS use leads to hyperactivation of the RAAS, promoting fibrosis and hypertrophy. Pharmacologic blockade of this system is critical to preventing cardiomyopathy progression.
- Prothrombotic Surveillance: Given the hypercoagulable state associated with increased levels of coagulation factors II, IX, and XI, ongoing assessment of thrombotic risk is warranted.[9]

In summary, physicians' approach to AAS users should be grounded in the science of prevention. By leveraging technologies such as resting and exercise strain imaging, stress echocardiography with GLS, and CCTA, clinicians no longer need to wait for a myocardial infarction to occur before intervening. Instead, they can act during the silent phase of disease, when pathology is already present but still amenable to treatment.

References

1. Abrahin OSC, Souza NSF, Sousa EC, Moreira JKR, Nascimento VC. Prevalence of the Use of Anabolic Androgenic Steroids by Physical Education Students and Professors who Work In Health Clubs. Rev Bras Med Esporte. 2013;19(1):27-30. doi: 10.1590/S1517-86922013000100005.
2. Baggish AL, Weiner RB, Kanayama G, Hudson JI, Lu MT, Hoffmann U, et al. Cardiovascular Toxicity of Illicit Anabolic-Androgenic Steroid Use. Circulation. 2017;135(21):1991-2002. doi: 10.1161/CIRCULATIONAHA.116.026945.
3. Carmo EC, Rosa KT, Koike DC, Fernandes T, Silva ND Jr, Mattos KC, et al. Association between Anabolic Steroids and Aerobic Physical Training Leads to Cardiac Morphological Alterations and Loss of Ventricular Function in Rats. Rev Bras Med Esporte. 2011;17(2):137-41. doi: 10.1590/S1517-86922011000200014.
4. Abdullah R, Bjørnebekk A, Hauger LE, Hullstein IR, Edvardsen T, Haugaa KH, et al. Severe Biventricular Cardiomyopathy in Both Current and Former Long-Term Users of Anabolic-Androgenic Steroids. Eur J Prev Cardiol. 2024;31(5):599-608. doi: 10.1093/eurjpc/zwad362.
5. D'Andrea A, Radmilovic J, Russo V, Sperlongano S, Carbone A, Di Maio M, et al. Biventricular Dysfunction and Lung Congestion in Athletes on Anabolic Androgenic Steroids: A Speckle Tracking and Stress Lung Echocardiography Analysis. Eur J Prev Cardiol. 2022;28(17):1928-38. doi: 10.1093/eurjpc/zwab086.
6. Grandperrin A, Schnell F, Donal E, Galli E, Hedon C, Cazorla O, et al. Specific Alterations of Regional Myocardial Work in Strength-Trained Athletes using Anabolic Androgenic Steroids Compared to Athletes with Genetic Hypertrophic Cardiomyopathy. J Sport Health Sci. 2023;12(4):477-85. doi: 10.1016/j.jshs.2022.07.004.
7. Perry JC, Schuetz TM, Memon MD, Faiz S, Cancarevic I. Anabolic Steroids and Cardiovascular Outcomes: The Controversy. Cureus. 2020;12(7):e9333. doi: 10.7759/cureus.9333.
8. Souza FR, Rochitte CE, Silva DC, Sampaio B, Passarelli M, Santos MRD, et al. Coronary Inflammation by Computed Tomography Pericoronary Fat Attenuation and Increased Cytokines in Young Male Anabolic Androgenic Steroid Users. Arq Bras Cardiol. 2023;120(11):e20220822. doi: 10.36660/abc.20220822.
9. Chang S, Münster AB, Gram J, Sidelmann JJ. Anabolic Androgenic Steroid Abuse: The Effects on Thrombosis Risk, Coagulation, and Fibrinolysis. Semin Thromb Hemost. 2018;44(8):734-46. doi: 10.1055/s-0038-1670639.

Review Article

Echocardiographic Assessment of Diastolic Dysfunction in Special Situations

Antonio Amador Calvilho Júnior[1]
Universidade Paulista,[1] Sorocaba, SP – Brazil

Central Illustration: Echocardiographic Assessment of Diastolic Dysfunction in Special Situations

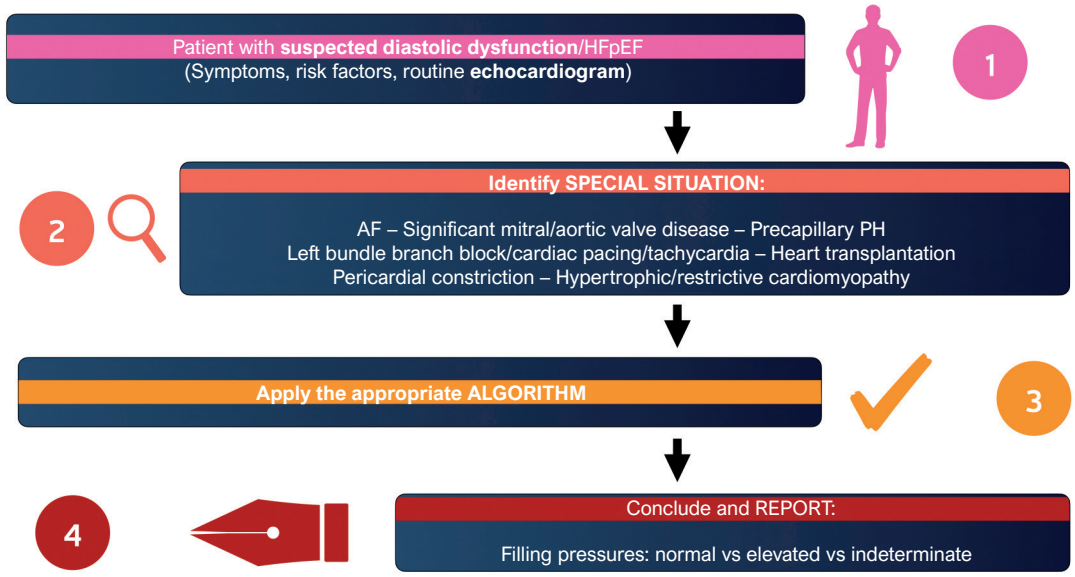

Arq Bras Cardiol: Imagem cardiovasc. 2026; 39(2):e20260029

Proposed framework for the echocardiographic assessment of LV diastolic function in special clinical situations. The figure summarizes the main clinical scenarios in which conventional algorithms may be limited and highlights the adapted diagnostic approaches recommended for each context . AF: Atrial fibrillation; PH: pulmonary hypertension. HFpEF: heart faillure with preserved ejection fraction.

Abstract

Echocardiographic assessment of diastolic function and left ventricular (LV) filling pressures is fundamental to the evaluation of dyspnea and the management of heart failure. However, conventional algorithms have limitations in several special clinical settings in which rhythm disturbances, valvular heart disease, pulmonary hypertension (PH), or structural cardiac abnormalities interfere with the interpretation of Doppler parameters. This article presents a practical approach to assessing diastolic function in conditions such as atrial fibrillation (AF), PH, mitral valve disease, mitral annular calcification, aortic valve disease, conduction disturbances, ventricular pacing, and restrictive cardiomyopathies. The main parameters applicable to each context, the technical aspects of image acquisition, and strategies for preparing a clear and clinically useful echocardiographic report are discussed.

Keywords

Doppler Echocardiography; Stroke Volume; Diastolic Heart Failure

Mailing Address: Antonio Amador Calvilho Júnior •
UNIP Sorocaba, Departamento Medicina. Av Independência, 210. Postal code: 18087-101. Bairro Iporanga, Sorocaba, SP – Brazil
E-mail: dr.calvilho@gmail.com
Manuscript received March 12, 2026, revised manuscript March 23, 2026, accepted March 25, 2026
Editor responsible for the review: Marcelo Tavares

DOI: https://doi.org/10.36660/abcimg.20260029i

Introduction

Left ventricular (LV) diastole is not a passive phase of the cardiac cycle. Relaxation, diastolic suction, and ventricular compliance, together with the interactions among the ventricle, left atrium, and pulmonary circulation, determine

symptoms, hemodynamics, and prognosis across a range of cardiac conditions.

In clinical practice, echocardiographic assessment of diastolic function is generally guided by two key questions: (1) Is diastolic dysfunction present? and (2) Are LV filling pressures elevated at the time of assessment?

The term "LV filling pressures" encompasses different invasive measurements that reflect LV pressure behavior during diastole. Right heart catheterization is used to estimate pulmonary artery wedge pressure (PAWP), whereas left heart catheterization allows measurement of mean left atrial pressure (mLAP), pre-A pressure, and LV end-diastolic pressure (LVEDP). Although these measurements reflect the same underlying pathophysiologic process, they may differ according to the stage and severity of diastolic dysfunction. LVEDP, for example, tends to rise earlier, which has implications for the interpretation of echocardiographic parameters, since some variables correlate better with LVEDP, such as E-wave velocity, whereas others more directly reflect PAWP or pre-A pressure.[1]

In special situations, the correlations between echocardiographic parameters and invasive measurements may be further influenced by factors specific to each clinical condition. A classic example is significant mitral stenosis, in which mLAP and, consequently, pulmonary capillary pressure are elevated without a corresponding increase in LV diastolic pressures. This example illustrates how certain conditions can dissociate atrial and ventricular pressures, reinforcing the need for specific assessment protocols tailored to each clinical context.

Special Situations and Diastolic Assessment

Atrial fibrillation (AF) is the best-known example of a special situation and probably the most widely debated, as beat-to-beat variability and the absence of the A wave affect the applicability of key echocardiographic measurements. In pulmonary hypertension (PH), tricuspid regurgitation (TR) and pulmonary artery systolic pressure (PASP) are no longer reliable indirect markers of left-sided filling pressure. In heart transplant recipients, atrial remodeling and anastomotic scarring may confound traditional indices. This article focuses on these scenarios and provides a practical framework for echocardiographers dealing with such situations.

Assessment Sequence

Diastolic function assessment is generally performed at the end of the echocardiographic examination, since special situations must first be excluded, a process that requires a comprehensive study (Central Illustration).[1-3] The checklist proposed in Table 1 outlines the most likely scenarios in sequence.

Which variables should be used in special situations

In both routine and special situations, isolated measurements should not be used for diagnosis; instead, integration of multiple echocardiographic variables is required. Table 2 summarizes the main clinical situations and the measurements most appropriate for each context.

Assessment of diastolic function in special situations encompasses multiple clinical scenarios, which may hinder the systematic application of diagnostic algorithms. It is therefore useful to recognize which parameters have specific limitations — such as left atrial dimensions in patients with AF — and which can be applied more consistently across different settings. Among the latter, peak TR velocity, except in cases of precapillary PH, and isovolumetric relaxation time (IVRT) stand out, as both have high feasibility and are relatively straightforward to interpret.

AF and PH have specific diagnostic algorithms in the most recent publications that are not based solely on the sequential application of the variables summarized in the

Table 1– Steps to be assessed before proceeding with echocardiographic evaluation of diastolic function

Clinical condition	Implications for diastolic function assessment
What is the presumed or confirmed rhythm (sinus rhythm, AF/flutter, pacemaker rhythm), and does the heart rate allow separation of the E and A waves?	In the presence of AF, specific algorithms should be prioritized. In sinus tachycardia with E–A wave fusion, the assessment should be adapted.
Is there significant mitral valve disease (stenosis, ≥ moderate failure, prosthesis) or ≥ moderate mitral annular calcification?	If so, the standard algorithm may not be applicable, and condition-specific algorithms should be used.[1]
Is there relevant PH or suspicion of precapillary PH?	If so, TR and PASP cannot be used as surrogates for left-sided filling pressure. A specific algorithm is available for assessment in the setting of concomitant precapillary PH.[1]
Do the two-dimensional findings suggest cardiac amyloidosis or hypertrophic cardiomyopathy? Has the structural analysis already provided a coherent overall picture (hypertrophy, LA size, valves, RV, pericardium)? The numerical findings must be consistent with the anatomy.	If so, a condition-specific algorithm should be used.[1]

LA: left atrium; AF: atrial fibrillation; PH: pulmonary hypertension; PASP: pulmonary artery systolic pressure; TR: tricuspid regurgitation; RV: right ventricle.

Table 2 – Main clinical situations and corresponding applicable measurements

Condition	Echocardiographic indicators of elevated filling pressure
AF	1. DT < 160 ms (reduced LVEF) 2. Peak acceleration rate of the E-wave velocity ≥ 1,900 cm/s² 3. IVRT ≤ 65 ms 4. DT of pulmonary venous diastolic flow velocity ≤ 220 ms 5. E/Vp ≥ 1.4 6. Septal E/e′ ≥ 11 7. Peak TR velocity > 2.8 m/s
Sinus tachycardia	1. Early filling pattern (reduced EF) 2. IVRT ≤ 70 ms 3. Pulmonary vein systolic fraction ≤ 40% 4. Mean E/e′ > 14 5. Use of compensatory beats to separate E and A waves
Hypertrophic cardiomyopathy (HCM)	1. Mean E/e′ > 14 2. Ar–A ≥ 30 ms 3. Peak TR velocity > 2.8 m/s 4. LAVI > 34 mL/m²
Restrictive cardiomyopathy	1. Mean E/e′ > 14 2. DT < 140 ms* 3. E/A > 2.5* 4. IVRT < 50 ms*
PH	1. E/A ≥ 2 → favors postcapillary PH 2. E/A ≤ 0.8 → favors precapillary PH 3. If E/A 0.8–2: Lateral E/e′ > 13, LAVI > 34 mL/m², and LA reservoir strain < 18% favor postcapillary PH
Mitral stenosis	1. IVRT < 60 ms* 2. Mitral A > 1.5 m/s 3. IVRT / TE–e′ < 4.2
Mitral regurgitation (MR)	1. IVRT < 60 ms* 2. Ar–A ≥ 30 ms 3. IVRT / TE–e′ < 5.6 4. Mean E/e′ > 14 (valid only if reduced EF)
Moderate to severe mitral annular calcification (MAC)	1. E/A < 0.8 → normal LAP 2. E/A > 1.8 → elevated LAP 3. E/A between 0.8–1.8: • IVRT ≥ 80 ms → normal LAP • IVRT < 80 ms → elevated LAP
Heart Transplant	1. E/e′ < 7 → normal LAP 2. E/e′ > 14 → elevated LAP 3. E/e′ 7–14: • E/SR_{IVRT} ≤ 200 cm → normal LAP • E/SR_{IVRT} > 200 cm → elevated LAP • If SR_{IVRT} is unavailable, use peak TR velocity: – ≤ 2.8 m/s → normal LAP – > 2.8 m/s → elevated LAP

**Variables that are specific but not sensitive for detecting elevated filling pressures in the contexts in which they are presented. Ar–A: difference between the duration of the pulmonary venous atrial reversal wave and that of the transmitral A wave; AF: atrial fibrillation; PH: pulmonary hypertension; LAP: left atrial pressure; PASP: pulmonary artery systolic pressure; TR: tricuspid regurgitation; SR: strain rate; LARS: left atrial reservoir strain; DT: deceleration time; TE–e′: time interval between the E and e′ waves; IVRT: isovolumetric relaxation time; RV: right ventricle; LAVI: left atrial volume index; LVEF: left ventricular ejection fraction; EF: ejection fraction. Adapted from Nagueh et al.[1]*

table. In contrast, among heart transplant recipients and patients with mitral annular calcification, the algorithms presented in current publications are often presented visually but essentially correspond to the same recommendations summarized in the table. Constrictive pericarditis may also be considered a special situation in the assessment of diastolic function; however, because of its distinct pathophysiologic and diagnostic features, it is traditionally discussed separately and therefore will not be addressed in this review.

Atrial fibrillation

The absence of the A wave and cycle-length variability reduces the accuracy of echocardiographic measurements in AF. In a multicenter study involving 148 patients, no single parameter showed an adequate correlation with PAWP, prompting Khan et al. to propose a diagnostic algorithm integrating multiple hemodynamic and structural markers. This algorithm, subsequently incorporated into the 2024 British recommendations and the 2025 American guidelines, allows estimation of ventricular filling pressures even in the absence of the organized atrial contraction characteristic of AF.[1,3,4]

The main parameters include E-wave velocity ≥ 100 cm/s, septal E/e' > 11, peak TR velocity > 2.8 m/s or PASP > 35 mmHg, E-wave deceleration time ≤ 160 ms, left atrial reservoir strain < 18%, pulmonary vein S/D ratio < 1, and body mass index > 30 kg/m². The interpretation of these criteria and their diagnostic sequence are illustrated in Figure 1.

The arrhythmic nature of AF requires additional care when acquiring echocardiographic measurements. To reduce the impact of beat-to-beat variability and improve reproducibility, recording 10 to 15 cardiac cycles at a high sweep speed and averaging multiple beats is recommended. Cycles should be selected with R–R intervals representative of the mean heart rate, ideally with similar preceding R–R intervals, while avoiding post-pause beats and very short cycles with wave fusion. The report should also explicitly state that the values represent averages obtained during AF and acknowledge the inherent beat-to-beat variability of this arrhythmia.

When the algorithm yields an indeterminate classification, the additional variables listed in Table 2 may be used as supportive elements in the interpretation. In addition, relatively low variability in E-wave velocity between consecutive cycles, despite irregular R–R intervals, may suggest elevated filling pressures. Although this finding is not formally included in diagnostic algorithms, it represents a qualitative sign that is often useful in the echocardiographic evaluation of patients with AF.

From a pathophysiologic standpoint, sustained elevation of left atrial pressure (LAP) tends to attenuate the impact of R–R interval variability on the transmitral gradient. Thus, despite rhythm irregularity, persistently elevated E-wave velocities with relatively little variation between consecutive cycles may provide an additional clue to increased filling pressures.

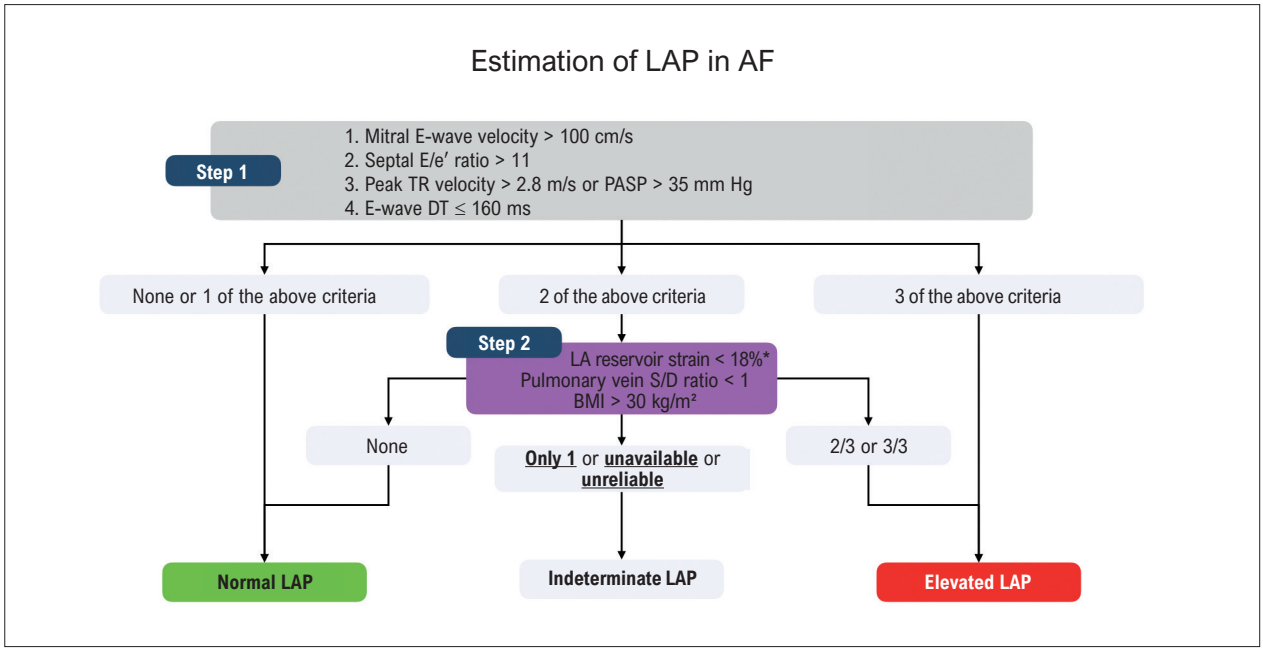

Figure 1 – *Algorithm for estimating LAP in patients with AF. Diagnostic algorithm integrating Doppler parameters and clinical variables to estimate LAP in patients with AF. The approach combines immediate hemodynamic markers with structural or functional consequences of chronically elevated filling pressures. Adapted from Khan et al.[4] AF: Atrial fibrillation; BMI: body mass index; LAP: left atrial pressure; TR: tricuspid regurgitation; LA: left atrial; LARS: left atrial reservoir strain; DT: deceleration time; PASP: pulmonary artery systolic pressure. *Cutoff value in the original study = 16% (Khan et al.[4]), modified to 18% in the 2025 American recommendations for diastolic function assessment (Nagueh et al.[1]).*

Although AF is one of the most common settings in which conventional algorithms for assessing diastolic function have limitations, other clinical scenarios also require specific adaptations in the interpretation of echocardiographic parameters, as discussed in the following sections.

PH with preserved EF: suspected noncardiac (precapillary) PH

In precapillary PH, peak TR velocity and PASP are elevated by definition and therefore cannot be used to infer LV filling pressure. The variables presented in Table 2 are essentially the same as those used in Figure 2, but organized as a flowchart based on the work of Inoue et al. and later incorporated into the 2025 American recommendations and the 2024 British recommendations.[1, 3, 5]

Mitral valve disease and annular calcification

In mitral valve disease, estimation of filling pressures should rely on integration of the variables presented in Table 2, as hemodynamic and structural alterations may affect the interpretation of individual parameters.

Among these conditions, moderate or severe mitral annular calcification deserves particular attention, as reduced annular motion may limit the interpretation of parameters that depend on mitral annular velocity, such as e′. In such cases, use of a specific, easy-to-remember, and clinically applicable algorithm is recommended, allowing direct, dichotomous determination of filling pressures and avoiding the undesirable outcome of an indeterminate classification.[1,6]

Aortic valve disease (aortic stenosis and aortic regurgitation)

In aortic valve disease, estimation of filling pressures is usually feasible, and the standard algorithm can generally be applied. However, it should be recognized that ventricular hypertrophy and myocardial remodeling, which are frequently associated with these conditions, may reduce left atrial reservoir strain and e′ before overt elevation of filling pressures occurs. Therefore, interpretation of these parameters should always take into account the clinical context, the severity of the valvular disease, and the presence of symptoms or signs of congestion.[1, 7]

Conduction disorders and ventricular pacing (left bundle branch block, ventricular pacing, and cardiac resynchronization therapy)

Ventricular dyssynchrony alters regional relaxation and the temporal relationship between transmitral flow and tissue Doppler signals, reducing the accuracy of e′ and E/e′. In first-degree AV block, these variables remain valid only in the absence of E–A fusion. In advanced AV block, when isolated A waves are present, a peak TR velocity > 2.8 m/s may suggest elevated filling pressures.[1]

Restrictive cardiomyopathies and amyloidosis

When a suggestive structural phenotype is identified—including increased ventricular wall thickness, characteristic abnormalities in longitudinal strain, LA enlargement, RV involvement, and PH—a condition-specific assessment is recommended. In these situations, the cutoff values

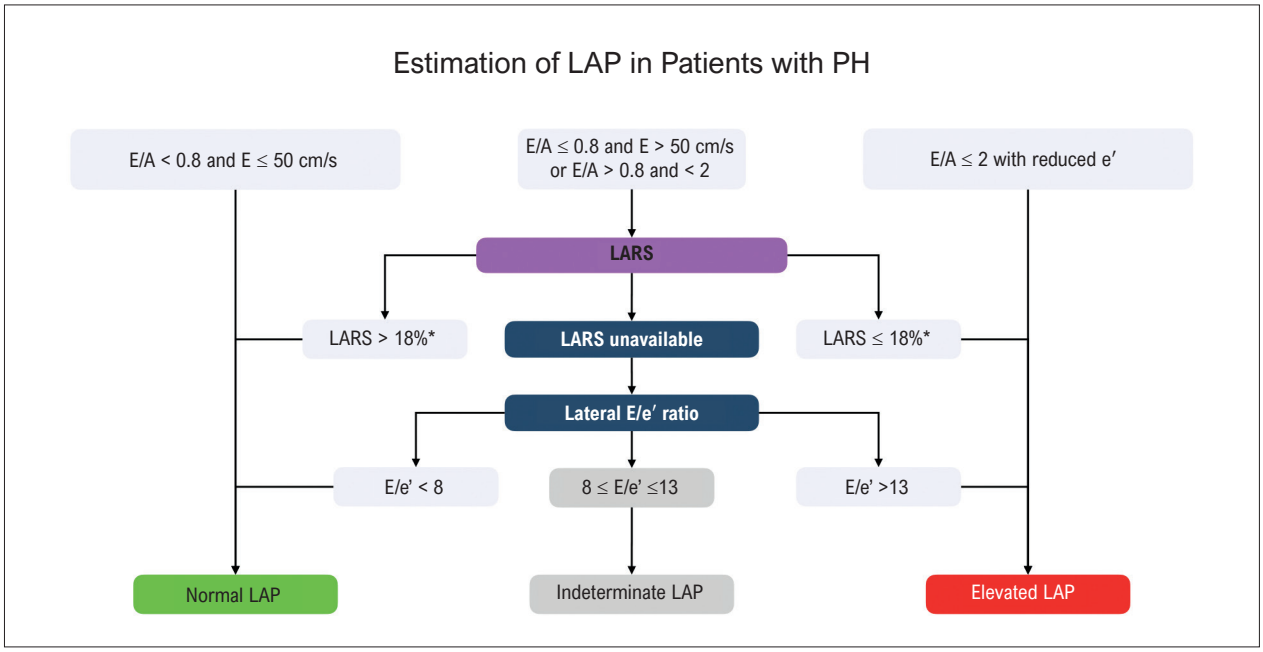

Figure 2 – *Echocardiographic approach to the assessment of diastolic function in PH. Interpretive strategy for echocardiographic parameters of diastolic function in patients with PH, highlighting variables that are useful for differentiating elevated left-sided filling pressures from primarily pulmonary vascular disease. Adapted from Inoue et al.[5] LAP: left atrial pressure; LARS: left atrial reservoir strain; PH: pulmonary hypertension. *Cutoff value in the original study = 16% (Inoue et al.[5]), modified to 18% in the 2025 American recommendations for diastolic function assessment (Nagueh et al.[1]).*

presented in Table 2 differ from those used in other conditions and are more stringent for characterizing elevated filling pressures.

Other special situations

The remaining conditions listed in Table 2 are generally self-explanatory and do not require additional visual algorithms for interpretation. In these settings, Table 2 may serve as a practical guide for selecting the most appropriate variables for each clinical context, thereby facilitating the application of general principles for assessing diastolic function.

Minimum acquisition and report writing (essential elements)

The 2025 ASE recommendations emphasize that the essential parameters must be included in the report, especially when assessment of filling pressures is requested.[1] To avoid confusion for the referring clinician and to maintain internal consistency of the report, the echocardiographer should specify which protocol was used and should primarily report the variables involved in determining filling pressures in that specific context.

In certain special situations, certain variables traditionally used to assess diastolic function should not be considered when estimating filling pressures. One example is significant mitral annular calcification, in which e′ velocity loses accuracy; reporting it with the same emphasis given in routine settings may mislead the treating physician, particularly because widely used clinical scores for the diagnosis of heart failure with preserved ejection fraction incorporate this measurement.[8, 9]

On the other hand, some variables may not be used to determine filling pressures in specific contexts, but should still be reported for their diagnostic or prognostic value. Left atrial dimensions, for example, do not reflect filling pressures in patients with AF but retain prognostic value. Similarly, PASP remains an important variable in the evaluation of patients with suspected precapillary PH.

Although the most recent recommendations still propose a diagnostic framework that first addresses the presence or absence of diastolic dysfunction and then determines filling pressures, the algorithms for special situations are essentially focused on estimating these pressures. In practice, this may create the impression that diastolic dysfunction is always present in such settings, which is not necessarily the case. Moreover, although undesirable, some algorithms applied to special situations may result in an indeterminate classification of filling pressures.

Therefore, meticulous measurement acquisition and appropriate contextualization of the variables used make the echocardiographic report clearer, help prevent misinterpretation, and allow a more reliable estimation of filling pressures across different clinical scenarios.

Conclusions

The most recent updates have introduced important advances in the echocardiographic assessment of filling pressures, including the incorporation of newly validated markers, such as left atrial reservoir strain, and the development of dedicated algorithms for conditions such as AF, PH, and heart transplantation. Taken together, these changes reflect a shift from a purely checklist-based approach to a more contextualized, pathophysiology-based evaluation, with the potential to reduce the frequency of indeterminate results.[1, 3, 4, 7, 10]

In practice, three approaches are particularly helpful: recognizing early when the standard algorithm does not apply; obtaining high-quality measurements from representative cardiac cycles; and reporting the findings clearly and in context, explicitly acknowledging the limitations of the method and recommending complementary testing when appropriate. In this way, echocardiography retains its central role in assessing filling pressures, even in the face of the complexity of special clinical situations.

Ultimately, the echocardiographer must recognize that, in special situations, the value of the examination lies not only in the application of algorithms, but also in the interpretation of hemodynamic signals in light of the clinical context.

Author Contributions

Conception and design of the research, acquisition of data, analysis and interpretation of the data, writing of the manuscript and critical revision of the manuscript for intellectual content: Calvilho-Júnior A.

Potential Conflict of Interest

No potential conflict of interest relevant to this article was reported.

Sources of Funding

There were no external funding sources for this study.

Study Association

This study is not associated with any thesis or dissertation work.

Ethics Approval and Consent to Participate

This article does not contain any studies with human participants or animals performed by any of the authors.

Use of Artificial Intelligence

During the preparation of this work, the author(s) used Chat GPT - Open AI for text formatting (grammar and spelling check). After using this tool/service, the author(s) reviewed and edited the content as needed and take full responsibility for the content of the published article.

Availability of Research Data

The underlying content of the research text is contained within the manuscript.

References

1. Nagueh SF, Sanborn DY, Oh JK, Anderson B, Billick K, Derumeaux G, et al. Recommendations for the Evaluation of Left Ventricular Diastolic Function by Echocardiography and for Heart Failure with Preserved Ejection Fraction Diagnosis: An Update from the American Society of Echocardiography. J Am Soc Echocardiogr. 2025;38(7):537-69. doi: 10.1016/j.echo.2025.03.011.
2. Nagueh SF, Smiseth OA, Appleton CP, Byrd BF 3rd, Dokainish H, Edvardsen T, et al. Recommendations for the Evaluation of Left Ventricular Diastolic Function by Echocardiography: An Update from the American Society of Echocardiography and the European Association of Cardiovascular Imaging. J Am Soc Echocardiogr. 2016;29(4):277-314. doi: 10.1016/j.echo.2016.01.011.
3. Robinson S, Ring L, Oxborough D, Harkness A, Bennett S, Rana B, et al. The Assessment of Left Ventricular Diastolic Function: Guidance and Recommendations from the British Society of Echocardiography. Echo Res Pract. 2024;11(1):16. doi: 10.1186/s44156-024-00051-2.
4. Khan FH, Zhao D, Ha JW, Nagueh SF, Voigt JU, Klein AL, et al. Evaluation of Left Ventricular Filling Pressure by Echocardiography in Patients with Atrial Fibrillation. Echo Res Pract. 2024;11(1):14. doi: 10.1186/s44156-024-00048-x.
5. Inoue K, Andersen OS, Remme EW, Khan FH, Andreassen AK, Skulstad H, et al. Echocardiographic Evaluation of Left Ventricular Filling Pressure in Patients with Pulmonary Hypertension. JACC Cardiovasc Imaging. 2024;17(5):566-7. doi: 10.1016/j.jcmg.2023.12.004.
6. Abudiab MM, Chebrolu LH, Schutt RC, Nagueh SF, Zoghbi WA. Doppler Echocardiography for the Estimation of LV Filling Pressure in Patients with Mitral Annular Calcification. JACC Cardiovasc Imaging. 2017;10(12):1411-20. doi: 10.1016/j.jcmg.2016.10.017.
7. Grapsa J, Argulian E, Smiseth OA. Diastolic Dysfunction: A Comparison of 2025 ASE, 2024 BSE and 2022 EACVI Guidelines. Eur Heart J Cardiovasc Imaging. 2025;26(11):1725-7. doi: 10.1093/ehjci/jeaf269.
8. Rahi W, Lababidi H, Hussain I, Quinones MA, Nagueh SF. Improving the Diagnosis of HFpEF: A Comparison of the H2FPEF Score and the 2025 ASE Diastolic Function Guideline Recommendations Using Invasive Hemodynamics as the Gold Standard. JACC Cardiovasc Imaging. 2026;19(2):166-174. doi: 10.1016/j.jcmg.2025.09.011.
9. Reddy YNV, Carter RE, Obokata M, Redfield MM, Borlaug BA. A Simple, Evidence-Based Approach to Help Guide Diagnosis of Heart Failure with Preserved Ejection Fraction. Circulation. 2018;138(9):861-70. doi: 10.1161/CIRCULATIONAHA.118.034646.
10. Lababidi H, Rahi W, Smiseth OA, Billick K, Inoue K, Khan FH, et al. New Algorithm for Estimating Left Ventricular Filling Pressure by Echocardiography. Circulation. 2025;152(7):424-35. doi: 10.1161/CIRCULATIONAHA.125.074974.

Mitral Valve Leaflet Hypoplasia in Adults: Role of Cardiovascular Imaging

Fábio Luis de Jesus Soares[1,2]
Cardio Pulmonary Hospital,[1] *Salvador, BA – Brasil*
Hospital Santa Izabel,[2] *Salvador, BA – Brasil*

Central Illustration: Mitral Valve Leaflet Hypoplasia in Adults: Role of Cardiovascular Imaging

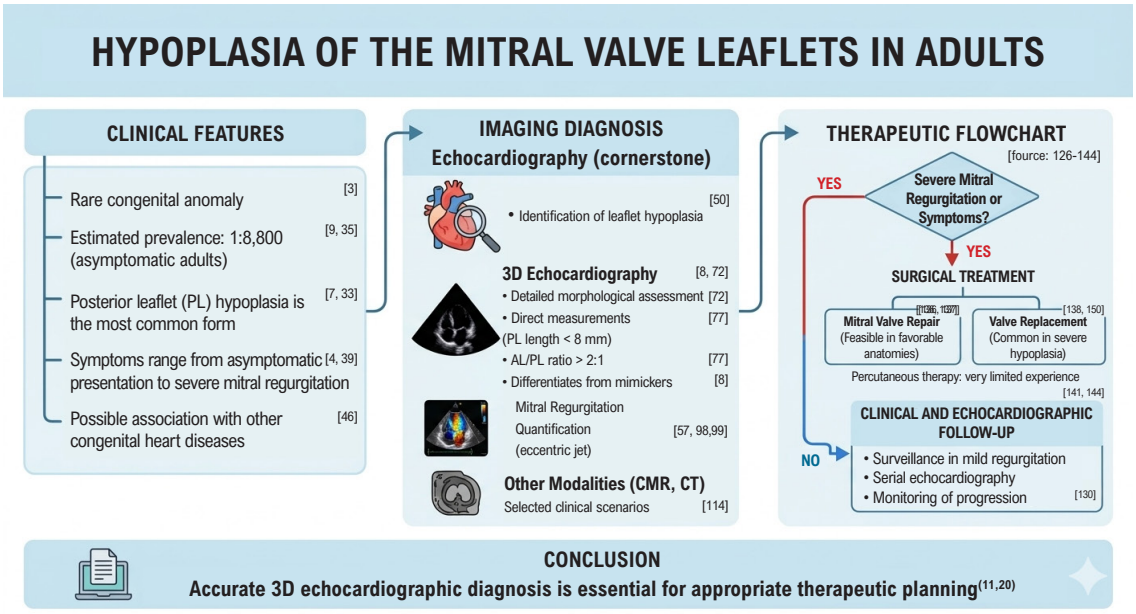

Arq Bras Cardiol: Imagem cardiovasc. 2026;39(2):e20260046

Mitral Valve Leaflet Hypoplasia in Adults

Abstract

Mitral valve leaflet hypoplasia is a rare congenital anomaly, traditionally described in childhood but increasingly recognized in adults, often as an incidental finding or during the evaluation of mitral regurgitation. Clinical presentation is heterogeneous and depends on leaflet anatomy, the subvalvular apparatus, and the severity of regurgitation. In this narrative literature review, including case reports, case series, and review articles from nationally and internationally recognized journals, epidemiological and clinical aspects are discussed, with particular emphasis on echocardiographic findings. Posterior leaflet hypoplasia is the most common form and may be partial or complete. Three-dimensional echocardiography plays a central role in anatomical assessment, enabling direct measurements of leaflet area and length and helping differentiate true hypoplasia from mimicking entities such as mitral cleft, functional restriction, or subvalvular abnormalities. The estimated prevalence in asymptomatic adults is approximately 1:8,800. Therapeutic management is primarily determined by the severity of mitral regurgitation, with valve repair being feasible only in selected anatomical scenarios. Therefore, refined anatomical understanding, particularly through three-dimensional echocardiography, is essential for accurate diagnosis and appropriate therapeutic planning in this rare yet clinically relevant condition.

Keywords

Mitral Valve; Congenital Abnormalities; Three-Dimensional Echocardiography

Mailing Address: Fábio Luis de Jesus Soares •
Cardio Pulmonary Hospital. Av. Garibaldi, 2199. CEP: 40170-130. Ondina, Salvador, BA – Brazil
E-mail: fljsoares@yahoo.com.br
Manuscript received April 15, 2026, revised manuscript April 22, 2026, accepted April 25, 2026
Editor responsible for the review: Marcelo Tavares

DOI: https://doi.org/10.36660/abcimg.20260046i

Introduction

Congenital abnormalities of the mitral valve (MV) form a spectrum that includes prolapse, clefts, duplications,

SUMÁRIO

congenital stenosis, subvalvular apparatus abnormalities, and, more rarely, hypoplasia of one or both leaflets. Among these, posterior leaflet hypoplasia is the most frequently described in the literature and often results in a functional unicuspid mitral valve phenotype.[1]

Historically, mitral leaflet hypoplasia was considered incompatible with life and was predominantly diagnosed in childhood in the context of severe mitral regurgitation (MR). However, over the past two decades, case reports, small series, and literature reviews have described presentations in adults, often asymptomatic or with mild symptoms, identified incidentally on routine echocardiograms[2] (Central Illustration).

From an imaging standpoint, this is a fascinating entity: the MV may maintain adequate coaptation through compensatory elongation of the opposite leaflet, annular remodeling, and left ventricular (LV) adaptations. When these mechanisms fail, MR of varying degrees predominates, generally without significant stenosis.[3]

This article reviews mitral valve leaflet hypoplasia in adults, with special focus on echocardiographic characterization, the role of other imaging modalities, and therapeutic implications.

Prevalence

Posterior mitral leaflet hypoplasia is considered a rare congenital anomaly. In a prospective analysis of 26,484 echocardiographic examinations, Bar et al. identified three cases of asymptomatic posterior leaflet hypoplasia in young adults, estimating a prevalence of approximately 1:8,800 among asymptomatic patients undergoing echocardiography.[2]

A recent systematic literature review that compiled case reports and case series identified approximately 60–70 cases of posterior leaflet hypoplasia/aplasia in adults, reinforcing the exceptional nature of the condition.[2,4] Hypoplasia of the anterior leaflet, the mitral annulus, or the entire MV (as in variants of Shone's complex) is even less frequent, with only isolated cases published.[1]

The true prevalence is likely underestimated, as mild forms without significant MR may go unrecognized on routine echocardiography, particularly when attention is focused solely on regurgitation severity rather than detailed valve morphology.

Clinical Presentation

The clinical spectrum in adulthood is broad. Reported cases range from incidental findings in asymptomatic patients, often evaluated for a soft systolic murmur, to presentations with severe MR, dyspnea, and significant left-sided chamber dilation.[5]

Reported clinical manifestations include:

- **Asymptomatic**: mild hypoplasia with preserved coaptation due to elongated anterior leaflet, without significant MR.[6]
- **Mild symptoms**: palpitations, fatigue, and exertional dyspnea, generally associated with moderate MR.[7,8]
- **Advanced presentations**: dyspnea in higher functional classes, edema, atrial fibrillation, and dilation of the left atrium and LV in the context of severe chronic MR.[3]
- In many reports, there is an **association with other congenital heart diseases**, such as: bicuspid aortic valve, ostium secundum atrial septal defect, left ventricular noncompaction cardiomyopathy, and genetic syndromes (e.g., Marfan syndrome).[4, 6]

Atypical ischemic symptoms, such as nonspecific chest pain, have also been described, although generally secondary to chronic volume overload or coexisting comorbidities rather than the hypoplasia itself.[9,10]

Echocardiographic Findings

Echocardiography is the cornerstone of the diagnosis of MV leaflet hypoplasia, allowing not only morphological identification but also hemodynamic quantification of the associated MR and evaluation of cardiac chambers.

Two-Dimensional Transthoracic Echocardiography

Typical findings include (Figure 1):

- **Marked reduction in the length of one leaflet**, most commonly the posterior leaflet, which may appear as a small rudimentary structure with limited mobility in parasternal long-axis and apical four-chamber views.[5,11]

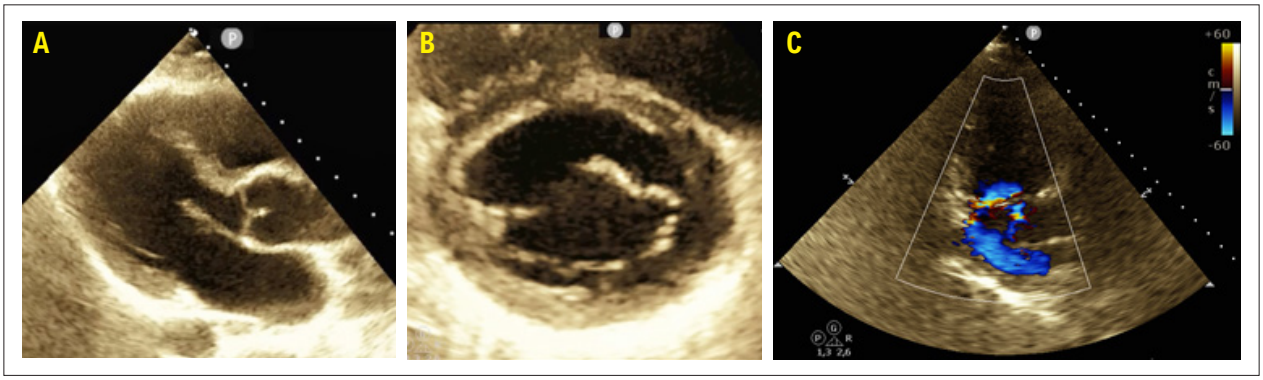

Figure 1 – *Posterior mitral leaflet hypoplasia on transthoracic echocardiography: (A) parasternal long-axis view demonstrating an anterior leaflet disproportionately elongated relative to the posterior leaflet; (B) mitral valve short-axis view demonstrating absence of stenosis; (C) apical two-chamber view demonstrating eccentric jet.*

• **Opposite leaflet (usually anterior) elongated and sometimes thickened**, projecting deeply into the ventricular cavity, often with a myxomatous appearance and occasionally associated prolapse, serving as a compensatory mechanism for coaptation.[6]

• **Coaptation line displaced** toward the hypoplastic leaflet, resulting in an eccentric MR jet directed toward that side.[4]

• **Subvalvular apparatus** generally preserved, although shortening or anomalous chordal insertion into the hypoplastic leaflet may occur, contributing to restriction.

• **Absence of significant stenosis**, with preserved valve area and low transmitral gradients in most cases; when stenosis is present, it is usually related to annular hypoplasia or more diffuse MV involvement.[12]

Some authors propose **comparative measurements**: the ratio between anterior and posterior leaflet lengths (typically > 2:1 in cases of severe posterior leaflet hypoplasia) and assessment of the effective coaptation area.[13]

Transesophageal Echocardiography (TEE) and 3D

The complex mitral anatomy requires systematic analysis, and three-dimensional echocardiography (3D TEE and 3D TTE) has become the most important tool for characterizing hypoplasia.

Although universal measurement standards have not yet been established, three parameters are consistently reported in series and case reports[3,4] (Figure 2):

a) Leaflet length

The normal posterior leaflet (PL) measures on average **10–15 mm** (varying with body surface area [BSA]). Findings suggestive of hypoplasia include:

• **Length < 8 mm** (criterion used in several case series)
• **Anterior-to-posterior leaflet ratio > 2:1**, with > 2.3–2.5:1 frequently cited in significant hypoplasia

b) Leaflet area (3D planimetry)

PL areas < **1.0–1.2 cm²** are reported in clinically relevant hypoplasia. The anterior leaflet (AL) area is generally preserved or compensatorily increased.

c) Coaptation height

Coaptation is displaced toward the hypoplastic leaflet. Abnormal findings include:

• **Coaptation height < 2 mm over PL**

• **Elongated coaptation over the AL, with displacement > 5 mm from the anatomic center**

Based on these criteria, posterior leaflet hypoplasia may be categorized as partial or total:

Partial hypoplasia

• PL present but **shortened**, **restricted,** or **underdeveloped** (Figure 3);

• Chordae often thin or abnormally inserted;

• Compensatory anterior leaflet function, maintaining some degree of coaptation.

In published cases, predominant hypoplasia includes:
• **P2**: most common (40–60% of reported cases);

• **P1**: less frequent;

• **P3**: usually associated with chordal anomalies and subvalvular restriction.

Total hypoplasia (aplasia)

Reported in a few adult cases and considered a "true unicuspid mitral valve."

• Complete anatomic absence of the PL in the atrial "en face" view (Figure 4);

• Aberrant subvalvular insertions;

• Coaptation sustained exclusively by the anterior leaflet, often markedly elongated;

• Generally associated with severe MR, although mild MR due to anterior leaflet compensation has been described.

Furthermore, 3D imaging clearly differentiates **true hypoplasia** from mitral cleft, segmental prolapse, functional restriction, and leaflet elongation without congenital hypoplasia.

Doppler and Regurgitation Quantification

Color Doppler demonstrates an eccentric jet directed opposite the hypoplastic leaflet, frequently wall-hugging (Coanda effect), which may underestimate MR severity if assessed solely by jet area (Figure 5).[3]

Therefore, the following are recommended:

• **Calculation of regurgitant volume and effective regurgitant orifice area (EROA)** using the PISA method, when feasible;

• Assessment of **vena contracta**, preferably in multiple views;

• Integration with indirect parameters: left atrial size, LV diameters and volumes, and pulmonary artery systolic pressure;

• True coaptation area;

• 3D regurgitant volume;

• Anatomic regurgitant orifice area (3D EROA), useful in eccentric jets;

• Complete mitral annular reconstruction (diameters, nonplanar angle, saddle height), frequently altered in significant hypoplasia cases.[5]

In pure hypoplasia with adequate compensation by the opposite leaflet, MR may be absent or mild; in cases with annular dilation and associated prolapse, MR tends to be severe.[13]

Other Imaging Modalities

Although echocardiography is the first-line method, **cardiac magnetic resonance (CMR)** and **computed tomography (CT)** may complement evaluation in selected situations.

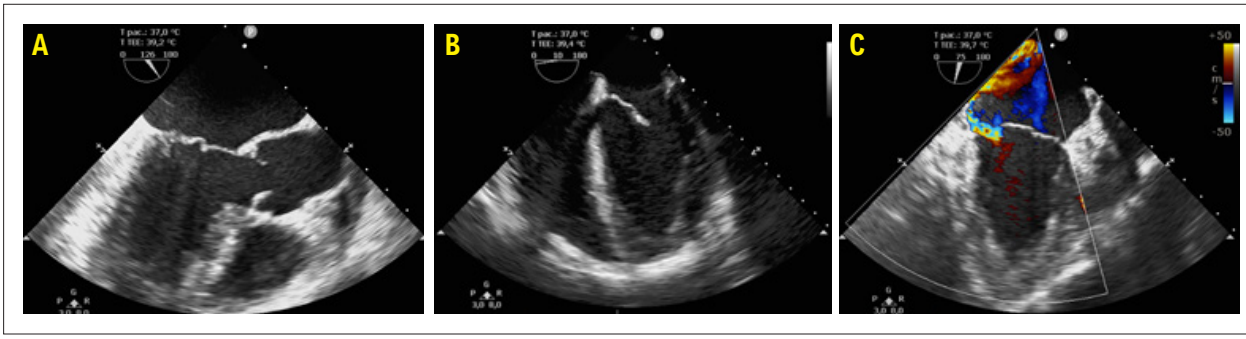

Figure 2 – *Transesophageal echocardiography demonstrating coaptation displaced toward the posterior leaflet (A), an anterior-to-posterior leaflet ratio > 2:1 (B), and the eccentric jet resulting from ineffective coaptation (C).*

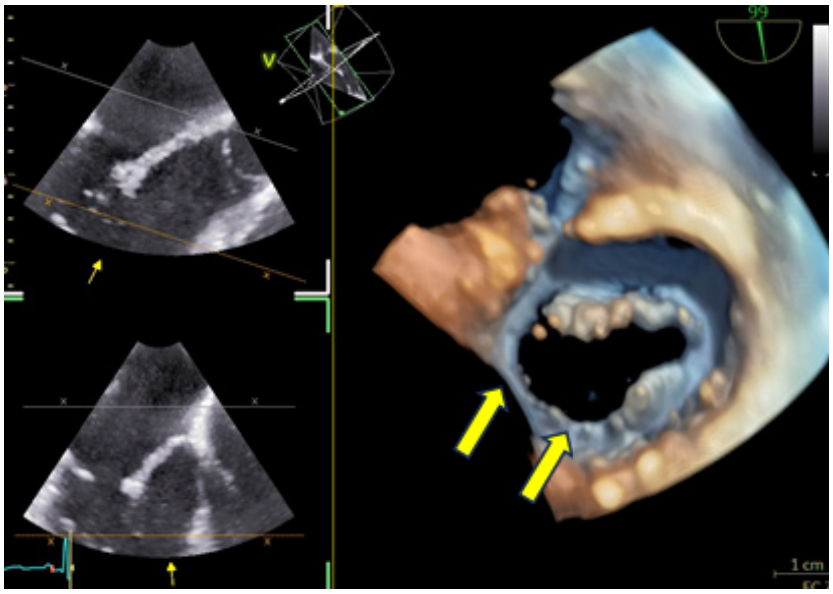

Figure 3 – *Three-dimensional transesophageal echocardiography with ventricular view of the mitral valve demonstrating partial posterior leaflet hypoplasia (segments P2 and P3 – yellow arrows).*

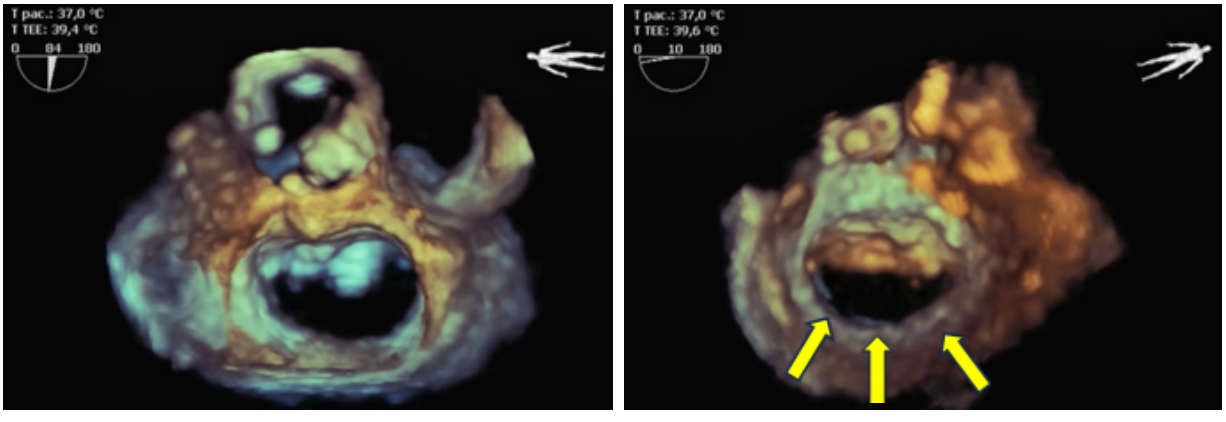

Figure 4 – *Three-dimensional transesophageal echocardiography with atrial and ventricular views of the mitral valve demonstrating complete posterior leaflet hypoplasia (segments P1, P2, and P3 – yellow arrows).*

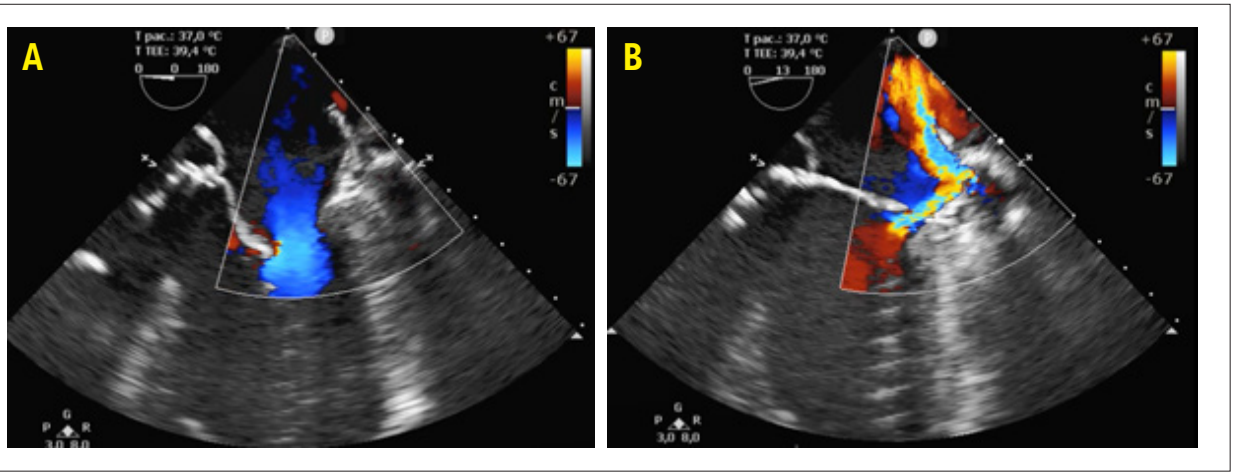

Figure 5 – *Two-dimensional transesophageal echocardiography demonstrating antegrade (A) and eccentric retrograde flows.*

Cardiac Magnetic Resonance

CMR contributes primarily in three aspects:

1. Precise volumetric and functional assessment of the LV and left atrium, useful for quantifying the impact of chronic MR and aiding surgical decision-making.

2. Regurgitation quantification by phase-contrast flow (difference between LV stroke volume and ascending aortic flow), providing a measure independent of echocardiography.

3. Tissue characterization of the mitral annulus and intervalvular fibrosa region in cases with suspected fibroelastosis, lipomatosis, or fibrosis associated with annular or anterior leaflet hypoplasia.[12]

Case reports show that CMR may confirm annular restriction with limited opening even in the absence of a significant gradient and exclude additional structural heart disease.[1]

Cardiac Computed Tomography

Cardiac CT may be useful in:

- Patients with suboptimal echocardiographic windows;
- Detailed anatomic assessment of the mitral annulus and its relationships with adjacent structures, particularly in the planning of complex surgeries or concomitant procedures (e.g., aortic valve replacement in patients with bicuspid aortic valve and mitral leaflet hypoplasia).[11]

However, due to the low prevalence of the entity and the high sensitivity of echocardiography (particularly 3D TEE), CMR and CT remain complementary rather than routine modalities.

Treatment

There are no specific guidelines for managing MV leaflet hypoplasia in adults; decisions generally follow recommendations for primary MR, adapted to the peculiar anatomic context.

Clinical and Echocardiographic Follow-up

Asymptomatic patients with mild or no MR and without significant chamber dilation may be followed clinically, with serial echocardiography to monitor MR progression, ventricular remodeling, and the emergence of symptoms or arrhythmias.[6]

Follow-up intervals are typically annual or biennial, depending on MR severity and remodeling degree.

Surgical Approach

Most adult patients described in the literature with severe MR or limiting symptoms have undergone surgical treatment. Options include:

- **Mitral valve repair**: technically challenging when the hypoplastic leaflet is very short with limited coaptation area. In some cases, leaflet augmentation with pericardium, annuloplasty, and correction of opposite leaflet prolapse are feasible;[4]
- **Mitral valve replacement:** often the most common solution in scenarios of severe hypoplasia, small annulus, or multiple associated anomalies in which durable repair is unlikely.[9]

Some reports question whether repair should always be attempted, particularly when challenging anatomy increases the risk of early reoperation.[3]

Percutaneous Therapy

Experience with **transcatheter edge-to-edge repair (MitraClip/PASCAL-type procedures)** in leaflet hypoplasia is very limited. The reduced height of the hypoplastic leaflet increases the risk of incomplete leaflet grasp, residual regurgitation, and functional stenosis after clipping.

In practice, these patients are rarely considered good candidates, except in highly selected cases with favorable opposite leaflet anatomy and high surgical risk. Current literature includes only indirect mentions, without robust series specific to this population.[3]

Conclusion

Mitral valve leaflet hypoplasia in adults, particularly of the posterior leaflet, is a rare, likely underdiagnosed entity with a

wide spectrum of clinical presentation - from incidental finding to symptomatic severe MR.

Transthoracic and transesophageal echocardiography, particularly with three-dimensional reconstruction, constitute the diagnostic cornerstone, enabling precise characterization of valve morphology, MR quantification, and planning of surgical or percutaneous interventions. Complementary modalities such as CMR and CT add anatomic and functional information in selected situations.[2,3,12]

From a therapeutic standpoint, management follows principles of primary MR, with clinical surveillance in mild cases and surgical indication in symptomatic patients or those with significant structural impact. Mitral repair may be feasible in favorable anatomies, but severe hypoplasia often leads to valve replacement. Evidence for percutaneous therapies remains limited and based on extrapolation.[2,13]

Given the still-limited number of reported cases and series, there is room for **multicenter registries** and **standardized descriptions** to better understand natural history, predictors of decompensation, and long-term outcomes of different therapeutic strategies. For the echocardiographer and cardiovascular imaging specialist, maintaining a high index of suspicion in the presence of "unusual" MV morphology is essential to avoid missing this rare - but clinically relevant - diagnosis.

Author Contributions

Conception and design of the research, data acquisition, analysis and interpretation of data, writing of the manuscript, and critical revision of the manuscript for important intellectual content: Fares FLJ.

Potential Conflict of Interest

No potential conflict of interest relevant to this article was reported.

Sources of Funding

There were no external funding sources for this study.

Study Association

This study is not associated with any thesis or dissertation work.

Ethics Approval and Consent to Participate

This article does not contain any studies with human participants or animals performed by any of the authors.

Use of Artificial Intelligence

The authors did not use any artificial intelligence tools in the development of this work.

Availability of Research Data

The underlying content of the research text is contained within the manuscript.

References

1. Séguéla PE, Houyel L, Acar P. Congenital Malformations of the Mitral Valve. Arch Cardiovasc Dis. 2011;104(8):465-79. doi: 10.1016/j.acvd.2011.06.004.
2. Koenig B, Ionescu A, Galli E. Posterior Mitral Valve Hypoplasia: Three Clinical Cases and a Review of the Literature. Biomedicines. 2025;13(5):1078. doi: 10.3390/biomedicines13051078.
3. Pourafkari L, Baghbani-Oskouei A, Toufan M, Ghaffari S, Nader ND. Hypoplastic Posterior Mitral Valve Leaflet: A Case Report and Review of the Literature. Echocardiography. 2018;35(7):1052-5. doi: 10.1111/echo.13898.
4. Parato VM, Masia SL. Hypoplasia or Absence of Posterior Leaflet: A Rare Congenital Anomaly of the Mitral Valve in Adulthood - Case Series. J Cardiovasc Echogr. 2018;28(1):45-7. doi: 10.4103/jcecho.jcecho_73_17.
5. Bhardwaj A, Pillai AA, Balaguru S. A Case of Hypoplastic Posterior Mitral Leaflet-Related Severe Mitral Regurgitation Associated with Ostium Secundum Atrial Septal Defect. Eur Heart J. 2022;43(36):3497. doi: 10.1093/eurheartj/ehac371.
6. Yazdan-Ashoori P, Rohani A, Mulji AS, van Spall HG. Hypoplasia of the Posterior mitral Valve Leaflet Detected in Late Adulthood. Eur Heart J. 2015;36(7):456. doi: 10.1093/eurheartj/ehu335.
7. Shah J, Jain T, Shah S, Mawri S, Ananthasubramaniam K. Rare Case of Unileaflet Mitral Valve. J Cardiovasc Ultrasound. 2016;24(2):168-9. doi: 10.4250/jcu.2016.24.2.168.
8. Murphy C, Madeloso L, Chandrala P. Hypoplasia of the Posterior Mitral Leaflet Diagnosed in Adulthood. Eur Heart J Case Rep. 2019;3(2):ytz083. doi: 10.1093/ehjcr/ytz083.
9. Fazlinezhad A, Azari MA, Bigdellu L. Severe Hypoplasia of Posterior Mitral Valve Leaflet Presented with Atypical Chest Pain: A Case Report. Razavi J Med. 2016;5(1):22-3. doi: 10.30483/rijm.2016.118354.
10. Gabaldón-Pérez A, Marcos-Garcés V, Muñoz Gil J, Gascó FJC, Santas E. Hypoplasia of the Posterior Mitral Valve Leaflet: Don't Forget to Look Beyond the Mitral Valve. Echocardiography. 2021;38(1):142-3. doi: 10.1111/echo.14910.
11. Velarde-Acosta K, Ramirez JYM, Medina-Maguiña JM, Baltodano-Arellano R. Hypoplastic Posterior Leaflet Mitral Valve Associated with Bicuspid Aortic Valve. CASE. 2024;8(3Part A):151-6. doi: 10.1016/j.case.2023.12.025.
12. Zavar R, Sani ZA, Kermani-Alghoraishi M, Alizadehsani R, Behjati M. Congenital Hypoplastic Mitral Valve Annulus: An Incidental Finding in a 30-Year-Old Male with Pericarditis. Multidiscip Cardio Annal. 2023;14(1):e137811. doi: 10.5812/mca-137811.
13. Karaduman A, Yılmaz C, Balaban İ, Aytürk M, Sarı M, Bayram Z, et al. An Echocardiographic Study of a Rare Cause of Mitral Regurgitation: Hypoplastic Posterior Mitral Valve Leaflet. Anatol J Cardiol. 2024;29(3):124-31. doi: 10.14744/AnatolJCardiol.2024.4710.

Recognition of Clinical Stages and Myocardial Damage in Aortic Stenosis: Beyond Diagnosis – To Op or Not To Op

Daniel Franca Vasconcelos[1]

Universidade de Brasília, Faculdade de Medicina, Hospital Universitário de Brasília,[1] Brasília, DF – Brazil

Central Illustration: Recognition of Clinical Stages and Myocardial Damage in Aortic Stenosis: Beyond Diagnosis – To Op or Not To Op

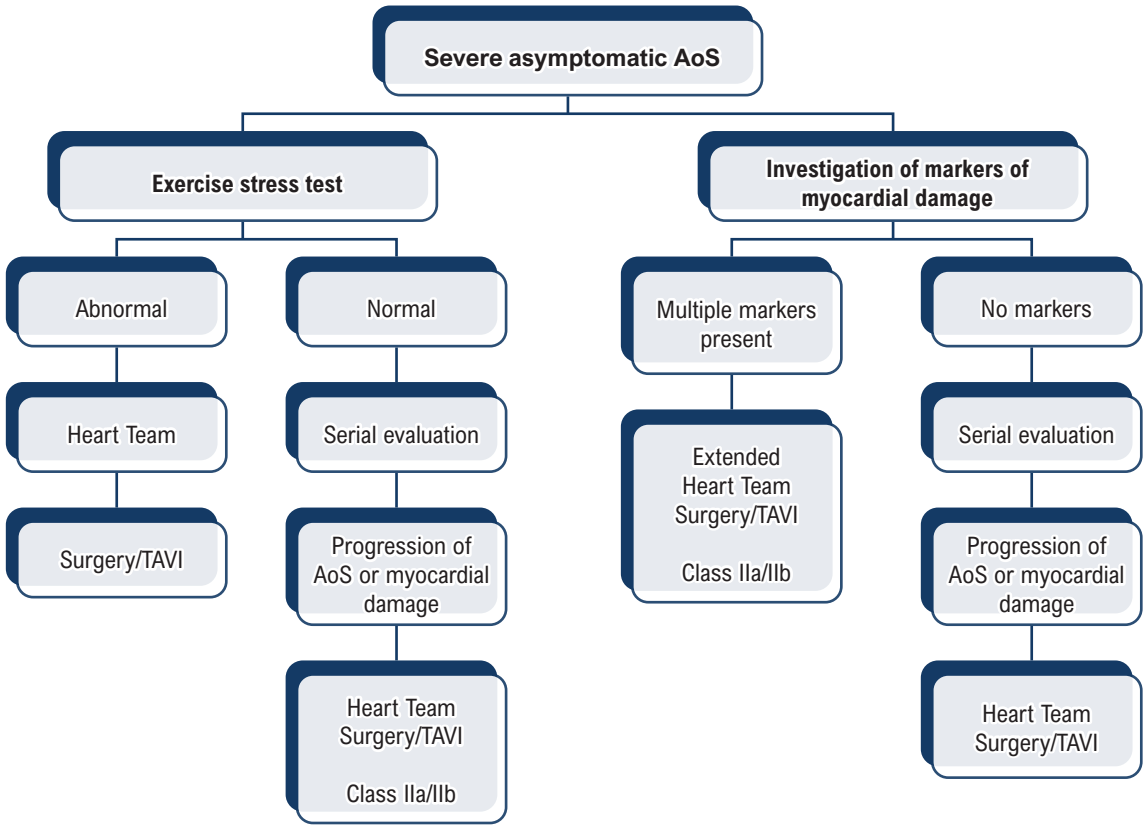

Arq Bras Cardiol: Imagem cardiovasc. 2026;39(2):e20260054

Proposed flowchart for guiding the management of patients with severe aortic stenosis, differentiating between healthy and frail patients. AoS: aortic stenosis; TAVI: transcatheter aortic valve implantation.

Keywords

Aortic Valve Stenosis; Echocardiography; Magnetic Resonance Imaging

Mailing Address: Daniel Franca Vasconcelos •
Universidade de Brasília. Hospital Universitário de Brasília. Postal code: 70910-900. Brasília, DF – Brazil
E-mail: dfrancav@uol.com.br
Manuscript received April 7, 2026, revised manuscript April 22, 2026, accepted April 22, 2026
Editor responsible for the review: Marcelo Tavares

DOI: https://doi.org/10.36660/abcimg.20260054i

Abstract

Severe aortic stenosis is a progressive clinical entity that has historically developed alongside descriptions of pathological anatomy, cardiovascular semiology, heart surgery, and percutaneous cardiovascular interventions. Indication for valve replacement in patients with severe aortic stenosis is still based on symptom onset. With advances in surgical techniques, especially transcatheter implantation, the focus has shifted to identifying early markers of myocardial damage that may indicate irreversible myocardial injury. This review article seeks to provide a comprehensive analysis

of methods for identifying myocardial damage in patients with severe aortic stenosis, including clinical evaluation, electrocardiography (ECG), echocardiography, cardiac magnetic resonance imaging (CMR), and plasma biomarkers. It also discusses the staging of myocardial damage and the optimal timing for therapeutic intervention based on clinical, functional, and structural findings. Recent studies designed to address how to manage asymptomatic patients with aortic stenosis have yielded divergent results. Accordingly, the aim is to assist clinicians in deciding the optimal timing for valve replacement, taking individual patient characteristics into account.

Introduction

Aortic stenosis is the most frequently surgically treated valvular heart disease in the current population.[1] The clinical entity has evolved concomitantly with descriptions of pathological anatomy, cardiovascular semiology, cardiac surgery, and, recently, percutaneous cardiovascular interventions.

In 1663, the French physician Lazare Rivière described the first anatomopathological finding of a stenotic aortic valve.[1] Subsequently, Giovanni Battista Morgagni and Jean-Nicolas Corvisar described an "ossified aortic valve" that did not allow the passage of relevant-sized structures. In 1819, Laënnec described ossified aortic stenosis as a valvular clinical entity with the currently recognized semiological characteristics.[2]

The twentieth century was characterized by detailed anatomopathological description, knowledge of the pathophysiology of the disease, and the development of surgical techniques with increasingly sophisticated prostheses, followed by the development of percutaneous interventions in the twenty-first century. It is currently possible to estimate the degree of progression of aortic stenosis based on echocardiographic epidemiological studies.[3]

Notwithstanding advances in knowledge of pathophysiology, the only current therapeutic option for calcified aortic valve stenosis remains valve replacement.[4] Current guidelines, including the Brazilian guideline, recommend that valve replacement be indicated in patients with severe aortic valve stenosis (peak Doppler velocity > 4.0 m/s, mean gradient > 40 mmHg, valve area < 1.0 cm^2, or indexed valve area < 0.6 cm^2/m^2) who present with symptoms, or in patients with severe stenosis and reduced ejection fraction (< 50%).[5]

With the advent of transcatheter aortic valve implantation (TAVI), it has become possible to perform valve replacement in frail patients with high surgical risk, for whom surgical intervention would be prohibitive.[6] The enthusiasm stemming from the favorable results of percutaneous intervention and the development of new techniques for assessing myocardial damage has led to greater interest in identifying early markers of myocardial damage to indicate valve replacement.[7]

The central question that therefore follows is: Since percutaneous intervention has proven to be safe, why not indicate valve replacement in patients with severe calcified stenosis before symptoms appear? Although the procedure is considered safe, it is not without risks. In some situations, it can worsen the clinical condition and quality of life, in addition to the fact that prosthesis durability has not been fully defined from an epidemiological point of view.[8] The mortality of asymptomatic patients under expectant management is less than 1% per year, much lower than that expected after surgical valve replacement. On the other hand, the durability of the new prostheses (valve prostheses) has not been tested.

Regarding expectant management, several studies have attempted to identify myocardial damage through electrocardiography (ECG), exercise stress testing, reduction in ejection fraction and myocardial strain by echocardiography, transvalvular gradient response to physical stress echocardiography, myocardial fibrosis and edema by cardiac magnetic resonance imaging (CMR), and plasma biomarkers such as B-type natriuretic peptide (BNP) and N-terminal pro-B-type natriuretic peptide (NT-proBNP).[9]

In spite of all these advances, studies comparing expectant management with early intervention have not demonstrated benefits, and there are still challenges in defining the optimal timing for intervention.[10] The purpose of this article is to review the methods for identifying myocardial damage and suggest the most appropriate timing for valve replacement intervention, before irreversible myocardial damage occurs, as well as to propose designs for future studies.

Epidemiological implications

Calcified aortic valve stenosis has a prevalence of 0.4% in the general population, increasing to 1.7% at age 65 and 3.4% at age 75; in other words, it increases significantly after 65 years of age.[11] Bicuspid aortic valve has a prevalence of 0.5% to 1.0% in the population and is responsible for approximately 50% of valve interventions, especially in younger patients.[12] Surgery for calcified aortic valve stenosis represents 47% of all valve surgeries performed.[12]

In spite of recent knowledge about the pathophysiology of calcified valve disease, to date there is no specific clinical treatment for this condition.[13] Symptom onset represents the defined threshold for the indication of valve replacement. From symptom onset, expectant management (without intervention) is associated with a 50% mortality rate within 2 years.[14]

Pathophysiology

Calcified aortic valve disease shares the same pathophysiological mechanisms and risk factors as atherosclerotic disease. In the initial phase, the inflammatory process predominates, followed by the calcification phase.[15] More recently, the deposition of lipoproteins, such as apoA1, apoB, apoE and lipoprotein(a), has been highlighted, followed by inflammation, oxidative stress, osteogenic differentiation of interstitial cells, and subsequent calcification.[15]

Risk factors for the development of calcified valvular disease include bicuspid aortic valve, age, male sex, smoking, systemic arterial hypertension, dyslipidemia, obesity, metabolic syndrome, diabetes mellitus, elevated

lipoprotein(a), mediastinal radiotherapy, chemotherapy, and rheumatological diseases.[15,16] Regarding the risk of more rapid progression to severe aortic stenosis, the following stand out: advanced age, female sex, hemodynamic severity of the initial stenosis, degree of valve calcification, active smoking, uncontrolled systemic arterial hypertension, metabolic syndrome, hyperparathyroidism, chronic renal failure, and elevated lipoprotein(a).[16]

The advent of percutaneous intervention in patients with prohibitive surgical risk has opened a window of therapeutic opportunity for these patients. On the other hand, a trend has emerged to perform this type of procedure in situations where the cost-benefit should be carefully discussed in the context of a multidisciplinary Heart Team. The concept of an extended Heart Team includes the participation of nephrologists, geriatricians, neurologists, nutritionists, patients, and family members, especially for the population of frail patients with multiple morbidities.[17] Despite the lower risk compared to conventional surgery, studies in patients with high frailty have shown results that question the indiscriminate indication of early intervention.[18]

Adaptation to pressure overload and myocardial damage

Following sustained pressure overload, an increase in myofibrillar content is observed, with a consequent increase in left ventricular mass. This increase in mass leads to a reduction in coronary microcirculation density and an increase in coronary vascular resistance. Coronary reserve is progressively reduced, initially only during exertion, and subsequently at rest as well.[19]

Consequently, the myocardium is subjected to repeated ischemia, initially manifesting as diastolic dysfunction.[19] With recurrent ischemia, fibrosis subsequently develops. Initially, this fibrosis is interstitial, diffuse, and reversible after valve replacement. In later stages, the fibrosis is substitutive, focal, and irreversible. Subsequently, changes in the functional geometry of the left ventricle occur, resulting in increased end-diastolic pressure. This increase is transmitted to pulmonary venous pressure, and symptoms of pulmonary congestion appear (dyspnea on exertion).[19] Ischemia may manifest with symptoms of angina. Impaired ejection flow, especially during exertion, is responsible for symptoms of pre-syncope and syncope, particularly during exertion.[19]

Once the mechanism of myocardial damage has been understood, it is imperative to use the available diagnostic tools in a rational and individualized manner. As previously mentioned, there is still no drug treatment for calcified aortic stenosis. Despite knowledge about the mechanisms of myocardial damage, we still do not fully understand the implications of early intervention before the onset of symptoms.[19]

Identifying myocardial damage

Clinical evaluation

According to current guidelines, intervention in patients with severe aortic stenosis should be indicated when symptoms appear.[5] Although the classic symptoms (dyspnea, angina, and syncope) have been well defined, their identification can be challenging in certain populations.

Patients with aortic stenosis secondary to bicuspid aortic valve are typically younger (approximately 20 years younger than those with degenerative aortic stenosis), physically active, and without significant comorbidities.[20] In these cases, in addition to clinical history and physical examination with the goal of identifying symptoms, an exercise stress test is recommended in order to identify functional limitations and reproducible symptoms.[20]

In contrast, patients with degenerative calcified aortic stenosis present a completely different clinical profile. They are elderly, often with orthopedic problems, chronic lung diseases, and cognitive impairment. In this scenario, it is very difficult to adequately identify symptoms of ischemia or congestion.[21]

Regardless of profile, asymptomatic patients with severe aortic stenosis should be monitored periodically every 3 to 6 months, with the expectation of identifying emerging symptoms or changes on ECG and echocardiography.[5]

Electrocardiogram

ECG can provide important information related to left ventricular overload in the assessment of myocardial damage. An ECG with findings suggestive of left ventricular overload (left ventricular hypertrophy) in asymptomatic patients with severe aortic stenosis, estimated by the transvalvular gradient on echocardiography, represents a warning sign (yellow flag) that justifies intensified monitoring.[22] Studies of prognostic markers suggest that ventricular hypertrophy, identified by ECG, echocardiogram, or CMR, represents a worse outcome compared to patients without ventricular hypertrophy. The presence of arrhythmia, especially atrial fibrillation, can result from increased ventricular filling pressure secondary to diastolic dysfunction, followed by left atrial overload, and may indicate myocardial damage.

Exercise stress test

Exercise stress tests play an important role in the evaluation of asymptomatic patients with severe aortic stenosis. This test can reveal typical symptoms (dyspnea disproportionate to exertion, precordial angina, or syncope) that were not detected at rest, in up to 30% of individuals considered asymptomatic, thus guiding the decision to intervene. In addition to symptoms, a hypotensive response to exertion, ischemia on ECG, or the appearance of malignant arrhythmias are also indicators of greater severity, with a relative risk more than 7 times higher compared to patients with normal results.[23]

Echocardiography

Transthoracic echocardiography is the method of choice for evaluating aortic valve anatomy, quantifying stenosis severity, identifying associated valvular and diastolic dysfunction, estimating left ventricular filling pressures (E/e´ ratio), estimating left ventricular ejection fraction, assessing

right ventricular function, and estimating pulmonary arterial pressure.[24] Although the traditional cutoff point for systolic dysfunction is an ejection fraction of 50%, values above this threshold, but with significant progressive decline (> 10%), may represent relevant myocardial damage and justify valve replacement, in a manner similar to patients with cancer undergoing chemotherapy.[25]

Very severe aortic stenosis (Vmax > 5 m/s) or progression of stenosis severity (> 0.3 m/s/year) is associated with onset of symptoms and worsening mortality in the first year.[24] The European guideline considers this condition a class IIa indication for intervention.

Serial evaluation with progressive reduction of ventricular function is particularly informative. For example, a patient with an initial ejection fraction of 68% who shows a progressive reduction to 60% demonstrates a decline greater than 10%, which may signify significant myocardial damage in progression.[25]

Valvulo-arterial impedance (Zva) represents a marker of myocardial damage, calculated as systolic blood pressure (SBP) plus mean transvalvular gradient (MG) divided by the stroke volume indexed by body surface area (SVI), as follows: Zva = (SBP + MG) / SVI. Values greater than 4.5 have prognostic importance for indicating valve replacement.[26]

The left atrium undergoes enlargement proportionally to diastolic dysfunction, representing the chronic progression of atrial overload. Left atrial enlargement and elevated pulmonary artery systolic pressure represent signs of myocardial damage, as do right ventricular dysfunction and tricuspid regurgitation.[27]

Genereux et al. analyzed patients from the PARTNER 2 study, who were grouped and classified according to the presence or absence of cardiac damage detected by echocardiography before aortic valve replacement in the following manner: no extravalvular cardiac damage (stage 0), left ventricular damage (stage 1), left atrial or mitral valve damage (stage 2), pulmonary vasculature or tricuspid valve damage (stage 3), or right ventricular damage (stage 4). Among the 1,661 patients with echocardiographic data, 1-year mortality was 4.4% in stage 0, 9.2% in stage 1, 14.4% in stage 2, 21.3% in stage 3, and 24.5% in stage 4 (p for trend < 0.0001). The extent of cardiac damage was independently associated with higher mortality after aortic valve replacement (hazard ratio 1.46 for each stage increment, 95% confidence interval 1.27–1.67, p < 0.0001). These results suggest that stages other than 0 and 1 demonstrate structural and functional changes in which symptoms were likely already present and which had prognostic importance. In this case as well, the sum of myocardial damage markers suggests that valve replacement before the onset of symptoms may be an acceptable approach, even though the results have been controversial to date.[28]

Global longitudinal strain

Echocardiographic assessment may also include global longitudinal myocardial strain, which has been shown to be a more sensitive tool for identifying early systolic dysfunction.[9] Although the traditional cutoff points for strain in patients with ventricular dysfunction and patients with aortic stenosis are −17% and −14%, respectively, progressive strain reduction can also be interpreted as evidence of progressive myocardial damage.[9,29] Studies have correlated reduced myocardial strain with the onset of symptoms. Reduced strain also has prognostic value after valve replacement.[29]

Atrial strain is an additional tool that can be used when equipment with this feature is available. Although the data are controversial, atrial strain can identify atrial dysfunction before remodeling and predict the onset of atrial fibrillation during the course of the disease and post-operatively[30] (Figure 1).

Stress echocardiography

Although current guidelines do not recommend stress echocardiography as a tool for stratifying asymptomatic patients with severe aortic stenosis,[5] its use during physical or pharmacological stress (dobutamine) to assess the transvalvular gradient, electrocardiographic tracing, and ventricular functional response continues to be investigated.[9] Studies comparing patients with positive versus negative stress tests, subsequently undergoing valve intervention, show variability in results, without significant and consistent differences in long-term prognosis between groups.[31] Further studies are needed to define the role of stress echocardiography in the management of asymptomatic patients with severe aortic stenosis.

Cardiac magnetic resonance imaging

CMR has emerged as an important non-invasive marker of myocardial damage in severe aortic stenosis.[32] In addition to assessing the severity of stenosis with results comparable to echocardiography, it is now possible, by means of native T1 mapping, to identify and quantify diffuse interstitial myocardial fibrosis lesions that may be partially reversible after valve replacement. Late gadolinium enhancement allows identification of focal fibrosis, which is usually irreversible, and it is an important indicator for early valve replacement.[32,33]

Some initial studies have suggested that anticipating valve replacement in patients with fibrotic changes detected by CMR could favorably modify the clinical and functional outcomes.[34] However, the recently published randomized EVOLVED study with 224 patients did not demonstrate benefits in anticipating valve replacement before the onset of symptoms, even in the presence of myocardial fibrosis detected by CMR.[35] Likewise, Myhr et al., comparing 42 symptomatic patients with 80 asymptomatic patients, showed that the presence of myocardial fibrosis identified by CMR with late enhancement did not demonstrate significant differences in relation to progression after valve replacement[36] (Figure 2; Video 1).

On the other hand, another recently published randomized study by Généreux et al. (EARLY TAVR), albeit with some methodological limitations, evaluated a significantly larger sample (901 patients), suggesting favorable results for early percutaneous intervention in asymptomatic patients with severe aortic stenosis.[36] Although their conclusions

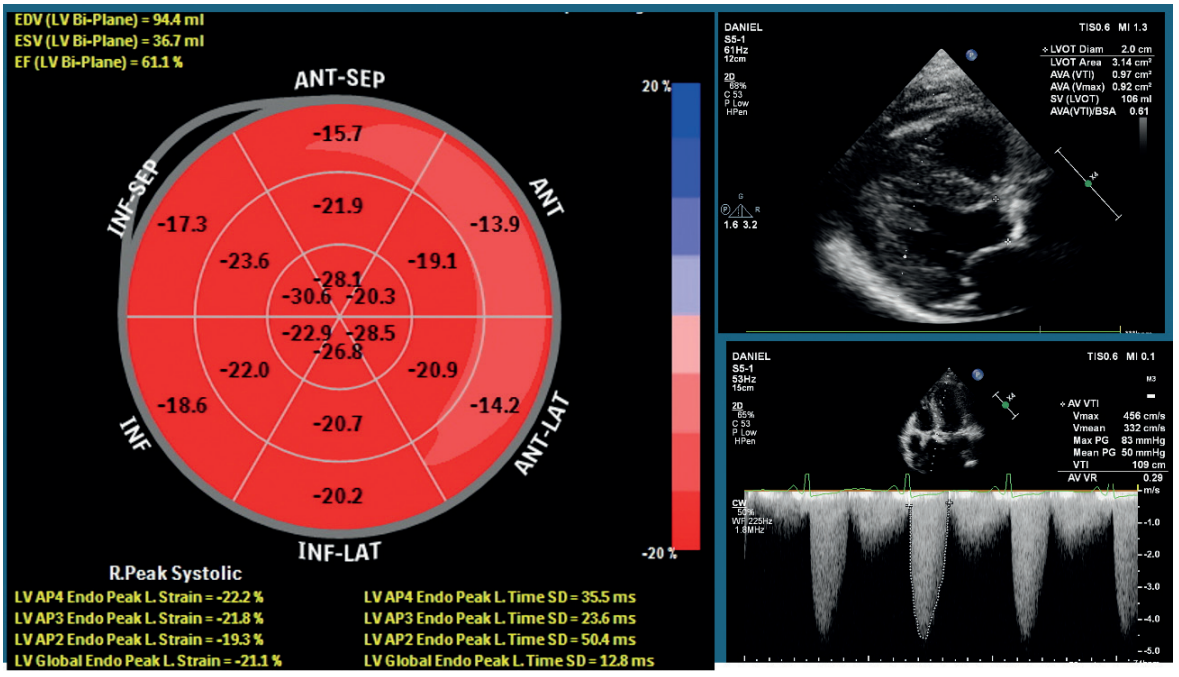

Figure 1 – *Two-dimensional transthoracic echocardiography with color Doppler demonstrating severe aortic stenosis. Top right: Parasternal longitudinal view showing left ventricular hypertrophy and calcified aortic valve. Bottom right: Transvalvular velocity > 4.5 m/s and mean gradient = 50 mmHg. Left: Bull's eye map showing normal global longitudinal strain = 21.1%.*

were favorable, mortality and prognosis were similar. The intervention reduced the outcome of hospitalization. A large part of these hospitalizations resulted from decompensation in the clinical follow-up group, in patients who underwent intervention in the subsequent 90 days. Similar results were found in the AVATAR study (Aortic Valve Replacement Versus Conservative Treatment in Asymptomatic Severe Aortic Stenosis).[37]

Plasma biomarkers

Elevated BNP and NT-proBNP levels are correlated with increased ventricular filling pressure and predict worse prognosis in severe aortic stenosis.[38] Elevated values may reflect myocardial damage with consequent diastolic dysfunction.[38] Similarly to other markers of myocardial damage, perhaps progressive worsening in serial evaluations, when associated with other markers, may indicate the need for early valve replacement.

Other biochemical markers have also shown prognostic value in surgical outcome during preoperative evaluation. High-sensitivity troponin T has important prognostic value. Elevations in troponin T, even slight ones, in patients with severe aortic stenosis correlate with worse clinical progression and a higher risk of adverse events.[39] This marker can identify structural cellular damage that is already present in the myocardium.[39] Osteopontin, a glycoprotein secreted by cells linked to inflammatory and remodeling processes, has been shown to be a marker of irreversible myocardial damage. Studies have shown that osteopontin predicts adverse clinical outcomes in patients after treatment of severe aortic stenosis with TAVI.[40] Annexin A1, studied in pericardial fluid of patients with severe aortic stenosis, has been shown to be a marker of atrial fibrillation associated with aortic stenosis, representing a marker of atrial remodeling.[41] Plasma ACE2 activity has also been shown to be associated with severe myocardial fibrosis and to predict mortality in patients with aortic stenosis.[42] Elevated levels indicate pathological myocardial remodeling processes with the development of fibrosis.[7]

Although biomarkers can identify patients with worse prognosis, current guidelines still do not mention their role in decision-making.

Discussion: When to intervene?

In spite of the multiple diagnostic tools available and the numerous published studies, the optimal timing to perform aortic valve replacement (to op) remains controversial and without absolute consensus (not to op).[7] In the real world, we have observed increasingly frequent indications for TAVI placement in patients under 65 years of age. Despite the safety of the procedure, long-term results have shown that mortality is higher in the percutaneous intervention group. The **Central Illustration** presents a proposed flowchart to guide the follow-up of asymptomatic patients with severe aortic stenosis.

Clinical experience suggests prudence and common sense in decision-making. In young, healthy, and asymptomatic patients with severe calcified aortic valve stenosis, close follow-up is recommended with consultations every 3 to 6 months, including:

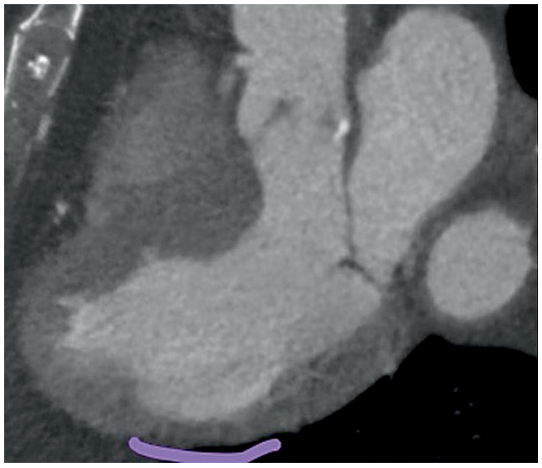

Figure 2 – *Cardiac magnetic resonance imaging in a patient with severe aortic stenosis. Late gadolinium enhancement demonstrates a pattern of focal subendocardial fibrosis. These changes represent evidence of irreversible structural myocardial damage (image kindly provided by Dr. Luiz Augusto Quaglia).*

- Serial ECG
- Echocardiogram with evaluation of ejection fraction and myocardial strain
- Exercise stress test (if appropriate for the patient's clinical profile)
- Plasma biomarkers (BNP/NT-proBNP, high-sensitivity troponin T)
- CMR with T1 and T2 maps and late gadolinium enhancement (less frequently, in selected situations)

Progressive changes with worsening ventricular function, whether due to ejection fraction or myocardial strain, left atrial enlargement, stenosis progression, and signs of elevated pulmonary arterial pressure, coupled with an abnormal exercise stress test (whether due to ischemia, decreased pressure, or malignant arrhythmias), may represent grounds for recommending valve replacement.[15]

In elderly patients with frailty that poses difficulties in adequately assessing symptoms, in addition to the parameters listed above (with the exception of exercise stress test, which may be contraindicated), assessment should integrate the multidimensional concept of frailty (extended Heart Team) to assist in the decision between performing elective valve intervention or clinical management with rigorous follow-up.[43]

For all patients, the classification of myocardial damage proposed by Genereux et al., after evaluating the population

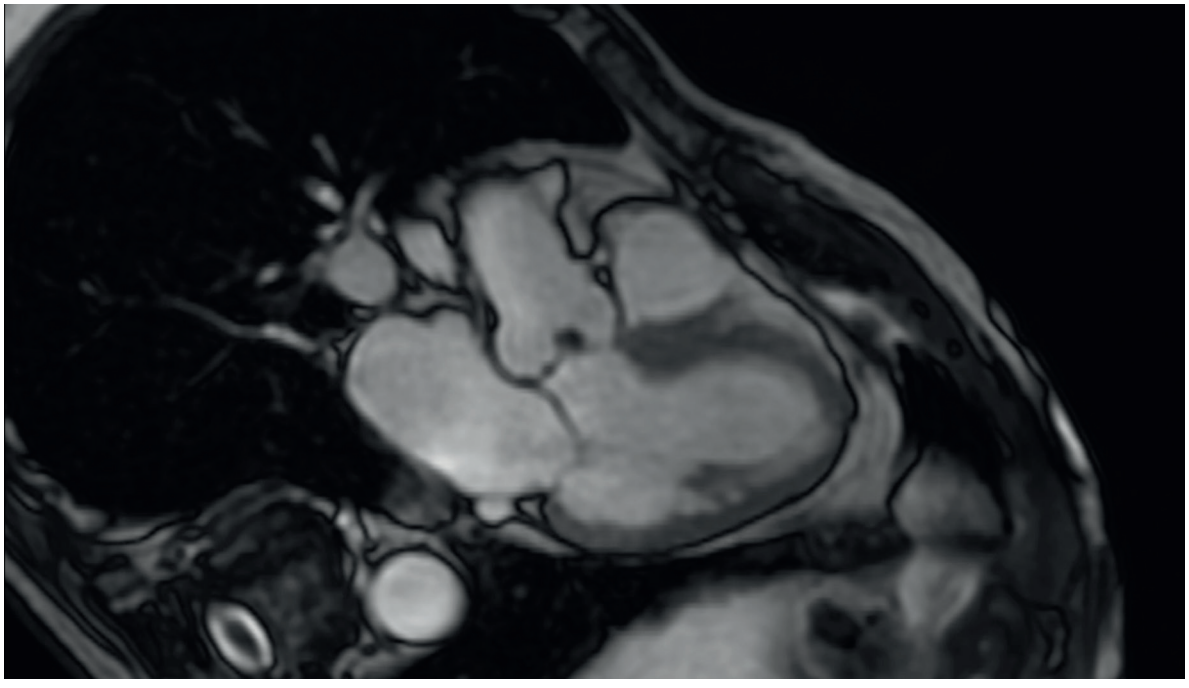

Video 1 – *Cardiac magnetic resonance imaging demonstrating severe aortic stenosis with myocardial structural remodeling and focal fibrosis. Courtesy of Dr. Luiz Augusto Quaglia. In: http://abcimaging.org/supplementary-material/2026/3902/ABCImag-2026-0054_AR_Video_1.mp4*

of the PARTNER study, can assist in identifying the initial stages of myocardial damage and justify the surgical indication described above. When applying the classification, it is important to bear in mind that all stages, except stage 0, are associated with a worse prognosis, justifying further monitoring and anticipation of intervention when appropriate.[7]

Conclusion

Severe aortic stenosis poses a challenge in current clinical management, characterized by the technical possibility of safe percutaneous intervention, but without absolute clarity regarding the optimal timing. Advances in the pathophysiological understanding of the disease and the development of sophisticated diagnostic tools (strain echocardiography, CMR with tissue mapping, and specific biomarkers) allow for the identification of myocardial damage in progressive stages before the onset of symptoms. Although the pathophysiological rationale points to intervention based on the identification of myocardial damage markers, studies conducted to date have yielded controversial results. Characteristics of the disease's phenotypic expression, which influence ventricular remodeling, worsening diastolic and systolic function, atrial remodeling, and the reaction of the pulmonary microcirculation, can affect the timing of symptom onset. Well-designed studies with consistent results are needed to incorporate the intervention approach into the guidelines.

An individualized and risk-stratified approach is recommended, considering the patient's clinical profile (young versus elderly, frail versus healthy), the presence and progression of markers of structural and functional myocardial damage, associated comorbidities, and the patient's informed preferences. The decision regarding closer follow-up intervals versus elective intervention should be based on multidisciplinary discussion within the context of an extended Heart Team. In the elderly population, whether asymptomatic or symptomatic, in the presence of a phenotype of left ventricular hypertrophy, the possibility of amyloid disease should always be considered.

Acknowledgements

The author would like to thank the echocardiography and CMR teams who contributed to compilation of the clinical images presented in this manuscript.

Author Contributions

Conception and design of the research, acquisition of data, analwysis and interpretation of the data, writing of the manuscript and critical revision of the manuscript for intellectual content: Vasconcelos DF.

Potential Conflict of Interest

No potential conflict of interest relevant to this article was reported.

Sources of Funding

There were no external funding sources for this study.

Study Association

This study is not associated with any thesis or dissertation work.

Ethics Approval and Consent to Participate

This article does not contain any studies with human participants or animals performed by any of the authors.

Use of Artificial Intelligence

The authors did not use any artificial intelligence tools in the development of this work.

Availability of Research Data

The underlying content of the research text is contained within the manuscript.

References

1. Vaslef SN, Roberts WC. Early Descriptions of Aortic Valve Stenosis. Am Heart J. 1993;125(5 Pt 1):1465-74. doi: 10.1016/0002-8703(93)91036-e.
2. Kuijpers P. History in Medicine: The Aortic Valve [Internet]. Sophia Antipolis: European Society of Cardiology; 2020 [cited 2026 May 28]. Available from:https://www.escardio.org/communities/councils/cardiology-practice/scientific-documents-and-publications/ejournal/volume-18/history-in-medicine-the-aortic-valve/.
3. Rosenhek R, Binder T, Porenta G, Lang I, Christ G, Schemper M, et al. Predictors of Outcome in Severe, Asymptomatic Aortic Stenosis. N Engl J Med. 2000;343(9):611-7. doi: 10.1056/NEJM200008313430903.
4. Lindman BR, Merryman WD. Unloading the Stenotic Path to Identifying Medical Therapy for Calcific Aortic Valve Disease: Barriers and Opportunities. Circulation. 2021;143(15):1455-7. doi: 10.1161/CIRCULATIONAHA.120.052531.
5. Tarasoutchi F, Montera MW, Ramos AIO, Sampaio RO, Rosa VEE, Accorsi TAD, et al. Atualização das Diretrizes Brasileiras de Valvopatias: Abordagem das Lesões Anatomicamente Importantes. Arq. Bras. Cardiol. 2017;109(6 Suppl 2):1-34. doi: 10.5935/abc.20180007.
6. Leon MB, Smith CR, Mack M, Miller DC, Moses JW, Svensson LG, et al. Transcatheter Aortic-Valve Implantation for Aortic Stenosis in Patients Who Cannot Undergo Surgery. N Engl J Med. 2010;363(17):1597-607. doi: 10.1056/NEJMoa1008232.
7. Drăgan A, Mateescu AD. Novel Biomarkers and Advanced Cardiac Imaging in Aortic Stenosis: Old and New. Biomolecules. 2023;13(11):1661. doi: 10.3390/biom13111661.
8. Kapadia SR, Leon MB, Makkar RR, Tuzcu EM, Svensson LG, Kodali S, et al. 5-Year Outcomes of Transcatheter Aortic Valve Replacement Compared with Standard Treatment for Patients with Inoperable Aortic Stenosis (PARTNER 1): A Randomised Controlled Trial. Lancet. 2015;385(9986):2485-91. doi: 10.1016/S0140-6736(15)60290-2.
9. Stein EJ, Fearon WF, Elmariah S, Kim JB, Kapadia S, Kumbhani DJ, et al. Left Ventricular Hypertrophy and Biomarkers of Cardiac Damage and Stress in Aortic Stenosis. J Am Heart Assoc. 2022;11(7):e023466. doi: 10.1161/JAHA.121.023466.

10. Généreux P, Banovic M, Kang DH, Giustino G, Prendergast BD, Lindman BR, et al. Aortic Valve Replacement vs Clinical Surveillance in Asymptomatic Severe Aortic Stenosis: A Systematic Review and Meta-Analysis. J Am Coll Cardiol. 2025;85(9):912-22. doi: 10.1016/j.jacc.2024.11.006.

11. Santangelo G, Bursi F, Faggiano A, Moscardelli S, Simeoli PS, Guazzi M, et al. The Global Burden of Valvular Heart Disease: From Clinical Epidemiology to Management. J Clin Med. 2023;12(6):2178. doi: 10.3390/jcm12062178.

12. Sievers HH, Schmidtke C. A Classification System for the Bicuspid Aortic Valve from 304 Surgical Specimens. J Thorac Cardiovasc Surg. 2007;133(5):1226-33. doi: 10.1016/j.jtcvs.2007.01.039.

13. Rajamannan NM, Evans FJ, Aikawa E, Grande-Allen KJ, Demer LL, Heistad DD, et al. Calcific Aortic Valve Disease: Not Simply a Degenerative Process: A Review and Agenda for Research from the National Heart and Lung and Blood Institute Aortic Stenosis Working Group. Executive summary: Calcific Aortic Valve Disease-2011 Update. Circulation. 2011;124(16):1783-91. doi: 10.1161/CIRCULATIONAHA.110.006767.

14. Kelly TA, Rothbart RM, Cooper CM, Kaiser DL, Smucker ML, Gibson RS. Comparison of Outcome of Asymptomatic to Symptomatic Patients Older than 20 Years of Age with Valvular Aortic Stenosis. Am J Cardiol. 1988;61(1):123-30. doi: 10.1016/0002-9149(88)91317-3.

15. Lindman BR, Clavel MA, Mathieu P, Iung B, Lancellotti P, Otto CM, et al. Calcific Aortic Stenosis. Nat Rev Dis Primers. 2016;2:16006. doi: 10.1038/nrdp.2016.6.

16. Lindman BR. Progression Rate of Aortic Stenosis: Why Does It Matter? JACC Cardiovasc Imaging. 2023;16(3):329-31. doi: 10.1016/j.jcmg.2022.12.002.

17. Mack MJ, Leon MB, Smith CR, Miller DC, Moses JW, Tuzcu EM, et al. 5-Year Outcomes of Transcatheter Aortic Valve Replacement or Surgical Aortic Valve Replacement for High Surgical Risk Patients with Aortic Stenosis (PARTNER 1): A Randomised Controlled Trial. Lancet. 2015;385(9986):2477-84. doi: 10.1016/S0140-6736(15)60308-7.

18. Huded CP, Huded JM, Friedman JL, Benck LR, Lindquist LA, Holly TA, et al. Frailty Status and Outcomes after Transcatheter Aortic Valve Implantation. Am J Cardiol. 2016;117(12):1966-71. doi: 10.1016/j.amjcard.2016.03.044.

19. Carabello BA. Clinical Practice. Aortic Stenosis. N Engl J Med. 2002;346(9):677-82. doi: 10.1056/NEJMcp010846.

20. Roberts WC, Ko JM. Frequency by Decades of Unicuspid, Bicuspid, and Tricuspid Aortic Valves in Adults Having Isolated Aortic Valve Replacement for Aortic Stenosis, with or without Associated Aortic Regurgitation. Circulation. 2005;111(7):920-5. doi: 10.1161/01.CIR.0000155623.48408.C5.

21. Manzo R, Ilardi F, Nappa D, Mariani A, Angellotti D, Molaro MI, et al. Echocardiographic Evaluation of Aortic Stenosis: A Comprehensive Review. Diagnostics. 2023;13(15):2527. doi: 10.3390/diagnostics13152527.

22. Taniguchi T, Morimoto T, Shiomi H, Ando K, Kanamori N, Murata K, et al. Initial Surgical versus Conservative Strategies in Patients with Asymptomatic Severe Aortic Stenosis. J Am Coll Cardiol. 2015;66(25):2827-38. doi: 10.1016/j.jacc.2015.10.001.

23. Amato MC, Moffa PJ, Werner KE, Ramires JA. Treatment Decision in Asymptomatic Aortic Valve Stenosis: Role of Exercise Testing. Heart. 2001;86(4):381-6. doi: 10.1136/heart.86.4.381.

24. Baumgartner H, Falk V, Bax JJ, De Bonis M, Hamm C, Holm PJ, et al. 2017 ESC/EACTS Guidelines for the Management of Valvular Heart Disease. Eur Heart J. 2017;38(36):2739-91. doi: 10.1093/eurheartj/ehx391.

25. Lancellotti P, Magne J, Dulgheru R, Clavel MA, Donal E, Vannan MA, et al. Outcomes of Patients with Asymptomatic Aortic Stenosis Followed Up in Heart Valve Clinics. JAMA Cardiol. 2018;3(11):1060-8. doi: 10.1001/jamacardio.2018.3152.

26. Hachicha Z, Dumesnil JG, Pibarot P. Usefulness of the Valvuloarterial Impedance to Predict Adverse Outcome in Asymptomatic Aortic Stenosis. J Am Coll Cardiol. 2009;54(11):1003-11. doi: 10.1016/j.jacc.2009.04.079.

27. Tastet L, Tribouilloy C, Maréchaux S, Vollema EM, Delgado V, Salaun E, et al. Staging Cardiac Damage in Patients with Asymptomatic Aortic Valve Stenosis. J Am Coll Cardiol. 2019;74(4):550-63. doi: 10.1016/j.jacc.2019.04.065.

28. Généreux P, Pibarot P, Redfors B, Mack MJ, Makkar RR, Jaber WA, et al. Staging Classification of Aortic Stenosis Based on the Extent of Cardiac Damage. Eur Heart J. 2017;38(45):3351-8. doi: 10.1093/eurheartj/ehx381.

29. Kempny A, Diller GP, Kaleschke G, Orwat S, Funke A, Radke R, et al. Longitudinal Left Ventricular 2D Strain is Superior to Ejection Fraction in Predicting Myocardial Recovery and Symptomatic Improvement after Aortic Valve Implantation. Int J Cardiol. 2013;167(5):2239-43. doi: 10.1016/j.ijcard.2012.06.012.

30. Meimoun P, Djebali M, Botoro T, Djou Md U, Bidounga H, Elmkies F, et al. Left Atrial Strain and Distensibility in Relation to Left Ventricular Dysfunction and Prognosis in Aortic Stenosis. Echocardiography. 2019;36(3):469-77. doi: 10.1111/echo.14258.

31. Leurent G, Donal E, de Place C, Chabanne C, Gervais R, Fougerou C, et al. Argument for a Doppler Echocardiography during Exercise in Assessing Asymptomatic Patients with Severe Aortic Stenosis. Eur J Echocardiogr. 2009;10(1):69-73. doi: 10.1093/ejechocard/jen163.

32. Myhr KA, Andrés-Jensen L, Larsen BS, Kristensen CB, Køber N, Tischer SG, et al. Myocardial Fibrosis in Severe Asymptomatic versus Symptomatic Aortic Stenosis: A Cardiac Magnetic Resonance Cross-Sectional Study. Int J Cardiovasc Imaging. 2025;41(11):2159-71. doi: 10.1007/s10554-025-03519-2.

33. Treibel TA, López B, González A, Menacho K, Schofield RS, Ravassa S, et al. Reappraising Myocardial Fibrosis in Severe Aortic Stenosis: An Invasive and Non-Invasive Study in 133 Patients. Eur Heart J. 2018;39(8):699-709. doi: 10.1093/eurheartj/ehx353.

34. Azevedo CF, Nigri M, Higuchi ML, Pomerantzeff PM, Spina GS, Sampaio RO, et al. Prognostic Significance of Myocardial Fibrosis Quantification by Histopathology and Magnetic Resonance Imaging in Patients with Severe Aortic Valve Disease. J Am Coll Cardiol. 2010;56(4):278-87. doi: 10.1016/j.jacc.2009.12.074.

35. Loganath K, Craig NJ, Everett RJ, Bing R, Tsampasian V, Molek P, et al. Early Intervention in Patients with Asymptomatic Severe Aortic Stenosis and Myocardial Fibrosis: The EVOLVED Randomized Clinical Trial. JAMA. 2025;333(3):213-21. doi: 10.1001/jama.2024.22730.

36. Généreux P, Schwartz A, Oldemeyer JB, Pibarot P, Cohen DJ, Blanke P, et al. Transcatheter Aortic-Valve Replacement for Asymptomatic Severe Aortic Stenosis. N Engl J Med. 2025;392(3):217-27. doi: 10.1056/NEJMoa2405880.

37. Banovic M, Putnik S, Penicka M, Doros G, Deja MA, Kockova R, et al. Aortic Valve Replacement versus Conservative Treatment in Asymptomatic Severe Aortic Stenosis: The AVATAR Trial. Circulation. 2022;145(9):648-58. doi: 10.1161/CIRCULATIONAHA.121.057639.

38. Nakatsuma K, Taniguchi T, Morimoto T, Shiomi H, Ando K, Kanamori N, et al. B-Type Natriuretic Peptide in Patients with Asymptomatic Severe Aortic Stenosis. Heart. 2019;105(5):384-90. doi: 10.1136/heartjnl-2018-313746.

39. Hadziselimovic E, Greve AM, Sajadieh A, Olsen MH, Kesäniemi YA, Nienaber CA, et al. Association of High-Sensitivity Troponin T with Outcomes in Asymptomatic Non-Severe Aortic Stenosis: A Post-Hoc Substudy of the SEAS Trial. EClinicalMedicine. 2023;58:101875. doi: 10.1016/j.eclinm.2023.101875.

40. Lutz M, von Ingersleben N, Lambers M, Rosenberg M, Freitag-Wolf S, Dempfle A, et al. Osteopontin Predicts Clinical Outcome in Patients after Treatment of Severe Aortic Stenosis with Transcatheter Aortic Valve Implantation (TAVI). Open Heart. 2017;4(2):e000633. doi: 10.1136/openhrt-2017-000633.

41. Fragão-Marques M, Vitorino R, Barroso I, Falcão-Pires I, Leite-Moreira A, Trindade F. Pericardial Fluid Annexin A1 Is a Marker of Atrial Fibrillation in Aortic Stenosis: A Proteomics Analysis. J Pers Med. 2022;12(2):264. doi: 10.3390/jpm12020264.

42. Ramchand J, Patel SK, Kearney LG, Matalanis G, Farouque O, Srivastava PM, et al. Plasma ACE2 Activity Predicts Mortality in Aortic Stenosis and Is Associated with Severe Myocardial Fibrosis. JACC Cardiovasc Imaging. 2020;13(3):655-64. doi: 10.1016/j.jcmg.2019.09.005.

43. Afilalo J, Alexander KP, Mack MJ, Maurer MS, Green P, Allen LA, et al. Frailty Assessment in the Cardiovascular Care of Older Adults. J Am Coll Cardiol. 2014;63(8):747-62. doi: 10.1016/j.jacc.2013.09.070.

Review Article

My Approach to Transcatheter Closure of Atrial Septal Defect: Step-by-Step and Current Contraindications

Angele Azevedo Alves Mattoso,[1,2] *Joberto Pinheiro Sena,*[1] *Gilson Soares Feitosa Filho,*[1] *Maria Lúcia Duarte*[1]
Hospital Santa Izabel,[1] *Salvador, BA – Brazil*
Clínica Proalívio Day Hospital,[2] *Salvador, BA – Brazil*

Abstract

All patients who are candidates for transcatheter closure of an ostium secundum atrial septal defect (ASD) should undergo a detailed echocardiographic assessment using 2D transesophageal echocardiography (TEE) prior to the procedure. It is essential for a comprehensive analysis of interatrial septal anatomy and for determining defect eligibility for the procedure. The type, number, size, location and morphology of the ASD, as well as the quality of the surrounding septal tissue and its relationship with adjacent cardiac structures, should be carefully assessed. 3D TEE may complement this assessment by providing additional relevant anatomical information. During the procedure, TEE plays a fundamental role in real-time guidance, allowing proper deployment of the septal occluder device as well as immediate assessment of the result and early detection of potential complications. This article presents a practical approach to transcatheter closure of ostium secundum ASD, with emphasis on echocardiographic aspects in the pre-procedural, intraprocedural, and post-procedural phases.

Introduction

Ostium secundum atrial septal defect (ASD) is the most common form of interatrial septal defect (IASD) and can often be treated with percutaneous transcatheter closure. Currently, this method is the preferred approach when anatomy is favorable.[1] Pre-procedural transthoracic echocardiography is usually sufficient in most pediatric patients. However, in adults, transesophageal echocardiography (TEE) is recommended for better characterization of septal anatomy. This examination is generally performed in patients previously identified as candidates for closure, based on the following indications:

- Isolated ostium secundum ASD with a pulmonary-to-systemic flow ratio (Q_P/Q_S) > 1.5;
- Signs of right ventricular (RV) volume overload;
- Absence of cyanosis;
- Absence of significant or irreversible pulmonary hypertension.

Guidelines from the American College of Cardiology/American Heart Association recommend ASD closure in patients with RV dilation, regardless of symptom presence (Class I). On the other hand, small defects (diameter < 5 mm), in the absence of RV dilation, do not require intervention, as they are not considered hemodynamically significant nor capable of altering the clinical course.[2]

In addition, it is essential to exclude the presence of associated congenital anomalies that would indicate surgical correction, such as anomalous pulmonary venous connections, as well as the presence of intracardiac thrombi.

The main aspects of transcatheter closure of ostium secundum ASD will be described below, with emphasis on echocardiographic findings and the role of echocardiography at different stages of the procedure.

Anatomy of the interatrial septum

A detailed understanding of cardiac anatomy is essential for performing structural interventions. Ostium secundum ASD corresponds to a true discontinuity, single or multiple, in the embryonic septum primum, which forms the floor of the fossa ovalis. This structure is located in the central portion of the IAS.

The fossa ovalis is surrounded by the septum secundum, an invagination of the atrial roof filled with epicardial fat. It is considered a "false septum," as this adipose layer lies outside the atrial cavities. Ostium secundum defects are bounded by rims of septal tissue adjacent to the limiting structures of the right atrium (RA).

Among the most relevant adjacent structures are the aortic root, located anteriorly, and the venous inflows draining into the RA, including the superior vena cava (SVC), inferior vena cava (IVC), and the coronary sinus. These structures maintain a close anatomical relationship with the left atrium (LA)[1,3,4] (Central Illustration).

The size of the defect and the integrity of the septal rims are determinants of successful transcatheter ASD closure.

Size and shape of ostium secundum atrial septal defect

Ostium secundum ASDs show wide variation in size and morphology, and may present as elliptical, round, slit-like, or slightly irregular shapes (Figure 1). In some cases, persistent

Keywords

Heart Septal Defects, Atrial; Catheterization; Echocardiography

Mailing Address: Angele Azevedo Alves Mattoso •
Hospital Santa Izabel - SCMBA. Praça Conselheiro Almeida Couto. Postal code: 40050-410. Salvador, BA – Brazil
E-mail: angelealves@bol.com.br
Manuscript received February 27, 2026, revised manuscript March 9, 2026, accepted March 10, 2026
Editor responsible for the review: Marcelo Tavares

DOI: https://doi.org/10.36660/abcimg.20260020i

CONTENTS

Central Illustration: My Approach to Transcatheter Closure of Atrial Septal Defect: Step-by-Step and Current Contraindications

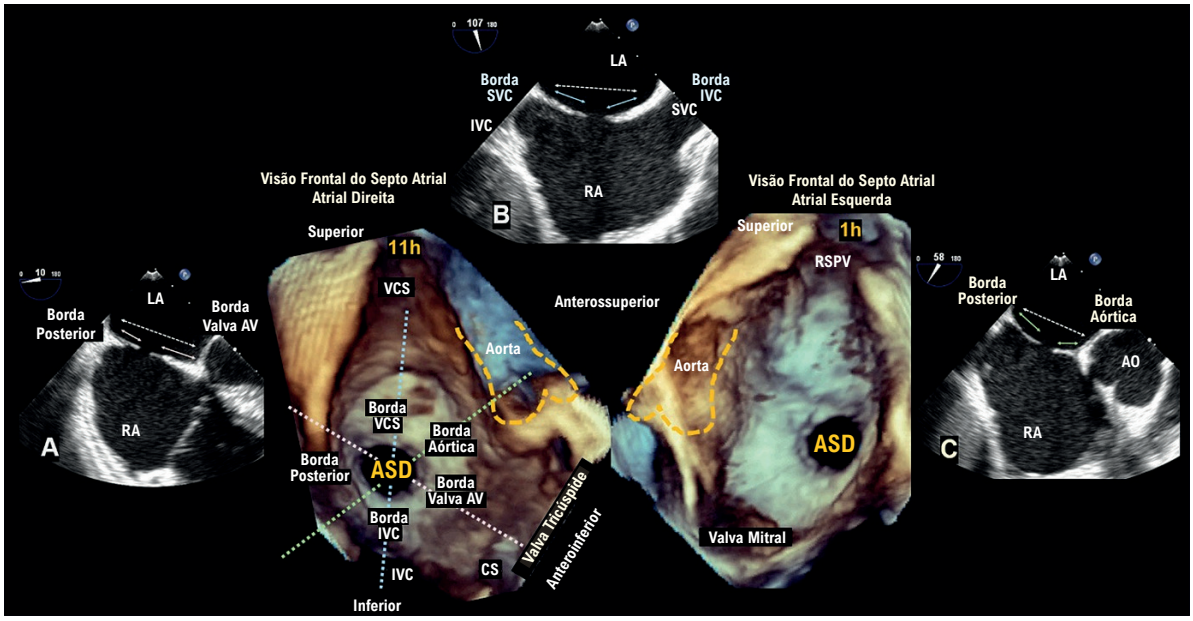

Arq Bras Cardiol: Imagem cardiovasc. 2026;39(2):e20260020

Images obtained by TEE illustrate the anatomical assessment of ostium secundum ASD and its suitability for transcatheter closure. The central images show the 3D frontal (en face, zoom mode) view of the ASD and IAS in the recommended anatomical orientation, highlighting adjacent structures from the perspectives of the right and left atria, respectively. The 2D images show the standardized planes for defect measurement: A) four-chamber view; B) bicaval view; C) aortic valve short-axis view. These views allow assessment of ASD diameter and its rims (yellow, blue, and green arrows) as well as IAS length (white arrows). The dashed lines overlaid on the frontal 3D image indicate the cutting planes used to obtain the 2D images. AO: aorta; ASD: atrial septal defect; CS: coronary sinus; IAS: interatrial septum; IVC: inferior vena cava; LA: left atrium; RA: right atrium; RSPV: right superior pulmonary vein; SVC: superior vena cava; TEE: transesophageal echocardiography.

septum primum strands may cross the defect, resulting in multiple communications and the formation of fenestrations. In large defects, the septum primum is often reduced or nearly absent.[1]

The size of these communications may range from a few millimeters to more than 30 mm in diameter. Large defects, defined as > 20 mm in children or > 30 mm in adults, represent greater technical complexity and are often associated with deficient septal rims, which may require modified closure strategies.

Defect measurement is recommended during both systole and diastole. An ASD is considered dynamic when it shows at least a 50% variation in its dimension throughout the cardiac cycle. In general, the size of the septal occluder device (SOD) is determined based on the largest linear diameter of the defect, usually obtained during diastole.

Assessment of ASD size should preferably be performed using 2D echocardiography combined with color Doppler. In addition, these defects may progressively enlarge over time, following cardiac growth and aging.[1,4]

Dimension and quality of ostium secundum atrial septal defect rims

Ostium secundum ASD may be located in different regions of the fossa ovalis, either centrally or peripherally (Figure 2, Panels A and B). This variability determines the amount of surrounding septal tissue, known as rims, that delimit the defect. A detailed assessment of such rims is essential to determine eligibility for transcatheter closure, as this is the tissue where the SOD will be anchored.

Rims are named according to adjacent anatomical structures and are classified as follows[1,4,5] (Central Illustration):

- Aortic rim (anterosuperior): between the ASD and the aortic valve annulus and aortic root;
- Atrioventricular valve rim (anteroinferior): between the ASD and the atrioventricular valves;
- Superior vena cava rim (posterosuperior): between the ASD and the SVC;
- Inferior vena cava rim (posteroinferior): between the ASD and the IVC;

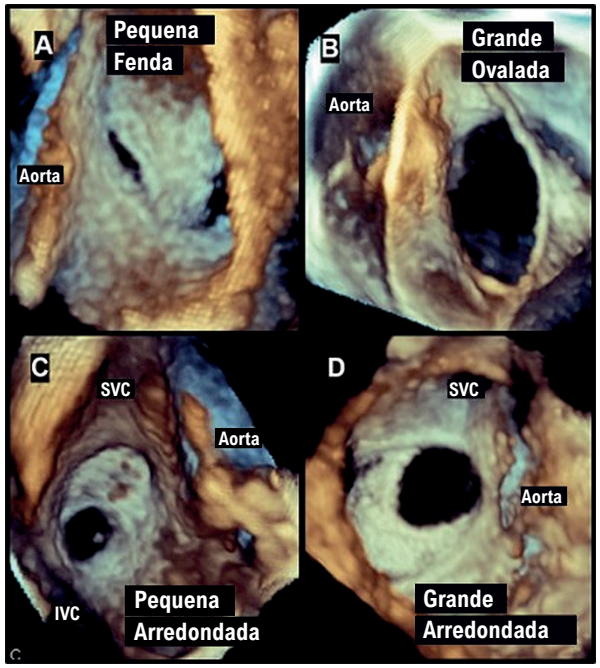

Figure 1 – *3D transesophageal echocardiography images, in zoom mode, illustrate representative examples of different sizes and shapes of ostium secundum ASD, obtained from en face views of the interatrial septum.*

- Posterior rim: between the ASD and the posterior atrial walls.

Additionally, the rim related to the right superior pulmonary vein (RSPV), located posteriorly between the ASD and such a vein, may also be assessed.

By convention, a rim length > 5 mm is considered adequate, representing a favorable feature for transcatheter closure. Rims measuring 3-5 mm are classified as deficient, whereas those < 3 mm are considered insufficient. The presence of rims < 5 mm may make the procedure more challenging and require specific technical strategies, although it is not an absolute contraindication.

The integrity of the posterosuperior, posteroinferior, and anteroinferior rims is particularly relevant for procedural success. In contrast, deficiency of the aortic rim, although associated with a potential risk of erosion, is not a contraindication, and adaptation of the SOD to the aorta is often desirable.[4]

In addition to length, the structural quality of the rims should also be assessed. Thin and redundant rims, especially in the posterior and posteroinferior regions, may be associated with additional fenestrations, characterizing multiple defects (Figure 2C).

General imaging protocol of the interatrial septum

2D transesophageal echocardiography

2D TEE forms the basis of imaging assessment of the IAS. Since ostium secundum ASD may be located anywhere within

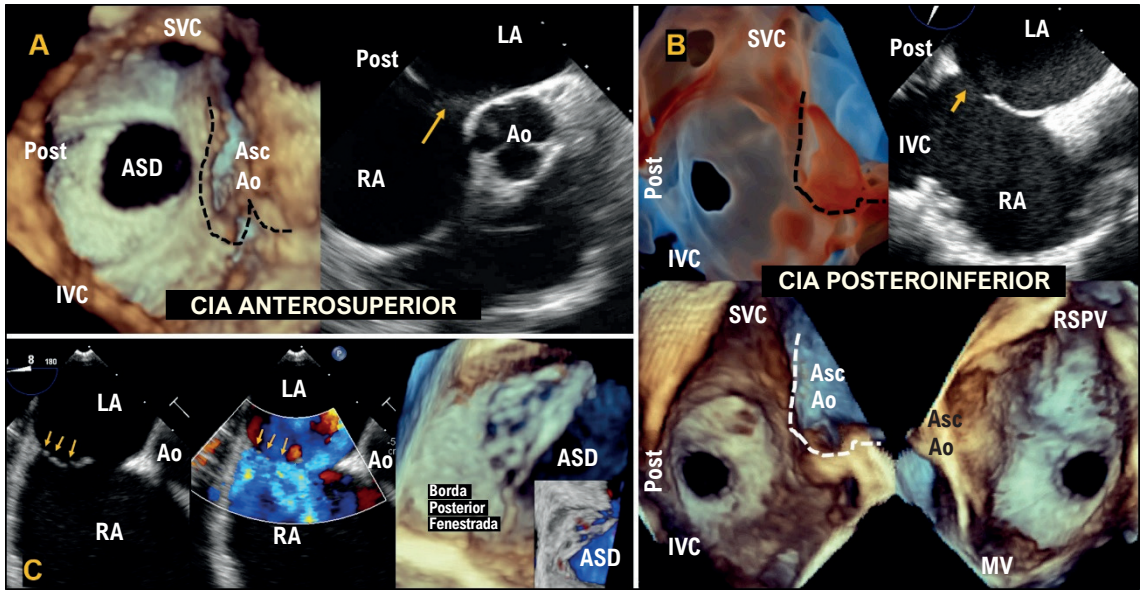

Figure 2 – *Examples of TEE images of ostium secundum ASDs. A) ASD located in the anterosuperior region of the IAS, visualized by 3D TEE from the RA perspective and by 2D TEE (arrow); B) ASD located in the posteroinferior region of the IAS, demonstrated by 3D TEE from multiple perspectives and by 2D TEE (arrow); C) Image of the posterior rim showing multiple small fenestrations, observed on 2D TEE and with greater detail on 3D TEE. Ao: aorta; ASD: atrial septal defect; IAS: interatrial septum; IVC: inferior vena cava; LA: left atrium; Post: posterior; RSPV: right superior pulmonary vein; SVC: superior vena cava; TEE: transesophageal echocardiography.*

the fossa ovalis, image acquisition should begin at 0° and the transducer angle should be progressively increased in 15° increments up to approximately 120°, allowing complete septal evaluation.

2D images should be optimized before applying color Doppler. The color Doppler scale may be adjusted to lower values (≈ 35-40 cm/s) to facilitate detection of low-velocity flows, such as in small fenestrations or smaller defects.

Most standard views are obtained at the mid-esophageal level, including:

- Four-chamber view (0°-30°): allows assessment of the posterior rim and atrioventricular valves;
- Inflow-outflow or aortic valve short-axis view (45°-60°): demonstrates the posterior and aortic (anterosuperior) rims;
- Bicaval view (90°-120°): allows evaluation of the posterosuperior (SVC) and posteroinferior (IVC) rims.

Clockwise rotation of the probe from the aortic valve short-axis view (45°-60°) enables visualization of the right pulmonary veins. Withdrawing the probe to the upper esophagus, combined with progressive angular sweep from 0°, allows better assessment of the superior portion of the septum.

In the bicaval view at 120°, in cases of superiorly located ASD, the posterosuperior rim can be visualized. Additional clockwise rotation allows identification of right pulmonary venous drainage, aiding in the differentiation between superior sinus venosus defect and superiorly located ostium secundum ASD.

When the posteroinferior rim is not adequately visualized in the bicaval view, maneuvers such as probe retroflexion or gradual angle reduction to approximately 60° may bring the IVC into the imaging field. This rim is often the most difficult to delineate by TEE, but its assessment is essential, as its deficiency, observed in approximately 3.3% of cases, is associated with a higher risk of SOD dysfunction. Nevertheless, in selected cases, percutaneous closure may be performed with appropriate technical adjustments.

The deep transgastric position may also be used to obtain a sagittal bicaval view. Initially, the RV inflow is identified at 90°, followed by increasing the angle to 100°-120° and slight clockwise rotation of the probe.[1,4,5]

3D transesophageal echocardiography

The IAS has a complex 3D anatomy, and 3D TEE provides additional relevant anatomical information. This modality allows acquisition of en face views of the ASD from both RA and LA perspectives, enabling detailed evaluation of defect rims and their relationship with adjacent structures.

In addition, 3D TEE allows real-time characterization of defect shape (especially in elliptical or multiple defects) and measurement of its minimum and maximum dimensions throughout the cardiac cycle. It also enables direct visualization of the SOD after implantation, as well as immediate assessment of its positioning and potential complications.

The technique also allows biplanar or triplanar acquisition, with simultaneous display of orthogonal planes (e.g., aortic valve short-axis and bicaval views), with high temporal resolution, which is particularly useful for guiding transcatheter procedures (Figure 4, Panel D).

3D volumetric acquisition is performed from standard 2D projections, such as the aortic short-axis or bicaval views. Before 3D acquisition, it is essential to optimize the 2D image. Proper gain adjustment is critical to avoid artifacts that may falsely simulate multiple defects, which cannot be corrected during post-processing.

3D TEE offers different acquisition modes, particularly real-time (narrow-angle) and wide-sector zoom modes.

3D display

According to anatomical convention, in the en face view, the IAS and ASD should be rotated so that the SVC is positioned at approximately the 11 o'clock position, the IVC along the inferior vertical axis, and the aorta anteriorly, directed toward the upper right corner of the image, from the RA perspective.

From the LA perspective, the 3D image is inverted along the superior-inferior axis. In this configuration, the RSPV, adjacent to the SVC, is positioned superiorly (approximately at the 1 o'clock position), the aortic root occupies the anterosuperior left region, and the mitral valve is located in the anteroinferior portion (Central Illustration).

These orientations should be used as an initial reference for systematic image interpretation.[1]

Complex ostium secundum atrial septal defect

Morphological variables may make transcatheter closure of ostium secundum ASD more challenging (Figure 3). ASD is considered complex, with potential surgical indication, in the following situations:

- Large ASD: diameter > 30 mm;
- Multiple ASDs or multifenestrated IAS: multiple fenestrations are present in approximately 2.7% of cases and are often associated with IAS aneurysm.[1] Characterization of the number, size, and location of the defects is essential for SOD selection and for anticipating procedural complexity;
- IAS aneurysm: may compromise SOD stability and positioning, influencing device selection;
- Deficient or non-firm rims (thin and redundant): may impair proper device anchoring.

These anatomical variations may favor the use of specific devices for multiple fenestrations or, in some cases, require implantation of more than one SOD. Defects exceeding the size of available devices may require surgical management.

In addition, measurement of IAS length (Central Illustration) is recommended, as devices with an occluder disc larger than 90% of this length may be associated with a higher risk of cardiac erosion.

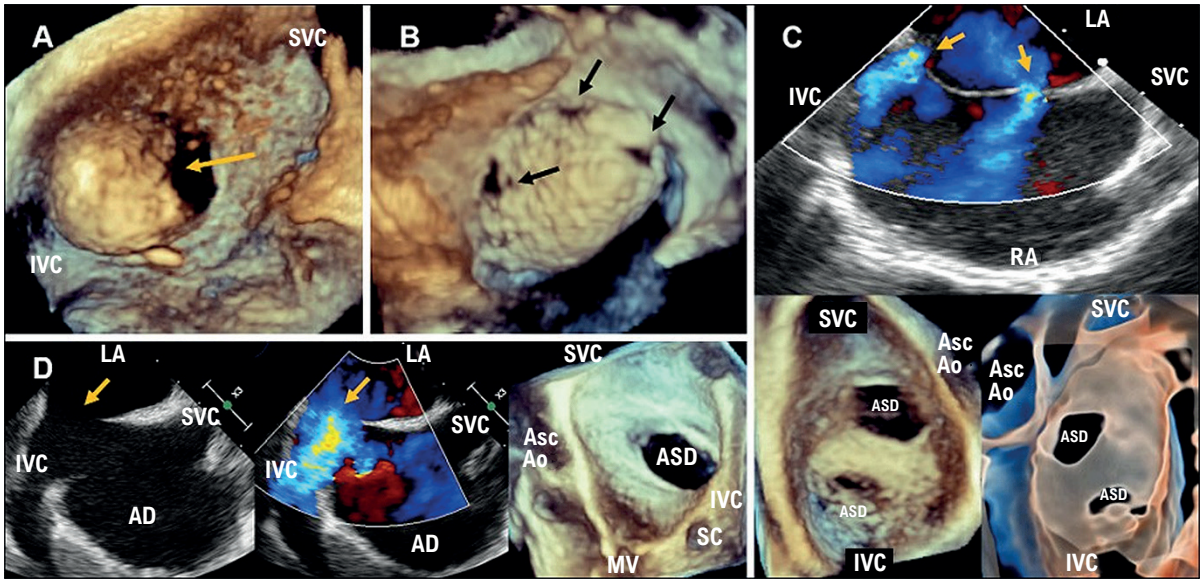

Figure 3 – *Examples of images obtained by TEE of complex ostium secundum ASDs. A) 3D frontal view demonstrating ASD associated with an IAS aneurysm (yellow arrow); B) 3D TEE frontal view showing ASD associated with an aneurysmal and multifenestrated IAS (black arrows); C) 2D TEE images (upper panel, yellow arrows) and 3D TEE images (lower panel) demonstrating an IAS with two ASDs; D) 2D TEE images (right panel, yellow arrow) and 3D TEE images (left panel) showing ASD with absence of the posteroinferior rim. RA: right atrium; LA: left atrium; Asc Ao: ascending aorta; ASD: atrial septal defect; TEE: transesophageal echocardiography; IAS: interatrial septum; IVC: inferior vena cava; SVC: superior vena cava; MV: mitral valve.*

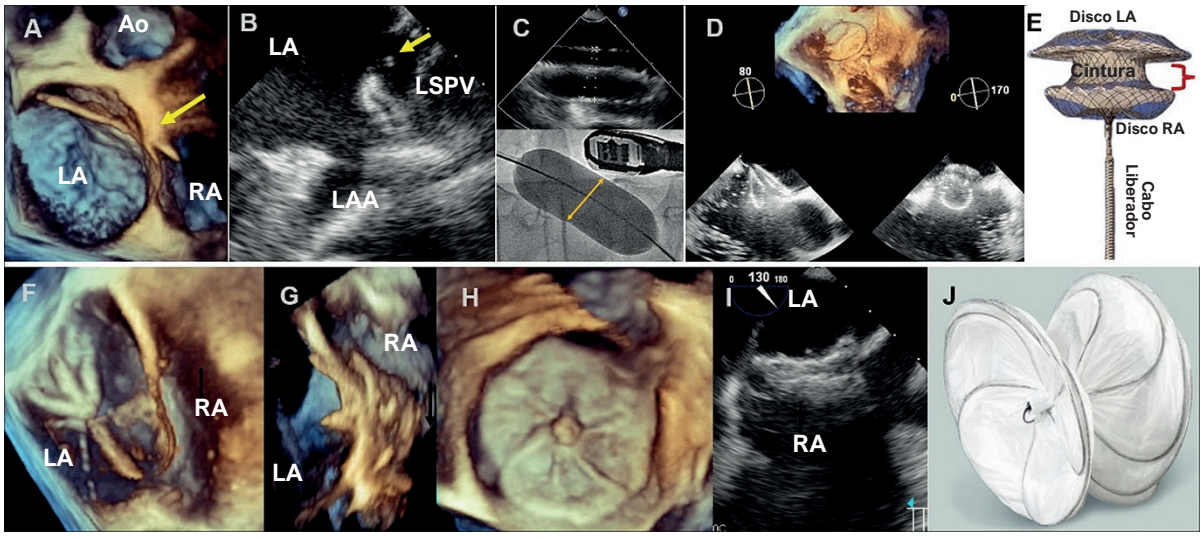

Figure 4 – *mages obtained during the transcatheter closure procedure of ostium secundum ASD. A) 3D TEE image demonstrating the guidewire crossing the IAS; B) 2D TEE image showing the catheter positioned in the LSPV (yellow arrow); C) Measurement of the stretched ASD diameter by TEE (upper panel) and fluoroscopy (lower panel); D) Multiplanar reconstruction by 3D TEE demonstrating the positioning of the Amplatzer septal occluder device in the IAS; E) Schematic illustration of the Amplatzer device; F) Formation of the left atrial disc of a non-self-centering device in the LA, with a "tulip-like" appearance, visualized by 3D TEE; G) Profile view of the device; H) Frontal view of the device; I) 2D TEE image of the implanted device; J) Illustration of a non-self-centering device. RA: right atrium; LA: left atrium; LAA: left atrial appendage; Ao: aorta; ASD: atrial septal defect; TEE: transesophageal echocardiography; IAS: interatrial septum; LSPV: left superior pulmonary vein.*

Septal occluder device

Several SODs are available for percutaneous transcatheter closure of ostium secundum ASD. The Amplatzer-type device consists of two self-expanding discs connected by a self-centering waist, made of nitinol mesh, allowing recapture and repositioning during implantation. The LA disc has a larger diameter due to higher pressure in this chamber compared to the RA. The main reference for device selection is the waist diameter, which should correspond to the defect size (Figure 4, Panel E).

Non-self-centering devices, specifically developed for multifenestrated IAS, consist of two discs of equal diameter connected by a thin waist positioned at the central defect. In this configuration, the disc size on both sides of the septum maximizes coverage of multiple fenestrations. In these cases, the central ASD is the main reference for sizing, and disc diameter is the most relevant parameter (Figure 4, Panel J).

Transcatheter closure of ostium secundum atrial septal defect

Echocardiography provides essential information at all stages of the procedure, including patient selection, SOD choice, intraprocedural guidance, complication monitoring, and outcome assessment.

A key step during the procedure is ASD measurement. This evaluation is performed by echocardiography, as previously described, and complemented by angiography using a sizing balloon.

Balloon sizing is based on the concept of stretched diameter, in which the ASD diameter measured by TEE is smaller than the diameter obtained after balloon inflation. Although TEE is essential for rim assessment, it does not allow precise determination of their structural composition. The sizing balloon is therefore crucial to expand the septal rims until they provide adequate resistance for device anchoring. This measurement defines the minimum SOD size required for proper fixation.[4-6]

Measurement of stretched diameter is performed using the stop-flow technique. This technique consists of gradual balloon inflation until interruption of left-to-right flow, which should be confirmed by echocardiography with color Doppler. Ideally, the balloon presents a central constriction ("waist"), indicating proper positioning and centering within the defect (Figure 4, Panel C). The balloon waist corresponds to the reference for the diameter of the device to be implanted.

The selected balloon should have a diameter larger than initially estimated to allow adequate septal stretching. In general, an increase of approximately 30%-35% compared with the initial measurement is observed. Inflation should not exceed the point of flow interruption or the balloon's maximum volume to avoid excessive defect distension. The presence of a waist without flow interruption may indicate multiple communications within the fossa ovalis.

After determining defect diameter, SOD size may be selected according to different criteria: diameter equal to the defect, one size larger, stretched diameter plus 0-2 mm, or, in cases of thick and firm rims, 20%-30% larger than the measurement obtained by TEE.

Step-by-step guidance for transcatheter closure of ostium secundum atrial septal defect

1. Initially, TEE should be used to assess the ASD in terms of morphology, location, and rim characteristics;
2. Venous access is generally obtained via the IVC, visualized in the bicaval view. At this stage, the guidewire is directed superiorly toward the IAS, aiming to cross the defect and reach the LA. The course of the wire should be clearly identified in the RA to avoid entry into the RA appendage, a structure adjacent to the SVC and a potential site of atrial perforation. It is also important to check for the presence of a Chiari network due to the risk of wire entanglement; therefore, complex maneuvers within the RA should be avoided;
3. The guidewire is then advanced to cross the IAS (Figure 4A);
4. Once in the LA, the wire is directed posteriorly toward the left superior pulmonary vein (LSPV), a structure considered safe for stabilization. TEE confirms appropriate positioning of the wire in the LSPV and excludes its passage into the left atrial appendage (LAA), a trabeculated, thin-walled structure at risk of perforation (Figure 4, Panel B);
5. The sizing balloon is then advanced;
6. The balloon should be inflated with its center aligned with the defect. Confirmation of the stop-flow technique is performed by TEE, with measurement of the stretched ASD diameter;
7. The SOD is selected;
8. The balloon should only be removed after the selected SOD has been properly prepared for implantation;
9. Subsequently, the guidewire and delivery sheath are advanced through the IAS to the ideal position, usually within the LA body or the LSPV, with confirmation by TEE;
10. The dilator and guidewire are then removed, maintaining the sheath positioned within the LA. The SOD is then advanced through the sheath;
11. Next, the delivery sheath is repositioned in the LA body, and the left atrial disc is deployed under echocardiographic guidance, ensuring that the device remains away from the LAA, mitral valve, and atrial free wall. The LA disc is then pulled back until it is positioned against the IAS at the level of the defect, while the connecting waist is released with continuous traction toward the RA;
12. Finally, the right atrial disc is deployed on the right side of the IAS (Figure 4, Panel D);
13. When using an Amplatzer-type SOD, a stability test ("tug test") may be performed under echocardiographic and fluoroscopic monitoring to confirm device stability;

14. After confirming positioning and stability, the SOD is released.

In the case of non-self-centering devices, the procedure follows the same general principles as standard ASD closure, with the difference that device selection is primarily guided by echocardiography. In this situation, balloon use is not necessarily mandatory, as defect sealing does not depend on the device waist but rather on its discs. The ratio between SOD diameter and defect diameter should be greater than 2:1, and the selected device diameter should not exceed 90% of the measured septal length.

In these cases, the left atrial disc is initially formed within the LA body under fluoroscopic and echocardiographic guidance (Figure 4F). Once formed, TEE is used to guide its positioning against the left atrial surface of the IAS. The LA disc is kept supported against the septum while the delivery catheter is pulled toward the RA, allowing formation of the right atrial disc (Figure 4, Panels G, H and I).

In cases of multifenestrated ASD, 2D TEE, and especially 3D TEE, should be used to measure the distance between the center of the main defect and the most distant defect, corresponding to the radius. This value is then multiplied by 2 in order to obtain the required device diameter. To verify that the selected SOD will not interfere with adjacent structures, the following should be measured:

- From the center of the central defect to the aortic root;
- From the center of the central defect to the SVC rim;

If the required SOD size exceeds the safely permitted size, the device should not be implanted.

Assessment of final result

Assessment by 2D and 3D TEE of the SOD, IAS, and adjacent structures should be performed from multiple windows before device release, allowing recapture and repositioning if necessary.

Proper positioning of the SOD should be confirmed, as well as the presence of interposed septal tissue between the discs, evidenced by slight separation of the discs on profile view. The device and its rims should be carefully evaluated using color Doppler to detect residual shunts.

Small residual shunts tend to decrease or disappear with progressive endothelialization of the device over a few months; however, they may persist in approximately 3% of cases after 1 year of implantation.[6] In many cases, residual flow is observed along the retroaortic rim immediately after implantation and before device release. This finding results from tension exerted by the delivery cable, which displaces the RA disc inferiorly, separating it from the septum.

This tension and residual flow tend to resolve after the SOD is released from the delivery cable. However, the operator must ensure that residual leakage is not due to device undersizing or slippage from the LA to the RA, especially in the presence of a deficient retroaortic rim.

Interference with pulmonary veins, the coronary sinus, atrioventricular valve function, and potential deformation of the aortic root should be carefully evaluated and excluded before device release. After SOD release, all these assessments should be systematically repeated.

Author Contributions

Conception and design of the research and writing of the manuscript: Mattoso AAA; critical revision of the manuscript for intellectual content: Sena JP, Feitosa-Filho GS, Duarte ML.

Potential Conflict of Interest

No potential conflict of interest relevant to this article was reported.

Sources of Funding

There were no external funding sources for this study.

Study Association

This study is not associated with any thesis or dissertation work.

Ethics Approval and Consent to Participate

This article does not contain any studies with human participants or animals performed by any of the authors.

Use of Artificial Intelligence

The authors did not use any artificial intelligence tools in the development of this work.

Availability of Research Data

The underlying content of the research text is contained within the manuscript.

References

1. Silvestry FE, Cohen MS, Armsby LB, Burkule NJ, Fleishman CE, Hijazi ZM, et al. Guidelines for the Echocardiographic Assessment of Atrial Septal Defect and Patent Foramen Ovale: From the American Society of Echocardiography and Society for Cardiac Angiography and Interventions. J Am Soc Echocardiogr. 2015;28(8):910-58. doi: 10.1016/j.echo.2015.05.015.
2. Warnes CA, Williams RG, Bashore TM, Child JS, Connolly HM, Dearani JA, et al. ACC/AHA 2008 Guidelines for the Management of Adults with Congenital Heart Disease: A Report of the American College of Cardiology/American Heart Association Task Force on Practice Guidelines (Writing Committee to Develop Guidelines on the Management of Adults with Congenital Heart Disease). Circulation. 2008;118(23):e714-833. doi: 10.1161/CIRCULATIONAHA.108.190690.
3. Mattoso AAA, Sena JP, Hotta VT. The Role of Echocardiography in the Assessment of the Interatrial Septum and Patent Foramen Ovale as an

Emboligenic Source. Arq Bras Cardiol. 2023;120(9):e20220903. doi: 10.36660/abc.20220903.

4. Hahn RT, Saric M, Faletra FF, Garg R, Gillam LD, Horton K, et al. Recommended Standards for the Performance of Transesophageal Echocardiographic Screening for Structural Heart Intervention: From the American Society of Echocardiography. J Am Soc Echocardiogr. 2022;35(1):1-76. doi: 10.1016/j.echo.2021.07.006.

5. Bechis MZ, Rubenson DS, Price MJ. Imaging Assessment of the Interatrial Septum for Transcatheter Atrial Septal Defect and Patent Foramen Ovale Closure. Interv Cardiol Clin. 2017;6(4):505-24. doi: 10.1016/j.iccl.2017.05.004.

6. Yared K, Baggish AL, Solis J, Durst R, Passeri JJ, Palacios IF, et al. Echocardiographic Assessment of Percutaneous Patent Foramen Ovale and Atrial Septal Defect Closure Complications. Circ Cardiovasc Imaging. 2009;2(2):141-9. doi: 10.1161/CIRCIMAGING.108.832436.

My Approach to a Standardized Assessment of the Tricuspid Valve: A Contemporary Analysis

Halsted Alarcão Gomes Pereira da Silva,[2] Alexandre Costa Souza,[3] Adenalva Beck[1]

Hospital Sírio Libanês,[1] Brasília, DF – Brazil

Instituto Dante Pazzanese de Cardiologia,[2] São Paulo, SP – Brazil

Hospital São Rafael/Rede D'or,[3] Salvador, BA – Brazil

Central Illustration: My Approach to a Standardized Assessment of the Tricuspid Valve: A Contemporary Analysis

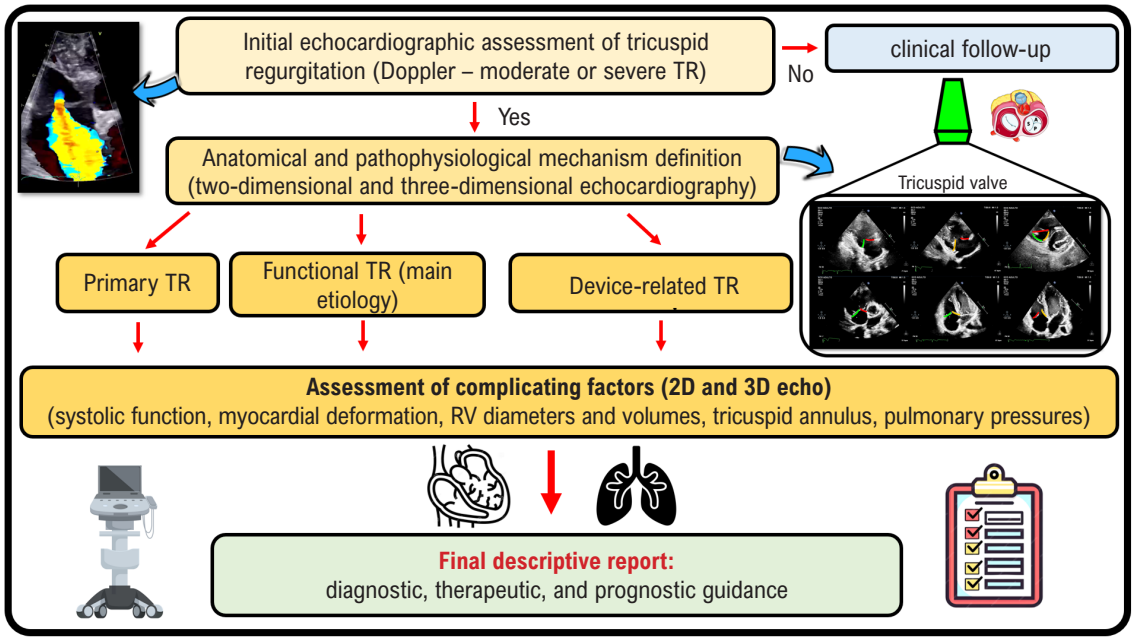

Arq Bras Cardiol: Imagem cardiovasc. 2026;39(2):e20260034

Abstract

Tricuspid regurgitation (TR) remains one of the most frequent valvular diseases encountered in echocardiographic practice. Mild cases generally do not require further investigation or specific treatment. Moderate and severe valvular disease, however, require more detailed anatomical and etiological assessment to better understand the underlying pathophysiological mechanism.

Two-dimensional echocardiographic analysis is the initial examination of choice and should be performed in a standardized manner, with individual identification of the leaflets using the main transthoracic echocardiographic windows. The description of complementary parameters – such as right ventricular (RV) systolic function, myocardial deformation assessed by longitudinal strain, right-sided chamber diameters and volumes, and estimation of pulmonary pressures – guides the clinician regarding potential therapeutic strategies and provides relevant prognostic information.

In this context, the 2025 European Society of Cardiology (ESC) guideline reinforces the importance of a standardized and comprehensive evaluation of the tricuspid valve and its hemodynamic repercussions. Most of this assessment can be performed using widely available two-dimensional transthoracic echocardiography.

Keywords

Tricuspid Valve; Tricuspid Valve Insufficiency; Pulmonary Hypertension.

Mailling Address: Halsted Alarcão Gomes Pereira da Silva •
Instituto Dante Pazzanese de Cardiologia. Rua Dr Dante Pazzanese, 500. Postal code: 04012-909. São Paulo, SP – Brazil
E-mail: halstedufg@hotmail.com
Manuscript received March 12, 2026, revised manuscript March 23, 2026, accepted March 25, 2026
Editor responsible for the review: Marcelo Tavares

DOI: https://doi.org/10.36660/abcimg.20260034i

CONTENTS

Introduction

The tricuspid valve (TV) is an important cardiac structure in echocardiographic evaluation, especially in conditions such as functional tricuspid regurgitation, pulmonary hypertension, and right ventricular dysfunction, where detailed analysis can influence therapeutic decisions. The tricuspid valve complex is an integrated anatomic-functional unit composed of valve leaflets, chordae tendineae, papillary muscles, and the valvular annulus, dynamically interacting with the right ventricle (RV), right atrium (RA), and pulmonary circulation. This integration contributes to hemodynamic function by ensuring unidirectional flow during the cardiac cycle and preventing regurgitation that would impair systolic efficiency.[1]

General Anatomy and Leaflet Structure

The TV is the most apical cardiac valve, positioned between the RA and the RV, with the largest orifice among the atrioventricular valves (typically 7–9 cm^2 in healthy adults, according to echocardiographic assessment). Its septal insertion is usually ≤10 mm more apical than the mitral valve plane, a classic echocardiographic finding that aids in anatomical characterization. The leaflets are asymmetrical and show numerical variability, with approximately 54% of cases presenting three cusps and 46% subdivided into the other types (two, four and five cusps). They are identified as anterior (or anterosuperior), septal, and posterior (or inferior/mural):

- **Anterior cusp:** The largest and most mobile, extending from the anterior infundibular region of the RV to the inferolateral wall, contributing to broad coaptation during diastole, essential for valve function.
- **Septal Cusp:** The smallest and least mobile, anchored to the interventricular septum, with a more apical insertion, relevant in the evaluation of dysfunctions associated with ventricular alterations.
- **Posterior Cusp:** Located along the posterior margin of the tricuspid annulus, extending between the septal leaflet and the RV free wall, playing a stabilizing role during ventricular contractions.

Coaptation occurs at the annular plane or slightly below it (with a coaptation height of 5–10 mm), functioning as a reserve mechanism in moderate annular dilation, as emphasized in tricuspid regurgitation assessment guidelines. Three-dimensional echocardiography is recommended to map these dynamics and identify pathological changes – such as tethering or dilation – that impair valvular competence.[2]

The Annulus as a Dynamic Structure

The tricuspid annulus has a non-planar geometry, with an oval saddle-shaped configuration (similar to the letter "D"), and dynamic dimensions that respond to preload and the cardiac cycle: approximately 10–15% shortening in diameters and 15–25% reduction in area during systole in healthy individuals. This annular contractility, which can be assessed by echocardiography, may be characterized in greater detail using three-dimensional (3D) techniques when available, contributing to the understanding of leaflet coaptation and the forces exerted on the subvalvular apparatus. Pathological measurements include a diastolic diameter ≥ 40 mm or ≥ 21 mm/m^2, preferably obtained in the apical four-chamber (4C) view, with body-surface-area indexing for prognostic purposes and intervention planning.

Subvalvular Apparatus: Chordae Tendineae and Papillary Muscles

The subvalvular apparatus consists of chordae tendineae that are less distensible than those of the mitral valve, arranged in a fan-shaped distribution, and three papillary muscle groups: anterior and posterior (well defined and anchored to the RV free wall) and septal. These structures anchor the cusps, preventing prolapse or eversion during systole, and are particularly sensitive to RV dilation, which may lead to tethering and functional regurgitation.

Epidemiology and Clinical Impact

Tricuspid regurgitation (TR) is a relatively common echocardiographic finding in the general population, with higher prevalence in women and in older patients. Mild TR is, in most cases, a benign condition that does not require further investigation. Significant TR is defined when regurgitation is ≥ moderate in severity and has an age- and sex-adjusted estimated prevalence of 0.55%, with a gradual increase associated with aging (4% in individuals ≥ 75 years).[2] Similar to mitral regurgitation, this condition should be interpreted along a continuous spectrum of severity, in which greater regurgitation correlates with higher risk of death and cardiovascular complications, independent of comorbidities, ventricular function, and pulmonary pressures.

Only 8-10% of patients with TR present clear anatomical abnormalities of the tricuspid valve complex (primary TR). These may result from various conditions such as infectious endocarditis, rheumatic disease, carcinoid syndrome, congenital anomalies (Ebstein anomaly), thoracic radiation, myxomatous disease, as well as trauma or iatrogenic valvular injury (e.g., endomyocardial biopsy). TR related to cardiac implantable electronic devices (CIEDs) represents a distinct entity requiring specific diagnostic and management approaches. In patients with CIEDs, diagnostic efforts should aim to determine whether the lead is the cause of TR (CIED-related TR) or merely incidental (CIED-associated TR).

In patients with secondary TR, the tricuspid valve leaflets are structurally normal, and regurgitation is caused by annular dilation and/or leaflet tethering due to right atrial (RA) dilation and/or right ventricular (RV) dilation and dysfunction. Based on key morphological and hemodynamic characteristics, two phenotypes of secondary TR have been proposed:

- **Atrial secondary TR**: primarily due to atrial fibrillation and characterized by the absence of significant leaflet tethering, but with marked dilation of the right atrium (RA) and annulus, along with preserved right ventricular (RV) size/function, pulmonary pressure, and left ventricular (LV) function.
- **Ventricular secondary TR:** caused by annular dilation and leaflet restriction as a consequence of left-sided ventricular or valvular disease (post-capillary pulmonary hypertension), pre-capillary pulmonary hypertension, or primary RV cardiomyopathy/ischemia (also after left-sided valve surgery).

In advanced stages of the disease, these two phenotypes may no longer be distinguishable; therefore, early characterization is essential for determining prognosis. Currently, there is no evidence of a direct impact on patient management; thus, current recommendations for intervention primarily consider primary versus secondary TR.

Diagnostic Evaluation Focused on Severity and Prognostic Aspects

A comprehensive transthoracic echocardiographic examination of the tricuspid valve requires a methodical approach to correctly identify the associated pathology. In two-dimensional echocardiography, it is not possible to visualize all three leaflets simultaneously, and there is considerable variability regarding which leaflets appear in each acquired image.

In the parasternal RV inflow view, the anterior leaflet always appears in the proximal field. In the distal field, the leaflet may be either the septal or the posterior one, depending on the transducer angulation.

In the short-axis view, the leaflet adjacent to the aortic valve generally corresponds to either the septal or the anterior leaflet, whereas the leaflet adjacent to the RV free wall is usually the posterior leaflet.

In the apical four-chamber view, the septal leaflet is positioned along the ventricular septum. The leaflet related to the free wall may be either the anterior or the posterior one, depending on the transducer angulation: when the aorta is visualized, it is the anterior leaflet; when the coronary sinus is seen, it is the posterior leaflet.

Figure 1 illustrates the main echocardiographic windows used in the two-dimensional assessment of the tricuspid valve, with identification of the corresponding leaflets visualized.

Compared with transthoracic echocardiography (TTE), transesophageal echocardiography is generally more limited in obtaining ideal windows for severity quantification due to the acquisition of off-axis imaging planes and the greater distance between the probe and the tricuspid valve.

Three-dimensional echocardiography provides unique views of the TV, allowing simultaneous visualization of all three or more leaflets and the entire annulus. Adding color Doppler to a full-volume acquisition not only makes it possible to analyze the mechanism and locate the TR jet, but also to quantify the size of the effective regurgitant orifice (ERO).[4]

Assessment of the right heart chambers

The RV is usually dilated in the presence of hemodynamically significant TR. Septal position produces a D-shaped LV, more evident in diastole (a pattern of RV volume overload). When TR is related to pulmonary hypertension, there is septal flattening throughout the

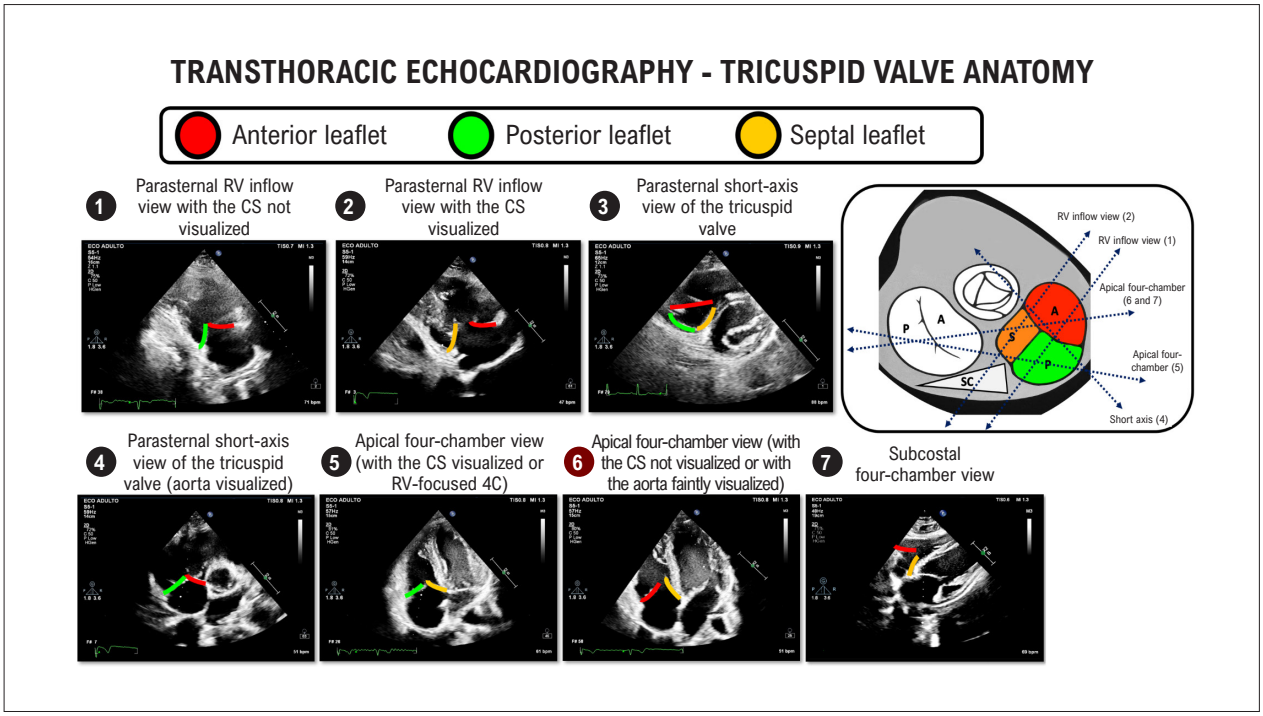

Figure 1 – *Two-dimensional transthoracic echocardiographic assessment of the tricuspid valve. Images 1, 2, 3, 4, 5, 6, and 7 demonstrate the main echocardiographic windows used for tricuspid valve evaluation and the corresponding leaflets visualized in a patient with normal anatomy. Anatomical variations should be considered, particularly in the parasternal short-axis and apical four-chamber views. Although not shown above, the apical two-chamber RV view generally displays the anterior and posterior leaflets of the tricuspid valve; RV: right ventricular; CS: coronary sinus; S: septal; A: anterior; P: posterior; adapted from Hungerford et al.[3]*

entire cardiac cycle, reflecting both diastolic and systolic RV overload (a pattern of RV pressure overload).

Parameters of RV systolic function are important for monitoring the effects of chronic primary TR and detecting deterioration of RV cardiac function. Assessing RV systolic function is challenging in this context because these parameters are load-dependent. A tricuspid annular plane systolic excursion (TAPSE) <1.7 cm and a right ventricular fractional area change (FAC) <35% are suggestive of RV dysfunction, although tricuspid annular excursion in particular may yield false-positive and false-negative results. In the presence of a valve with normal anatomy, abnormal RV function is more likely to be the cause rather than the consequence of TR. Significant chronic TR also leads to enlargement of the right atrium and the inferior vena cava. Finally, right atrial enlargement in patients with permanent atrial fibrillation and concomitant tricuspid annular dilation (>35 mm) may result in secondary tricuspid regurgitation of atrial etiology.[3]

Echocardiographic assessment of TR severity

1. Color-flow imaging

Color Doppler assessment of TR severity involves a critical analysis of the jet components: jet area, *vena contracta* (VC), and the flow convergence zone, with each of these components described below.

Jet area: Jet area is one of the color Doppler parameters used to evaluate the severity of regurgitation. However, there may be considerable overlap in jet areas among patients with mild versus moderate TR. In addition, eccentric regurgitant jets that impinge on the atrial wall appear smaller than centrally directed jets with a similar regurgitant volume. In general, a color Doppler jet area >10 cm^2 is consistent with severe TR; however, because several hemodynamic and anatomical factors affect the appearance of a central jet, jet area is often considered only a semiquantitative parameter. In cases of massive TR with lack of tricuspid leaflet coaptation, TR velocity may be so low that no aliasing occurs, making jet area calculation inaccurate.

Vena contracta: Visualization of the VC is technically less demanding than the PISA method and can be used semiquantitatively or qualitatively. When obtained from the apical four-chamber view and the parasternal RV inflow view, a VC width >0.7 cm identifies severe TR and is a marker of worse prognosis (Nyquist limit between 50–70 cm/s). Three-dimensional color Doppler can be used to measure both VC area and width. When comparing 2D and 3D color Doppler VC measurements, the maximum VC diameter is often larger on 3D Doppler imaging. The 3D VC area correlates well with the effective regurgitant orifice area (EROA). Based on currently available data, a VC area >0.4 cm^2 is a reasonable cutoff value for determining severe TR.

Flow convergence: The proximal flow convergence method is applicable to TR, but there is less experience with it than with MR. The PISA method for TR is subject to all the limitations seen in its application to MR. In particular, contour flattening as blood approaches the orifice may be exaggerated in TR, since the peak velocity is generally lower than in MR, resulting in underestimation of the regurgitant flow. Because the regurgitant orifice is often noncircular in TR, the standard PISA approach leads to additional underestimation. The 2D PISA method underestimates the effective regurgitant orifice area compared with 3D PISA and with the 3D VC area.[4]

2. Regurgitant volume

In theory, TR volume can be calculated by subtracting the flow across a non-regurgitant valve from the forward flow across the tricuspid annulus. However, this approach is rarely used in clinical practice, partly due to the difficulty in accurately estimating the shape of the tricuspid annulus (which is not circular) and the lack of uniformity in the site where velocity is measured across the annulus.

The optimal cutoff value for defining severe TR is still not well established. A comparative study in patients with significant mitral regurgitation (MR) and TR found that, for the same EROA obtained using the 2D PISA method (0.4 cm^2), the regurgitant volume cutoff values differed between TR (45 mL/beat) and MR (60 mL/beat). This difference is a direct consequence of the typically lower velocity of TR compared with MR, suggesting that, in clinical practice, different regurgitant volume thresholds need to be used, although a similar grading scheme may be applied for EROA.[4]

3. Pulsed and Continuous-Wave Doppler

It is important to note that TR jet velocity is not related to the regurgitant flow volume. In fact, very severe TR is often associated with a low jet velocity, with near equalization of RV and right atrial systolic pressures. Similar to MR, the continuous-wave Doppler characteristics of the TR jet that help assess regurgitation severity include signal intensity and the contour of the velocity curve. In severe TR, a dense spectral envelope is observed. A triangular jet contour with an early peak in maximum velocity indicates elevated right atrial pressure and a prominent regurgitant pressure wave (V wave) in the right atrium. It should be noted that this pattern may also be present in patients with milder degrees of TR who have markedly elevated right atrial pressure (reduced right atrial compliance).

Pulsed-wave Doppler evaluation of the hepatic veins helps corroborate the assessment of TR severity. As TR severity increases, the normally dominant systolic forward wave becomes less prominent. In severe TR, systolic flow reversal occurs. However, hepatic vein flow patterns are also influenced by right atrial and right ventricular compliance, respiration, preload, pacemaker rhythms, complete heart block, and atrial fibrillation/flutter. Systolic flow reversal is a specific sign of severe TR, provided that the modulating conditions mentioned above are considered during interpretation.[4]

Integrative approach to the assessment of tricuspid regurgitation (TR)

The ideal approach to evaluating TR severity is to integrate multiple parameters of tricuspid regurgitation, avoiding reliance on a single measurement. It is also important to distinguish between the regurgitant volume and its

hemodynamic consequences, particularly when considering acute versus chronic regurgitation.

If qualitative or semiquantitative parameters fall within the intermediate range between mild and severe, the TR severity is more likely to be moderate. Accurate quantification of TR severity is more challenging than in aortic or mitral valve disease. In cases where TTE provides limited assessment of regurgitation, when there is significant internal inconsistency, or when findings are discordant with the clinical presentation, additional evaluation using other imaging modalities may be necessary to more precisely assess the mechanism and severity of TR.[4]

Although the more recent classification proposed by Hahn et al.[1] in 2017 includes the categories of massive and torrential TR, this article will maintain the classification proposed by the American Society of Echocardiography (ASE) in its latest guideline, which divides severity into mild, moderate, and severe, in order to facilitate identification and reporting in outpatient echocardiography studies. Table 1 describes the main parameters used to grade the severity of TR.

Guideline Update

State of the Art in Tricuspid Valve Assessment in 2026

What's New in the 2025 European Society of Cardiology (ESC/EACTS) Guideline

Organization of Intervention and Reference Centers / "Heart Team"

The 2025 guideline reinforces the central role of the Heart Team and specialized reference centers with expertise in

Table 1 – Structural, qualitative, semiquantitative, and quantitative parameters for determining the severity of tricuspid regurgitation according to the recommendations of the American Society of Echocardiography (ASE)

ASSESSMENT OF CHRONIC TRICUSPID REGURGITATION SEVERITY - ECHOCARDIOGRAPHY			
PARAMETERS	**MILD**	**MODERATE**	**IMPORTANT**
STRUCTURAL			
Morphology of the tricuspid valve	Normal or slightly abnormal leaflets	Slightly abnormal leaflets	Severe valvular lesions (flail leaflet, severe retraction, large perforation)
RV and LV size	Usually normal	Normal or mild dilation	Dilated chambers *RV and RA size may remain within the "normal" range in patients with acute severe TR
Inferior vena cava diameter	IVC ≤ 20 mm	IVC between 21 and 25 mm	IVC > 25 mm
QUALITATIVE DOPPLER			
Jet area	Small, narrow, and central	Moderate and central	Large or eccentric jet with Coanda effect
Convergence zone	Not visible, transient, or small	Intermediate size and duration	Large PISA throughout systole
Continuous wave Doppler	Weak/partial/parabolic	Dense, parabolic or triangular	Dense, often triangular CW Doppler signal
SEMIQUANTITATIVE PARAMETERS			
Jet area (cm^2)	Not defined	Not defined	> 10 cm^2
Vena contracta width (cm)	< 0.3 cm	0.3 - 0.69 cm	≥ 0.7 cm
PISA radius	≤ 0.5 cm	0.6 - 0.9 cm	> 0.9 cm
Hepatic vein flow	Systolic-dominant	Systolic attenuation	Systolic flow reversal
Tricuspid inflow	Dominant A-wave	Variable	E-wave > 1.0 m/s
QUANTITATIVE			
EROA (cm^2)	< 0.20 cm^2	0.20 - 0.39 cm^2	≥ 0.40 cm^2
Regurgitant volume (PISA)	< 30 mL	30 - 44 mL	≥ 45 mL

TR: tricuspid regurgitation; RA: right atrial; RV: right ventricular; IVC: inferior vena cava; PISA: proximal isovelocity surface area; EROA: effective regurgitant orifice area.[4]

valvular heart disease to determine the optimal timing and modality of intervention, standardizing care pathways and prioritizing early evaluation. The official document and its supporting materials emphasize shared decision-making and practical decision pathways, with a focus on more concise and operational recommendations.

Advances in Imaging and Quantification

The 2025 European guideline consolidates 3D echocardiography, cardiac computed tomography, and cardiac magnetic resonance as key components in the screening and evaluation of valvular heart disease, assigning these modalities a more clearly defined role than in the 2021 guideline within the integrated cardiovascular imaging assessment. For the tricuspid valve, the update maintains the classic criteria for TR quantification (qualitative, semiquantitative, and quantitative), without changes to reference values (Figure 2). However, the new document reinforces a more contextualized interpretation of these parameters, integrating them with measurements of the tricuspid valve complex obtained through 3D assessment (annulus, gap, coaptation height, and tethering), as well as functional metrics of the RV – such as global and free-wall strain – which now contribute to severity grading and to defining the optimal therapeutic strategy.[5]

Functional Stratification of the RV and Tricuspid Valve Remodeling

The guideline now places greater emphasis on the consequences of TR by integrating RV function and remodeling, as well as tricuspid annular dilation and dynamics, into the decision-making process. In 2025, functional stratification of the right ventricle is based primarily on conventional echocardiographic parameters such as TAPSE and RV S', and can be refined by additional measures, including right ventricular ejection fraction by three-dimensional echocardiography (3D RVEF), RV strain, and three-dimensional anatomical assessment of the annulus and tricuspid apparatus when appropriate, to help determine the optimal timing and strategy for intervention. Figure 3 summarizes this framework, highlighting the integration between valvular mechanism parameters and conventional TR quantification.

In Figure 4, the main echocardiographic images are shown based on this sequential analysis, integrating two-dimensional acquisitions, color Doppler, and three-dimensional anatomical and volumetric assessment of the RV. This approach allows for a more holistic understanding of the mechanisms underlying TR as well as its hemodynamic repercussions.

Criteria for Tricuspid Valve Intervention

The update maintains the principle of earlier intervention in significant TR, especially when associated with left-sided valve disease, and reinforces the importance of concomitant treatment in these scenarios. The 2025 document adopts an organizational logic similar to that applied to the aortic and mitral valves, consolidating the role of the Heart Team as the central decision-making body for the tricuspid valve as well. As with left-sided valvular disease, management is now guided by multimodality imaging assessment and interdisciplinary discussion in reference centers, which determine the timing and modality of intervention—surgical or transcatheter—in an individualized, risk-based manner.

Specific considerations: sex, multimorbidity, combined valve disease

The 2025 guideline emphasizes patient-centered evaluation, incorporating sex, comorbidities, and combined

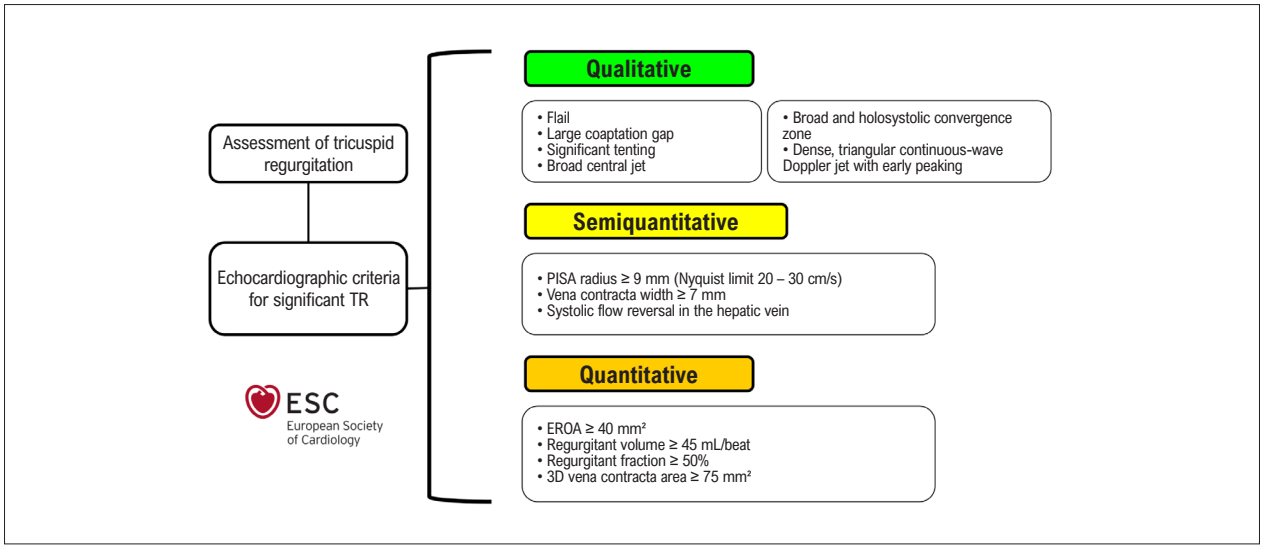

Figure 2 – *Structural, qualitative, semiquantitative, and quantitative parameters for determining the severity of tricuspid regurgitation according to the recommendations of the 2025 European Society of Cardiology guideline. "TR": tricuspid regurgitation; "PISA": proximal isovelocity surface area; EROA: effective regurgitant orifice area.*[2]

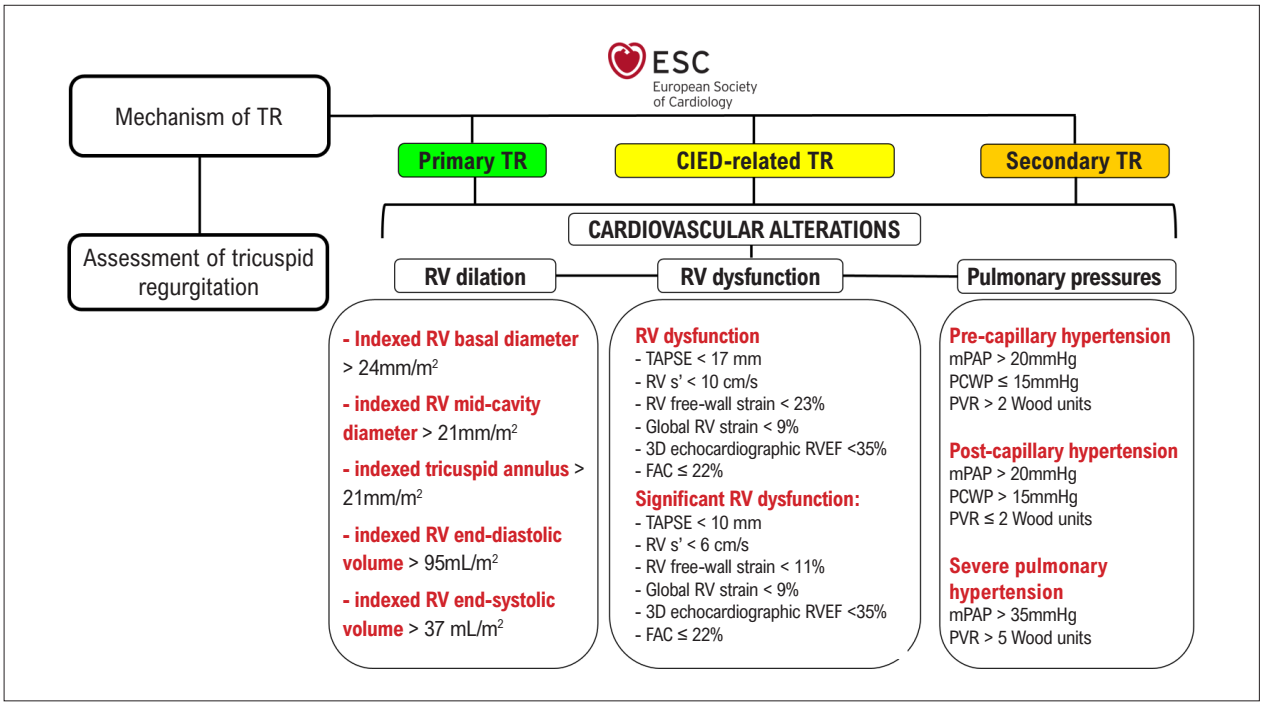

Figure 3 – *Additional integrated analysis complementing the quantification of TR severity, highlighting the main prognostic factors associated with worse cardiovascular outcomes according to the 2025 European Society of Cardiology guideline. "TR": tricuspid regurgitation; "RV": right ventricle; "TAPSE": tricuspid annular plane systolic excursion; "RVEF": right ventricular ejection fraction; "FAC": fractional area change; mPAP: mean pulmonary artery pressure; "PCWP": pulmonary capillary wedge pressure; "PVR": pulmonary vascular resistance; "CIED": cardiac implantable electronic device.*[2]

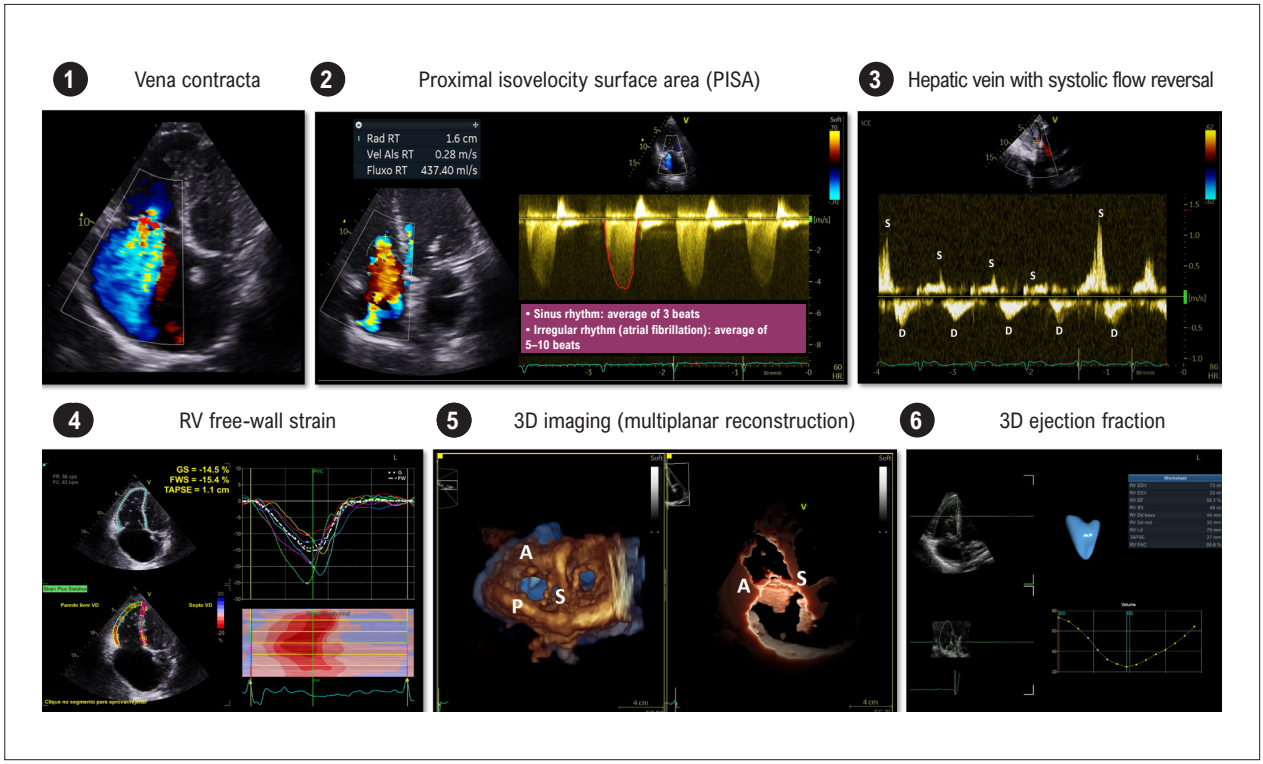

Figure 4 – *Fundamental two-dimensional and three-dimensional echocardiographic images for anatomical assessment, quantification, and prognostic analysis in patients with significant tricuspid regurgitation; "S": septal leaflet; "A": anterior leaflet; "P": posterior leaflet; "RV": right ventricle*

valvular disease into the decision-making process. In the context of TR, this means weighing frailty, RV dysfunction, pulmonary hypertension, and involvement of left-sided valves to determine the appropriate timing and modality of intervention, with referral to high-volume centers when a transcatheter approach is feasible.

Impacts on the tricuspid valve and practical recommendations

The 2025 ESC/EACTS guideline consolidates the understanding that TR should be approached with the same rigor applied to left-sided valvular disease. This repositioning has direct implications for clinical practice by reinforcing the central role of echocardiography in early disease detection, functional stratification of the right ventricle, and determination of the appropriate timing for intervention.

From an echocardiographic standpoint, assessment remains grounded in systematic two-dimensional analysis and conventional Doppler parameters, which are widely available and essential for the initial characterization of tricuspid regurgitation severity, mechanism, and hemodynamic impact. In this context, integration with additional anatomical and functional measurements allows for progressive refinement of diagnostic reasoning. Three-dimensional (3D) echocardiography, when available, serves as a complementary tool, contributing to a more detailed characterization of tricuspid annular geometry, coaptation patterns, and leaflet tethering.

Functional parameters of the right ventricle – such as TAPSE, tricuspid annular systolic velocity, three-dimensional right ventricular ejection fraction (3D RVEF), and global longitudinal strain – should be interpreted in an integrated manner, considering load-dependent limitations and the clinical context. This combined approach supports a more robust evaluation, particularly in scenarios where therapeutic decision-making requires greater anatomical or functional precision, as illustrated in the central figure of the article.

In clinical practice, this conceptual evolution translates into three main developments.

First, earlier detection of structural and functional abnormalities, in which identification of significant annular dilation or early right ventricular dysfunction justifies more frequent reassessment and timely referral for Heart Team discussion.

Second, a clearer definition of the optimal timing for intervention, particularly in patients with significant tricuspid regurgitation associated with left-sided valve disease, favoring concomitant treatment and reducing progression to advanced stages of right ventricular remodeling. Third, the gradual incorporation of transcatheter therapies, considered in selected scenarios – especially in patients with high surgical risk or with favorable anatomy better characterized by advanced imaging modalities.

In the daily routine of the echocardiography laboratory, this approach implies valuing a well-executed and standardized two-dimensional evaluation, using three-dimensional echocardiography as a complementary tool whenever pertinent, and monitoring right ventricular function parameters with the same regularity applied to left-sided valvular diseases. This set of principles supports a more consistent, accessible practice aligned with contemporary recommendations, enabling individualized decisions grounded in multidisciplinary teams.

Trends and Future Perspectives

Advances in tricuspid valve assessment are expected to focus on the integration of emerging technologies that enhance diagnostic precision and the ability to dynamically characterize cardiac remodeling. The incorporation of artificial intelligence algorithms into echocardiography and tomography routines should enable automatic anatomical segmentation, more stable measurements of the tricuspid annulus, and refined three-dimensional analysis of coaptation, favoring interpretations that are less examiner-dependent and more comparable across institutions.

In the therapeutic context, continuous development of devices for transcatheter repair or replacement of the tricuspid valve is observed, with greater suitability for the anatomical spectrum of primary and secondary regurgitation. As these devices achieve technological maturity and wider availability in specialized centers, decision-making is expected to incorporate more objective metrics of right ventricular function, extent of tethering, and annular geometry, expanding the ability to select interventions with greater physiological precision.

The progressive understanding of tricuspid regurgitation phenotypes, particularly the atrial phenotype, enables more informative categorizations of the hemodynamic behavior of the valvopathy and of the mechanisms of structural progression. This differentiation tends to improve management strategies that consider not only the severity of regurgitation but also the trajectory of right atrial and ventricular remodeling.

Finally, the field is moving toward models that integrate clinical data, biomarkers, two-dimensional and three-dimensional echocardiographic parameters, and machine learning–derived variables, with the potential to generate predictive platforms capable of estimating disease progression and functional impact in the medium and long term. These approaches favor a more anticipatory view of the pathophysiological process, with therapeutic choices based on quantitative projections and individualized risk stratification.

Conclusion

Transthoracic echocardiography remains the primary imaging modality for assessing the etiology, mechanism, and severity of tricuspid valve disease. A comprehensive evaluation requires integrating data from multiple echocardiographic windows and modalities, which may include three-dimensional transthoracic and transesophageal imaging, as well as complementary examinations such as cardiac CT and cardiac MRI.

New guidelines, such as the most recent European Society of Cardiology publication, provide direction for a systematic and standardized assessment of imaging findings, taking into account the patient's clinical context, the structural disease affecting the tricuspid valve complex, and the impact on related chambers such as the right ventricle.

The rapid expansion of tricuspid interventional cardiology has renewed interest in the detailed evaluation of this valve

and reaffirms echocardiography—particularly its structural analysis—as the cornerstone of clinical decision-making. This approach enables more appropriate selection of patients who are likely to benefit from intervention.

Author Contributions

Conception and design of the research and writing of the manuscript: Silva HAGP, Souza AC; critical revision of the manuscript for intellectual content: Silva HAGP, Souza AC, Beck A.

Potential Conflict of Interest

No potential conflict of interest relevant to this article was reported.

Sources of Funding

There were no external funding sources for this study.

Study Association

This study is not associated with any thesis or dissertation work.

Ethics Approval and Consent to Participate

This article does not contain any studies with human participants or animals performed by any of the authors.

Use of Artificial Intelligence

The authors did not use any artificial intelligence tools in the development of this work.

Availability of Research Data

The underlying content of the research text is contained within the manuscript.

References

1. Hahn RT, Zamorano JL. The Need for a New Tricuspid Regurgitation Grading Scheme. Eur Heart J Cardiovasc Imaging. 2017;18(12):1342-3. doi: 10.1093/ehjci/jex139.
2. Praz F, Borger MA, Lanz J, Marin-Cuartas M, Abreu A, Adamo M, et al. 2025 ESC/EACTS Guidelines for the Management of Valvular Heart Disease. Eur Heart J. 2025;46(44):4635-736. doi: 10.1093/eurheartj/ehaf194.
3. Hungerford SL, Rye EE, Hansen PS, Bhindi R, Choong C. Key Echocardiographic Considerations for Tricuspid Valve Transcatheter Edge-to-Edge Repair. J Am Soc Echocardiogr. 2023;36(4):366-80.e1. doi: 10.1016/j.echo.2023.01.013.
4. Zoghbi WA, Adams D, Bonow RO, Enriquez-Sarano M, Foster E, Grayburn PA, et al. Recommendations for Noninvasive Evaluation of Native Valvular Regurgitation: A Report from the American Society of Echocardiography Developed in Collaboration with the Society for Cardiovascular Magnetic Resonance. J Am Soc Echocardiogr. 2017;30(4):303-71. doi: 10.1016/j.echo.2017.01.007.
5. Vahanian A, Beyersdorf F, Praz F, Milojevic M, Baldus S, Bauersachs J, et al. 2021 ESC/EACTS Guidelines for the Management of Valvular Heart Disease. Eur Heart J. 2022;43(7):561-632. doi: 10.1093/eurheartj/ehab395.

Review Article

My Approach to Agitated Saline Contrast Echocardiography in Pediatric Patients

Karen Saori Shiraishi Sawamura,[1,2] *Márcio Miranda Brito*[3]
Universidade de São Paulo, Instituto da Criança,[1] *São Paulo, SP – Brazil*
Hospital Israelita Albert Einstein,[2] *São Paulo, SP – Brazil*
Universidade Federal do Norte do Tocantins,[3] *Araguaina, TO – Brazil*

Abstract

Agitated saline contrast is a simple, safe, widely available echocardiography technique. It is particularly useful for evaluating right-to-left shunts and pulmonary vascular abnormalities in the pediatric population. This article presents a practical approach to using this technique in pediatric echocardiography. It reviews the underlying physiological principles, the technical aspects of preparation and image acquisition, and the main clinical applications.

What is agitated saline contrast?

Agitated saline contrast consists of the intravenous (IV) administration of normal saline that has been vigorously agitated, a process that promotes the formation of microbubbles from gases dissolved in the fluid under hydrostatic pressure. These microbubbles have a mean diameter greater than 9 μm, which prevents their passage through the pulmonary capillary bed under normal physiological conditions.[1]

After injection, immediate opacification of the right-sided chambers occurs. The microbubbles have a short half-life and dissolve rapidly as they pass through the pulmonary circulation. Therefore, in an intact cardiopulmonary system, they are not observed in the left-sided chambers.

The detection of microbubbles in the left atrium (LA) or left ventricle indicates diversion of blood flow beyond the pulmonary capillary bed, consistent with the presence of an intracardiac or intrapulmonary shunt. Under normal conditions, microbubbles (> 9 μm) do not traverse the pulmonary capillaries and dissolve within the lungs. Thus, any visualization of contrast in the left side of the heart is considered abnormal and indicates deviation from normal capillary flow.

Keywords

Ecocardiography; Contrast Echocardiography; Patent Foramen Ovale; Atrial Septal Defect; Hepatopulmonary Syndrome.

Mailing Address: Karen Saori Shiraishi Sawamura •
Universidade de São Paulo Instituto da Criança. Av. Dr. Enéas Carvalho de Aguiar, 647. Postal code: 05403-000. São Paulo, SP – Brazil
E-mail: kasaori@gmail.com
Manuscript received March 25, 2026, revised manuscript April 6, 2026, accepted April 6, 2026
Editor responsible for the review: Marcelo Tavares

DOI: https://doi.org/10.36660/abcimg.20260041i

Which echocardiographic view should be used?

For evaluation with agitated saline, the preferred echocardiographic view is the apical four-chamber view, as it provides optimal visualization of the interatrial septum, minimizes shadowing artifacts over the left-sided chambers, and facilitates identification of microbubble passage from the right atrium (RA) to the LA.

If an adequate apical window cannot be obtained, the subcostal four-chamber view is an appropriate alternative, particularly in the pediatric population, in which this window often provides superior image quality.

Image acquisition should begin before the arrival of microbubbles in the RA and be maintained for at least 10-20 heartbeats after opacification of this chamber, allowing proper temporal assessment of contrast appearance in the left-sided chambers. The use of harmonic imaging is recommended to increase diagnostic sensitivity.[2] In addition, when feasible, physiological maneuvers such as Valsalva or coughing should be synchronized with contrast arrival in the RA to enhance detection of right-to-left shunts.

How should the solution be prepared?

Preparation requires peripheral IV access in an upper limb (preferably the right one) and a standardized technique to ensure adequate microbubble formation.

The technique consists of vigorous agitation by rapidly transferring the solution between two syringes connected by a three-way stopcock approximately 20 times, promoting appropriate microbubble formation (Central Illustration). Before IV administration, any visibly large air bubbles should be discarded to ensure procedural safety.

Injection should be performed immediately after agitation, as microbubbles have a short half-life.[1–3] On echocardiography, the contrast appears as hyperechoic material within the right-sided chambers, allowing dynamic assessment of its distribution and potential passage into the left-sided chambers. Recommended preparation options for pediatric use are described in Table 1.

Materials

- Peripheral IV access (preferably in an upper limb);
- Two 10 mL syringes;
- Three-way stopcock.

Review Article

Central Illustration: My Approach to Agitated Saline Contrast in Pediatric Patients: Clinical Applications

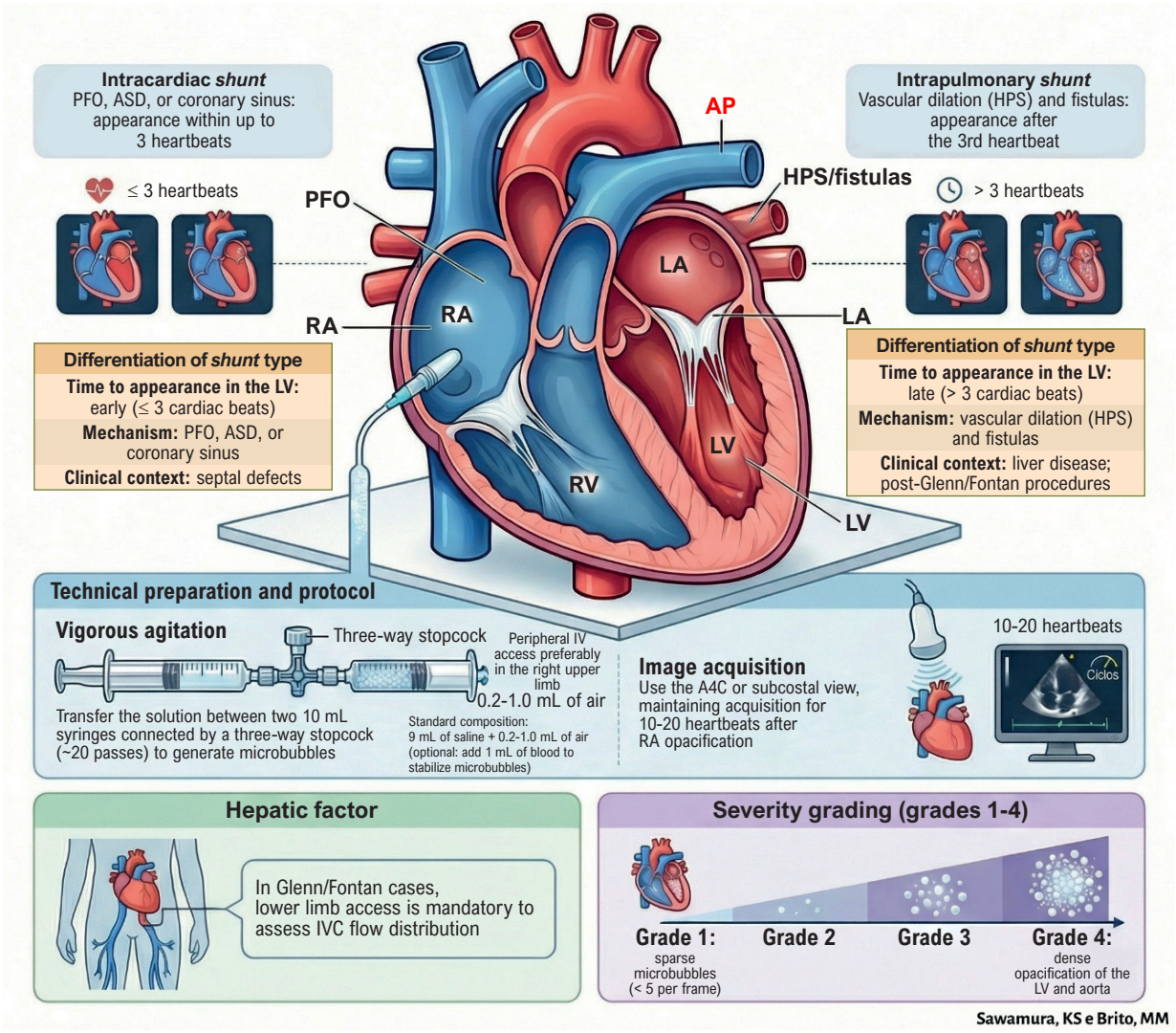

Arq Bras Cardiol: Imagem cardiovasc. 2026;39(2):e20260041

My Approach to Agitated Saline Contrast in Pediatric Patients: Clinical Applications. A4C: apical four-chamber view; ASD: atrial septal defect; HPS: hepatopulmonary syndrome; IVC: inferior vena cava; IV: intravenous; LV: left ventricle; PFO: patent foramen ovale; RA: right atrium; PA: pumonary artery.

Table 1 – Composition of agitated saline contrast for echocardiography

Option	Composition
A – Saline	9 mL of normal saline (0.9%) + 0.2-1 mL of air
B – With blood	8 mL of normal saline (0.9%) + 1 mL of blood + 0.2-1 mL of air

Before IV administration, any visibly large air bubbles should be discarded to ensure procedural safety.

Main indications in pediatric echocardiography

a) Investigation of intracardiac shunts

Agitated saline is widely used in pediatric echocardiography for the investigation and characterization of intracardiac shunts, particularly patent foramen ovale (Figure 1) and atrial septal defects, including coronary sinus-type defects (Figure 2).[2]

The key technical criterion for diagnosing an intracardiac shunt is the early appearance of microbubbles in the left-sided chambers, typically within the first 3 heartbeats after RA opacification. In sedated patients, brief abdominal compression may be applied to increase the sensitivity of the test.

This technique also assists in the characterization of venous anomalies, such as persistent left superior vena cava (SVC), unroofed coronary sinus, and arteriovenous fistulas.[4,5]

b) Hepatopulmonary syndrome (HPS) in pediatrics

HPS in pediatric patients occurs in the context of liver disease or portal hypertension and is characterized by intrapulmonary vascular dilation, partly mediated by increased nitric oxide production. This process leads to the formation of pulmonary microfistulas and disruption of the ventilation-perfusion relationship, allowing poorly oxygenated blood to enter the systemic circulation.

Diagnosis is based on the triad of underlying liver disease, evidence of intrapulmonary vascular dilation on echocardiography, and an increased alveolar-arterial gradient on arterial blood gas analysis. Clinically, it presents predominantly with hypoxemia of variable severity.[6,7]

On echocardiography, a delayed appearance of microbubbles in the left-sided chambers (> 3 heartbeats) is observed (Figure 3). This pattern differentiates HPS from intracardiac shunts, in which contrast appears early.[7]

c) Arteriovenous fistulas after Glenn/Fontan procedures

Following Glenn/Fontan surgeries, the development of pulmonary arteriovenous fistulas is related to the hemodynamic alterations inherent to single-ventricle physiology. The absence of pulsatile pulmonary flow, exclusion of hepatic flow with consequent deprivation of the so-called "hepatic factor," and chronically elevated central venous pressure promote endothelial dysfunction and pulmonary vascular remodeling, favoring microfistula formation.[2,8]

Clinically, these patients may present with persistent or progressive cyanosis. On agitated saline echocardiography, the characteristic finding is delayed appearance of microbubbles in the left-sided chambers, consistent with an intrapulmonary shunt pattern (Figure 4).

The origin of the shunt determines the site of contrast injection[9]:

- **Upper limb access (cephalic or basilic veins)** allows evaluation of SVC drainage into the pulmonary arteries and is useful for detecting pulmonary arteriovenous fistulas in cases of uneven flow distribution;

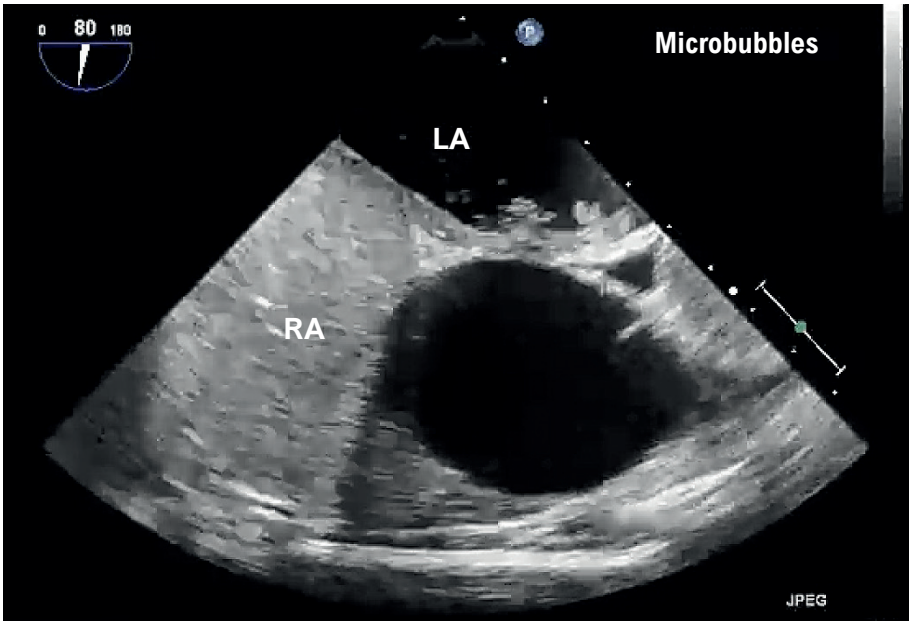

Figure 1 – *Transesophageal echocardiography demonstrating opacification of the RA after infusion of agitated saline contrast via peripheral IV access, with early passage of microbubbles into the LA through a PFO. IV: intravenous; LA: left atrium; PFO: patent foramen ovale; RA: right atrium.*

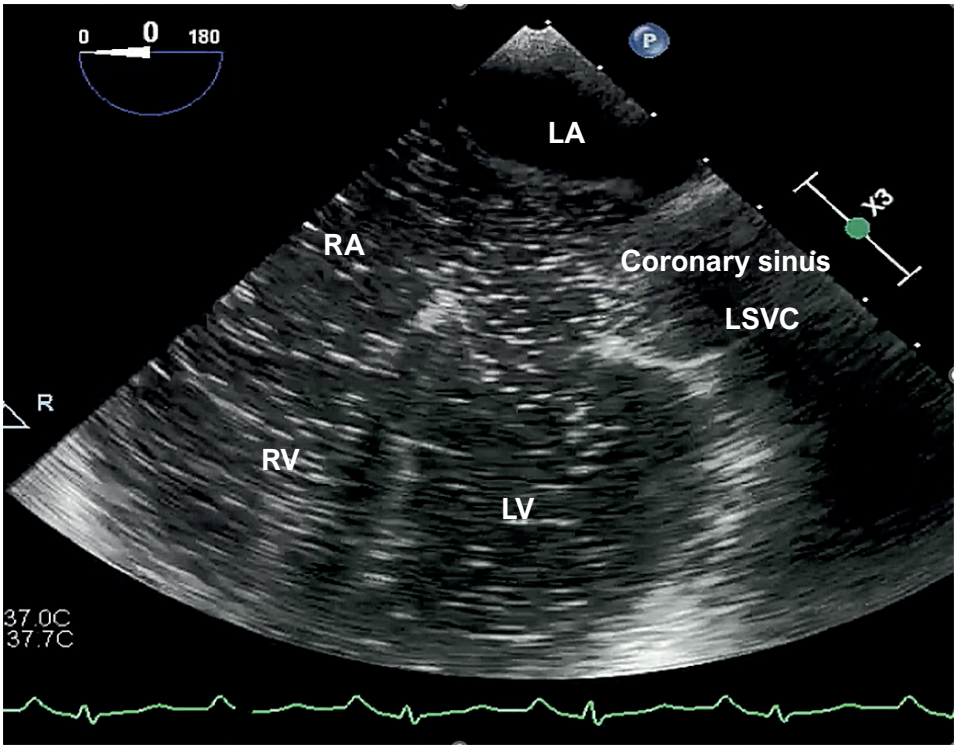

Figure 2 – *Transesophageal echocardiography in the four-chamber view after infusion of agitated saline contrast via peripheral IV access in the left upper limb, demonstrating opacification of the coronary sinus, the LSVC, and the LV, secondary to the presence of a coronary sinus-type ASD. ASD: atrial septal defect; LA: left atrium; LSVC: left superior vena cava; LV: left ventricle; RA: right atrium; RV: right ventricle.*

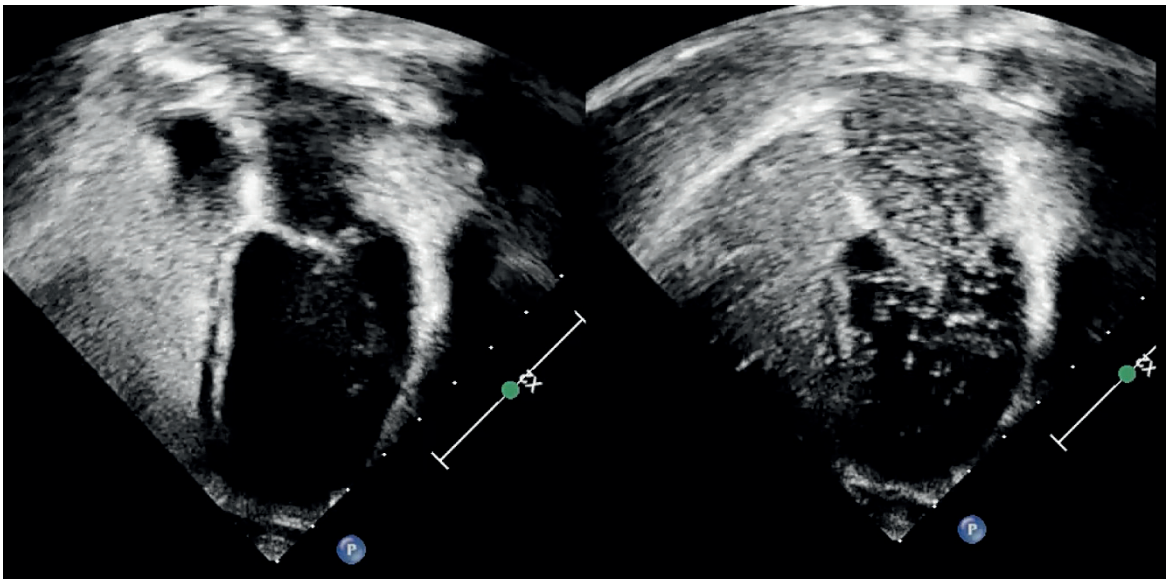

Figure 3 – *Transthoracic echocardiography in the apical four-chamber view demonstrating delayed appearance of microbubbles (> 3 heartbeats) in the left-sided chambers after infusion of agitated saline via peripheral IV access. IV: intravenous.*

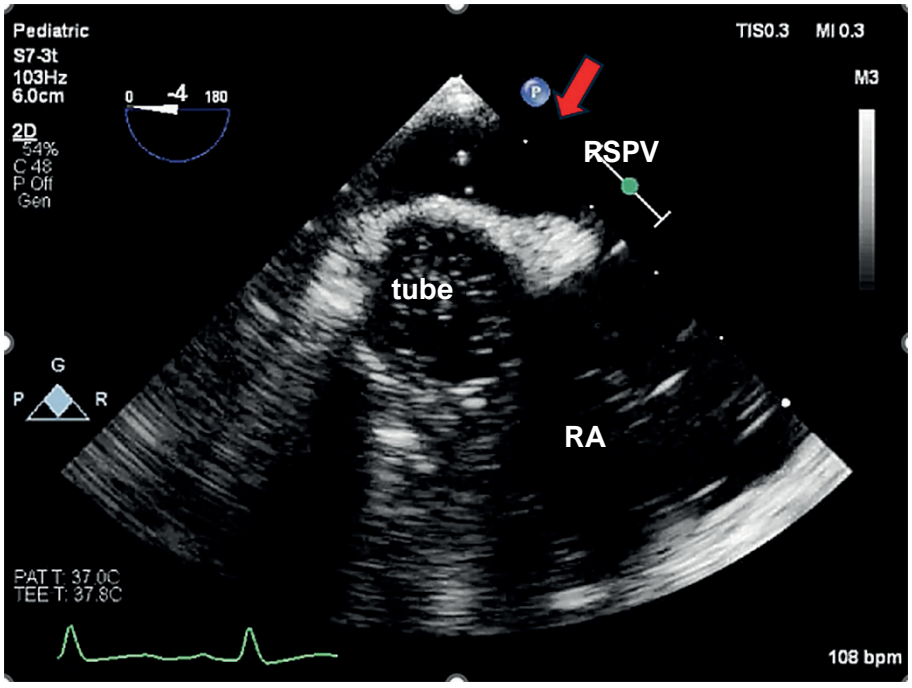

Figure 4 – *Transesophageal echocardiography in a patient following extracardiac Fontan surgery. The arrow indicates the RSPV, where microbubbles are observed after injection of agitated saline via peripheral IV access, which suggests the presence of pulmonary microfistulas. IV: intravenous; RA: right atrium; RSPV: right superior pulmonary vein.*

- **Lower limb access (saphenous or femoral veins)** is mandatory to assess the distribution of the hepatic factor. Early appearance of microbubbles in the left-sided chambers after injection via the inferior vena cava confirms the presence of an intrapulmonary shunt.

d) Pericardiocentesis

Agitated saline injection can be used during pericardiocentesis to confirm, under echocardiographic guidance, correct positioning of the needle or catheter within the pericardial space, particularly when the aspirate is bloody or there is uncertainty regarding instrument location.

The appearance of microbubbles in the pericardial space after the injection of 3–5 mL of agitated saline allows differentiation between the pericardial space and the cardiac chambers, as shown in Figure 5, reducing the risk of inadvertent puncture of intracardiac structures.[10]

Classification

Severity grading:[9]

- **Grade 1:** sparse microbubbles in the LA (< 5 bubbles per frame);
- **Grade 2:** 5-25 microbubbles in the LA;
- **Grade 3:** > 25 microbubbles without complete cavity opacification;
- **Grade 4:** dense LA opacification, similar to right-sided chambers, with contrast visible in the systemic ventricle and aorta.

Technical differentiation between intracardiac and intrapulmonary shunts

The distinction is based on the timing of microbubble appearance in the left-sided chambers (Table 2).

Conclusion

Agitated saline contrast is a simple, safe, highly useful technique in pediatric echocardiography. It enables the identification and differentiation of intracardiac and intrapulmonary shunts, the characterization of systemic venous anomalies, the assessment of alterations related to single-ventricle physiology, and procedural support, such as image-guided pericardiocentesis.

When applied judiciously and with appropriate monitoring, it improves diagnostic accuracy, enhances procedural safety, and reduces the need for invasive or higher-cost methods, thereby optimizing clinical decision-making.

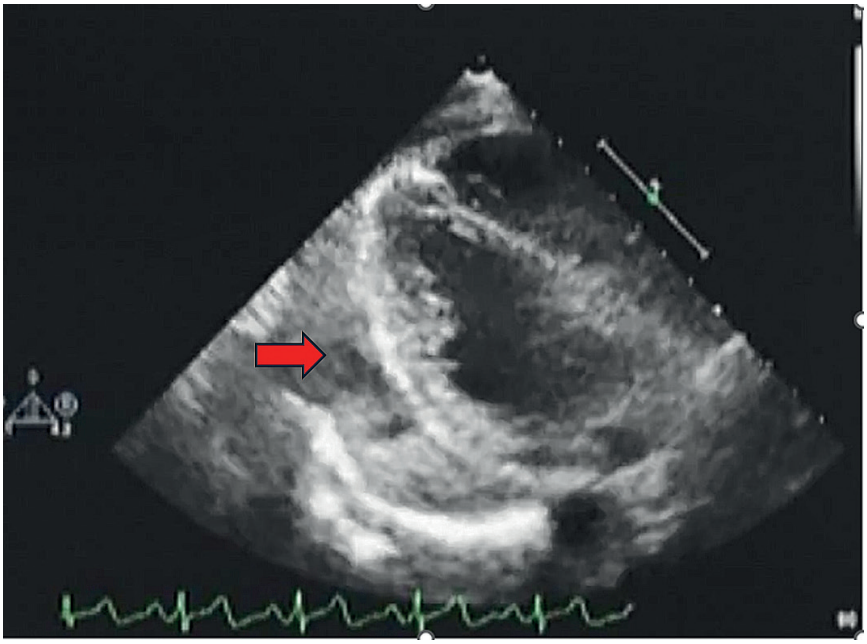

Figure 5 – *Transthoracic echocardiography with infusion of agitated saline into the pericardial space to confirm correct needle positioning during puncture.*

Author Contributions

Conception and design of the research, acquisition of data, analysis and interpretation of the data, writing of the manuscript, and critical revision of the manuscript for intellectual content: Sawamura KSS, Brito MM.

Potential Conflict of Interest

No potential conflict of interest relevant to this article was reported.

Table 2 – Technical differentiation between intracardiac and intrapulmonary shunts

Characteristic	Intracardiac shunt	Intrapulmonary shunt
Time to appearance in the LV	Early (≤ 3 heartbeats)	Late (> 3-6 heartbeats)
Mechanism	Intracardiac communication	Pulmonary vascular dilation, microfistulas
Clinical example	PFO, ASD	HPS, post-Glenn/Fontan

ASD: atrial septal defect; HPS: hepatopulmonary syndrome; PFO: patent foramen ovale.

Sources of Funding

There were no external funding sources for this study.

Study Association

This study is not associated with any thesis or dissertation work.

Ethics Approval and Consent to Participate

This article does not contain any studies with human participants or animals performed by any of the authors.

Use of Artificial Intelligence

During the preparation of this work, the authors used NotebookLM to create the central figure. After using this tool/service, the authors reviewed and edited the content as needed and take full responsibility for the content of the published article.

Availability of Research Data

The underlying content of the research text is contained within the manuscript.

References

1. Gupta SK, Shetkar SS, Ramakrishnan S, Kothari SS. Saline Contrast Echocardiography in the Era of Multimodality Imaging--Importance of "Bubbling It Right". Echocardiography. 2015;32(11):1707-19. doi: 10.1111/echo.13035.
2. Lopez L, Saurers DL, Barker PCA, Cohen MS, Colan SD, Dwyer J, et al. Guidelines for Performing a Comprehensive Pediatric Transthoracic Echocardiogram: Recommendations from the American Society of Echocardiography. J Am Soc Echocardiogr. 2024;37(2):119-70. doi: 10.1016/j.echo.2023.11.015.
3. Porter TR, Abdelmoneim S, Belcik JT, McCulloch ML, Mulvagh SL, Olson JJ, et al. Guidelines for the Cardiac Sonographer in the Performance of Contrast Echocardiography: A Focused Update from the American Society of Echocardiography. J Am Soc Echocardiogr. 2014;27(8):797-810. doi: 10.1016/j.echo.2014.05.011.
4. Labovitz AJ, Noble VE, Bierig M, Goldstein SA, Jones R, Kort S, et al. Focused Cardiac Ultrasound in the Emergent Setting: A Consensus Statement of the American Society of Echocardiography and American College of Emergency Physicians. J Am Soc Echocardiogr. 2010;23(12):1225-30. doi: 10.1016/j.echo.2010.10.005.
5. Watzinger N, Brussee H, Fruhwald FM, Schumacher M, Zweiker R, Stoschitzky K, et al. Pericardiocentesis Guided by Contrast Echocardiography. Echocardiography. 1998;15(7):635-40. doi: 10.1111/j.1540-8175.1998.tb00661.x.
6. Rodríguez-Roisin R, Krowka MJ. Hepatopulmonary Syndrome--A Liver-Induced Lung Vascular Disorder. N Engl J Med. 2008;358(22):2378-87. doi: 10.1056/NEJMra0707185.
7. Brito MM, Seda J Neto, Fonseca EA, Pugliese R, Danesi VB, Candido HL, et al. Outcomes of Liver Transplantation in Pediatric Recipients with Cardiovascular Disease. Pediatr Transplant. 2018;22(1). doi: 10.1111/petr.13081.
8. Bhatt AB, Foster E, Kuehl K, Alpert J, Brabeck S, Crumb S, et al. Congenital Heart Disease in the Older Adult: A Scientific Statement from the American Heart Association. Circulation. 2015;131(21):1884-931. doi: 10.1161/CIR.0000000000000204.
9. Rana BS, Thomas MR, Calvert PA, Monaghan MJ, Hildick-Smith D. Echocardiographic Evaluation of Patent Foramen Ovale Prior to Device Closure. JACC Cardiovasc Imaging. 2010;3(7):749-60. doi: 10.1016/j.jcmg.2010.01.007.
10. Holmes DR Jr, Nishimura R, Fountain R, Turi ZG. Iatrogenic Pericardial Effusion and Tamponade in the Percutaneous Intracardiac Intervention Era. JACC Cardiovasc Interv. 2009;2(8):705-17. doi: 10.1016/j.jcin.2009.04.019.

My Approach to Echocardiographic Assessment of Left Ventricular Filling Pressures: From Ambiguity to Precision With New Guidelines

Marco Stephan Lofrano Alves,[1,2] Larissa Maria Vosgerau,[1] Marcelo Vitola Dreckmann,[1] Roberto D´Ávila Martins,[1] Cláudia Biondo Zanlorensi,[1] Eduardo Henrique Bonotto[1]

Universidade Federal do Paraná,[1] Curitiba, PR – Brazil

SEMEC,[2] Curitiba, PR – Brazil

Abstract

The echocardiographic estimation of left ventricular (LV) filling pressures is a cornerstone in the assessment of heart failure, particularly in patients with heart failure with preserved ejection fraction (HFpEF). The 2016 American Society of Echocardiography/European Association of cardiovascular Imaging algorithm standardized this evaluation using key variables, but a substantial proportion of cases remained indeterminate in clinical practice. The recent update of the American guideline reorganized the approach into a hierarchical framework, incorporating age-related adjustments and formalizing the role of left atrial strain (LAS) as a tie-breaking parameter, while also providing a more detailed characterization of special clinical scenarios. In parallel, the 2024 British Society of Echocardiography guideline emphasizes the pathophysiological interpretation of ventricular filling, complementing the operational framework proposed by the American document. Multicenter studies with invasive validation support these updates, establishing LAS as a robust marker of increased filling pressures. In this article, we present My Approach to echocardiographic assessment of LV filling pressures, based on an initial morphofunctional evaluation, followed by structured screening (Step 1) and further refinement (Step 2) incorporating LAS and additional parameters. We also provide a comparison between guidelines, discuss common pitfalls and algorithm limitations, and include case-based videos for practical application.

Introduction

The echocardiographic assessment of left ventricular (LV) filling pressures has evolved from a mitral Doppler-centered approach to an integrated model incorporating both morphological and functional parameters, supported by increasingly structured algorithms. The 2016 American Society of Echocardiography (ASE)/European Association of cardiovascular Imaging (EACVI) guideline for assessing LV diastolic function by echocardiography marked a pivotal step in this transition by proposing a simplified framework based on four core variables;[1] however, a substantial proportion of examinations remained indeterminate with respect to filling pressure estimation. This limits diagnostic accuracy, particularly in conditions such as heart failure with preserved ejection fraction (HFpEF).

In addition, specific clinical conditions (e.g., atrial fibrillation [AF], pulmonary hypertension, and valvular heart disease) have continued to pose challenges to the applicability and interpretation of these parameters.[2]

Recent updates have advanced this field along two complementary directions. The 2024 British Society of Echocardiography guideline for assessing LV diastolic function[3] reinforces the pathophysiological basis of ventricular filling and formalizes left atrial strain (LAS) as a refinement tool. In parallel, the ASE 2025 update reorganizes the decision-making process, incorporates age-related adjustments, and integrates atrial strain in a similar manner,[4] supported by multicenter studies with invasive validation (Table 1).[5]

This article translates these advances into daily clinical practice through My Approach to echocardiographic assessment of LV filling pressures, an approach designed to be practical, reproducible, and clinically meaningful while preserving a strong physiological foundation (Central Illustration).

Before the algorithm: the integrated view of the echocardiographer

The assessment of diastolic function should always begin with clinical contextualization (e.g., age, symptoms, cardiac rhythm, valvular heart disease, and hemodynamic status) because the algorithm addresses a specific clinical question and should not be applied indiscriminately.[3,4]

Before applying any flowchart, a two-dimensional morphofunctional assessment allows the echocardiographer to rapidly integrate patterns of hypertrophy, LA size, ventricular geometry, mitral annular motion, signs of pulmonary hypertension, and the overall visual impression of ventricular compliance. This approach enables the clinician to position the patient within a probable phenotype: low, intermediate, or high likelihood of increased filling pressures.

This initial impression does not replace the algorithm; rather, it prevents both the mechanical application of numerical thresholds and conclusions drawn without objective criteria. It serves as a conceptual framework that

Keywords

Left Ventricular Function; Echocardiography; Heart Failure

Mailing Address: Marco Stephan Lofrano Alves •
Universidade Federal do Paraná. RUA Mateus Leme, 3945, apt 504, 2. Postal code: 82200-000. Curitiba, PR – Brazil
E-mail: mslalves@hotmail.com
Manuscript received March 12, 2026, revised manuscript March 23, 2026, accepted March 25, 2026
Editor responsible for the review: Marcelo Tavares

DOI: https://doi.org/10.36660/abcimg.20260026i

Central Illustration: My Approach to Echocardiographic Assessment of Left Ventricular Filling Pressures: From Ambiguity to Precision With New Guidelines

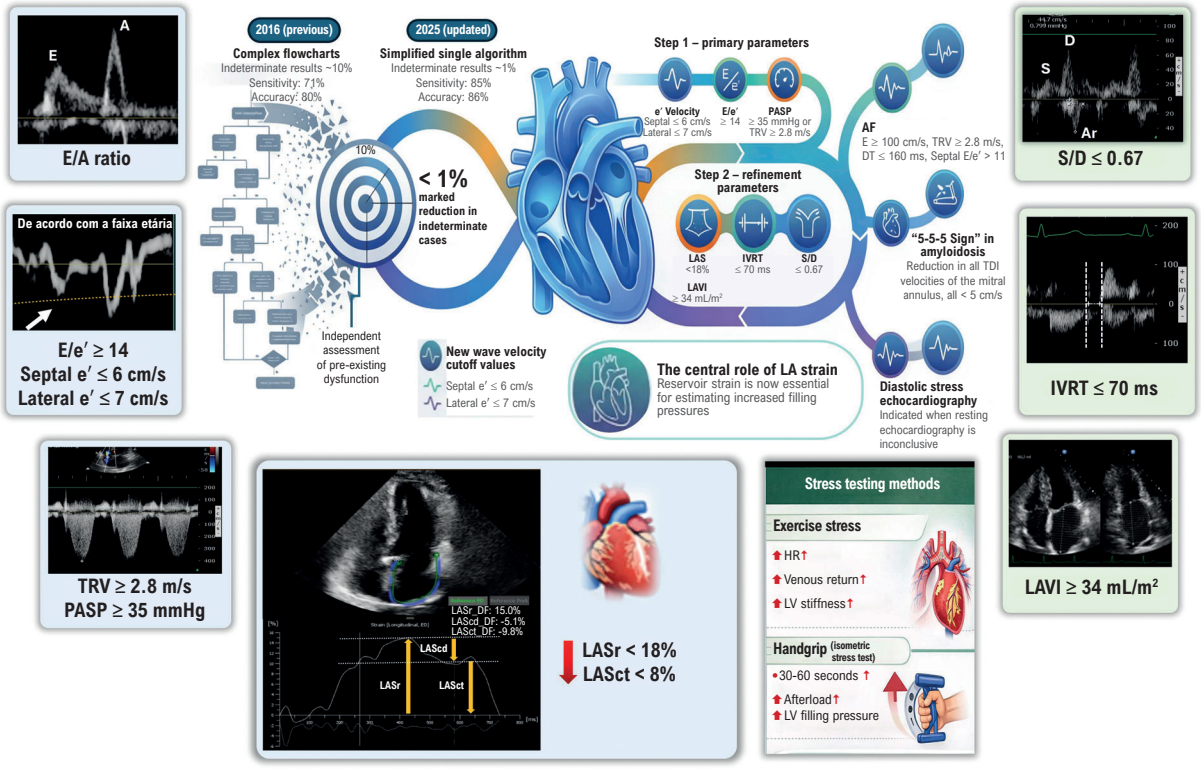

Arq Bras Cardiol: Imagem cardiovasc. 2026;39(2):e20260026

Integration and hierarchical application of parameters and techniques for the evaluation of LV filling pressures. The strategy begins with morphofunctional assessment and structured screening, followed by targeted refinement in indeterminate or discordant cases (Step 2), in which LAS and complementary parameters play a decisive role in the final diagnostic classification. AF: atrial fibrillation; DT: deceleration time; ED: end-diastole; HR: heart rate; IVRT: isovolumetric relaxation time; LAS: left atrial strain; LAScd: left atrial conduit strain; LASct: left atrial contraction strain; LASr: left atrial reservoir strain; LAVI: left atrial volume index; LV: left ventricular; PASP: pulmonary artery systolic pressure; TDI: tissue Doppler imaging; TRV: tricuspid regurgitation velocity.

guides interpretation and may be refined or corrected by the structured model.

Strategy overview: two steps, one clinical question

The assessment should be structured to answer a simple and clinically meaningful question: Is there consistent evidence of increased LV filling pressures? Table 2 summarizes the parameters used for this evaluation.

Step 1: initial screening

Updated guidelines emphasize that aging is associated with a physiological decline in myocardial relaxation. As a result, values considered abnormal in younger individuals may be expected in older people. Therefore, an isolated reduction in e′, particularly in older people, should not be automatically interpreted as indicative of increased filling pressures. Age-adjusted reference values are essential to support this interpretation.[4]

i. e′ velocity: relaxation with age adjustment

Both septal and lateral e′ velocities should be routinely assessed. A decreased e′ suggests impaired relaxation but does not necessarily indicate increased filling pressures, particularly in older individuals, in whom lower values are common and may occur in the presence of normal pressures.[3] Thus, e′ is highly informative for characterizing relaxation but must be interpreted in conjunction with other parameters.

New/current concept: the 2025 guideline refines normal reference thresholds and acknowledges that septal e′ ≤ 6 cm/s or lateral e′ ≤ 7 cm/s is frequently observed in individuals aged

Table 1 – Comparison between guidelines and recent evidence

Domain	ASE/EACVI (2016)[1]	ASE (2025)[4]	BSE (2024)[3]	My Approach to integration in practice
Objective	Standardization and simplification	Reduction of discordance and indeterminate cases; hierarchical framework	Emphasis on pathophysiology and interpretation	Integration of the 2025 framework with BSE physiological principles, using the 2016 model as the foundation
LAS	Not formally included	Formalized as a refinement parameter	Formalized as a refinement parameter	Preferred tie-breaking parameter
Age adjustment	Limited	Explicit incorporation	Recognized	Avoid overdiagnosis in older patients
LAVI	Core parameter	Supportive parameter; marker of chronicity	Structural parameter	Contextual support; not used in isolation
Gray zone	Frequent	Structured resolution strategy	Physiological interpretation	Step 2 refinement (LAS, IVRT, pulmonary venous flow)

ASE: American Society of Echocardiography; BSE: British Society of Echocardiography; EACVI: European Association of Cardiovascular Imaging; IVRT: isovolumetric relaxation time; LAS: left atrial strain; LAVI: LA volume index; PV: pulmonary vein.

Table 2 – Reference parameters for the assessment of LV filling pressures

Parameter	Abnormal threshold	Clinical interpretation/Action
Septal e′ velocity	≤ 6 cm/s	Decreased values suggest impaired relaxation; should be interpreted alongside other parameters.
Lateral e′ velocity	≤ 7 cm/s	Same interpretation as septal e′; should be interpreted alongside other parameters.
E/A ratio	≤ 0.8 or ≥ 2.0	E/A < 0.8 suggests impaired relaxation; E/A ≥ 2.0 suggests a restrictive filling pattern (should be interpreted alongside other parameters).
Average E/e′ ratio	≥ 14	Supports the presence of increased filling pressures.
PASP/TR velocity	≥ 35 mmHg / ≥ 2.8 m/s	When increased, supports increased filling pressures in the absence of pre-capillary pulmonary hypertension.
LASr	< 18%	Decreased values favor increased filling pressures; primary tie-breaking parameter.
LASct	< 8%	Marked decrease supports sustained increase of filling pressures; normal values may help exclude increased pressures (particularly when LASct > 14% and GLS ≥ 18%).
IVRT	< 70 ms	Shortened IVRT suggests increased filling pressures.
S/D ratio (pulmonary vein)	< 0.67	Diastolic predominance supports increased filling pressures; stronger association in decreased LVEF.
Ar-A difference (pulmonary vein)	> 30 ms	Suggests increased filling pressures, particularly in hypertrophic cardiomyopathy and MR.
LAVI	> 34 mL/m^2	Indicates chronic exposure to increased filling pressures; not diagnostic in isolation.
Diastolic stress echocardiography	Exercise E/e′ > 14; TR velocity > 2.8 m/s	Indicated when resting echocardiography does not explain symptoms; supports dynamic increase of filling pressures.
LUS/VExUS (adjunctive)	IVC > 2 cm; reversed hepatic/portal flow; B-line grading 0-3	Complementary assessment when clinical and imaging findings are discordant and resting echocardiography is inconclusive.

GLS: global longitudinal strain; IVC: inferior vena cava; IVRT: isovolumetric relaxation time; LASct: left atrial contractile strain; LASr: left atrial reservoir strain; LAVI: left atrial volume index; LUS: lung ultrasound; PASP: pulmonary artery systolic pressure; TR: tricuspid regurgitation; VExUS: venous excess ultrasound score; MR: mitral regurgitation.

> 60-70 years and, in isolation, does not define increased filling pressures.[4]

ii. E/e' ratio: useful but not definitive

The E/e' ratio remains a cornerstone parameter due to its practicality; however, it should be interpreted as supportive evidence rather than a standalone determinant.[3,4]

New/current concept: an average E/e' ≥ 14 supports the presence of increased filling pressures, whereas lower values make this less likely. However, an intermediate "gray zone" (particularly 8-14) is common and, according to the 2025 guideline, requires further refinement using additional parameters. Limitations must also be recognized in the presence of significant mitral valve disease, irregular rhythms without adequate beat averaging, and ventricles with preserved ejection fraction.[5,6]

iii. Tricuspid regurgitation velocity (TRV): a link to pulmonary hemodynamics

When adequately measured, TRV provides an indirect estimate of pulmonary pressure and may support the presence of increased LV filling pressures (post-capillary), provided that primary pulmonary disease (pre-capillary) is excluded. The cutoff of ≥ 2.8 m/s remains consistent across recent guidelines.[3]

New/current concept: the ASE update also considers an estimated pulmonary artery systolic pressure (PASP) ≥ 35 mmHg as suggestive of increased filling pressures, provided that right atrial pressure estimation based on inferior vena cava parameters is technically reliable.[4]

Step 2: refinement — where the recent updates have truly shifted practice

Step 2 focuses on the assessment of LA/LV remodeling markers and indicators of increased filling pressures.

i. E/A ratio and deceleration time (DT): the mitral pattern still matters

The E/A ratio remains a central physiological marker of transmitral filling, guiding the distinction between impaired relaxation and decreased compliance.[1] An E/A ratio ≤ 0.8 suggests impaired relaxation (common with aging), whereas E/A ≥ 2.0 combined with DT < 160 ms (particularly in patients with decreased LVEF) indicates a restrictive filling pattern and increased pressures.

The main limitation is pseudonormalization (E/A 0.8-2.0 in the presence of increased pressures), which underscores that E/A should never be interpreted in isolation.

New/current concept: the 2016 guideline emphasized its role in grading diastolic dysfunction, and the 2025 update preserves its physiological relevance while prioritizing a more objective and reproducible decision-making framework.[4]

ii. Left atrial volume index (LAVI): a marker of chronic exposure rather than current pressure

LAVI > 34 mL/m² is a well-established marker of chronic LA exposure to increased filling pressures, with important diagnostic and prognostic value in HF, AF, valvular heart disease, and cardiomyopathies.[7-9]

New/current concept: in the 2025 update, LAVI is no longer a central parameter but assumes a supportive role since it reflects chronic remodeling rather than current hemodynamic status. Therefore, it should be interpreted alongside markers that are less influenced by transient changes.

iii. Left atrial strain (LAS) (reservoir and contractile): the key contemporary tie-breaker

Recent studies have demonstrated a strong correlation between LAS and invasive measures of filling pressure, establishing left atrial reservoir strain (LASr) as a marker of increased pressures and left atrial contractile strain (LASct) as a tool to exclude them.[10,11]

New/current concept: atrial strain represents the most relevant practical innovation in current guidelines since it captures both LA function and hemodynamic history. LASr < 18% (particularly < 16%) suggests increased filling pressures by reflecting decreased atrial compliance, whereas LASct > 14% in patients with preserved EF effectively excludes increased pressures, even in the presence of borderline E/e' values.[4,10]

Technical acquisition: LAS should be measured in apical four- and two-chamber views, with the R-R interval defining the cardiac cycle. Adequate frame rates (> 60 fps), appropriate depth, and optimized image acquisition are essential. Speckle-tracking analysis should exclude pulmonary veins and the LA appendage. The average of both views should be reported (Figure 1, Video 1).

iv. Isovolumetric relaxation time (IVRT): useful in discordant or challenging scenarios

IVRT corresponds to the interval between aortic valve closure and mitral valve opening, reflecting early active ventricular relaxation.[12]

New/current concept: initially described as an auxiliary parameter in the 2009 guidelines and maintained as a complementary measure in 2016, IVRT has regained relevance as a refinement tool in discordant cases. Although not part of the primary decision-making core, a shortened IVRT (≤ 70 ms) suggests increased filling pressures, particularly when associated with a restrictive filling pattern or decreased atrial strain. It is especially useful when tissue Doppler measurements are unreliable, such as in AF or mitral annular calcification.[4]

v. Pulmonary venous flow (S/D and Ar-A): when additional confirmation is needed

Pulmonary venous flow assessment can be technically challenging but provides valuable information when adequately acquired. A diastolic predominance (S/D ≤ 0.67) supports increased filling pressures. However, patients with

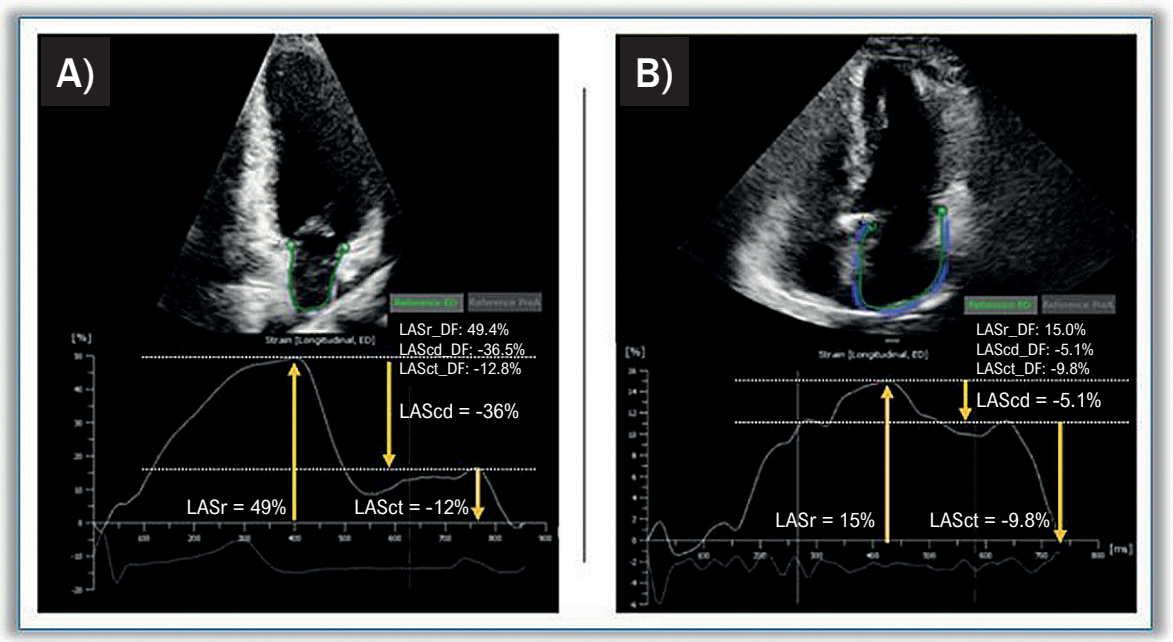

Figure 1 – *Role of LAS in refining the assessment of LV filling pressure. Assessment of LA deformation using speckle-tracking echocardiography. A) LASr, LAScd, and LASct measurements in a normal subject, with values of 49%, −36%, and −12%, respectively; B) corresponding strain curves from a patient with increased filling pressures, showing values of 15%, −5.1%, and −9.8%, respectively. LA: left atrium; LAS: LA strain; LAScd: LA conduit strain; LASct: LA contractile strain; LASr: LA reservoir strain; LV: left ventricle.*

preserved LVEF may exhibit S/D > 0.67 despite increased pressures, requiring confirmation with additional parameters.

An Ar-A duration difference > 30 ms may be useful in selected conditions, such as hypertrophic cardiomyopathy and mitral regurgitation (MR).[3,4,13]

vi. Additional supplementary parameters

When primary and refinement parameters are unavailable or unreliable, additional measures may support clinical interpretation. These include: peak diastolic pulmonary regurgitation velocity ≥ 2 m/s; pulmonary artery diastolic pressure ≥ 16 mmHg; mitral inflow L-wave velocity ≥ 50 cm/s; Ar-A duration > 30 ms; ≥ 50% reduction in mitral E/A during the Valsalva maneuver; E/Vp ≥ 2.5; A-wave transit time ≤ 45 ms; and IVRT/TE e′ < 2.

In addition, an LV mass index > 95 g/m² in women or > 115 g/m² in men may indicate structural remodeling consistent with diastolic dysfunction.[3,4]

Interpretation and integration of parameters (algorithm-based approach)

If all primary parameters assessed in Step 1 (e′, TRV, and E/e′) are within normal limits, LV filling pressures are considered normal. Conversely, if all three parameters are abnormal, increased filling pressures are present.

When e′ is decreased (based on age-adjusted reference values) and the E/A ratio is ≤ 0.8, this pattern is consistent with grade I diastolic dysfunction and normal filling pressures.

Diagnostic uncertainty arises in intermediate or discordant scenarios, including cases in which only e′ is decreased with E/A > 0.8, isolated increase of TRV/PASP or E/e′, or when any two primary variables are abnormal. In these situations, refinement using Step 2 parameters becomes essential.

These include LASr, IVRT, S/D, LAVI, and additional supplementary parameters. If one or more of these refinement markers are abnormal, increased filling pressures are confirmed. An E/A ratio < 2 supports the classification of grade II diastolic dysfunction, whereas E/A ≥ 2 indicates grade III diastolic dysfunction.[4]

Figure 2 shows the application of the algorithm.

Special situations

The 2025 guideline reinforces that a "one-size-fits-all" approach is not applicable. Specific clinical scenarios require adaptation of both acquisition and interpretation strategies (Table 3).

i. AF

Beat-to-beat variability increases the risk of measurement error; therefore, averaging multiple cardiac cycles is essential. Ideally, measurements should be obtained at a controlled heart rate < 100 bpm. Patients with decreased variability in mitral inflow tend to have increased filling pressures (Figure 3).[3,14]

My Approach to AF: the assessment follows a two-step framework. In Step 1, the following parameters are considered: E ≥ 100 cm/s, septal E/e′ ≥ 11, TRV > 2.8 m/s or PASP > 35 mmHg, and DT ≤ 160 ms.

If none or only one parameter is abnormal, filling pressures are considered normal. If ≥ three parameters are abnormal, filling pressures are increased. If two parameters are abnormal, refinement is required using Step 2 markers, including LASr < 18% and S/D < 1. BMI > 30 kg/m² further supports the diagnosis of HFpEF.

An average of 5-10 cardiac cycles should be used. If none of the parameters are abnormal, filling pressures are normal. If two of the three refinement parameters are abnormal, increased filling pressures are present. If only one parameter is abnormal or data are unavailable, the result should be considered indeterminate.

Caution: LASct is not present in AF; however, LASr remains informative. Very low values (< 16%) indicate decreased atrial compliance and increased filling pressures (Video 2).

ii. Mitral valve disease

In mitral stenosis, the E/e′ ratio should not be used. In significant MR, the E-wave may be increased due to volume overload rather than increased filling pressures.[3,4,15]

My Approach to mitral valve disease: in MR, greater emphasis should be placed on pulmonary venous flow patterns and IVRT. LAS should be interpreted cautiously, as regurgitant volume may artificially increase LASr.

iii. Cardiac amyloidosis

In this setting, isolated numerical values may fail to capture the underlying pathophysiology; the two-dimensional phenotype and overall functional pattern are key determinants. The presence of increased LV wall thickness associated with an "apical sparing" pattern on longitudinal strain should prompt evaluation for a restrictive diastolic filling pattern.[3,16]

My Approach to cardiac amyloidosis: a characteristic dissociation is often observed, with markedly decreased e′ velocities (septal and lateral < 5 cm/s) in contrast to a

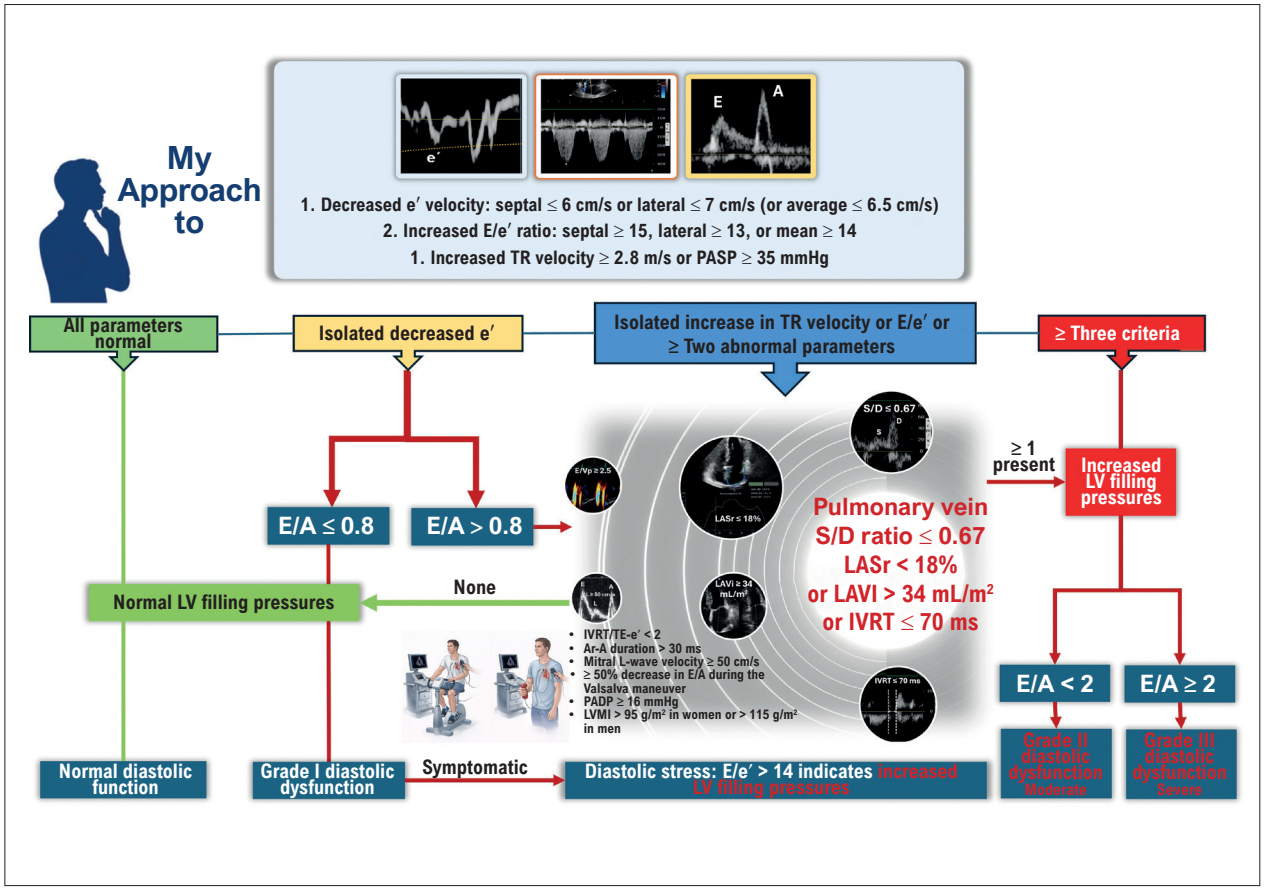

Figure 2 – *Decision algorithm for estimating LV filling pressures. Practical flowchart based on the 2025 ASE guideline. Step 1 relies on core parameters of myocardial relaxation and filling pressure assessment. In cases of discordance (e.g., a single abnormal parameter or borderline values), Step 2 is applied, prioritizing LASr and IVRT. Integration of these findings allows both grading of diastolic dysfunction and definitive classification of LV filling pressure status. ASE: American Society of Echocardiography; IVRT: isovolumetric relaxation time; LASr: left atrial reservoir strain; LAVI: left atrial volume index; LV: left ventricle; LVMI: LV mass index; PADP: pulmonary artery diastolic pressure; PASP: pulmonary artery systolic pressure; TR: tricuspid regurgitation.*

Table 3 – Clinical conditions requiring adaptation of the standard diastolic function algorithm

Clinical condition	Key considerations for assessing LV filling pressure
AF	Average 5-10 consecutive beats at a controlled heart rate. Consider E ≥ 100 cm/s, septal E/e′ ≥ 11, TR velocity ≥ 2.8 m/s, and DT ≤ 160 ms. LASr < 18% supports increased filling pressures. LA volume alone is not diagnostic.
Mitral stenosis	E/e′ should not be used. Prioritize IVRT, TE-e′ ratio, and mitral A-wave velocity. Filling pressures should be interpreted cautiously due to transmitral obstruction.
MR	The E wave is often increased due to volume overload rather than increased pressure. E/e′ may overestimate filling pressures. Ar-A duration and IVRT may provide supportive information.
Mitral annular calcification	Mechanical restriction reduces the reliability of e′. Greater emphasis should be placed on IVRT and the overall filling pattern rather than E/e′ alone.
Cardiac amyloidosis	Markedly decreased annular velocities (“5-5-5” sign: s′, e′, a′ < 5 cm/s) combined with a restrictive transmitral pattern. Apical sparing on longitudinal strain supports the diagnosis.
Sinus tachycardia/high-output states	Increased transmitral velocities may reflect increased cardiac output rather than increased filling pressures. IVRT and E/e′ should be interpreted within the clinical context.
Heart transplantation	Altered atrial geometry, denervation, and frequent sinus tachycardia modify Doppler patterns. Early diastolic predominance may be physiological, particularly in younger donors.
LVAD	Continuous-flow physiology alters conventional Doppler indices. E/A, E/e′, and pulmonary pressures should be interpreted in the context of device settings and clinical status.
Restrictive cardiomyopathy vs constrictive pericarditis	Preserved or increased medial e′ (> 8 cm/s) favors constriction, whereas decreased e′ (< 6 cm/s) supports restrictive cardiomyopathy. Assess for annulus reversus and respiratory variation.
Hypertrophic cardiomyopathy	LVOT obstruction and significant mitral regurgitation may increase LA pressure. Ar-A duration, LAVI, and TR velocity should be integrated into the assessment.
Pulmonary hypertension	Septal E/e′ may be misleading in RV pressure overload. Prefer lateral e′ and LAS to differentiate pre- vs post-capillary mechanisms.
Conduction abnormalities (LBBB, RV pacing, CRT)	Abnormal septal motion reduces the reliability of e′ and E/e′. Greater weight should be given to TR velocity, LA size, and LAS.
Athlete’s heart	Physiological chamber enlargement and increased diastolic volume may mimic diastolic dysfunction. Emphasize absence of symptoms, normal natriuretic peptides, and preserved LAS. Avoid automatic grading.

CRT: cardiac resynchronization therapy; DT: deceleration time; IVRT: isovolumetric relaxation time; LA: left atrium; LAS: LA strain; LASct: LA contractile strain; LASr: LA reservoir strain; LAVI: left atrial volume index; LBBB: left bundle branch block; LVAD: left ventricular assist device; LVOT: left ventricular outflow tract; RV: right ventricle; TR: tricuspid regurgitation; AF: atrial fibrillation; MR: mitral regurgitation.

high mitral E-wave and shortened DT. This classic restrictive pattern strongly supports the presence of increased filling pressures, often obviating the need for complex algorithmic assessment.

iv. Pulmonary hypertension

The E/e′ ratio, particularly the septal measurement, may be misleading in pre-capillary pulmonary hypertension. In such cases, greater emphasis should be placed on the lateral E/e′ and on LAS, especially when distinguishing pre- from post-capillary mechanisms in borderline scenarios[3,4,17] (Video 3).

The role of diastolic stress testing and invasive hemodynamic assessment

In patients with exertional dyspnea (New York Heart Association classes II and III) and a resting echocardiography that is normal or indeterminate, even after incorporation of LAS, evaluation should not be discontinued.[3,4,18]

Diastolic stress echocardiography using a supine bicycle or treadmill is recommended.[3,4] Maneuvers that increase LV preload, such as passive leg raising, may also help unmask increased filling pressures in patients with decreased ventricular compliance. These approaches may serve as alternatives when formal exercise testing is unavailable, although a negative result does not exclude clinically significant diastolic dysfunction.[3]

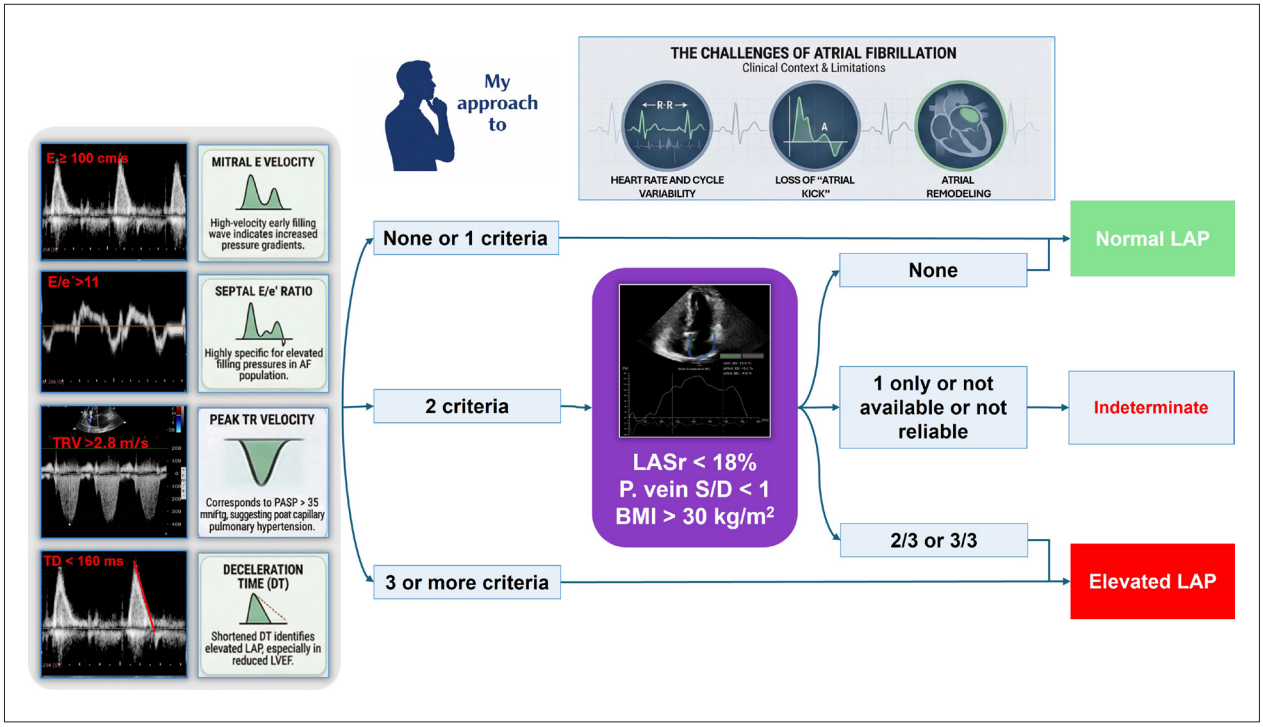

Figure 3 – *Algorithm for estimating mean LA in AF. Initial assessment is based on four parameters: mitral E velocity ≥ 100 cm/s, septal E/e' > 11, TR velocity > 2.8 m/s (or PASP > 35 mmHg), and DT ≤ 160 ms. The presence of none or only one abnormal parameter suggests normal LAP. When two parameters are abnormal, additional markers, including LASr < 18%, S/D < 1, and BMI > 30 kg/m², are used to refine classification as normal, increased, or indeterminate LAP. BMI: body mass index; DT: deceleration time; LA: left atrium; LAP: LA pressure; LASr: LA reservoir strain; LV: left ventricle; LVEF: LV ejection fraction; PASP: pulmonary artery systolic pressure; TR: tricuspid regurgitation; AF: atrial fibrillation.*

Some studies have also proposed handgrip stress to increase afterload.[19] In selected cases, stress echocardiography may be combined with simultaneous invasive hemodynamic assessment to confirm dynamic increases in pulmonary capillary pressure, thereby supporting the diagnosis of HFpEF when noninvasive findings are inconclusive.

My Approach to stress testing: I assess changes in the E/e′ ratio and TRV at peak exercise. An increase in average E/e′ > 14 or TRV > 2.8 m/s (or > 3.2 m/s in some studies to improve specificity) during exertion indicates dynamic increase of filling pressures and supports the diagnosis of HFpEF not evident at rest (Table 4; Video 4; Video 5).

Lung ultrasound (LUS) and venous excess ultrasound

LUS and the venous excess ultrasound (VExUS) score have emerged as complementary tools for the assessment of congestion. LUS identifies B-lines as markers of interstitial edema, whereas VExUS integrates inferior vena cava assessment with Doppler interrogation of intra-abdominal veins to characterize systemic venous congestion.

Although these methods do not replace diastolic function analysis, they expand bedside hemodynamic evaluation and may reinforce the suspicion of increased filling pressures in complex clinical scenarios.[4]

Artificial intelligence (AI) in the assessment of LV diastolic function

AI has emerged as a promising tool in the assessment of diastolic dysfunction and HFpEF, particularly due to its ability to integrate multiple echocardiographic and clinical variables into predictive models that outperform isolated parameters.

Machine learning algorithms can identify subtle phenotypic patterns, reduce the rate of indeterminate cases, and improve the estimation of filling pressures. Although still undergoing broad validation, AI is expected to function primarily as a decision-support tool, refining traditional algorithms without replacing the clinical judgment of the echocardiographer.[4,20]

What should be included in the report?

The echocardiographic report of diastolic function should address a clear clinical question rather than simply reproduce an algorithm. Classification as grade I, II, III, or indeterminate is insufficient on its own; it is essential to explicitly state whether there is consistent evidence of increased filling pressures and to describe the reasoning underlying this conclusion.

The echocardiographer should integrate available parameters and clearly articulate the interpretative logic, presenting key data alongside a direct and accountable conclusion. A high-quality report is one that informs clinical

Table 4 – Indications for diastolic stress testing and invasive hemodynamic assessment

Clinical condition	Indication/Purpose
Dyspnea with indeterminate HF despite baseline refinement	Clarify LV filling pressure behavior under stress conditions
Exercise intolerance (NYHA class II/III) with normal or inconclusive resting echocardiography	Detect dynamic elevation of LV filling pressures
Persistent symptoms after mitral valve repair or TEER	Evaluate residual or exercise-induced increase of filling pressures
Subtle clinical findings discordant with a "normal" resting echocardiography	Reproduce symptoms and assess hemodynamic response under stress
When to consider invasive hemodynamic assessment	**Purpose**
Indeterminate echocardiographic findings with high pre-test probability	Confirm diagnosis through cardiac catheterization
Persistent clinical suspicion despite noninvasive testing	Document dynamic increase of pulmonary capillary wedge pressure

HF: heart failure; LV: left ventricle; NYHA: New York Heart Association; TEER: transcatheter edge-to-edge repair.

management: technical rigor has value only when it translates into clarity and actionable insight.

Conclusion

The assessment of LV filling pressures has evolved from a rigid, algorithm-driven exercise to an integrated physiological interpretation. The 2025 ASE update provides greater flexibility, allowing adaptation of the assessment according to age and comorbidities.

Rather than representing a purely mechanical application of predefined criteria, this evaluation should be understood as the structured integration of physiological data in support of clinical decision-making. We measure velocities and deformation, but our ultimate goal is to understand the hemodynamic mechanisms underlying symptoms.

When performed with technical rigor and contextualized interpretation, echocardiography not only estimates filling pressures but also elucidates underlying mechanisms. This ability to translate quantitative data into clinically meaningful insight underpins its central role in contemporary cardiology practice.

Author Contributions

Conception and design of the research: Alves MSL, Bonotto EH; acquisition of data: Alves MSL, Vosgerau LM, Dreckmann MV, Bonotto EH; analysis and interpretation of the data: Alves MSL, Dreckmann MV, Bonotto EH; writing of the manuscript: Alves MSL, Vosgerau LM, Dreckmann MV, Martins RD, Zanlorensi CB; critical revision of the manuscript for intellectual content: Alves MSL, Vosgerau LM, Dreckmann MV, Zanlorensi CB, Bonotto EH.

Potential Conflict of Interest

No potential conflict of interest relevant to this article was reported.

Sources of Funding

There were no external funding sources for this study.

Study Association

This study is not associated with any thesis or dissertation work.

Ethics Approval and Consent to Participate

This article does not contain any studies with human participants or animals performed by any of the authors.

Use of Artificial Intelligence

During the preparation of this work, the author(s) used ChatGPT to improve the readability and language quality of the manuscript. After using this tool/service, the author(s) reviewed and edited the content as needed and take full responsibility for the content of the published article.

Availability of Research Data

The underlying content of the research text is contained within the manuscript.

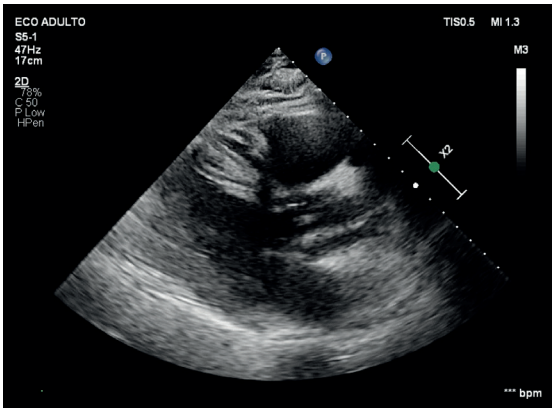

Video 1 – *HFpEF with inconclusive resting assessment, clarified by LAS. In: http://abcimaging.org/supplementary-material/2026/3902/ABCImag-2026-0026_AR_Video_1.mp4*

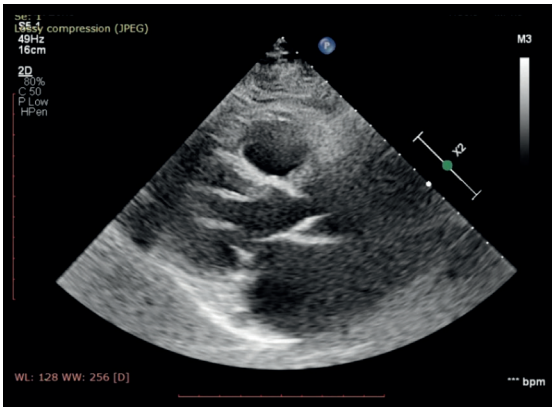

Video 2 – *AF: importance of beat averaging and the use of IVRT and LAS for refinement. In: http://abcimaging.org/supplementary-material/2026/3902/ABCImag-2026-0026_AR_Video_2.mp4*

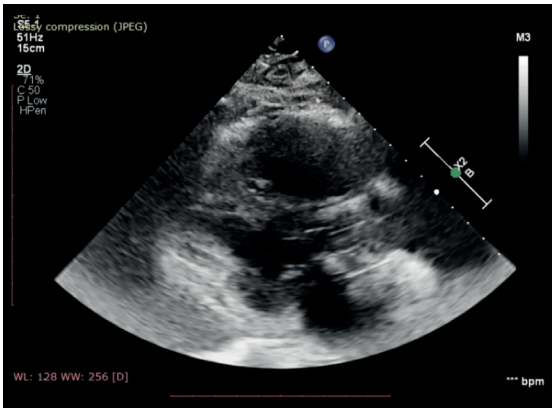

Video 3 – *Pre-capillary pulmonary hypertension with borderline parameters and preserved LAS. In: http://abcimaging.org/supplementary-material/2026/3902/ABCImag-2026-0026_AR_Video_3.mp4*

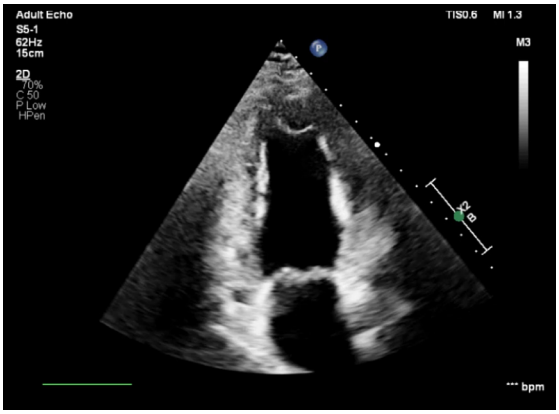

Video 4 –*Passive leg raising demonstrating increased filling pressures in a patient with exertional dyspnea. In: http://abcimaging.org/supplementary-material/2026/3902/ABCImag-2026-0026_AR_Video_4.mp4*

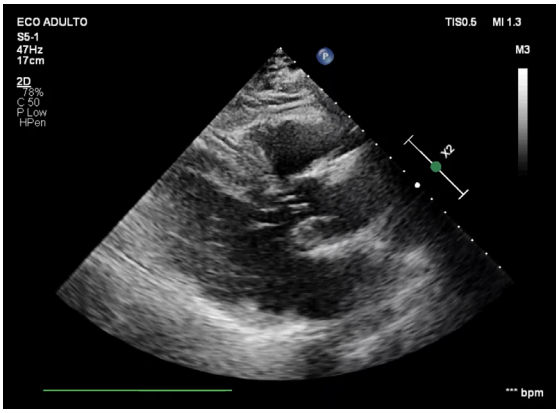

Video 5 – *Diastolic stress testing with handgrip confirming increased filling pressures in unexplained dyspnea. In: http://abcimaging.org/supplementary-material/2026/3902/ABCImag-2026-0026_AR_Video_5.mp4*

References

1. Nagueh SF, Smiseth OA, Appleton CP, Byrd BF 3rd, Dokainish H, Edvardsen T, et al. Recommendations for the Evaluation of Left Ventricular Diastolic Function by Echocardiography: An Update from the American Society of Echocardiography and the European Association of Cardiovascular Imaging. J Am Soc Echocardiogr. 2016;29(4):277-314. doi: 10.1016/j.echo.2016.01.011.
2. van de Bovenkamp AA, Enait V, de Man FS, Oosterveer FTP, Bogaard HJ, Vonk Noordegraaf A, et al. Validation of the 2016 ASE/EACVI Guideline for Diastolic Dysfunction in Patients with Unexplained Dyspnea and a Preserved Left Ventricular Ejection Fraction. J Am Heart Assoc. 2021;10(18):e021165. doi: 10.1161/JAHA.121.021165.
3. Robinson S, Ring L, Oxborough D, Harkness A, Bennett S, Rana B, et al. The Assessment of Left Ventricular Diastolic Function: Guidance and Recommendations from the British Society of Echocardiography. Echo Res Pract. 2024;11(1):16. doi: 10.1186/s44156-024-00051-2.
4. Nagueh SF, Sanborn DY, Oh JK, Anderson B, Billick K, Derumeaux G, et al. Recommendations for the Evaluation of Left Ventricular Diastolic Function by Echocardiography and for Heart Failure with Preserved Ejection Fraction Diagnosis: An Update from the American Society of Echocardiography. J Am Soc Echocardiogr. 2025;38(7):537-69. doi: 10.1016/j.echo.2025.03.011.
5. Lababidi H, Rahi W, Smiseth OA, Billick K, Inoue K, Khan FH, et al. New Algorithm for Estimating Left Ventricular Filling Pressure by Echocardiography. Circulation. 2025;152(7):424-35. doi: 10.1161/CIRCULATIONAHA.125.074974.
6. Nagueh SF, Middleton KJ, Kopelen HA, Zoghbi WA, Quiñones MA. Doppler Tissue Imaging: A Noninvasive Technique for Evaluation of Left

Ventricular Relaxation and Estimation of Filling Pressures. J Am Coll Cardiol. 1997;30(6):1527-33. doi: 10.1016/s0735-1097(97)00344-6.

7. Nedios S, Koutalas E, Sommer P, Arya A, Rolf S, Husser D, et al. Asymmetrical Left Atrial Remodelling in Atrial Fibrillation: Relation with Diastolic Dysfunction and Long-Term Ablation Outcomes. Europace. 2017;19(9):1463-9. doi: 10.1093/europace/euw225.
8. Ahmeti A, Bytyçi FS, Bielecka-Dabrowa A, Bytyçi I, Henein MY. Prognostic Value of Left Atrial Volume Index in Acute Coronary Syndrome: A Systematic Review and Meta-Analysis. Clin Physiol Funct Imaging. 2021;41(2):128-35. doi: 10.1111/cpf.12689.
9. Cameli M, Lisi M, Giacomin E, Caputo M, Navarri R, Malandrino A, et al. Chronic Mitral Regurgitation: Left Atrial Deformation Analysis by Two-Dimensional Speckle Tracking Echocardiography. Echocardiography. 2011;28(3):327-34. doi: 10.1111/j.1540-8175.2010.01329.x.
10. Inoue K, Khan FH, Remme EW, Ohte N, García-Izquierdo E, Chetrit M, et al. Determinants of Left Atrial Reservoir and Pump Strain and Use of Atrial Strain for Evaluation of Left Ventricular Filling Pressure. Eur Heart J Cardiovasc Imaging. 2021;23(1):61-70. doi: 10.1093/ehjci/jeaa415.
11. Lundberg A, Johnson J, Hage C, Bäck M, Merkely B, Venkateshvaran A, et al. Left Atrial Strain Improves Estimation of Filling Pressures in Heart Failure: A Simultaneous Echocardiographic and Invasive Haemodynamic Study. Clin Res Cardiol. 2019;108(6):703-15. doi: 10.1007/s00392-018-1399-8.
12. Appleton CP, Hatle LK, Popp RL. Relation of Transmitral Flow Velocity Patterns to Left Ventricular Diastolic Function: New Insights from a Combined Hemodynamic and Doppler Echocardiographic Study. J Am Coll Cardiol. 1988;12(2):426-40. doi: 10.1016/0735-1097(88)90416-0.
13. Kuecherer HF, Muhiudeen IA, Kusumoto FM, Lee E, Moulinier LE, Cahalan MK, et al. Estimation of Mean Left Atrial Pressure from Transesophageal Pulsed Doppler Echocardiography of Pulmonary Venous Flow. Circulation. 1990;82(4):1127-39. doi: 10.1161/01.cir.82.4.1127.
14. Khan FH, Zhao D, Ha JW, Nagueh SF, Voigt JU, Klein AL, et al. Evaluation of Left Ventricular Filling Pressure by Echocardiography in Patients with Atrial Fibrillation. Echo Res Pract. 2024;11(1):14. doi: 10.1186/s44156-024-00048-x.
15. Diwan A, McCulloch M, Lawrie GM, Reardon MJ, Nagueh SF. Doppler Estimation of Left Ventricular Filling Pressures in Patients with Mitral Valve Disease. Circulation. 2005;111(24):3281-9. doi: 10.1161/CIRCULATIONAHA.104.508812.
16. Pagourelias ED, Mirea O, Duchenne J, Van Cleemput J, Delforge M, Bogaert J, et al. Echo Parameters for Differential Diagnosis in Cardiac Amyloidosis: A Head-to-Head Comparison of Deformation and Nondeformation Parameters. Circ Cardiovasc Imaging. 2017;10(3):e005588. doi: 10.1161/CIRCIMAGING.116.005588.
17. Inoue K, Andersen OS, Remme EW, Khan FH, Andreassen AK, Skulstad H, et al. Echocardiographic Evaluation of Left Ventricular Filling Pressure in Patients with Pulmonary Hypertension. JACC Cardiovasc Imaging. 2024;17(5):566-7. doi: 10.1016/j.jcmg.2023.12.004.
18. Borlaug BA, Nishimura RA, Sorajja P, Lam CS, Redfield MM. Exercise Hemodynamics Enhance Diagnosis of Early Heart Failure with Preserved Ejection Fraction. Circ Heart Fail. 2010;3(5):588-95. doi: 10.1161/CIRCHEARTFAILURE.109.930701.
19. Samuel TJ, Beaudry R, Haykowsky MJ, Sarma S, Nelson MD. Diastolic Stress Testing: Similarities and Differences between Isometric Handgrip and Cycle Echocardiography. J Appl Physiol. 2018;125(2):529-35. doi: 10.1152/japplphysiol.00304.2018.
20. Akerman AP, Porumb M, Scott CG, Beqiri A, Chartsias A, Ryu AJ, et al. Automated Echocardiographic Detection of Heart Failure with Preserved Ejection Fraction Using Artificial Intelligence. JACC Adv. 2023;2(6):100452. doi: 10.1016/j.jacadv.2023.100452.

My Approach to Left Atrial Function: From Basic Assessment to Atrial Stiffness

Halsted Alarcão Gomes Pereira da Silva,[1] *Helder Moura Gomes,*[2] *Alexandre Costa Souza*[3]

Hospital São Geraldo,[1] *Juína, MT – Brazil*
Hospital Metropolitano Dom José Maria Pires,[2] *João Pessoa, PB – Brazil*
Hospital São Rafael,[3] *Salvador, BA – Brazil*

Central Illustration: My Approach to Left Atrial Function: From Basic Assessment to Atrial Stiffness

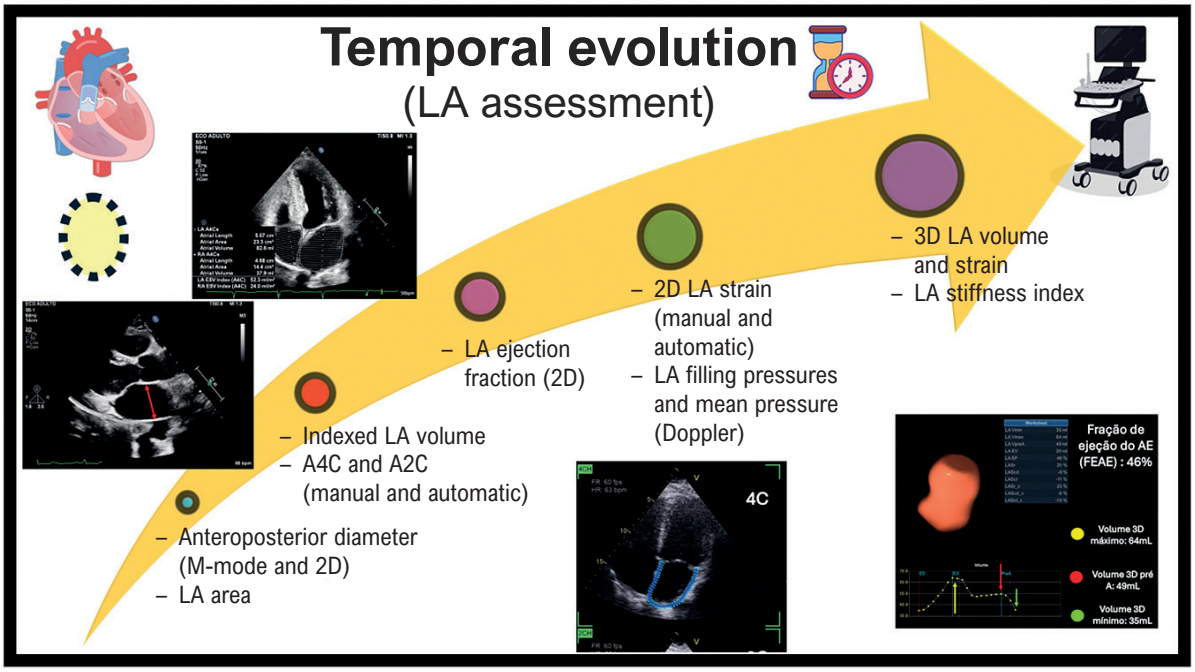

Arq Bras Cardiol: Imagem cardiovasc. 2026;39(2):e20260070

Temporal evolution of integrated left atrial analysis: a practical illustration of the technological evolution of echocardiography in the assessment of left atrial function. 2D: two-dimensional; 3D: three-dimensional; A2C: apical two-chamber view; A4C: apical four-chamber view; LA: left atrium.

Keywords

Strain, Left atrium; Ejection fraction

Mailing Address: Halsted Alarcão Gomes Pereira da SilvaX •
Instituto Dante Pazzanese de Cardiologia. Rua Dr Dante Pazzanese, 500. Postal code: 04012-909. São Paulo, SP – Brazil
E-mail: halstedufg@hotmail.com
Manuscript received May 4, 2026, revised manuscript May 4, 2026, accepted May 4, 2026
Editor responsible for the review: Marcelo Tavares

DOI: https://doi.org/10.36660/abcimg.20260070i

Abstract

The left atrium (LA) has historically been considered a passive chamber that conducts blood flow between the pulmonary veins and the left ventricle (LV). Advances in cardiovascular physiology and imaging techniques have highlighted its active role in modulating cardiac output, ventricular diastolic function, and the stratification of various heart diseases. Assessment of the LA has evolved over the years into a multiparametric functional approach, consolidated as an essential component of

modern echocardiography. The systematic incorporation of volumetric parameters, atrial strain, and atrial stiffness allows for a more precise characterization of cardiovascular pathophysiology and improves prognostic stratification, thus supporting more informed clinical decisions.

Introduction

For many years, the left atrium (LA) was analyzed solely as a segment of transition between the pulmonary veins and the left ventricle (LV), traditionally considered the primary pump of the heart. Over time, with a better understanding of the physiology of systolic and diastolic flows, this concept has given way to that of a chamber that plays a fundamental role in maintaining adequate cardiac output. It has likewise been established that alterations related to the LA directly influence pulmonary pressures and right chamber hemodynamics.

This review article provides a discussion ranging from the most basic concepts related to the LA to the new frontiers that have recently emerged with the understanding of the complex mechanics of this chamber in relation to cardiac function (Central Illustration).

Left atrial function and anatomy

The LA is located in the most posterior position of the heart, posterior and slightly superior to the right atrium (RA). It is separated from the RA by a fibromuscular wall called the interatrial septum. The posterior part of the LA is smooth and generally receives four pulmonary veins (two superior and two inferior), which return oxygenated blood from the lungs. The anterior portion of the LA is trabeculated and contains pectinate muscles, which are less numerous than those of the RA.

The LA fulfills three main physiological functions that influence the filling and performance of the LV (Figure 1).[1]

1. **Reservoir function:** During this phase, the LA functions as a reservoir, receiving blood from the pulmonary veins. It begins with the closure of the mitral valve (isovolumetric contraction), encompassing ventricular systole, and extends until isovolumetric relaxation.
   - **Main modulators:** The reservoir function of the LA is modulated by both biventricular contraction and LA compliance (chamber relaxation and stiffness).
2. **Conduit function:** During this phase, the LA acts as a conduit, with flow occurring passively, originating in the pulmonary veins and directed towards the LV. It begins immediately after mitral valve opening, encompassing the initial ventricular relaxation period and diastasis. It ends shortly before atrial contraction (P wave on the electrocardiogram).
   - **Main modulators:** The conduit function of the LA is predominantly modulated by LV relaxation and compliance, as well as early diastolic pressures.
3. **Contractile function:** During the contraction phase, the LA empties actively, contributing 20% to 30% of cardiac output in the absence of heart disease. This phase begins at the end of ventricular diastole, during the atrial contraction period.
   - **Main modulators:** LA contractile function is predominantly modulated by LV end-diastolic pressure and the intrinsic contractility of the LA.

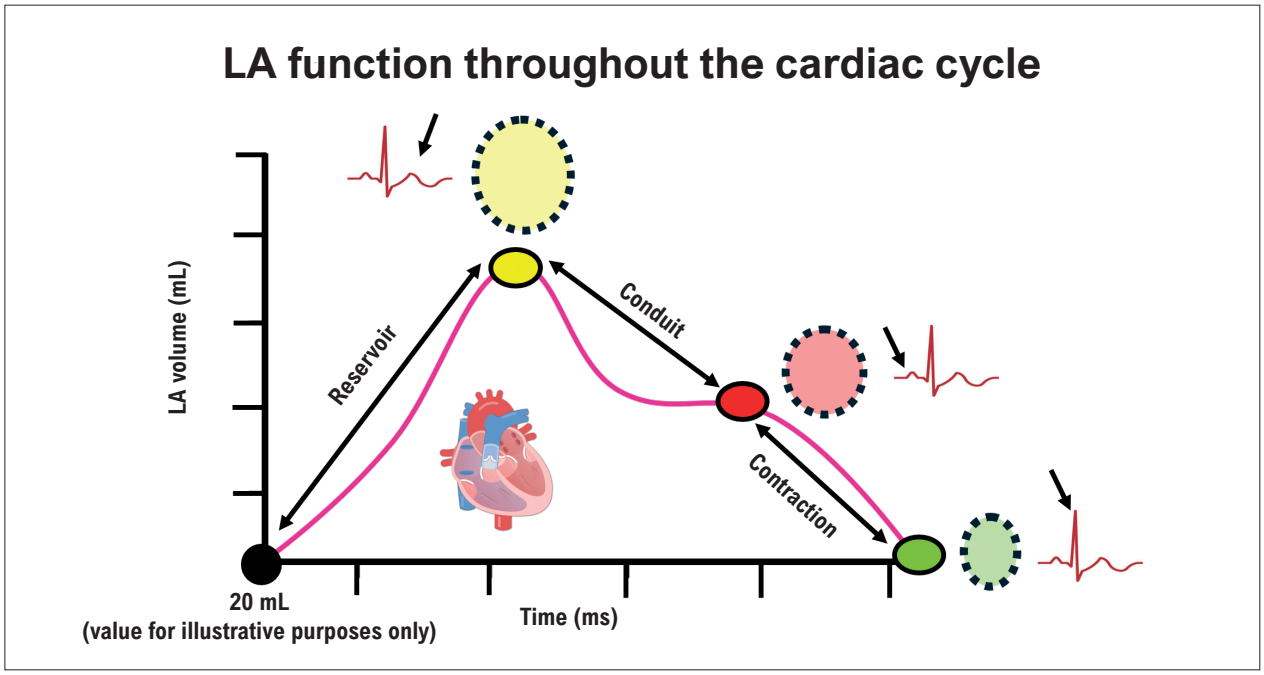

Figure 1 – *Phases of left atrial function throughout the cardiac cycle. The reservoir, conduit, and contraction phases are shown considering a volume × time curve. LA: left atrium. Source: The authors.*

There is currently extensive literature supporting the understanding of the prognostic correlation between LA function and maximum volume in diverse conditions, including atrial fibrillation (AF), heart failure (HF), coronary artery disease, mitral regurgitation, mitral stenosis, diastolic dysfunction, stroke, hypertrophic cardiomyopathy, and chronic kidney disease.[2] These data are essential for correct anatomical and functional characterization of this chamber during echocardiographic examination, avoiding erroneous diagnoses and inadequate treatment.

Linear dimensions and area measurements

The first method for quantifying LA dimensions was derived from linear measurements performed using M-mode. This parameter was fundamental for establishing normality and follow-up values, allowing studies to be conducted with more regular measurements and low variability in longitudinal follow-up. The most widely used linear dimension measurement is the anteroposterior diameter of the LA in the parasternal longitudinal axis, initially using M-mode echocardiography, subsequently performed using anatomical M-mode, and more recently guided by two-dimensional (2D) echocardiography.

It is worth noting that assessment of LA size using only the anteroposterior diameter assumes that, when the LA increases in size, all of its dimensions change proportionally, which is often not the case during atrial remodeling.

LA area has emerged as a more accurate analytical parameter than anteroposterior diameter for quantifying the size of both the LA and RA. For this measurement, atrial area planimetry should be performed in the apical two- and four-chamber views. Normal values for these cavities have been standardized and established over the years (LA ≤ 20 cm² and RA ≤ 18 cm²). Despite this improved accuracy in relation to diameter measurement, area assessment has not been shown to be a perfect substitute given that atrial volume is the ultimate measurement to be obtained. With the progressive improvement of 2D imaging, associated with the automation of volume acquisition and the more robust literature on normal values and prognostic data of atrial volumes, it is currently unnecessary to include LA area in the final report.[1]

2D echocardiographic assessment of left atrial volumes

Assessment of volumes and their prognostic correlation is supported by robust scientific evidence. Considerations regarding their acquisition and measurement are fundamental to avoid errors in measurement and consequent clinical interpretation.

First, it is necessary to understand that the longitudinal axes of the LV and LA often lie in different planes; consequently, dedicated LA acquisitions from the apical window should be obtained for more reliable measurements of atrial volume. The LA base should be visualized at its maximal diameter, indicating that the image plane passes through the maximum area of the central axis. The length should also be maximized to ensure correct alignment along the true axis of the LA (Figure 2).[1]

Length is measured from the mitral annulus to the superior wall of the LA. Long-axis lengths should not vary by more than 5 mm between the two echocardiographic views. If this variation is greater than 5 mm, the apical images should be reassessed. When tracing the endocardial borders, the LA appendage and pulmonary veins should be excluded from final analysis.[3]

Most ultrasound systems automatically calculate biplanar LA volume, after correctly delineating the atrial endocardium, using both the area-length method and the disc summation method (modified Simpson). For the area-length method, the shorter length obtained (in the two- or four-chamber view) is used to calculate LA volume. In contrast, for the disc summation method, the longer of the two measured lengths is used. It is worth noting that

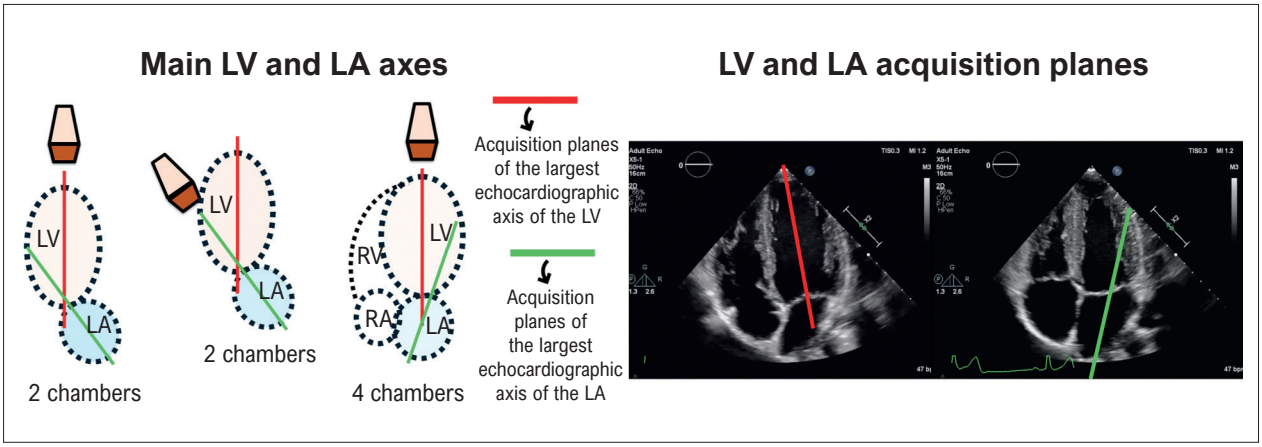

Figure 2 – *Dedicated echocardiographic acquisition of the LA. Left: A schematic drawing of the acquisition planes of the largest LA and LV axes. Right: The same schematic representation on 2D echocardiography in apical two- and four-chamber views. The longitudinal axes drawn for the LA (green line) and the LV (red line) are situated in different planes. LA: left atrium; LV: left ventricle; RA: right atrium; RV: right ventricle. Source: The authors.*

the area-length method consistently produces larger LA volumes than the disk summation method.[1]

The American Society of Echocardiography currently recommends the disk summation method for calculating LA volume, as it involves fewer geometric assumptions about LA shape. More recently, the semi-automated use of endocardial border tracking has provided volumes that correlate well with volumes acquired by three-dimensional (3D) echocardiography, computed tomography (CT), and cardiac magnetic resonance imaging (CMR), demonstrating lower interobserver variability than manual tracing. It is worth emphasizing that, despite the correlation, 2D echocardiographic volumes will always yield smaller values than those acquired by 3D methods. Given that volume calculation varies according to the technique, it is important for laboratories to consistently use the same technique.[1,4,5]

Patient size is one of the main determinants of LA size, and absolute LA volumes are larger in men than in women; therefore, indexing by body surface area partially corrects for this variability. Since 2015, the American Society of Echocardiography guideline for cardiac chamber quantification considers LA volume index values > 34 mL/m² to be abnormal. This value was based on observational studies with more than 6,000 patients without a history of AF or valvular heart disease, demonstrating that an indexed volume above 34 mL/m² was an independent predictor of death, HF, AF, and stroke (Figure 3).[6]

The main issue with the currently recommended grading values for LA volume (mildly enlarged = 35 to 41 mL/m², moderately enlarged = 42 to 48 mL/m², and severely enlarged > 48 mL/m²) is the narrow range between different categories. Consequently, even small measurement errors can result in incorrect classification of the degree of LA enlargement.[1]

A study published by Esther et al. in the *Journal of the American College of Cardiology* in 2022 demonstrated greater accuracy in classifying and stratifying LA dilation when using height-indexed and height-squared values in patients with overweight or obesity. Using individual data from over 17,000 patients, the use of height-indexed values reclassified LA abnormalities in up to 28% of patients when compared to indexing by body surface area, the parameter classically used in clinical practice. Table 1 displays normal values for these parameters.[7]

These calculations, even with the various additional indexing corrections, still consider geometric assumptions that underestimate the final volume, which should also be considered in interpretation.[1,4,5]

2D echocardiographic assessment of left atrial ejection fraction

After accurate volumetric acquisition of the LA during the cardiac cycle, an important parameter of atrial function can be obtained, namely, left atrial ejection fraction (LAEF). As shown in Figure 4,[1] LAEF, similar to LV ejection fraction, is calculated considering volumetric variation in different phases, at the following three moments of the cardiac cycle:

- **Atrial volume at the end of ventricular systole:** maximum LA volume (LAVmax)
- **Atrial volume immediately before atrial contraction:** LA volume before the P wave (LAVpreA)

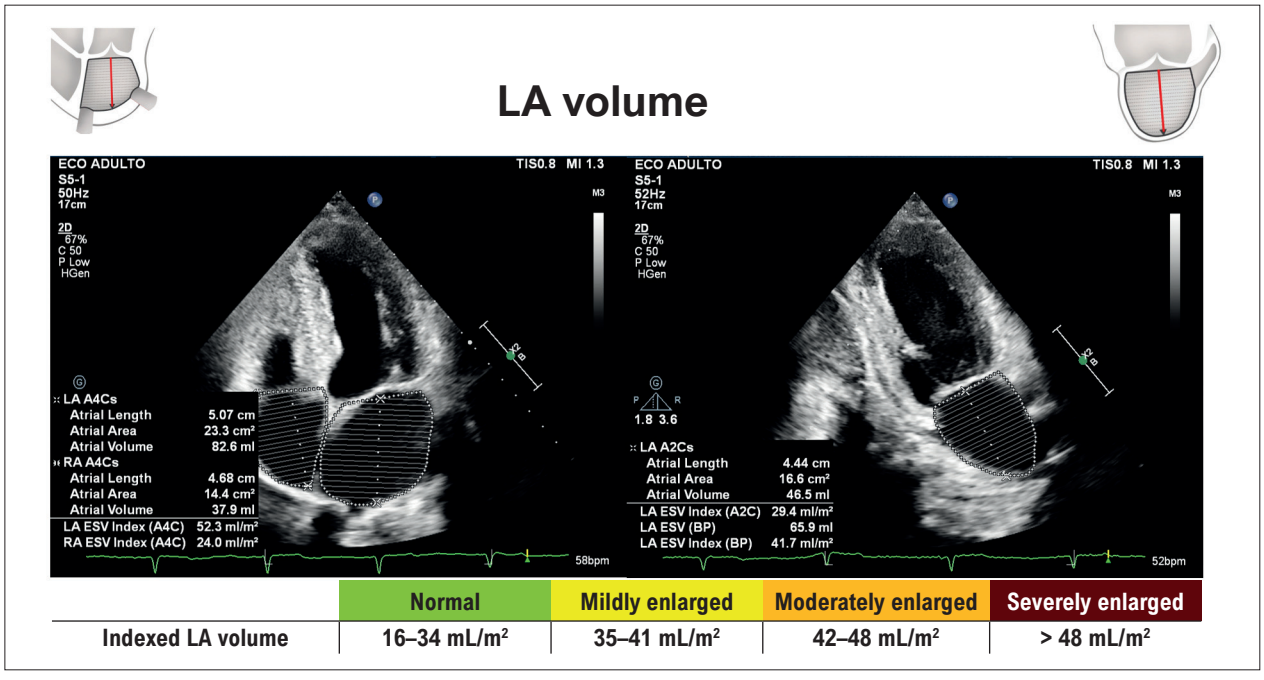

Figure 3 – *Calculation of left atrial volume using the biplane method (Simpson) and grading of enlargement according to the 2015 American Society of Echocardiography Guideline. LA: left atrium.*

Table 1 – Normal and left atrial dilation values, considering body surface area, height, and height squared

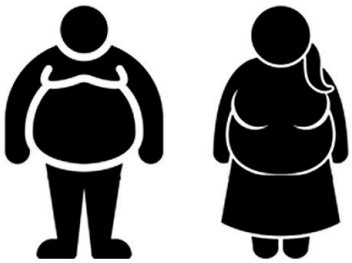

	Normal values	LA dilation
LA volume indexed by body surface area	Men: ≤ 34 mL/m²	Men: ≥ 35 mL/m²
	Women: ≤ 34 mL/m²	Women: ≥ 35 mL/m²
LA volume indexed by height	Men: ≤ 35.7 mL/m	Men: ≥ 35.8 mL/m
	Women: ≤ 33.7 mL/m	Women: ≥ 33.8 mL/m
LA volume indexed by height²	Men: ≤ 18.5 mL/m²	Men: ≥ 18.6 mL/m²
	Women: ≤ 16.5 mL/m²	Women: ≥ 16.6 mL/m²

LA: left atrium. Adapted from Davis et al. J Am Coll Cardiol Img, 2022.[7]

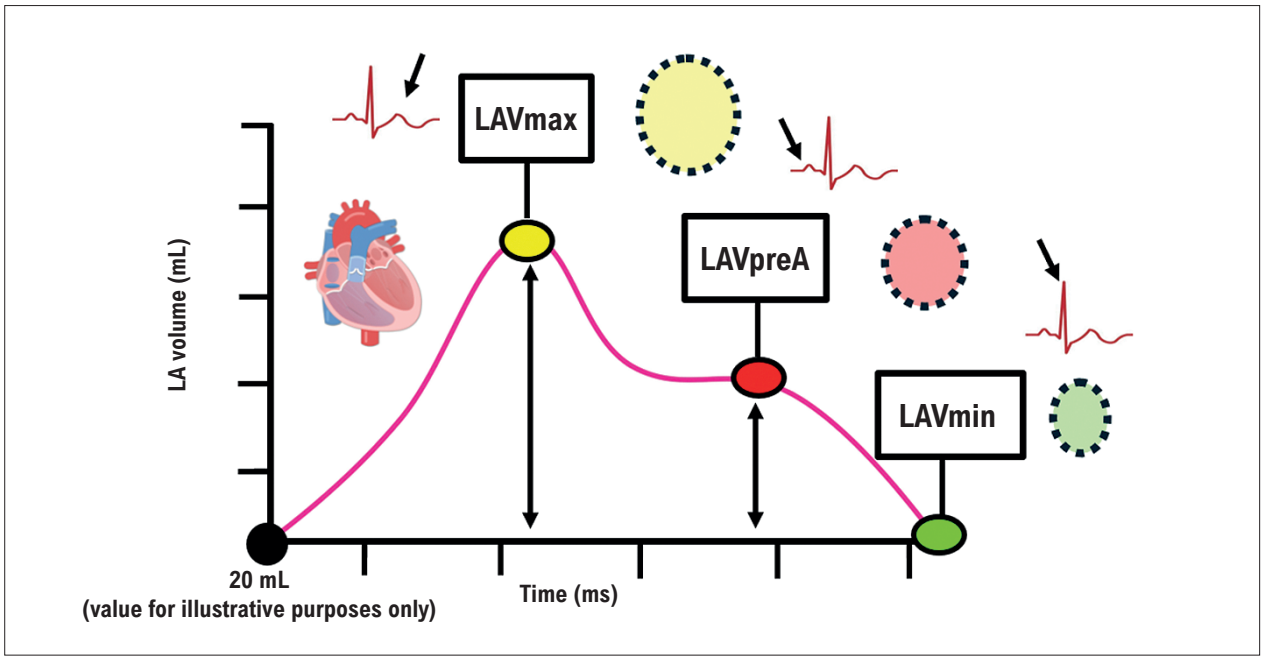

Figure 4 – *Left atrial volumes throughout the cardiac cycle: LAVmax (end of T wave), LAVpreA (before P wave), and LAVmin (R wave). LA: left atrium; LAVmax: maximum left atrial volume; LAVmin: minimum left atrial volume; LAVpreA: left atrial volume immediately before atrial contraction.*

- **Atrial volume at the end of ventricular diastole:** minimum LA volume (LAVmin).

Based on these volumes, the following three main values are obtained: total ejection fraction (reservoir) derived from LAVmax and LAVmin, passive ejection fraction (conduit) derived from LAVmax and LAVpreA, and active ejection fraction (contraction) derived from LAVpreA and LAVmin, according to the formulas below:[1]

1. **Total LAEF (global reservoir function) = (LAVmax – LAVmin) / LAVmax × 100**
2. **Passive LAEF = (LAVmax – LAVpreA) / LAVmax × 100**
3. **Active LAEF = (LAVpreA – LAVmin) / LAVpreA × 100**

Note: In the literature, ejection fraction and emptying fraction can be found as equivalent terms.

Figure 5 illustrates an example of LA volume calculation, as well as the derivation of LAEF, which showed the strongest prognostic correlation in most studies.[1,8]

It is worth noting that the active ejection fraction, as it depends on atrial contraction, cannot be assessed in the absence of sinus rhythm.

These parameters can be assessed using different imaging techniques: 2D and 3D echocardiography, CT, or CMR. Using dedicated software for quantifying LA volume, volumetric and functional assessment at different stages has become more accurate, reproducible, and less time-consuming compared to classic 2D analysis.

Tables 2 and 3 show the normal values for LA volumes and function according to published data from a study conducted by the World Alliance Societies of

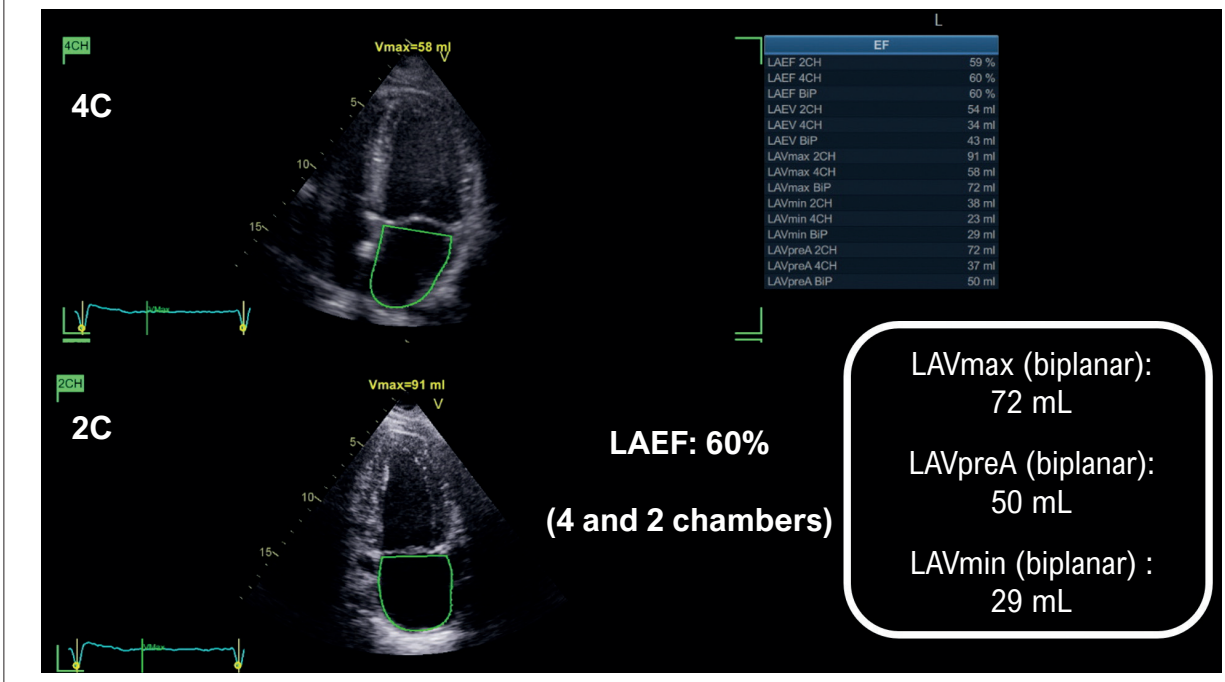

Figure 5 – *Biplane tracing of the LA and calculation of the total ejection fraction, which in this case is preserved. 2C: two-chamber view; 4C: four-chamber view; LA: left atrium; LAEF: left atrial ejection fraction; LAVmax: maximum left atrial volume; LAVmin: minimum left atrial volume; LAVpreA: left atrial volume immediately before atrial contraction.*

Table 2 – Comparison of left atrial volumetric and functional parameters between 2D and 3D methods (WASE Study, 2022)

Normal values for LA size and function derived from 1,765 healthy adults (results from the World Alliance Societies of Echocardiography Study)		
Volume parameters	**2D**	**3D**
Maximum volume (mL)	45.9 ± 15.7	49.9 ± 14.1
Maximum indexed volume (mL/m²)	25.7 ± 7.9	28.1 ± 6.9
Minimum volume (mL)	*	19.0 ± 7.2
Minimum indexed volume (mL/m²)	*	10.7 ± 3.7
Pre-A volume (mL/m²)	*	31.6 ± 10.8
Indexed pre-A volume (mL/m²)	*	17.8 ± 5.5
Reservoir volume (mL)	*	30.9 ± 9.0
Indexed reservoir volume (mL/m²)	*	17.4 ± 4.5
Conduit volume (mL)	*	18.4 ± 6.4
Indexed conduit volume (mL/m²)	*	10.4 ± 3.4

*Values are shown as mean ± standard deviation. 2D: two-dimensional echocardiography; 3D: three-dimensional echocardiography; LA: left atrium; pre-A: immediately before atrial contraction. *Data not provided by WASE, 2022.*

Table 3 – Reference values for left atrial volumes and ejection fractions (WASE Study, 2022)

Normal values for LA size and function derived from 1,765 healthy adults (results from the World Alliance Societies of Echocardiography Study)		
Function parameters	**2D**	**3D**
Ejection fraction (%)	65.7 ± 8.4	62.2 ± 7.7
Passive ejection fraction (%)	*	37.7 ± 11.0
Active ejection fraction (%)	*	39.5 ± 9.5
Reservoir strain (%)	42.1 ± 10.0	*
Conduit strain (%)	27.7 ± 9.7	*
Contractile strain (%)	14.4 ± 6.3	*

*Values are shown as mean ± standard deviation.2D: two-dimensional echocardiography; 3D: three-dimensional echocardiography; LA: left atrium. * Data not provided by WASE, 2022.*

Echocardiography. Despite these international data, it is important to emphasize that reference values for analysis of atrial function by 2D and 3D methods have not yet been standardized and incorporated into echocardiography guidelines.[9]

In patients with severe aortic stenosis, LAEF has proven useful for prognostic assessment. Cutoff values below 37% have shown superiority even in relation to maximum velocity and mean gradient for predicting mortality.[10]

Regarding arrhythmias, when evaluating only patients with AF, reduced LAEF was associated with worse cardiovascular outcomes, regardless of LV ejection fraction.[11]

Considering the clinical importance of LAEF and the increasing availability of this tool in echocardiography equipment, this parameter should be routinely reported.

3D echocardiographic assessment of left atrial volumes

In the last two decades, 3D echocardiography has become the modality of choice for volumetric quantification of cardiac chambers, with stronger correlation with CMR and less inter- and intraobserver variability. In a multicenter study with 92 patients with varying LA volumes, the agreement for the classification of enlarged LA using a cutoff point > 34 mL/m² showed a kappa coefficient of agreement of 0.88 between 3D echocardiography and CMR, compared to a kappa of 0.71 for the same analysis with 2D echocardiography and CMR.[12]

Some of the main advantages of this method include:

1. **High accuracy:** No geometric assumptions regarding LA shape, resulting in less underestimation compared to CMR
2. **Greater reproducibility:** Semi-automatic identification of cardiac borders, reducing foreshortened measurements.
3. **Acceptable temporal resolution:** Resolution > 20 volumes per second compared to CT and CMR
4. **Dynamic characterization of size and shape:** Continuous analysis throughout the cardiac cycle, allowing assessment of atrial functional phases.
5. **Single-beat acquisition:** Feasible analysis in patients who present frequent atrial or ventricular arrhythmias

Figure 6 shows the volumetric values and calculations performed using specific software for semi-automatic measurement.

Similar to 2D echocardiographic assessment of LA volumes, indexing 3D LA volumes to body surface area reduced sex differences. A small, yet significant increase in LA volume on 3D echocardiography has been observed with aging.

Currently, the main limitations of this analysis are temporal resolution, as well as the limited data regarding normal reference and prognostic values among diverse diseases.

Left atrial strain

Assessment of LA function by means of strain allows for more detailed analysis of each phase of atrial physiology. The ability to discriminate between passive and active movement, angle independence, reduced tethering effects, lower load dependence, and tracking of the movement of each segment of the atrial wall allow for a better understanding of atrial function.

LA strain is preferably measured by the speckle tracking method. For this purpose, the endocardial borders of the LA are manually or automatically traced on high-quality 2D images obtained at a frame rate between 50 and 90 frames/second. The need to acquire images in dedicated, non-shortened windows (as opposed to a conventional window optimized for the LV) to obtain LA strain measurements is a relatively recent concept and an essential parameter.

The European Society of Cardiovascular Imaging and the American Society of Echocardiography recommend using the LA strain value obtained from apical two- and four-chamber images, avoiding shortening, although strain analysis from the apical four-chamber window alone is also commonly performed and has proven accurate and reproducible. Dedicated software for LA strain analysis should be used, when available, to reduce variability and measurement errors.

As an additional recommendation, it is advised to obtain an image with the acquisition focused on the LA and a region of interest with a thickness of approximately 3 mm, due to the thin atrial wall.[1,13]

Two different temporal trigger approaches are available to quantify LA strain using the speckle tracking method. The first approach uses the beginning of the QRS complex

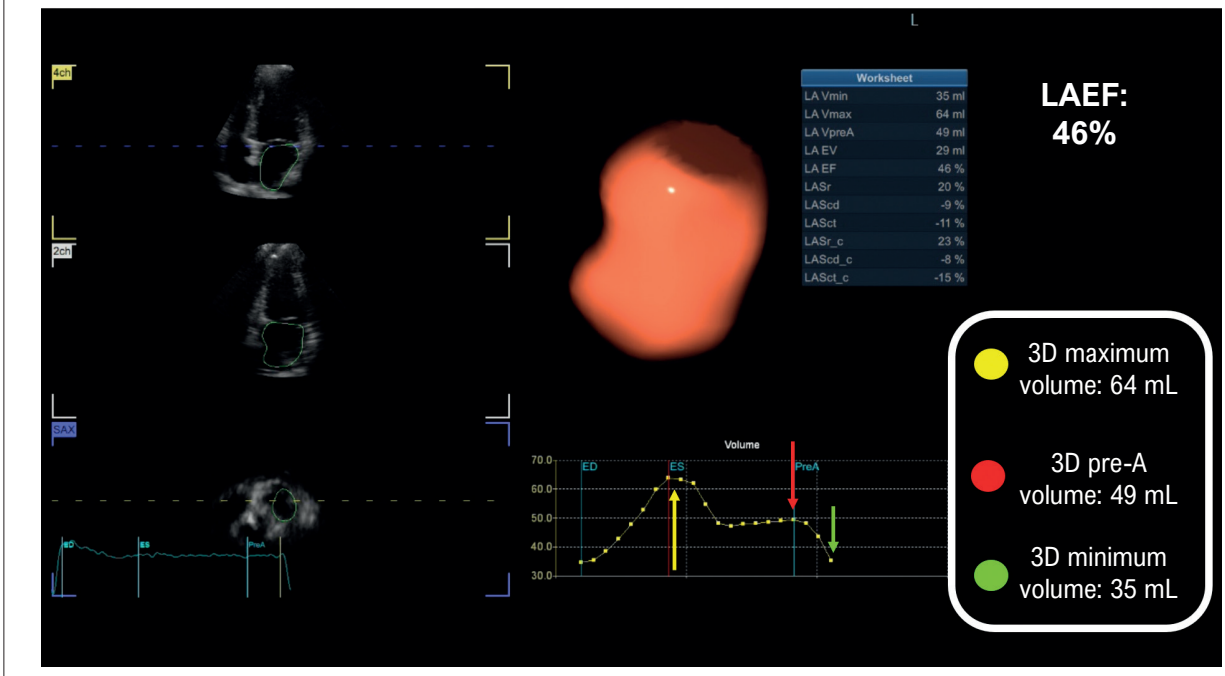

Figure 6 – *Semi-automatic 3D volumetric analysis of the LA (example of dedicated software). 3D: three-dimensional; LAEF: left atrial ejection fraction; pre-A: immediately before atrial contraction.*

derived from the electrocardiogram as a starting point (R-R trigger) and measures two key types of LA strain:

1. **Left atrial reservoir strain (LASr):** Analyzed at the end of LV systole (corresponding to aortic valve closure)
2. **Left atrial contraction strain (LASct):** Analyzed subsequently, corresponding to LA contraction.

The difference between LASr and LASct represents left atrial conduit strain (LAScd).

The second approach uses the P wave of the electrocardiogram as a starting point (P-P trigger), allowing the measurement of two deformations: the first descending, which corresponds to SAEct, and the second ascending, which corresponds to atrial relaxation and reservoir function.

Atrial parameters are smaller for the P-P interval-gated analysis compared to R-R gating. It is important to emphasize the impossibility of applying this analysis to patients with AF when P-P gating is used. Another point to highlight is that most studies published around the world have used R-R gating, making it the recommended method for measuring LA deformation.[13]

Figure 7 shows the main phases of LA deformation using R-R interval-gated analysis as a parameter.

Figure 8 shows both LA strain curve patterns, R-R or P-P interval, depending on the gating chosen.

Figure 9 illustrates the analysis of these three components of LA strain in a patient with hypertension, but without structural heart abnormalities.

The clinical importance of LASr has been reinforced by several studies demonstrating its independent prognostic value. The main studies conducted to date have validated this parameter as a prognostic marker in the following scenarios:[13]

- Acute myocardial infarction
- Chronic coronary syndrome
- Cardio-oncology
- ≥ moderate valvular disease (single or multiple valves)
- Dilated cardiomyopathy
- Acute or chronic HF
- Cardiac resynchronization therapy
- Athlete's heart
- Takotsubo syndrome

Normal LASr, LAScd, and LASct values are provided in Tables 4 and 5; however, the only recommended deformation parameter for LA function is global longitudinal deformation or LASr.

Segments adjacent to the mitral annulus, particularly in the inferior wall, normally exhibit higher strain values than those in the mid and superior (roof) segments of the LA. The lowest LA strain values are found in the LA roof, in the region of pulmonary vein insertion, where the heart is anchored to the mediastinum.

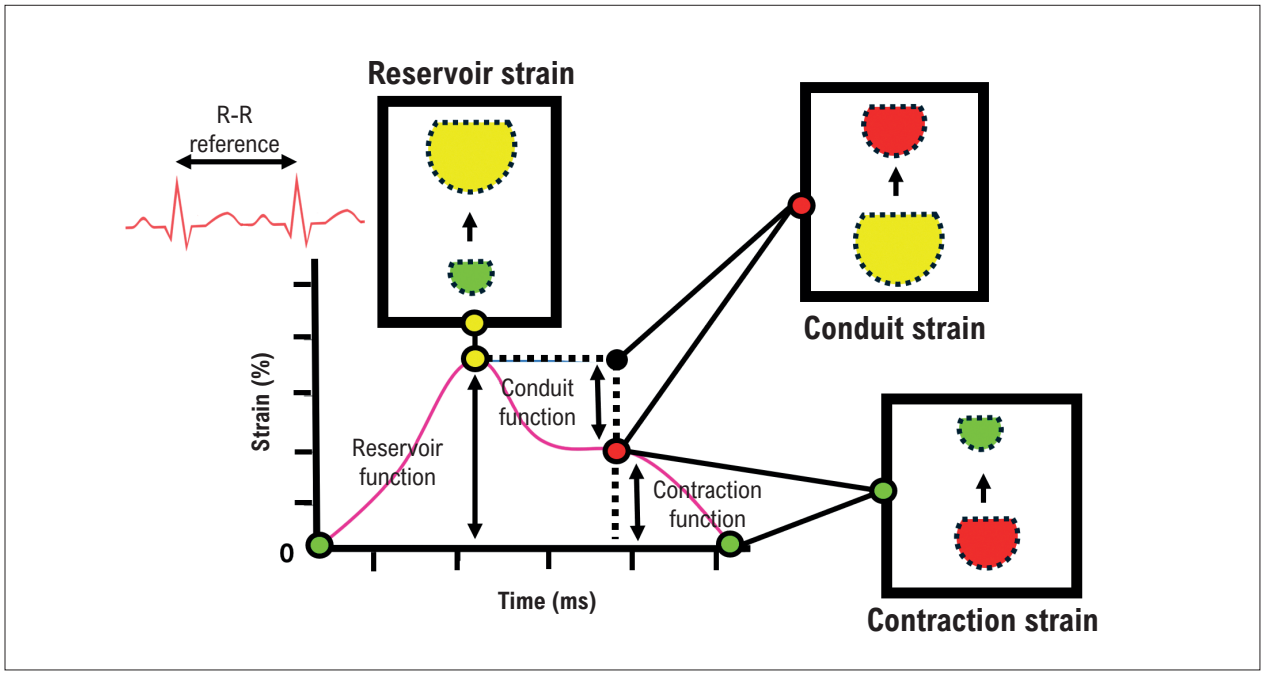

Figure 7 – *Left atrial strain curve (speckle tracking) with R-R gating: reservoir, conduit, and contraction strain.*

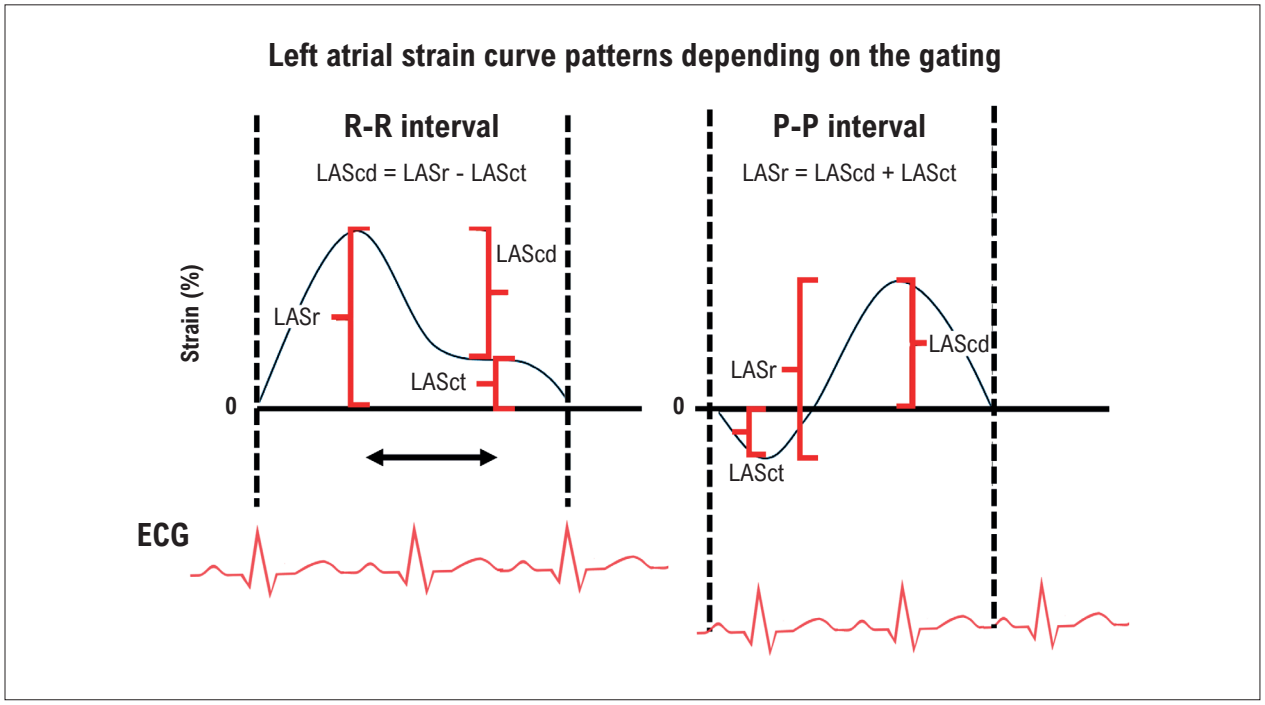

Figure 8 – *Two zero-reference approaches for left atrial strain assessment, and their respective curves. The strain values obtained with both techniques can be mathematically converted to one another. ECG: electrocardiogram; LAScd: left atrial conduit strain; LASct: left atrial contraction strain; LASr: left atrial reservoir strain.*

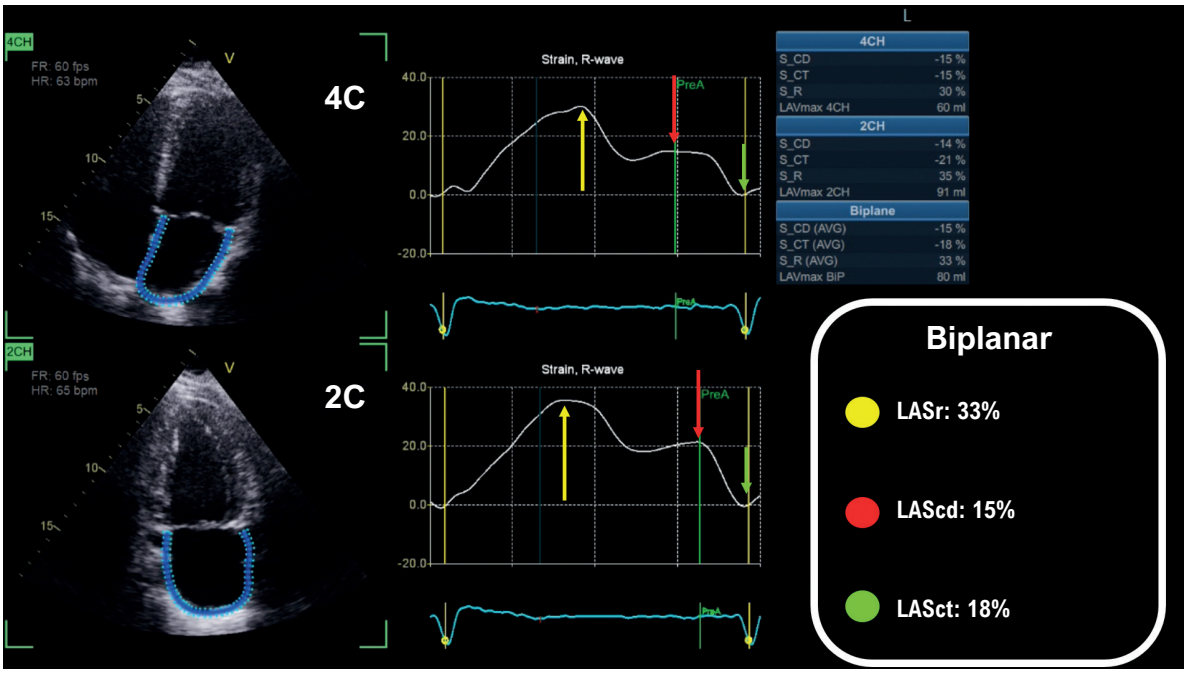

Figure 9 – *Analysis of left atrial strain in three phases (arrows: yellow = LASr; red = LAScd; green = LASct) in a patient with hypertension. Analysis was performed using dedicated software to measure left atrial longitudinal strain using automated left atrial endocardial tracking in apical two- and four-chamber views, following the recommendations of the European Association of Cardiovascular Imaging/American Society of Echocardiography/Industry Task Force to standardize deformation imaging.13 2C: two-chamber view; 4C: four-chamber view; LA: left atrium; LAScd: left atrial conduit strain; LASct: left atrial contraction strain; LASr: left atrial reservoir strain.*

Regional differences in LA strain may potentially be useful for assessing LA dyssynchrony, a parameter used as an indirect measure of heterogeneous LA fibrosis and dysfunction that can predict AF recurrence after radiofrequency ablation.

Mechanical dispersion of the LA or LA dyssynchrony, calculated as the standard deviation of the time to maximum strain of LA segments, was also evaluated for both reservoir and contractile strain, and both measures demonstrated value in predicting AF recurrence.[1,13]

The main limitations are related to the very thin LA walls, the interatrial septum which is often associated with hypermobility or aneurysm, the dependence on geometric assumptions in the regions of pulmonary vein and LA appendage insertion, in addition to the image field being presented in the most distal segment on echocardiographic analysis, and the fact that the LA is located in the most distant field during echocardiographic analysis.

The LA in assessment of diastolic function

Initially based on invasive hemodynamic studies, the assessment of LV stiffness and compliance constituted the initial pillars for identifying increased filling pressures and the development of LV diastology. In the case of patients with reduced ejection fraction, the elevation of filling pressures was more easily understood in light of systolic dysfunction. In patients with preserved ejection fraction, this interpretation became less straightforward, which prompted a deeper study of diastolic function.

With the incorporation of Doppler into echocardiography, there was a leap in quality in the non-invasive assessment of filling pressures, and studies emerged classifying another type of HF, diastolic HF, a term that would later be superseded by the preferred term heart failure with preserved left ventricular ejection fraction (HFpEF). The first guideline that guided the systematic assessment of LV diastole was published in 2009, already considering atrial variables for this assessment.

The LA and LV are structures arranged in series in the circulatory system, with the atrium serving the antechamber for the LV. Due to this close connection, LV diastolic function has a great influence on LA pressure and function. LA assessment, therefore, provides valuable information that can corroborate the identification and grading of LV diastolic dysfunction. This assessment was initially limited to analysis of transmitral flow and pulmonary venous flow. With the advent of new technologies, the identification of increased LA pressure has been made possible by more accurate variables: tissue Doppler of the mitral annulus during initial ventricular filling (e′ wave) and its relationship with the mitral E wave, with a mean E/e′ ratio greater than 14 being indicative of increased LA pressure. These variables, although important, may not be conclusive in some scenarios such as an E/e′ ratio between 8

and 14, mitral annulus calcification, atrial arrhythmias, and fusion of the E and A waves.

In 2025, the latest update of the guidelines for assessing LV diastolic function expanded the range of tools for this assessment. Among other variables, LASr less than or equal to 18% was included as another data point to be considered in this analysis. This addition was especially useful in the analysis of patients with preserved ejection fraction, a group in which strain alteration has high specificity for identifying increased LA pressure. With these additions and a new assessment flowchart, all patients previously classified as having indeterminate diastolic function (18.8% applying the 2016 criteria) were classified as having normal diastolic function or classified as having some degree of diastolic dysfunction, reducing the likelihood of inadequate quantification of diastolic dysfunction.[15]

In practice, this new guideline added parameters that increased the importance of the LA in diastology. The American Society of Echocardiography's Recommendations for the Evaluation of Left Ventricular Diastolic Function by Echocardiography and for HF With Preserved Ejection Fraction can be consulted for further guidance on diastolic assessment.[16]

Left atrial stiffness index

Impaired LA strain is closely related to the clinical presentation and diagnosis of HFpEF. When LA strain is used in conjunction with pulmonary artery occlusion pressure, invasively measured by catheterization, or with the E wave velocity/mitral e' velocity ratio (E/e'), the LA stiffness index can be derived.[17,18]

The LA stiffness index can be estimated using the following two echocardiographic variables:

- **LASr:** peak longitudinal LA strain
- E/e' ratio

The E/e'/LASr ratio is a relatively simple and non-invasive parameter to obtain and has shown good correlation with NT-proBNP and conventional echocardiographic diastolic parameters, including E/e', indexed LA volume, and right ventricular systolic pressure. Kim et al. published an interesting retrospective study in the *Journal of the American College of Cardiology* in 2022, with 307 patients, demonstrating that the LA stiffness index showed stronger prognostic performance in predicting all-cause mortality and HF-related hospitalization than classic diastolic parameters, including E/e', indexed LA volume, maximum tricuspid regurgitation velocity, and LASr during follow-up. An E/e'/LASr value > 0.26 had an area under the curve of 0.743 (95% confidence interval: 0.681 to 0.806; $p < 0.001$).

In that study, patients with invasively assessed LV end-diastolic pressure ≥ 16 mmHg and LV ejection fraction ≥ 50%, when presenting with an increased LA stiffness index (> 0.26), showed worse medium- and long-term prognosis compared to patients with the same characteristics and LA stiffness index ≤ 0.26, suggesting the potential use of this parameter as a prognostic biomarker based on echocardiographic imaging.[18]

New technologies (HeartModel)

New technologies have been incorporated into echocardiographic analysis, allowing for greater reproducibility and speed in acquiring images and volumetric data. Volumetric assessments on 3D echocardiography, classically available on ultrasound devices, are presented as semi-automatic measurements, often requiring additional

Table 4 – Reference values for left atrial reservoir, conduit, and contraction strain[13,14]

Normal values Meta-analysis including 2,542 healthy individuals		
Phases	**Valores de referência**	
LASr		**39%** (95% CI: 38%–41%) • Values < 23% associated with worse prognosis • Diastolic guidelines (values < 18% associated with increased LV filling pressures)
LAScd		**23%** (95% CI: 21%–25%)
LASct		**18%** (95% CI: 16%–19%)

CI: confidence interval; LAScd: left atrial conduit strain; LASct: left atrial contraction strain; LASr: left atrial reservoir strain; LV: left ventricle.

Table 5 – Main reference studies on LASr in relation to prognosis in various scenarios[13]

		LASr
Atrial fibrillation Her et al. JACC, 2021		LASr < 23% predicts recurrence of AF after ablation.
HFpEF Singh et al. JACC, 2022		LASr was an early and sensitive marker of increased LV filling pressure.
Valvular diseases Addetia et al. JASE, 2023		LASr < 25% in severe mitral regurgitation identified patients with worse prognosis regardless of ejection fraction.
Oncology Zhang et al. EHJ CV Imaging, 2024		LASr < 25% predicts cardiotoxicity earlier than LV strain.

HFpEF: heart failure with preserved left ventricular ejection fraction; LASr: left atrial reservoir strain; LV: left ventricle; AF: atrial fibrillation

adjustments for each of the analyzed cardiac segments, which would ultimately consume additional time that is often unavailable in clinical practice.

Companies such as Philips and General Electric have developed specific software for accurate and fully automatic measurements with single-click acquisition, allowing even echocardiography operators without extensive experience to easily perform this analysis.

In a feasibility and accuracy study with 159 patients, Tsang et al. demonstrated that the fully automatic software (HeartModel, Philips Healthcare) showed a strong correlation with the semi-automatic measurement with manual correction (r = 0.87 to 0.96). Additionally, the agreement between automated volumetric analysis and CMR was also significant (r = 0.84 to 0.95). The average acquisition and analysis time for LV and LA volumes was 37 seconds for the automatic HeartModel software, compared to 79 seconds for the same acquisition, but with minor manual adjustments made by the operator, and 212 seconds for 2D assessment by Simpson's method, with a final reduction of 82% in acquisition time.[19] An interesting finding of this analysis was that human post-processing changes did not lead to significant improvements compared to automatic volumetric analysis, using CMR as a reference.

Figure 10 illustrates acquisition using the Philips HeartModel A.I. software with automatic volumetric evaluation.

Figure 11 presents a step-by-step approach to structured left atrial (LA) analysis, encompassing the essential data that should be obtained from the echocardiographic study, as well as a summary table highlighting the strengths and limitations of the main parameters discussed throughout the text.

Conclusion

LA assessment has evolved from morphological analysis restricted to the anteroposterior diameter to an integrated functional approach that is capable of characterizing the three phases of the atrial cycle (reservoir, conduit, and contraction). This progression, which ranges from 2D volumetry to strain and atrial stiffness index, reflects a conceptual shift in recent literature. The LA is not a passive chamber, but rather an active determinant of cardiac performance and an independent prognostic marker in various clinical settings, such as AF, HF, and valvular heart disease.

The systematic incorporation of these parameters into routine echocardiography is, therefore, clinically justified. The inclusion of LA reservoir strain in the most recent diastolic function guideline exemplifies how this integration is already underway. As new technologies increase reproducibility and reduce acquisition time, LA functional analysis is likely to become consolidated as an essential component of echocardiographic reports, supporting more precise characterization and more informed clinical decision-making.

Author Contributions

Conception and design of the research, analysis and interpretation of the data and writing of the manuscript:

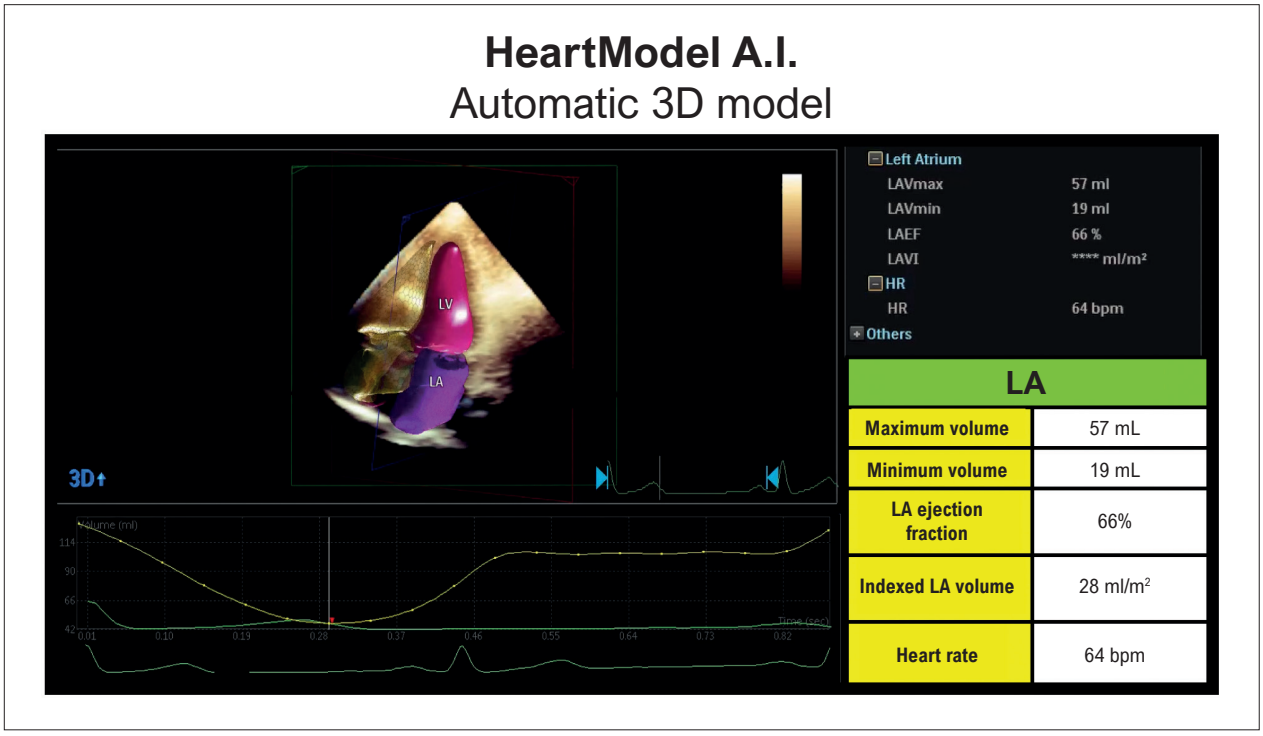

Figure 10 – *Automated 3D transthoracic quantification of left heart chambers using specific HeartModel A.I. software. LA: left atrium; 3D: three-dimensional.*

Take-home messages:

1. Linear dimensions: These dimensions should no longer be used, as they are not related to the actual size of the LA, especially if the LA is enlarged.

2. 2D LA volume assessment:

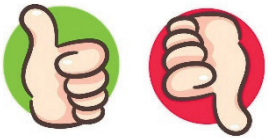

- **Strengths:**
  - Easy to perform
  - Widely available
  - Does not require dedicated software
  - Large body of data on normal values and data demonstrating prognostic value in various cardiac conditions
- **Weaknesses:**
  - Underestimates actual LA volume
  - Relies on geometric assumptions to calculate volume
  - Reasonable, but not optimal, interobserver variability and reproducibility

3. 3D LA volume assessment:

- **Strengths:**
  - Does not rely on geometric assumptions (more precise volumes)
  - Lower interobserver variability (ideal for serial measurements)
- **Weaknesses:**
  - Low spatial resolution
  - Requires a specific transducer for image acquisition, as well as software
  - Increased costs and limited supporting data on normal values and prognosis

4. LA reservoir strain:

- **Strengths:**
  - Uses conventional grayscale analysis
  - Easy to perform and highly reproducible
  - Demonstrated prognostic value in HFpEF (already incorporated into guidelines)
  - Increasingly available dedicated software packages
- **Weaknesses:**
  - Variability between providers has yet to be evaluated in large-scale studies
  - Prognostic value independent of LV longitudinal strain still needs to be established

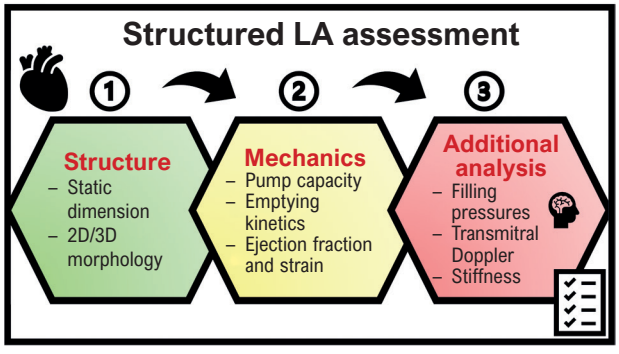

Figure 11 – *Top: Comparison of the pros and cons of different techniques: linear dimensions, LA volumes by the 2D biplane method, LA volumes by the 3D method, and LA reservoir strain. Bottom: Flowchart for a structured analysis of the left atrium using anatomical, functional, and hemodynamic data. These parameters should be reported at the end of the echocardiography report. 2D: two-dimensional; 3D: three-dimensional; LA: left atrium; HFpEF: heart failure with preserved left ventricular ejection fraction; LV: left ventricle. 2D: two-dimensional; 3D: three-dimensional; HFpEF: heart failure with preserved left ventricular ejection fraction; LA: left atrium; LV: left ventricle.*

Silva HAGP, Gomes HM; critical revision of the manuscript for intellectual content: Silva HAGP, Gomes HM, Souza AC.

Potential conflict of interest

No potential conflict of interest relevant to this article was reported.

Sources of funding

There were no external funding sources for this study.

Study association

This study is not associated with any thesis or dissertation work.

Ethics approval and consent to participate

This article does not contain any studies with human participants or animals performed by any of the authors. This article does not contain any studies with human participants or animals performed by any of the authors.

Use of Artificial Intelligence

The authors did not use any artificial intelligence tools in the development of this work.

Data Availability Statement

The underlying content of the research text is contained within the manuscript.

References

1. Thomas L, Muraru D, Popescu BA, Sitges M, Rosca M, Pedrizzetti G, et al. Evaluation of Left Atrial Size and Function: Relevance for Clinical Practice. J Am Soc Echocardiogr. 2020;33(8):934-952. doi: 10.1016/j.echo.2020.03.021.
2. Mangia M, D'Andrea E, Cecchetto A, Beccari R, Mele D, Nistri S. Current and Clinically Relevant Echocardiographic Parameters to Analyze Left Atrial Function. J Cardiovasc Dev Dis. 2024;11(8):241. doi: 10.3390/jcdd11080241.
3. Mitchell C, Rahko PS, Blauwet LA, Canaday B, Finstuen JA, Foster MC, et al. Guidelines for Performing a Comprehensive Transthoracic Echocardiographic Examination in Adults: Recommendations from the American Society of Echocardiography. J Am Soc Echocardiogr. 2019;32(1):1-64. doi: 10.1016/j.echo.2018.06.004.
4. Badano LP, Miglioranza MH, Mihăilă S, Peluso D, Xhaxho J, Marra MP, et al. Left Atrial Volumes and Function by Three-Dimensional Echocardiography: Reference Values, Accuracy, Reproducibility, and Comparison with Two-Dimensional Echocardiographic Measurements. Circ Cardiovasc Imaging. 2016;9(7):e004229. doi: 10.1161/CIRCIMAGING.115.004229.
5. Agner BF, Kühl JT, Linde JJ, Kofoed KF, Åkeson P, Rasmussen BV, et al. Assessment of Left Atrial Volume and Function in Patients with Permanent Atrial Fibrillation: Comparison of Cardiac Magnetic Resonance Imaging, 320-Slice Multi-Detector Computed Tomography, and Transthoracic Echocardiography. Eur Heart J Cardiovasc Imaging. 2014;15(5):532-40. doi: 10.1093/ehjci/jet239.
6. Lang RM, Badano LP, Mor-Avi V, Afilalo J, Armstrong A, Ernande L, et al. Recommendations for Cardiac Chamber Quantification by Echocardiography in Adults: An Update from the American Society of Echocardiography and the European Association of Cardiovascular Imaging. J Am Soc Echocardiogr. 2015;28(1):1-39.e14. doi: 10.1016/j.echo.2014.10.003.
7. Davis EF, Crousillat DR, He W, Andrews CT, Hung JW, Danik JS. Indexing Left Atrial Volumes: Alternative Indexing Methods Better Predict Outcomes in Overweight and Obese Populations. JACC Cardiovasc Imaging. 2022;15(6):989-97. doi: 10.1016/j.jcmg.2022.02.006.
8. Thomas L, Marwick TH, Popescu BA, Donal E, Badano LP. Left Atrial Structure and Function, and Left Ventricular Diastolic Dysfunction: JACC State-of-the-Art Review. J Am Coll Cardiol. 2019;73(15):1961-77. doi: 10.1016/j.jacc.2019.01.059.
9. Singh A, Singulane CC, Miyoshi T, Prado AD, Addetia K, Bellino M, et al. Normal Values of Left Atrial Size and Function and the Impact of Age: Results of the World Alliance Societies of Echocardiography Study. J Am Soc Echocardiogr. 2022;35(2):154-164.e3. doi: 10.1016/j.echo.2021.08.008.
10. Ferreira J, Gonçalves V, Marques-Alves P, Martins R, Monteiro S, Teixeira R, et al. Left Atrial Functional Assessment and Mortality in Patients with Severe Aortic Stenosis with Sinus Rhythm. Cardiovasc Ultrasound. 2021;19(1):1. doi: 10.1186/s12947-020-00231-0.
11. Inciardi RM, Giugliano RP, Claggett B, Gupta DK, Chandra A, Ruff CT, et al. Left Atrial Structure and Function and the Risk of Death or Heart Failure in Atrial Fibrillation. Eur J Heart Fail. 2019;21(12):1571-9. doi: 10.1002/ejhf.1606.
12. Mor-Avi V, Yodwut C, Jenkins C, Kühl H, Nesser HJ, Marwick TH, et al. Real-Time 3D Echocardiographic Quantification of Left Atrial Volume: Multicenter Study for Validation with CMR. JACC Cardiovasc Imaging. 2012;5(8):769-77. doi: 10.1016/j.jcmg.2012.05.011.
13. Thomas JD, Edvardsen T, Abraham T, Appadurai V, Badano L, Banchs J, et al. Clinical Applications of Strain Echocardiography: A Clinical Consensus Statement from the American Society of Echocardiography Developed in Collaboration with the European Association of Cardiovascular Imaging of the European Society of Cardiology. Eur Heart J Cardiovasc Imaging. 2026;27(3):335-68. doi: 10.1093/ehjci/jeag006.
14. Pathan F, D'Elia N, Nolan MT, Marwick TH, Negishi K. Normal Ranges of Left Atrial Strain by Speckle-Tracking Echocardiography: A Systematic Review and Meta-Analysis. J Am Soc Echocardiogr. 2017;30(1):59-70.e8. doi: 10.1016/j.echo.2016.09.007.
15. Hafez A, Farina JM, Ahmed S, Awad K, Pietri MP, Scalia IG, et al. Reclassifying Left Ventricular Diastolic Function with the 2025 American Society of Echocardiography Guideline versus the 2016 Algorithm. J Am Soc Echocardiogr. 2026:S0894-7317(26)00087-8. doi: 10.1016/j.echo.2026.02.013.
16. Nagueh SF, Sanborn DY, Oh JK, Anderson B, Billick K, Derumeaux G, et al. Recommendations for the Evaluation of Left Ventricular Diastolic Function by Echocardiography and for Heart Failure with Preserved Ejection Fraction Diagnosis: An Update from the American Society of Echocardiography. J Am Soc Echocardiogr. 2025;38(7):537-69. doi: 10.1016/j.echo.2025.03.011.
17. Mathias IS, Rahi W, Ramos A, Na J, Angulo C, Rothstein P, et al. Validation of Noninvasive Left Atrial Stiffness Against Left Atrial Operating Chamber Stiffness by Cardiac Catheterization. JACC Cardiovasc Imaging. 2024;17(8):1000-2. doi: 10.1016/j.jcmg.2024.03.004.
18. Kim D, Seo JH, Choi KH, Lee SH, Choi JO, Jeon ES, et al. Prognostic Implications of Left Atrial Stiffness Index in Heart Failure Patients with Preserved Ejection Fraction. JACC Cardiovasc Imaging. 2023;16(4):435-45. doi: 10.1016/j.jcmg.2022.11.002.
19. Tsang W, Salgo IS, Medvedofsky D, Takeuchi M, Prater D, Weinert L, et al. Transthoracic 3D Echocardiographic Left Heart Chamber Quantification Using an Automated Adaptive Analytics Algorithm. JACC Cardiovasc Imaging. 2016;9(7):769-82. doi: 10.1016/j.jcmg.2015.12.020.

My Approach to Assessing Mitral Regurgitation with Splay: What Does It Mean for Severity?

Gustavo Nishida,[1] *Natasha Soares Simões dos Santos,*[1] *Jorge Eduardo Assef,*[1] *Andrea de Andrade Vilela*[1]
Instituto Dante Pazzanese de Cardiologia,[1] *São Paulo, SP – Brazil*

Central Illustration: My Approach to Assessing Mitral Regurgitation with Splay: What Does It Mean for Severity?

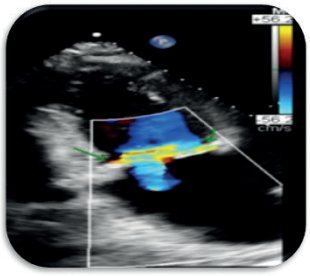

- Side-lobe artifact
- Red flag for significant MR
- Not all cases of splay indicate significant MR; not all cases of significant MR show splay
- Reassessment/complementary imaging: caution regarding underestimation when grading MR severity
- Potential diagnostic and prognostic value

Arq Bras Cardiol: Imagem cardiovasc. 2026;39(2):e20260024

MR: mitral regurgitation.

Abstract

Echocardiographic assessment of mitral regurgitation (MR) is multiparametric and often challenging. The artifact known as splay has been described as an additional tool for estimating the severity of regurgitation. The term refers to a side-lobe artifact that forms a horizontal arc on color Doppler imaging. This same phenomenon can also be observed in other valvular heart diseases, such as aortic regurgitation. In 2020, Wiener et al. reported that splay was present in 81% of cases of significant MR, reaching 93% in eccentric jets, whereas the prevalence was only 16% in mild MR. Verbeke et al. associated the artifact with larger regurgitant volumes. A splay width greater than 29 mm was identified as an independent predictor of adverse cardiovascular outcomes. Although its presence alone does not denote severe MR, splay acts as a red flag, suggesting that regurgitation may be greater than it appears and indicating the need for careful reassessment of the transthoracic echocardiogram or, possibly, complementary transesophageal echocardiography. Further evidence and systematic evaluations are needed to investigate the best strategy for incorporating these data into the multiparametric approach to MR.

Keywords

Severity of Illness Index; Mitral Valve Insufficiency; Echocardiography

Mailing Address: Gustavo Nishida •
Instituto Dante Pazzanese de Cardiologia. Avenida Dr Dante Pazzanese, 500. Postal code: 04012-909. São Paulo, SP – Brazil
E-mail: gustavonishida@yahoo.com.br
Manuscript received March 12, 2026, revised manuscript March 23, 2026, accepted March 25, 2026
Editor responsible for the review: Marcelo Tavares

DOI: https://doi.org/10.36660/abcimg.20260024i

The challenge of grading mitral regurgitation severity

Echocardiographic assessment of mitral regurgitation (MR) is multiparametric and often challenging. Especially in the presence of multiple, eccentric, non-homogeneous

CONTENTS

jets throughout the cardiac cycle or non-circular regurgitant orifices, it is paramount to combine qualitative and quantitative data that can guide the grading of valvular regurgitation.[1,2] In this context, an artifact has been described as an additional finding in the assessment of MR.

Splay: a valuable artifact

The term splay refers to a side-lobe artifact that appears as a horizontal arc on color Doppler imaging, dispersing signal and usually observed along the atrial surface of the valve, extending beyond anatomical boundaries[3] (Figure 1).

Ultrasound transducers emit energy not only in the main direction (central axis of the beam), but also in lateral directions, forming secondary lobes of lower intensity. When these side lobes encounter highly reflective structures, such as cardiac walls or valves, they may generate echoes that are incorrectly mapped by the imaging system, as if they originated from the main axis, resulting in artifacts on echocardiographic images.[4]

Considering the mechanism that gives rise to this artifact, splay can be documented in other valvular regurgitations, for example, aortic regurgitation (Figure 2).

Evidence of diagnostic and prognostic value

In 2020, Wiener et al.[3] described this artifact as a clue for detecting significant MR. In an analysis of 200 cases of MR documented by transthoracic echocardiography, half with significant regurgitation and half with mild regurgitation, the prevalence of splay was 81% and 16%, respectively. In eccentric jets, the prevalence reached 93% of cases. This sign was observed in proto-, meso-, tele-, and holosystolic jets; on the atrial and ventricular surface of the mitral annulus; in preserved and reduced left ventricular ejection fraction; in different etiologies (prolapse, rheumatic disease, mitral annulus calcification, functional); and using different commercially available echocardiogram brands. It has most frequently been documented in apical views, but it has also been observed in parasternal long- and short-axis views. The origin of the signal appears to be related to blood flow rate per unit area. With higher gain, lower ultrasound frequency, and lower Nyquist limit, higher prevalence and greater extent of splay are observed. In their study, harmonic imaging had little effect on splay.

In a single-center registry by Verbeke et al.[5] in Ghent, Belgium, a 27% prevalence of color Doppler splay was reported in 469 patients, correlating with greater effective regurgitant orifice area, regurgitant volume, and vena contracta width. They used a Vivid E9 echocardiographic system, GE Healthcare, equipped with an M5Sc-D transducer for all examinations. For color Doppler assessment, the following standardized parameters were applied for all patients: transmission frequency of 2.2 MHz, velocity scale of 3.5 kHz (aliasing velocity of 63 cm/s), and gain adjusted to −5 dB. Splay was more prevalent and showed greater width in patients with significant MR. In their cohort, splay

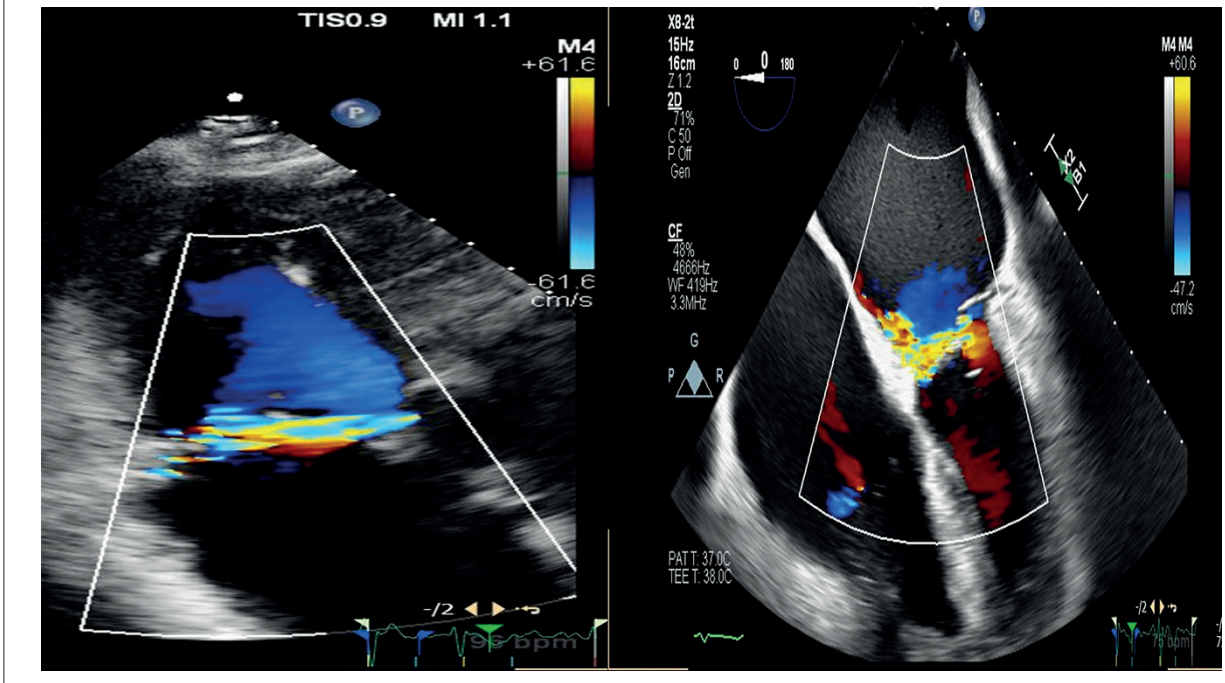

Figure 1 – *Splay in MR. On the left, transthoracic echocardiography in the apical 3-chamber view shows evidence of splay on color Doppler at the level of the mitral annulus. On the right, transesophageal echocardiography reveals significant MR with a medially directed eccentric jet.*

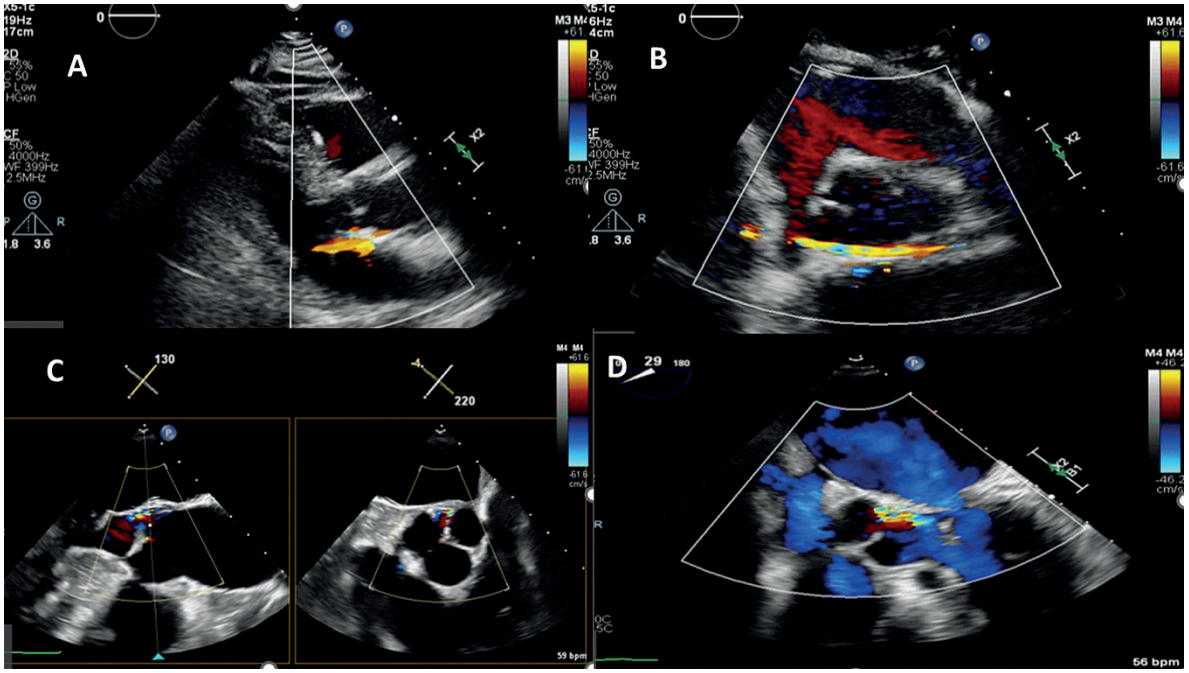

Figure 2 – *Splay in aortic regurgitation. In the upper images, transthoracic echocardiography in the parasternal long-axis (A) and short-axis (B) views shows evidence of splay, extending beyond anatomical boundaries. In the lower images (C and D), transesophageal echocardiogram reveals an eccentric aortic regurgitant jet originating from the commissural region.*

width greater than 29 mm was an independent predictor of cardiovascular outcomes, with additional prognostic value.

Final considerations

This is a relatively recent description of an echocardiographic sign that requires further evidence and studies to guide its systematic integration into echocardiographic practice. Although it does not necessarily indicate significant MR and is not indispensable for defining this severity, splay represents a potential tool signaling the possibility that regurgitation is more severe than appears. This red flag prompts careful reassessment of the transthoracic echocardiogram and, when appropriate, complementary transesophageal echocardiography when other findings lead us to suspect significant MR (Central Illustration).

In the words of Bertrand et al.,[6] splay is "the artifact that tells the truth," by signaling the possibility of significant MR.

Author Contributions

Conception and design of the research and writing of the manuscript: Nishida G; acquisition of data and analysis and interpretation of the data: Nishida G, Santos NSS; critical revision of the manuscript for intellectual content: Nishida G, Santos NSS, Assef JE, Vilela AA.

Potential Conflict of Interest

No potential conflict of interest relevant to this article was reported.

Sources of Funding

There were no external funding sources for this study.

Study Association

This study is not associated with any thesis or dissertation work.

Ethics approval and consent to participate

This article does not contain any studies with human participants or animals performed by any of the authors.

Use of Artificial Intelligence

The authors did not use any artificial intelligence tools in the development of this work.

Availability of Research Data

The underlying content of the research text is contained within the manuscript.

References

1. Zoghbi WA, Adams D, Bonow RO, Enriquez-Sarano M, Foster E, Grayburn PA, et al. Recommendations for Noninvasive Evaluation of Native Valvular Regurgitation: A Report from the American Society of Echocardiography Developed in Collaboration with the Society for Cardiovascular Magnetic Resonance. J Am Soc Echocardiogr. 2017;30(4):303-71. doi: 10.1016/j.echo.2017.01.007.
2. Grayburn PA, Thomas JD. Basic Principles of the Echocardiographic Evaluation of Mitral Regurgitation. JACC Cardiovasc Imaging. 2021;14(4):843-53. doi: 10.1016/j.jcmg.2020.06.049.
3. Wiener PC, Friend EJ, Bhargav R, Radhakrishnan K, Kadem L, Pressman GS. Color Doppler Splay: A Clue to the Presence of Significant Mitral Regurgitation. J Am Soc Echocardiogr. 2020;33(10):1212-9.e1. doi: 10.1016/j.echo.2020.05.002.
4. Bertrand PB, Levine RA, Isselbacher EM, Vandervoort PM. Fact or Artifact in Two-Dimensional Echocardiography: Avoiding Misdiagnosis and Missed Diagnosis. J Am Soc Echocardiogr. 2016;29(5):381-91. doi: 10.1016/j.echo.2016.01.009.
5. Verbeke J, Kamoen V, Calle S, De Buyzere M, Timmermans F. Color Doppler Splay in Mitral Regurgitation: Hemodynamic Correlates and Outcomes in a Clinical Cohort. J Am Soc Echocardiogr. 2022;35(9):933-9. doi: 10.1016/j.echo.2022.04.006.
6. Bertrand PB, Nagata Y, Namasivayam M, Levine RA. The Artifact that Tells the Truth: Color Doppler Splay Unmasking Significant Mitral Regurgitation. J Am Soc Echocardiogr. 2020;33(10):1220-2. doi: 10.1016/j.echo.2020.08.003.

Single Coronary Artery and Stress Cardiomyopathy: An Association Demonstrated by Multimodality Imaging

Marcus Vinicius Silva Ferreira,[1] Julia Pereira Afonso dos Santos Tormin,[1] Roberto Nery Dantas Jr.,[1] Roberto Vitor Almeida Torres,[1] Renan Andreos Cordeiro,[1] José de Arimateia Batista Araújo-Filho,[1] Luiz Francisco Cardoso[1]

Hospital Sirio-Libanes,[1] São Paulo, SP – Brazil

Case Report

A 58-years-old female patient was admitted with retrosternal chest pain described as a continuous, oppressive tightness that had started two days earlier, after a tooth extraction procedure performed under ineffective local anesthesia. The patient's past medical history included diabetes, dyslipidemia, and ovarian cancer, and she was receiving aspirin, rosuvastatin, metformin, dapagliflozin, and semaglutide. Physical examination was unremarkable. The chest pain protocol was initiated, and the initial electrocardiogram showed sinus rhythm with left anterior fascicular block, early repolarization in the inferior leads, and T-wave inversion in aVL, V1, and V2 (Figure 1A). The patient received 5 mg of sublingual isosorbide dinitrate, and blood samples were collected for laboratory testing. High-sensitivity troponin T (hs-cTnT) was 171 ng/L, confirming myocardial injury. An initial diagnosis of non–ST-elevation myocardial infarction (NSTEMI) was made, and the patient underwent coronary angiography (CA) for anatomic assessment (Figure 1 / Video S1).

Angiography revealed a single right coronary artery (RCA), which was further evaluated by coronary computed tomography angiography (CCTA; Figure 2). The left coronary branches originated from a large right marginal branch, with an anomalous course anterior to the right ventricular conus, followed by an ascending course of the left anterior descending (LAD) artery in the interventricular sulcus and subsequent branching into the circumflex (CX) and obtuse marginal (OM) arteries. However, no evidence of plaque or stenosis was identified. Left ventriculography (Video S1) revealed regional wall motion abnormalities, with midventricular akinesia and ballooning, which were further confirmed by echocardiography (Figure 3/ Video S2). These findings are typically described as the midventricular phenotype of stress cardiomyopathy (SCM).

Keywords

Coronary Vessels; Takotsubo Cardiomyopathy; Coronary Angiography; Echocardiography; Magnetic Resonance Imaging

Mailing Address: Marcus Vinicius Silva Ferreira •
Hospital Sírio-Libânes. Rua Dona Adma Jafet, 115. Postal code: 01308-050. São Paulo, SP – Brazil
E-mail: marcusvsferreira@gmail.com
Manuscript received March 23, 2026, revised manuscript April 6, 2026, accepted April 6, 2026
Editor responsible for the review: Marcelo Tavares

DOI: https://doi.org/10.36660/abcimg.20260023i

The patient received supportive care, with improvement in pain and a decrease in hs-cTnT to 39 ng/L. Cardiac magnetic resonance (CMR), performed four days later, before hospital discharge, revealed a preserved ejection fraction with mild hypokinesia of the midventricular anterior and septal walls (Figure 4/Video S3). The T2-weighted short tau inversion recovery (STIR) sequence demonstrated edema in the mid-anterior and septal walls, with mild mid-wall late gadolinium enhancement, interpreted as a subacute finding of SCM. The patient was discharged after seven days, with complete pain resolution and no complications during hospitalization.

Discussion

Isolated single coronary artery (SCA) is a rare congenital anomaly in which a single artery arises from a single coronary ostium and supplies the entire myocardium, branching in different patterns to perfuse the coronary territories.[1] Although most patients remain asymptomatic, some variants, particularly those with interarterial and intramural courses, may promote exercise-induced ischemia because of extrinsic compression caused by increased pulsation of the aorta and pulmonary artery. These patients are at increased risk of sudden cardiac death during exercise, particularly younger patients under 30 years of age, with a left coronary artery following an interarterial and intramural course.[2] In addition, an acute-angle takeoff and a tortuous course may result in abnormal blood flow and predispose to atherosclerotic disease because of endothelial injury.[3]

Recent reports have described SCM in patients with SCA, even in the absence of an interarterial course.[3-6] SCM is an acute and transient myocardial injury characterized by myocardial stunning, that is, transient regional left ventricular systolic dysfunction, triggered by an emotionally or physically stressful event. The classic presentation of SCM, known as Takotsubo syndrome consists of apical and midventricular akinesia, hypokinesia, or dyskinesia associated with basal hyperkinesia, resulting in apical ballooning. However, other phenotypes have also been described, including the midventricular pattern observed in the present case.[7] The mechanism of myocardial injury remains unclear. It has been hypothesized that dysregulation of the central autonomic nervous system and increased levels of stress-related neuropeptides may promote microvascular constriction, impaired perfusion, and ischemic stunning.[8]

Gräni et al.[6] reported a case of a single RCA with a deep subpulmonary intraseptal course of the LAD/CX, presenting with the classic apical ballooning phenotype

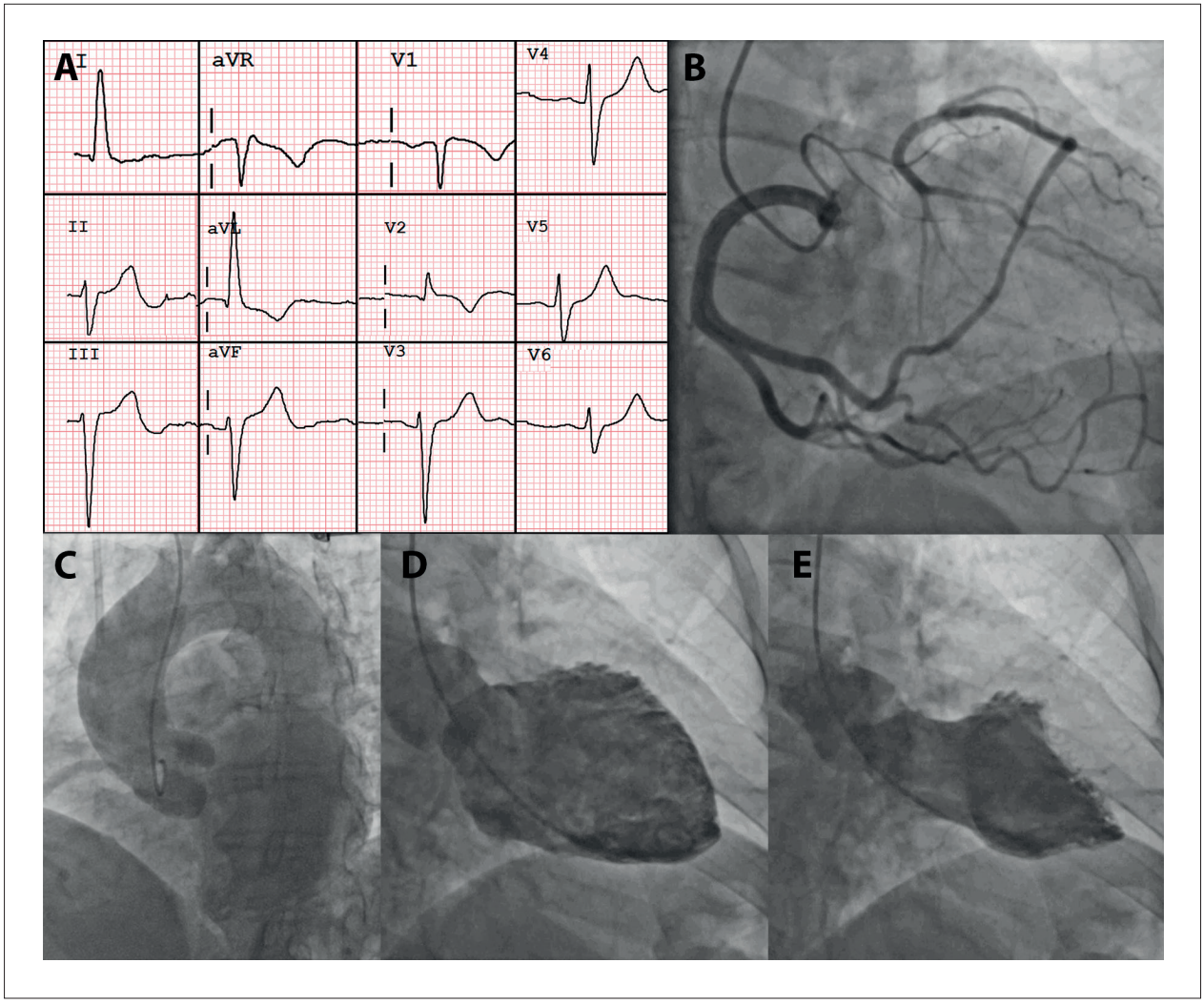

Figure 1 – *Initial Electrocardiogram and Percutaneous Angiography Findings. A) Initial electrocardiogram demonstrating T-wave inversion in aVL, V1 and V2. B) CA revealed a SCA emerging from the right coronary sinus with anomalous course anterior to the right ventricle (RV) conus and providing the left branches. No coronary stenosis was identified. C) Aortography revealed no abnormalities. D-E) Left ventriculography in diastole (D) and systole (E) demonstrating mid-ventricle akinesia and balooning.*

of SCM (Takotsubo syndrome). Despite the absence of an interarterial course, the transeptal path was hypothesized to contribute to vasospasm, endothelial dysfunction, and SCM. However, extrinsic compression as a potential mechanism was not observed in other reports.

Neiva et al[3] described a similar case of a single RCA, with hypoplastic LAD and CX arteries arising from a posterolateral branch that coursed anterior to the right ventricular conus, presenting with classic SCM and complete remission after seven days. Salazar Marín et al.[4] reported a case of a single RCA with a different branching pattern, characterized by independent origins of the LAD and CX, with prepulmonary and retroaortic courses, respectively, associated with classic SCM.

Across these reports, the anomalous origin of the LAD and CX was a common finding, though without the typical high-risk features for ischemia. However, Miura et al.[5] described a left SCA coursing in the posterior sulcus, supplying the posterior descending and posterior left ventricular arteries, and presenting with the same SCM phenotype. A specific epicardial coronary artery distribution alone could not explain the occurrence of SCM in these patients, and the mechanism of myocardial injury remains unclear. All reported cases, including the present one, had a favorable prognosis with complete remission of symptoms.

Conclusion

This case is the first to describe the association between a distinct SCM phenotype, the midventricular form, and an isolated right SCA. The potential association between SCM and SCA is of increasing interest, given the growing

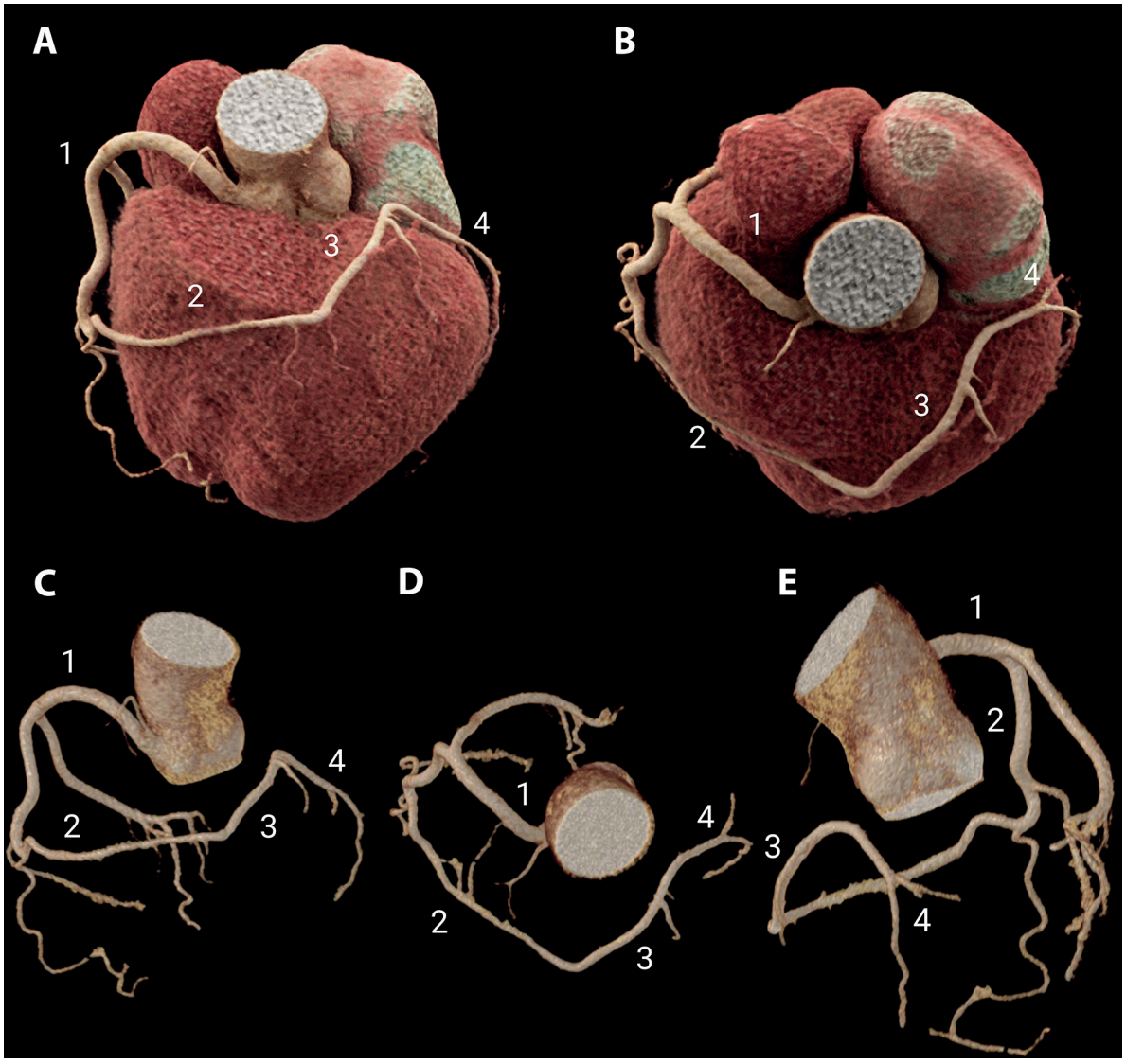

Figure 2 – *CCTA Findings. 3D rendered cardiac (A-B) and coronary reconstruction (C-E) better depicted coronary anatomy. 1) Single RCA emerging from the right sinus with normal course through the atrioventricular sulcus. 2) Elongated right marginal artery coursing anterior to the right ventricle conus to reach the anterior interventricular sulcus. 3) Anterior interventricular branch with ascending course with septal and diagonal branches (LAD artery territory). 4) Left atrioventricular branch coursing laterally and branching into left OM branches (left CX artery territory).*

number of reports despite the rarity of SCA. However, the mechanism predisposing patients with SCA to SCM remains unknown, and a high-risk coronary course alone was absent in most previous reports, as well as in the present case.

Author Contributions

Conception and design of the research: Ferreira MVS, Tormin JPAS, Dantas Jr. RN, Araújo-Filho JAB; Acquisition of data: Ferreira MVS, Tormin JPAS, Cordeiro RA, Cardoso LF; Analysis and interpretation of the data: Dantas Jr. RN, Araújo-Filho JAB; Torres RVA; Writing of the manuscript: Ferreira MVS, Tormin JPAS; Critical revision of the manuscript for intellectual content: Ferreira MVS, Tormin JPAS, Dantas Jr. RN, Torres RVA, Cordeiro RA, Cardoso LF, Araújo-Filho JAB.

Potential Conflict of Interest

No potential conflict of interest relevant to this article was reported.

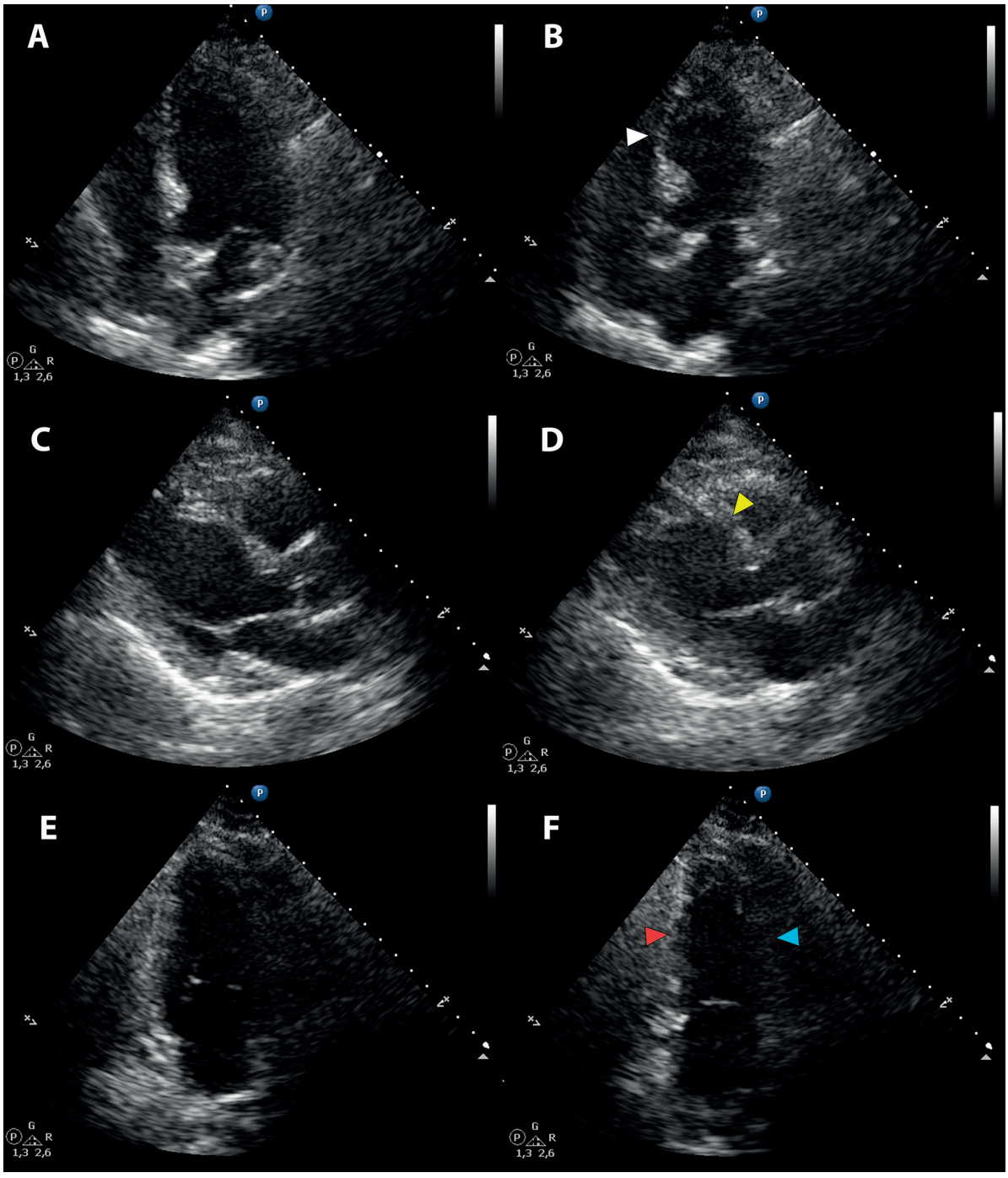

Figure 3 – *Transthoracic Echocardiogram (TTE) Findings. A-B) TTE Four-chamber view in diastole (A) and systole (B) demonstrating mid inferoseptal segment akinesia and bulging (white arrowhead). C-D) Parasternal long-axis view in diastole (C) and systole (D) demonstrating mid anteroseptal segment akinesia and bulging (yellow arrowhead). E-F) Two-chamber view in diastole (E) and systole (F) demonstrating mid inferior akinesia (red arrowhead) and mid anterior hypokinesia (blue arrowhead). TTE confirmed previous left ventriculography findings, which were suggestive of SCM.*

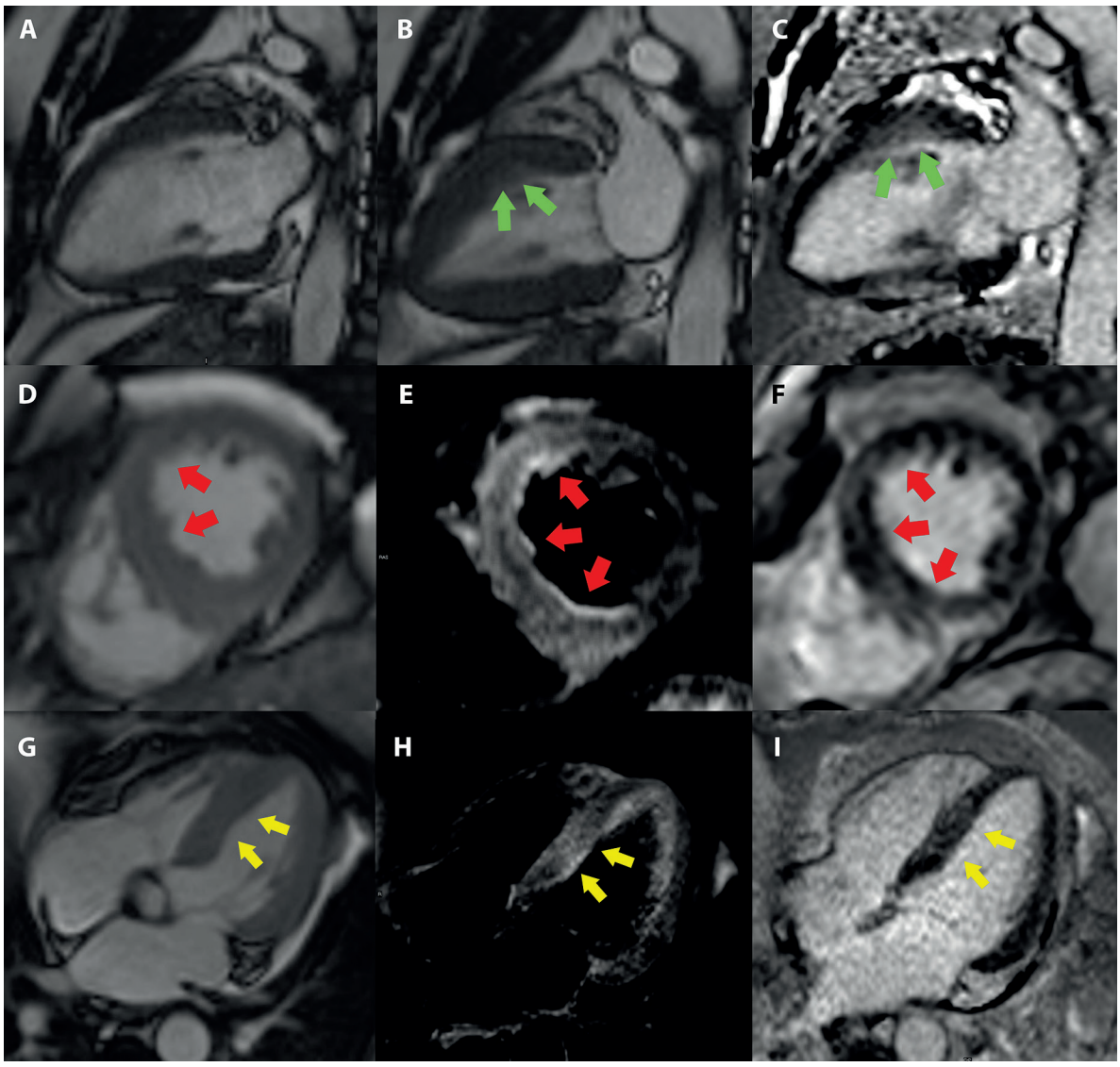

Figure 4 – *Cardiac Magnetic Resonance Findings (CMR). Steady-state free precession (SSFP) cine images were acquired in two-chamber view in diastole (A) and systole (B) and revealed mid anterior segment hypokinesia (green arrows). Phase-sensitive inversion recovery (PSIR) late gadolinium enhancement (LGE) in the same view (C), revealed patchy mid-wall enhancement in mid anterior and mid inferior segments (green arrows). Systolic cine (D), Short-tau inversion recovery (STIR) and PSIR imagens in mid-ventricle short axis view (E and F respectively) demonstrate mid anterior and anteroseptal hypokinesia, transmural oedema (E) and patchy mid-wall LGE (F) in mid anterior, anteroseptal, inferoseptal and inferior segments (red arrows). Four-chamber view systolic cine (G), STIR (H) and PSIR (I) images demonstrated hypokinesia, oedema and patchy mid-wall LGE in mid inferoseptal segment (yellow arrows).*

Sources of Funding

There were no external funding sources for this study.

Study Association

This study is not associated with any thesis or dissertation work.

Ethics Approval and Consent to Participate

This study was approved by the Ethics Committee of the Hospital Sírio Libanês / Sociedade Beneficente de Senhoras under the protocol number 7.226.271. All the procedures in this study were in accordance with the 1975 Helsinki Declaration, updated in 2013. Informed consent was obtained from all participants included in the study.

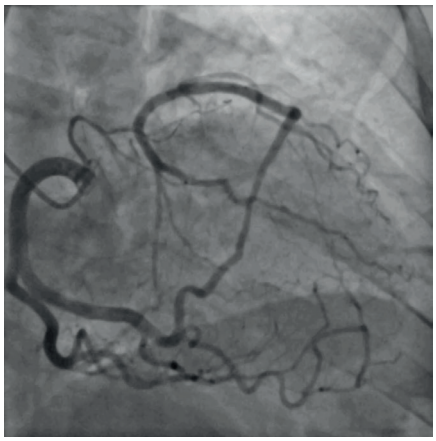

Video S1 – *Percutaneous CA and Left Ventriculography. View: http://abcimaging.org/supplementary-material/2026/3902/ABCImag-2026-0023_video_S1_-_Takotsubo.mp4*

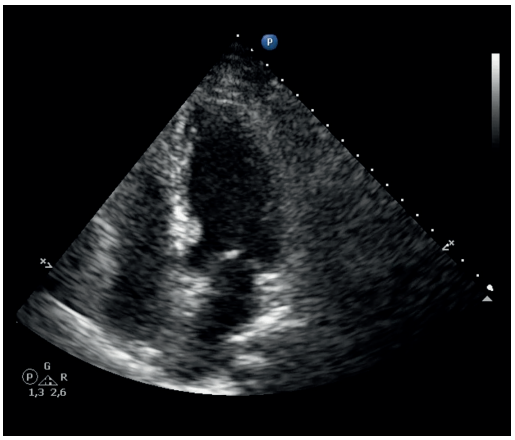

Video S2 – *Transthoracic Echocardiography. View: http://abcimaging.org/supplementary-material/2026/3902/ABCImag-2026-0023_video_S2_-_Takotsubo.mp4*

Use of Artificial Intelligence

The authors did not use any artificial intelligence tools in the development of this work.

Availability of Research Data

The underlying content of the research text is contained within the manuscript.

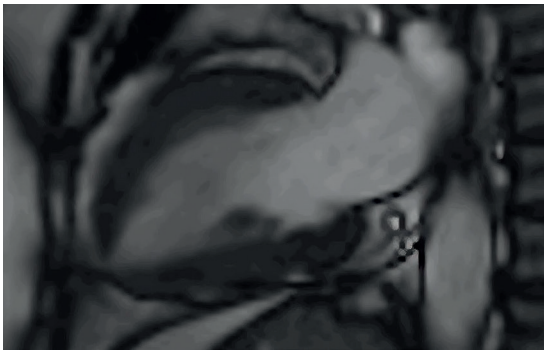

Video S3 – *Cine Cardiac Magnetic Resonance Sequences. View: http://abcimaging.org/supplementary-material/2026/3902/ABCImag-2026-0023_video_S3_-_Takotsubo.mp4*

References

1. Lipton MJ, Barry WH, Obrez I, Silverman JF, Wexler L. Isolated Single Coronary Artery: Diagnosis, Angiographic Classification, and Clinical Significance. Radiology. 1979;130(1):39-47. doi: 10.1148/130.1.39.
2. Taylor AJ, Rogan KM, Virmani R. Sudden Cardiac Death Associated with Isolated Congenital Coronary Artery Anomalies. J Am Coll Cardiol. 1992;20(3):640-7. doi: 10.1016/0735-1097(92)90019-j.
3. Neiva J, Silva MP, Pires-Morais G, Dias A, Ponte M, Caeiro D, et al. Right Single Coronary Artery as an Incidental Finding in Takotsubo Syndrome and Acute Heart Failure: Case Report and Review of the Literature. Rev Port Cardiol. 2019;38(3):215-23. doi: 10.1016/j.repc.2018.06.013.
4. Salazar Marín S, Hanna F, Ramírez N, Valencia JM. Takotsubo Cardiomyopathy and Single Coronary Artery: A Unique Combination. Rev Colomb Cardiol. 2016;23(4):303.e1-303.e6. doi: 10.1016/j.rccar.2015.10.001.
5. Miura S, Manabe O, Naya M, Ando A, Usami A, Miyazaki C, et al. Multimodality Evaluation of Takotsubo Cardiomyopathy in an Isolated Single Coronary Artery Anomaly. J Nucl Cardiol. 2022;29(2):874-80. doi: 10.1007/s12350-020-02312-z.
6. Gräni C, Grunwald C, Windecker S, Siontis GCM. Coronary Artery Anomaly in Takotsubo Cardiomyopathy: Cause or Innocent Bystander? Tex Heart Inst J. 2020;47(1):44-6. doi: 10.14503/THIJ-18-6809.
7. Singh T, Khan H, Gamble DT, Scally C, Newby DE, Dawson D. Takotsubo Syndrome: Pathophysiology, Emerging Concepts, and Clinical Implications. Circulation. 2022;145(13):1002-19. doi: 10.1161/CIRCULATIONAHA.121.055854.
8. Galiuto L, De Caterina AR, Porfidia A, Paraggio L, Barchetta S, Locorotondo G, et al. Reversible Coronary Microvascular Dysfunction: A Common Pathogenetic Mechanism in Apical Ballooning or Tako-Tsubo Syndrome. Eur Heart J. 2010;31(11):1319-27. doi: 10.1093/eurheartj/ehq039.

Giant Atrial Myxoma in a Pregnant Patient: A Case Report

Roberto Ramos Barbosa,[1] Caio Badiani Prando,[1] Victor Macedo Bianchini,[1] Lucas Crespo de Barros,[1] Larissa Novaes Paganini,[1] Gracielly Barros,[1] Darlan Dadalt,[1] Sergio Luis Santos Guedes,[1] Vinicius Eduardo Araújo Costa,[1] Marcus Gustavo Tito,[1] Tiago Bernardo Nery,[1] Marcio Vinicius de Nardi de Angeli,[1] Maria Eduarda Vichi Gomes Viana,[1] Mariana Oliveira Roncato,[1] João Paulo Moulin Auad,[1] Guilherme Freitas Fernandes de Oliveira,[1] Renato Giestas Serpa,[1] Osmar Araujo Calil,[1] Luiz Fernando Machado Barbosa[1]

Hospital da Santa Casa de Misericórdia de Vitória,[1] Vitória, ES – Brazil

Introduction

Atrial myxoma is the most prevalent primary heart tumor.[1,2] Clinical manifestations of myxomas are usually nonspecific, and they may present with dyspnea, fatigue, reduced functional capacity, edema, and, eventually, cerebral embolic events with focal neurological deficits.[3] Although they are classified as benign neoplasms, most commonly located in the left atrium, they can cause obstruction of intracardiac blood flow and, when friable, systemic embolism with consequent tissue ischemia.[2,4]

In spite of higher prevalence in women (65%), diagnosis during pregnancy is considered uncommon, with greater challenges in treatment and an increased risk of fetal death.[5] We report the case of a pregnant patient with a complication of atrial myxoma that manifested during labor.

Case report

A 28-year-old primigravida female patient, who was previously healthy, received low-risk prenatal care in the obstetrics department of a tertiary hospital. Her blood pressure was normal at all appointments, and she used multivitamins and calcium supplements. At the end of the third trimester of pregnancy, she began to report a progressive increase in dyspnea and orthopnea, associated with lower limb edema, without relieving factors.

At gestational age consistent with 37 weeks and 2 days, she was admitted to a routine-risk maternity ward linked to a tertiary hospital, reporting worsening of the symptoms mentioned during prenatal care. Fetal vitality assessment was performed using cardiotocography, which showed signs indicative of fetal compromise, mainly due to fetal bradycardia. The patient was referred to the surgical center for a cesarean section, which proceeded without complications, except for a persistent cough throughout the surgery and bleeding in multiple tissue planes, requiring intraoperative administration of tranexamic acid.

Five hours after the procedure, she developed a seizure of unclear etiology, associated with oliguria and progressive dyspnea, requiring orotracheal intubation due to decreased level of consciousness. She also presented significant periorbital and lower limb edema. On the same day, she was referred to a secondary care hospital due to the unavailability of resources for adequate diagnosis and management at the maternity ward. The electrocardiograms performed did not show any noteworthy alterations. Transthoracic echocardiography identified the presence of a large mass in the left atrium, associated with right heart chamber overload, diffuse right ventricular hypokinesia, and pulmonary hypertension, with estimated pulmonary artery systolic pressure (PASP) of 91 mmHg. The patient was subsequently referred to a tertiary cardiology referral center and cardiac surgery due to suspected mechanical obstruction of blood flow through the mitral valve.

Following successful extubation, she underwent a new transthoracic echocardiogram, which revealed significant left atrial dilation (linear measurement of 47 mm, indexed volume of 62.2 mL/m^2), with the presence of a large mobile mass in the left atrium, which projected into the mitral valve opening during diastole (Figure 1), associated with increased right ventricular dimensions (diastolic diameter of 45 mm), moderate systolic dysfunction, estimated PASP of 100 mmHg and borderline left ventricular systolic function (ejection fraction of 57%, using Simpson's method).

During hospitalization, the patient underwent surgical resection of the mobile mass identified on echocardiography. Through sternotomy and using cardiopulmonary bypass, a left atriotomy was performed with resection of the interatrial septum and identification of a 10-centimeter atrial myxoma (Figure 2) firmly adherent to the ostia of the right pulmonary veins, with a friable texture, which was resected with the right pulmonary vein and part of the left atrial wall. For complete resection, a right atriotomy with atrial septotomy was also necessary due to the extensive adherence of the myxoma. It was necessary to perform reconstruction of the interatrial septum, the left atrial wall, and the pulmonary veins, using a bovine pericardial patch. The procedure was completed without complications, and the surgical specimen was sent for histopathological analysis, which identified a myxoma measuring 10.0 × 8.6 × 3.3 cm and weighing 54 g, without associated malignant processes.

Before hospital discharge, a postoperative follow-up transthoracic echocardiogram was performed, showing a

Keywords

Myxoma; Heart Failure; Thoracic Surgery.

Mailing Address: Roberto Ramos Barbosa •
Hospital da Santa Casa de Misericórdia de Vitória. Rua Dr. João dos Santos Neves, 143. Postal code 29010-430. Vila Rubim, Vitória, ES – Brazil
E-mail: roberto.cardio@gmail.com
Manuscript received February 9, 2026, revised manuscript March 29, 2026, accepted April 29, 2026
Editor responsible for the review: Maria Otto

DOI: https://doi.org/10.36660/abcimg.20260010i

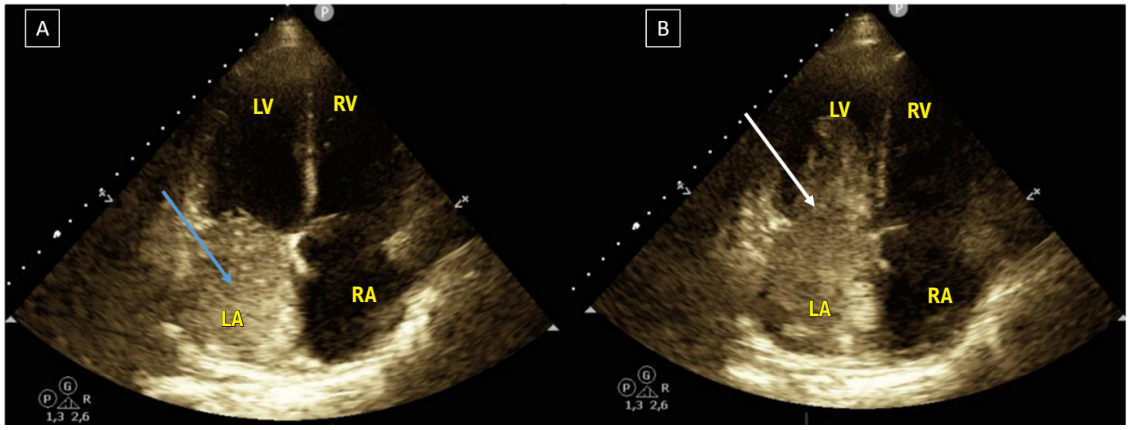

Figure 1 – *Transthoracic echocardiography in apical 4-chamber view. (A) Image suggestive of a mass in the left atrium (white arrow); (B) Image of the same mass projecting into the mitral valve orifice during diastole and occupying the left ventricle (blue arrow). LA: left atrium; LV: left ventricle; RA: right atrium; RV: right ventricle.*

Figure 2 – *Surgical specimen of the atrial myxoma (yellow arrow).*

significant reduction in PASP to 46 mmHg and preserved systolic and diastolic function in both ventricles. The patient was discharged from the hospital on the fourth postoperative day and remained asymptomatic during routine follow-up at the unit's outpatient clinic.

Discussion

Although the clinical picture is considered nonspecific, the symptoms of left atrial myxoma vary according to location, size, and mobility.[6,7] In the reported case, the prolapse of the mass through the mitral valve orifice obstructed the left ventricular inflow tract and pulmonary venous return, raising filling pressures and triggering symptoms of cough and dyspnea, followed by acute pulmonary edema. An oligosymptomatic clinical course was likely misinterpreted as normal progression of pregnancy, with symptom exacerbation at the end of gestation and further worsening during and immediately after surgery.

The most commonly indicated treatment for clinically significant atrial myxomas is complete surgical resection, which presents excellent clinical outcomes and a low incidence of tumor recurrence, especially when accompanied by periodic echocardiographic monitoring.[3,8,9] Various surgical techniques for left atrial myxoma resection, in addition to median sternotomy, have been described and are considered in different services, such as minimally invasive video-assisted surgery via minithoracotomy and right anterolateral minithoracotomy.[8] However, in addition to being indicated in individualized situations, they require a higher level of specialization and availability of specific resources.

In order to ensure a complete surgical approach and better results, intraoperative transesophageal echocardiography is recommended, given that the main goals of surgery also include prevention of tumor recurrence. Risk factors associated with recurrence include incomplete resection, intracardiac implantation, embolization, and intraoperative displacement of tumor material. For this reason, a clear and comprehensive operative field should be considered, in addition to intraoperative echocardiography to confirm the absence of tumor residues.[8]

Pregnancy is a condition in which several modifications occur in the maternal organism in order to ensure optimal fetal development, such as increased cardiac output, increased blood volume, and reduced peripheral vascular resistance.[10] Therefore, it is reasonable to consider whether the adaptations mentioned, especially maternal hypervolemia, may have contributed to our patient's clinical presentation. The hemodynamic changes at the end of pregnancy were added to those of the surgical trauma, culminating in a severe case of acute pulmonary edema, which required orotracheal intubation and initiated the urgent investigation of the cardiovascular abnormality.

We report a rare case of giant atrial myxoma in a pregnant patient, which manifested with typical symptoms of cardiac congestion and acute worsening after cesarean delivery, with a high risk of mortality. This highlights the importance of clinical reasoning and suspicion of possible differential diagnoses, especially given that, from an epidemiological perspective, atrial myxoma is rare during pregnancy, which can hinder diagnosis and delay appropriate treatment.

Author contribution

Research conception and design: Barbosa RR, Prando CB, de Barros LC. Data acquisition: Prando CB, Bianchini VM, Paganini LN, de Barros GR, Dadalt D, Guedes SLS, Costa VEA, Tito MG, Nery TB, de Angeli MVN, Viana MEVG, Roncato MO, Auad JPM. Data analysis and interpretation: Barbosa RR, de Barros LC, Paganini LN, de Barros GR, Dadalt D, Auad JPM, Barbosa LFM. Manuscript writing: Barbosa RR, Prando CB, Bianchini VM. Critical review of the manuscript for important intellectual content: Barbosa RR, de Barros LC, Barbosa LFM.

Author Contributions

Conception and design of the research: Barbosa RR, Prando CB, de Barros LC; acquisition of data: Prando CB, Bianchini VM, Paganini LN, de Barros G, Dadalt D, Guedes SLS, Costa VEA, Tito MG, Nery TB, de Angeli MVN, Viana MEVG, Roncato MO, Auad JPM, Serpa RG, Calil AO; analysis and interpretation of the data: Barbosa RR, de Barros LC, Paganini LN, de Barros G, Dadalt D, Auad JPM, Barbosa LFM; writing of the manuscript: Barbosa RR, Prando CB, Bianchini VM; critical revision of the manuscript for intellectual content: Barbosa RR, de Barros LC, Barbosa LFM.

Potential Conflict of Interest

No potential conflict of interest relevant to this article was reported.

Sources of Funding

There were no external funding sources for this study.

Study Association

This study is not associated with any thesis or dissertation work.

Ethics Approval and Consent to Participate

This study received approval from the Ethics Committee of the Escola Superior de Ciências da Santa Casa de Misericórdia de Vitória (EMESCAM), under protocol number CAAE 93811125.0.0000.5065, opinion number 8.000.875. All procedures involved in this study were conducted in accordance with the 1975 Declaration of Helsinki, updated in 2013.

Use of artificial intelligence

The authors did not use any artificial intelligence tools in the development of this work.

Availability of Research Data

The underlying content of the research text is contained within the manuscript.

References

1. Li Y, Yang W, Liao S, Zuo H, Liu M. Cardiac Myxomas as Great Imitators: A Rare Case Series and Review of the Literature. Heart Lung. 2022;52:182-9. doi: 10.1016/j.hrtlng.2022.01.010.
2. Silva RRP, Magalhães CJ, Silva RSVD, Rocha GAF, Cavalcanti PEF, Montenegro ST. Acute ST-Elevation Myocardial Infarction in a Young Adult: Rare Presentation of Giant Atrial Myxoma. Arq Bras Cardiol. 2024 Apr 22;121(3):e20230538. doi: 10.36660/abc.20230538.
3. Ramcharan P, Katwaroo A, Maharaj M, Seecheran V, Lalchansingh D, Seecheran R, et al. Giant Right Atrial Myxoma Presenting with Right Heart Failure. J Investig Med High Impact Case Rep. 2025;13:23247096251329706. doi: 10.1177/23247096251329706.
4. Marta L, Peres M, Alves M, Silva GF. Giant Left Atrial Myxoma Presenting as Acute Myocardial Infarction. Rev Port Cardiol. 2012;31(12):815-9. doi: 10.1016/j.repc.2012.04.013.
5. John AS, Connolly HM, Schaff HV, Klarich K. Management of Cardiac Myxoma during Pregnancy: A Case Series and Review of the Literature. Int J Cardiol. 2012;155(2):177-80. doi: 10.1016/j.ijcard.2011.05.069.
6. Xue XS, Liang JY, Bao SJ, Ma HF, Zhan B, Liu Y. Cardiac Myxoma: A Report of Two Cases and Review of the Literature. Radiol Case Rep. 2025;21(1):407-13. doi: 10.1016/j.radcr.2025.09.085.
7. Okongwu CC, Olaofe OO. Cardiac Myxoma: A Comprehensive Review. J Cardiothorac Surg. 2025;20(1):151. doi: 10.1186/s13019-024-03333-2.
8. Kavakli AS, Ozturk NK. Determination of Residual Mass in Left Ventricle by Intraoperative Transesophageal Echocardiography after a Giant and Floating Left Atrial Myxoma Resection. Braz J Anesthesiol. 2018;68(5):524-7. doi: 10.1016/j.bjan.2017.10.001.
9. Hernandez N, DiLeo M, Wong CK, Alam M. Sequelae and Surgical Management of Giant Cardiac Myxoma. Tex Heart Inst J. 2025;52(1):e248413. doi: 10.14503/THIJ-24-8413.
10. Avila WS, Alexandre ERG, Castro ML, Lucena AJG, Marques-Santos C, Freire CMV, et al. Brazilian Cardiology Society Statement for Management of Pregnancy and Family Planning in Women with Heart Disease - 2020. Arq Bras Cardiol. 2020;114(5):849-942. doi: 10.36660/abc.20200406.

A Hidden Connection: Anomalous Left Circumflex Artery Arising From the Right Pulmonary Artery Unveiled by Cardiovascular Computed Tomography

Mubariz Ahmed Hassan,[1] *Ashraf Alzahrani,*[1] *Mohammad Mhanna,*[1] *Ola Abdelkarim,*[1] *Rodrigo Bello,*[1] *Paulo Savoia,*[1] *Promporn Suksaranjit,*[1] *Kimberly Delcour*[1]

University of Iowa Hospitals and Clinics,[1] *Iowa, IA – USA*

Introduction

Congenital coronary artery anomalies are uncommon but clinically significant conditions that may present across a broad spectrum, ranging from incidental findings to myocardial ischemia, ventricular arrhythmias, heart failure (HF), and sudden cardiac death (SCD). In adults, anomalous coronary origins may be particularly challenging to recognize because symptoms are often nonspecific and may overlap with more prevalent causes of chest pain, dyspnea, or palpitations.

In rare cases, a coronary artery may originate from the pulmonary arterial circulation, resulting in myocardial perfusion that depends on collateral flow from the remaining coronary arteries arising from the aorta, thereby predisposing the myocardium to ischemia-related electrical instability. Noninvasive anatomical imaging plays a pivotal role in establishing a definitive diagnosis, particularly when conventional angiography is inconclusive.

We report an exceptionally rare case of an anomalous left circumflex artery (LCx) arising from the right pulmonary artery (RPA), identified after invasive coronary angiography failed to selectively engage the LCx. Subsequent cardiovascular computed tomography (CT) precisely delineated the anomalous origin and demonstrated a collateral-dependent perfusion pattern.

Case report

A 48-year-old man with a history of ventricular bigeminy, obstructive sleep apnea, and peripheral edema presented for evaluation of symptomatic premature ventricular contractions (PVCs). Initial ambulatory Holter monitoring demonstrated a high PVC burden (34%), rare atrial ectopy, and episodes of nonsustained supraventricular tachycardia. Transthoracic echocardiography revealed mildly reduced left ventricular (LV) systolic function, with an ejection fraction of 45%-50%. Following initiation of beta-blocker therapy, the patient developed progressive dyspnea, worsening palpitations, and functional limitation, leading to treatment discontinuation.

Coronary angiography was performed because of abnormal stress test findings and concern for underlying myocardial ischemia. During the procedure, selective engagement of the LCx was unsuccessful, raising suspicion for a congenital coronary anomaly. Subsequent cardiovascular CT clearly demonstrated an anomalous origin of the LCx from the RPA, with collateral retrograde perfusion supplied by a dominant right coronary artery (RCA), as shown in Figure 1-4.

This case highlights the critical role of advanced noninvasive imaging in the anatomical characterization of anomalous coronary artery origins, particularly when conventional angiography is inconclusive. Cardiovascular CT provided high-resolution 3D visualization that was essential for accurate diagnosis, risk stratification, and therapeutic planning in a patient initially evaluated for ventricular arrhythmia.

Discussion

Congenital coronary artery anomalies comprise a heterogeneous group of rare but clinically significant malformations, with an overall prevalence < 2% in the general population. Among these anomalies, anomalous origin of the LCx from the RPA is exceptionally rare, with only isolated cases reported in prior research.[1] Although many coronary anomalies remain asymptomatic, anomalous coronary origins may lead to myocardial ischemia, ventricular arrhythmias, HF, or SCD, particularly when myocardial perfusion depends on collateral circulation.

In the present case, the patient's high PVC burden, combined with the inability to selectively engage the LCx during invasive coronary angiography, raised suspicion for an anomalous coronary anatomy. Although invasive angiography remains the reference standard for coronary artery assessment, its diagnostic capability may be limited in cases involving anomalous vessels arising from non-aortic structures.[2] In this context, cardiovascular CT offers substantial advantages, including high spatial resolution, multiplanar reconstruction, and 3D anatomical visualization, all of which are essential for accurately defining anomalous coronary pathways.

Keywords

Coronary Vessels; Pulmonary Artery; X-Ray Computed Tomography; Cardiac Catheterization

Mailing Address: Mubariz Ahmed Hassan •
1000 Oakcrest St. Apt 303. Postal code: 52246. Iowa City, IA - USA.
E-mail: mubariz-hassan@uiowa.edu
Manuscript received April 30, 2026, revised manuscript May 4, 2026, accepted May 4, 2026
Editor responsible for the review: Marcelo Tavares

DOI: https://doi.org/10.36660/abcimg.20260040i

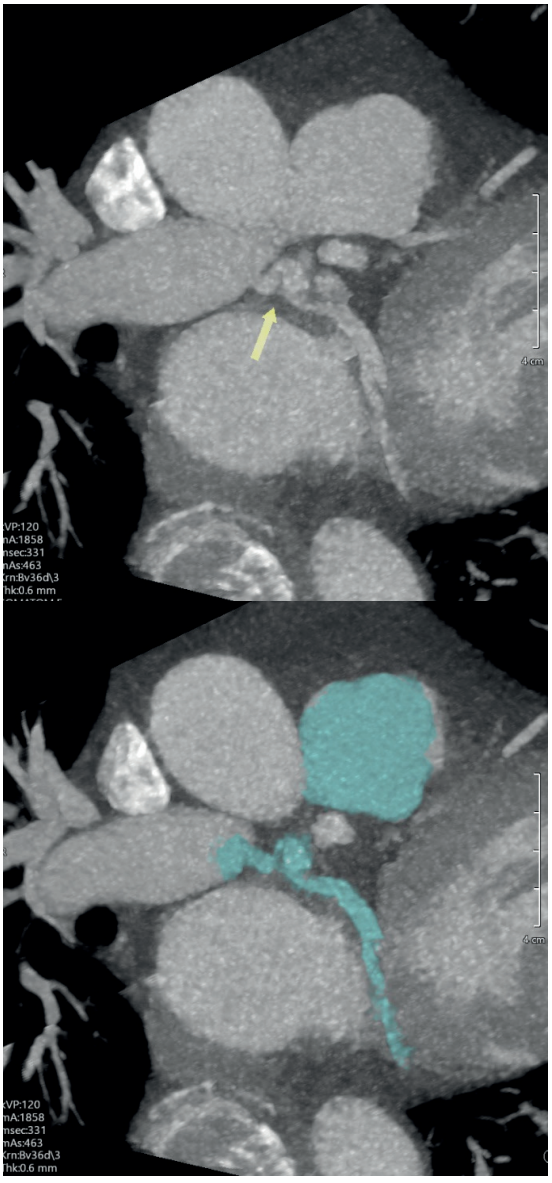

Figure 1 – *Yellow arrow indicating the stump of the RPA from which the LCx originates.*

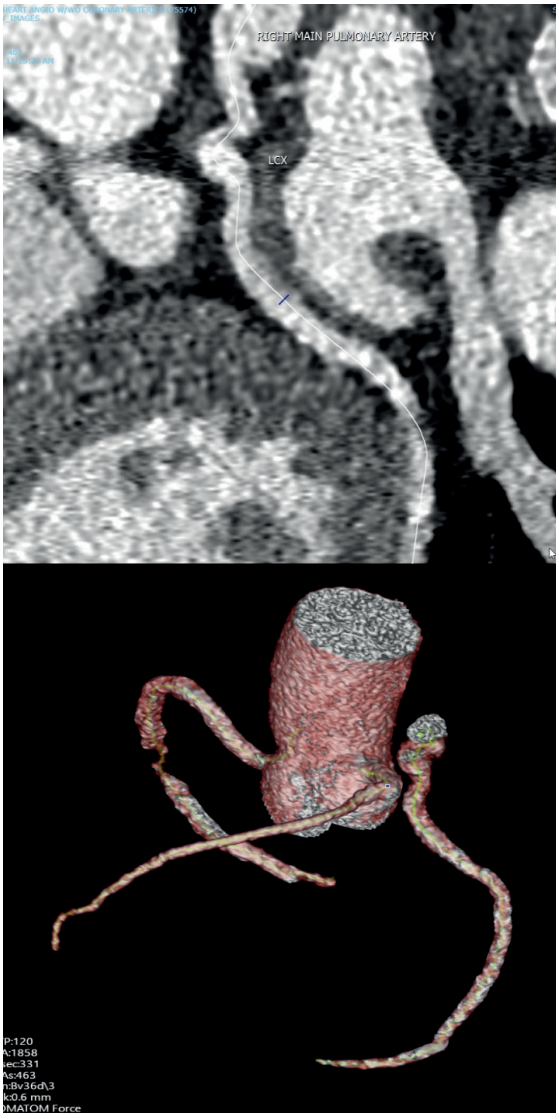

Figure 2 – *3D reconstruction generated using Vitrea software demonstrating the course of the LCx arising from the RPA. The image also shows the aortic root with a separate origin of the LCx from the left coronary cusp.*

In our patient, cardiovascular CT was instrumental not only in confirming the anomalous origin of the LCx from the RPA but also in demonstrating retrograde collateral perfusion from a dominant RCA to the LCx territory. Identification of this anatomy carries important implications for risk stratification, therapeutic decision-making, and long-term clinical management.[3] Furthermore, this case highlights the indispensable role of multimodality imaging in contemporary cardiovascular diagnostics, particularly when conventional techniques are inconclusive or potentially misleading.[4]

From a management perspective, recognition of a coronary artery originating from the pulmonary circulation is critical because treatment decisions are often guided by symptom burden, evidence of myocardial ischemia, ventricular function, arrhythmic profile, and the adequacy of collateral perfusion. Multidisciplinary assessment involving advanced cardiac imaging specialists, interventional cardiologists, electrophysiologists, and cardiothoracic surgeons may be necessary to individualize management strategies, which can range from clinical surveillance and functional evaluation to surgical or percutaneous intervention in selected high-risk cases. In this patient, advanced cardiovascular CT served as the definitive imaging modality for characterization of a rare congenital coronary anomaly initially investigated in the context of ventricular arrhythmia, underscoring the transformative role of noninvasive imaging in modern cardiovascular medicine.

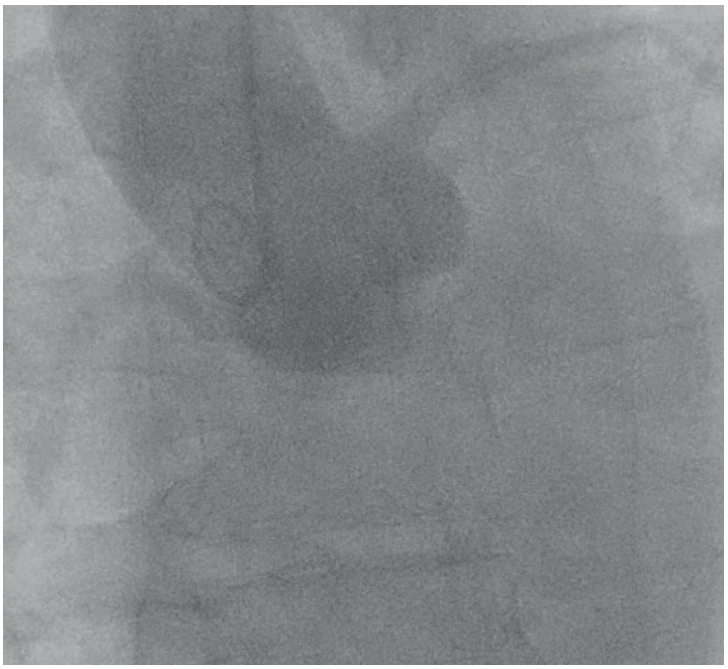

Figure 3 – *Aortography demonstrating the ostia of the left main coronary artery and RCA. No ostium of the LCx is identified.*

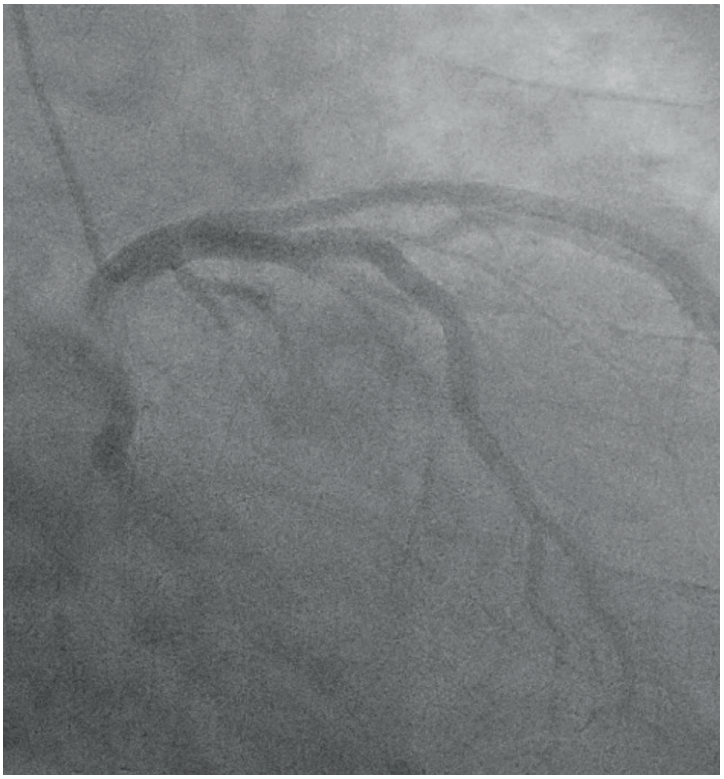

Figure 4 – *Right anterior oblique caudal projection demonstrating the left coronary system, including the left anterior descending artery and a large first diagonal branch, without visualization of the LCx.*

Conclusion

Anomalous origin of the LCx from the RPA is an exceptionally rare but clinically relevant congenital coronary anomaly, particularly in patients presenting with ventricular arrhythmias, LV dysfunction, or suspected myocardial ischemia. When invasive coronary angiography is nondiagnostic, especially in cases in which the LCx cannot be selectively engaged, cardiovascular CT may serve as the definitive imaging modality for accurate delineation of coronary origin and collateral perfusion patterns. Precise anatomical characterization is essential for appropriate diagnosis, risk stratification, and individualized management planning.

Author Contributions

Conception and design of the research: Hassan MA, Savoia P, Delcour K; acquisition of data: Hassan MA, Alzahrani A, Mhanna M, Abdelkarim O, Savoia P, Suksaranjit P, Delcour K; analysis and interpretation of the data and critical revision of the manuscript for intellectual content: Hassan MA, Alzahrani A, Mhanna M, Abdelkarim O, Bello R, Savoia P, Suksaranjit P, Delcour K; writing of the manuscript: Hassan MA, Abdelkarim O, Bello R, Savoia P, Delcour K.

Potential Conflict of Interest

No potential conflict of interest relevant to this article was reported.

Sources of Funding

There were no external funding sources for this study.

Study Association

This study is not associated with any thesis or dissertation work.

Ethics Approval and Consent to Participate

This article does not contain any studies with human participants or animals performed by any of the authors.

Use of Artificial Intelligence

The authors did not use any artificial intelligence tools in the development of this work.

Availability of Research Data

The underlying content of the research text is contained within the manuscript.

References

1. Faria B, Calvo L, Ribeiro S, Ruivo C, Lourenço A. Anomalous Origin of the Circumflex Coronary Artery from the Right Pulmonary Artery: Diagnosis Through Cardiac CT. Arq Bras Cardiol. 2021;117(1 suppl 1):8-11. doi: 10.36660/abc.20200060.
2. Korosoglou G, Ringwald G, Giannitsis E, Katus HA. Anomalous Origin of the Left Circumflex Coronary Artery from the Pulmonary Artery. A Very Rare Congenital Anomaly in an Adult Patient Diagnosed by Cardiovascular Magnetic Resonance. J Cardiovasc Magn Reson. 2008;10(1):4. doi: 10.1186/1532-429X-10-4.
3. Vergara-Uzcategui CE, Urquiza RV, Salinas P, Núñez-Gil IJ. Anomalous Origin of Left Circumflex Artery from the Right Pulmonary Artery of an Adult. REC Interv Cardiol. 2021;3(1):65-72. doi: 10.24875/RECICE.M20000128.
4. Harky A, Bashir M, Garner M, Hsia T. Anomalous Origin of the Circumflex Coronary Artery Presenting with Ventricular Fibrillation Cardiac Arrest. BMJ Case Rep. 2017;2017:bcr2016219184. doi: 10.1136/bcr-2016-219184.

Recurrent Intracardiac Masses in an Orthotopic Heart Transplant Recipient

Bilal Saeed,[1] Natdanai Punnanithinont,[2] Shareef Mansour,[3] Paulo Savoia,[1] Promporn Suksaranjit[1]

University of Iowa Health Care,[1] Iowa City, Iowa – USA
Harbor-UCLA Medical Center,[2] Torrance, Califórnia – USA
University of Texas,[3] Galveston, Texas – USA

Introduction

As long-term survival improves among heart transplant recipients, rare post-transplant complications, including intracardiac masses, are being increasingly recognized.[1]

Severe left atrial (LA) dilation and atrial arrhythmias may further contribute to blood stasis and thrombus formation in transplant recipients. LA thrombi in these patients may mimic neoplastic masses and represent important diagnostic and therapeutic challenges.[2] Contributing factors include atrial dilation, arrhythmias, foreign material, and the components of Virchow's triad, namely abnormal blood flow, endothelial injury, and hypercoagulability.[3,4]

We report a unique case of a heart transplant recipient who developed recurrent LA thrombi over a 15-year period, requiring surgical resection, long-term anticoagulation, and complex therapeutic decision-making due to bleeding complications.

Case report

A 73-year-old man with a history of orthotopic heart transplantation (OHT) with bicaval anastomosis, performed in 2002 at an outside academic institution, established cardiovascular care at our institution in 2009. During outpatient follow-up, an incidental LA mass was identified on transthoracic echocardiography (TTE). The mass measured 5.5 × 5.1 × 4.3 cm and was located along the posterolateral wall of the LA. The patient was asymptomatic at the time of diagnosis. His medical history was significant for sick sinus syndrome requiring dual-chamber pacemaker implantation, nonobstructive coronary allograft vasculopathy, and monoclonal gammopathy of undetermined significance.

Annual TTE surveillance over the following 7 years demonstrated progressive enlargement of the mass, reaching a maximum size of 7.9 × 6.2 cm. Cardiac computed tomography (CCT) (Figure 1) confirmed the presence of two large LA masses. The first mass originated from the posterolateral wall, with partial calcification and extension through the atrial wall. The second mass arose from the roof of the LA.

After 7 years of imaging surveillance, the patient underwent redo sternotomy with surgical resection of both masses. Histopathological analysis of the first mass demonstrated fibrinopurulent debris with focal dystrophic calcifications, whereas the second mass was confirmed to be thrombotic material. Grocott methenamine silver, periodic acid-Schiff, and Gram staining were all negative. An old epicardial defibrillator pad was also identified, along with an associated thrombus within the pericardial space, which was surgically excised.

The patient was admitted with hypertensive urgency 1 year later. On presentation, blood pressure was 185/112 mmHg, heart rate was 88 beats/min, SpO_2 was 98% on room air, and body temperature was normal. Electrocardiography demonstrated normal sinus rhythm with right bundle branch block. During hospitalization, repeat TTE demonstrated recurrence of a mass in the posterolateral LA measuring 3.7 × 4.1 cm. The lesion appeared homogeneous and broadly attached to the atrial wall, findings considered consistent with thrombus formation. Anticoagulation with

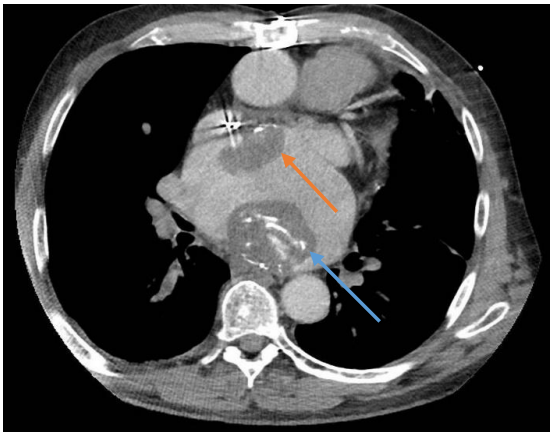

Figure 1 – *CCT demonstrating two LA masses. The larger mass (blue arrow) measured 8 × 6 × 5 cm and exhibited smooth borders with layered calcification. The smaller mass (orange arrow) measured 6 × 5 × 3 cm and was attached to the superior and medial aspects of the left atrium.*

Keywords

Heart Transplant; Left atrial; Heart Atria; Cardiac MRI; X-Ray Computed Tomography

Mailing Address: Bilal Saeed •
University of Iowa Health Care. 200 Hawkins Drive. Postal code: 52242-1007. Iowa City, Iowa – USA
E-mail: bilal-saeed@uiowa.edu
Manuscript received April 24, 2026, revised manuscript April 29, 2026, accepted April 29, 2026
Editor responsible for the review: Marcelo Tavares

DOI: https://doi.org/10.36660/abcimg.20260031i

warfarin was initiated, resulting in complete resolution of the mass 1 year later.

After 4 years of anticoagulation therapy, the patient developed persistent atrial flutter, which was initially managed medically. An additional 2 years later, he underwent electrical cardioversion. Shortly thereafter, he was hospitalized because of a large spontaneous right retroperitoneal hemorrhage and subsequently underwent right renal artery embolization, followed by discontinuation of warfarin therapy. His clinical course was further complicated by acute kidney injury requiring permanent dialysis.

After hospital discharge, routine TTE demonstrated recurrence of a mass along the roof of the LA measuring 7.3 × 6.3 cm. Cardiac magnetic resonance (CMR) was subsequently performed (Figures 2 and 3), revealing severe LA dilation and a large heterogeneous broad-based mass attached to the LA roof, measuring 7.9 × 7.1 × 6.1 cm. A second mass was identified within the pericardial space adjacent to the lateral wall, measuring 4.0 × 1.2 × 3.0 cm. No enhancement was observed on first-pass perfusion or late gadolinium enhancement (LGE) imaging (Figure 4), findings that favored thrombi rather than neoplastic lesions. Consequently, warfarin therapy was resumed.

Following another 8 months, the patient experienced progressive clinical deterioration, including worsening mental status. He ultimately elected hospice care and died several weeks later. Autopsy was declined.

Discussion

Advances in immunosuppressive therapy and surgical techniques have substantially improved long-term survival after heart transplantation.[5] Intracardiac masses remain a rare complication following OHT, and when present, they are typically identified within the first 1-2 years after surgery.[1] The most common intracardiac masses in this population include organizing thrombi and primary cardiac tumors, particularly myxomas.[2] However, differentiating among the various etiologies of intracardiac masses remains a significant diagnostic challenge and often requires a multimodality imaging approach.

The present case illustrates the unusual occurrence of recurrent thrombi in a patient who underwent OHT using the bicaval technique. Serial annual TTE examinations demonstrated progressive enlargement of the LA mass over several years before surgical resection. Additional imaging modalities, including CCT and CMR, played a critical role in anatomical characterization, as TTE alone could not reliably distinguish among thrombus, tumor, or foreign-body-associated lesions.

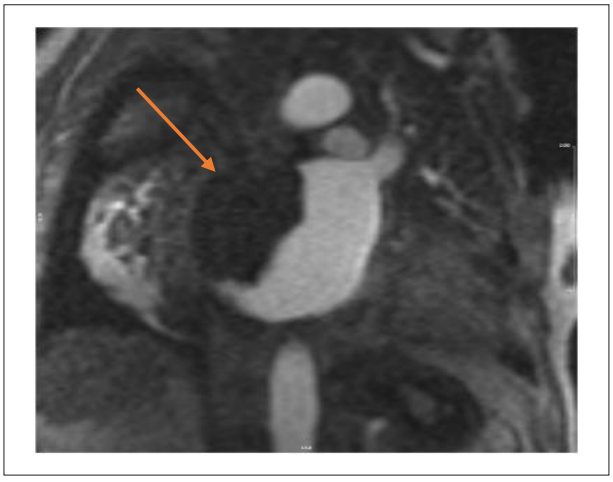

Figure 2 – *CMR first-pass perfusion imaging (two-chamber view) demonstrating a hypointense mass attached to the roof of the left atrium with a broad-based attachment and no contrast perfusion. The mass measured 7.9 × 7.1 × 6.1 cm.*

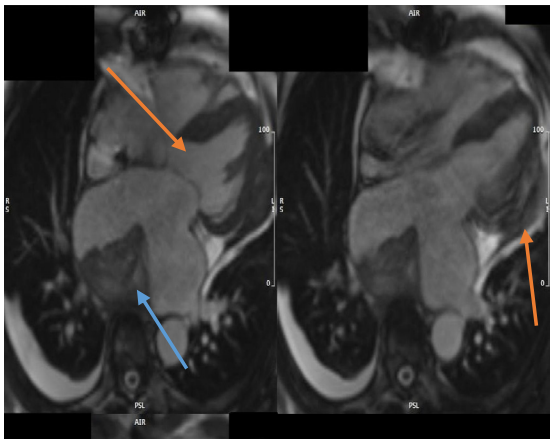

Figure 3 – *CMR cine steady-state free precession sequence (four-chamber view) demonstrating a mass within the pericardial space (orange arrow) adjacent to the lateral wall of the left ventricle, measuring 6.3 × 2.0 cm, along with a large broad-based LA mass (blue arrow) measuring 7.9 × 7.1 × 6.1 cm and exhibiting heterogeneous signal intensity.*

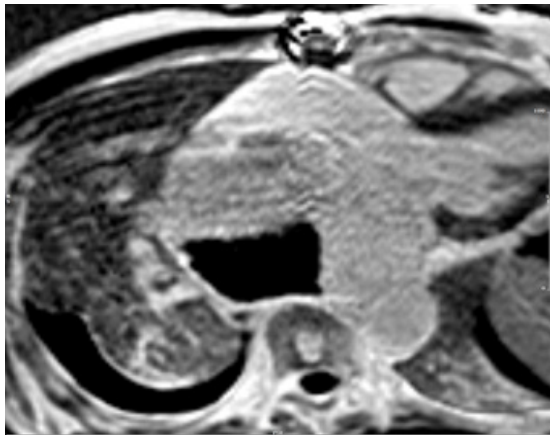

Figure 4 – *High-T1 LGE CMR (three-chamber view) demonstrating a hypointense LA mass with an etched appearance.*

In this patient, the initial large LA mass containing fibrinopurulent debris and dystrophic calcification may have represented a reactive process related to the retained epicardial defibrillator pad, contributing to stagnant intra-atrial blood flow in accordance with Virchow's triad.[3] Denudation of the extracellular matrix may promote conduction abnormalities, fibrosis, and endocardial infiltration, thereby facilitating thrombogenesis.[4]

The standard biatrial OHT technique, originally popularized by Shumway and colleagues because of its technical simplicity and shorter ischemic times, may result in anatomical and physiological alterations, including enlarged atrial chambers, blood stasis, atrial thrombosis, and valvular regurgitation. Consequently, the bicaval anastomotic technique was developed to better preserve atrial geometry, reduce atrial arrhythmias, and minimize asynchronous contraction between donor and recipient atrial tissue, all of which may contribute to thrombus formation.[6] Despite these theoretical advantages, our patient developed recurrent LA and pericardial thrombi even after removal of the retained surgical material and epicardial defibrillator pad.

Only a limited number of cases describing atrial thrombi confirmed by surgical resection and histopathological examination have been reported in patients undergoing bicaval OHT.[2,7-9]

CMR is particularly valuable for differentiating thrombus from cardiac tumors through tissue characterization. Imaging features favoring thrombus include absence of first-pass perfusion, lack of LGE, low signal intensity on delayed enhancement sequences, and the presence of a layered or "etched" appearance.[10-12]

Conclusion

We report a rare case of recurrent LA thrombi in an asymptomatic patient who underwent bicaval OHT. The mass was incidentally detected and demonstrated progressive enlargement over a 7-year period. Multimodality imaging, particularly CCT and CMR, was essential for diagnostic assessment, as TTE alone could not reliably differentiate thrombus from neoplasm or foreign-body-associated lesions.

The initial mass may have been associated with a retained epicardial defibrillator pad, which likely contributed to blood stasis and thrombus formation. Despite surgical resection, thrombus recurrence occurred within months, highlighting the persistent thrombotic risk in this population, even in the absence of atrial arrhythmias.

This case emphasizes the importance of multimodality imaging, histopathological confirmation when feasible, individualized anticoagulation strategies, and long-term surveillance in heart transplant recipients with intracardiac masses. Further studies are needed to better define thrombotic risk factors and optimal anticoagulation duration following bicaval OHT.

Author Contributions

Writing of the manuscript: Saeed B, Punnanithinont N; critical revision of the manuscript for intellectual content: Mansour S, Savoia P; chief author: Suksaranjit P.

Potential Conflict of Interest

No potential conflict of interest relevant to this article was reported.

Sources of Funding

There were no external funding sources for this study.

Study Association

This study is not associated with any thesis or dissertation work.

Ethics Approval and Consent to Participate

This article does not contain any studies with human participants or animals performed by any of the authors.

Use of Artificial Intelligence

The authors did not use any artificial intelligence tools in the development of this work.

Availability of Research Data

The underlying content of the research text is contained within the manuscript.

References

1. Velleca A, Shullo MA, Dhital K, Azeka E, Colvin M, DePasquale E, et al. The International Society for Heart and Lung Transplantation (ISHLT) Guidelines for the Care of Heart Transplant Recipients. J Heart Lung Transplant. 2023;42(5):e1-e141. doi: 10.1016/j.healun.2022.10.015.
2. Hale A, Vann J, Henderson P, Harrison T, Trehan S. A Case of a Left Atrial Mass in an Orthotopic Heart Transplant Recipient. CASE. 2019;4(1):33-8. doi: 10.1016/j.case.2019.10.011.
3. Lowe GD. Virchow's Triad Revisited: Abnormal Flow. Pathophysiol Haemost Thromb. 2003;33(5):455-7. doi: 10.1159/000083845.
4. Yamashita T. Virchow Triad and Beyond in Atrial Fibrillation. Heart Rhythm. 2016;13(12):2377-8. doi: 10.1016/j.hrthm.2016.09.007.
5. Lund LH, Khush KK, Cherikh WS, Goldfarb S, Kucheryavaya AY, Levvey BJ, et al. The Registry of the International Society for Heart and Lung Transplantation: Thirty-fourth Adult Heart Transplantation Report-2017; Focus Theme: Allograft Ischemic Time. J Heart Lung Transplant. 2017;36(10):1037-46. doi: 10.1016/j.healun.2017.07.019.
6. Dell'Aquila AM, Mastrobuoni S, Bastarrika G, Praschker BL, Agüero PA, Castaño S, et al. Bicaval versus Standard Technique in Orthotopic Heart Transplant: Assessment of Atrial Performance at Magnetic Resonance and Transthoracic Echocardiography. Interact Cardiovasc Thorac Surg. 2012;14(4):457-62. doi: 10.1093/icvts/ivr084.
7. Neuman Y, Tolstrup K, Blanche C, Luthringer D, Kobal S, Miyamoto T, et al. Pseudomyxoma Originating from the Interatrial Septum in a Heart Transplant Patient. J Am Soc Echocardiogr. 2005;18(7):e1. doi: 10.1016/j.echo.2004.09.014.

8. Yousefzai R, Trivedi S, Jain R, Cheema OM, Crouch JD, Thohan V, et al. Expecting the Unexpected: Right Atrial Mass in a Transplant Patient. ESC Heart Fail. 2015;2(4):164-7. doi: 10.1002/ehf2.12065.

9. Bartus K, Litwinowicz R, Kapelak B, Filip G, Wierzbicki K, Lee RJ. Giant Left Atrium Associated with Massive Thrombus Formation 14 Years after Orthotopic Heart Transplantation. Braz J Cardiovasc Surg. 2020;35(6):1010-2. doi: 10.21470/1678-9741-2018-0390.

10. Motwani M, Kidambi A, Herzog BA, Uddin A, Greenwood JP, Plein S. MR Imaging of Cardiac Tumors and Masses: A Review of Methods and Clinical Applications. Radiology. 2013;268(1):26-43. doi: 10.1148/radiol.13121239.

11. Weinsaft JW, Kim HW, Shah DJ, Klem I, Crowley AL, Brosnan R, et al. Detection of Left Ventricular Thrombus by Delayed-Enhancement Cardiovascular Magnetic Resonance Prevalence and Markers in Patients with Systolic Dysfunction. J Am Coll Cardiol. 2008;52(2):148-57. doi: 10.1016/j.jacc.2008.03.041.

12. Araoz PA, Eklund HE, Welch TJ, Breen JF. CT and MR Imaging of Primary Cardiac Malignancies. Radiographics. 1999;19(6):1421-34. doi: 10.1148/radiographics.19.6.g99no031421.

Dilated Cardiomyopathy as a Rare Initial Manifestation of ANCA-positive Microscopic Polyangiitis: Case Report

Karoline Gonzaga Costa,[1] *Maria Estefânia Bosco Otto,*[2] *André Felipe Lobão Fernandes,*[1] *Nathália de Macêdo Assunção,*[1] *Mariana Ubaldo Barbosa Paiva,*[2] *Rosyane Luz Rufino de Lima,*[1] *Rita Mikelle Soares Dias*[1]

Hospital Universitário de Brasilia, Brasília,[1] *DF – Brasil*

Universidade de Brasilia,[2] *Brasília, DF – Brasil*

Introduction

Antineutrophil cytoplasmic antibody (ANCA)-associated vasculitis constitute a group of systemic small-vessel inflammatory diseases characterized by pauci-immune necrotizing vasculitis and multisystem involvement, including granulomatosis with polyangiitis (GPA), eosinophilic granulomatosis with polyangiitis (EGPA), and microscopic polyangiitis (MPA).[1-4] MPA is classically associated with rapidly progressive glomerulonephritis and alveolar hemorrhage, conditions that carry high morbidity and mortality when not promptly recognized and treated.[1,4]

In addition to predominant renal and pulmonary involvement, there is growing evidence that patients with ANCA-associated vasculitis have an increased cardiovascular risk, related not only to traditional factors but also to disease-specific mechanisms such as persistent inflammation, endothelial dysfunction, and accelerated atherosclerosis.[5-8] Studies suggest a higher incidence of major cardiovascular events (myocardial infarction, stroke, and heart failure) compared with the general population.[6]

Cardiac involvement, although more frequently described in EGPA and GPA, can also occur in MPA, manifesting as myocarditis, pericarditis, coronary or microvascular vasculitis, and ventricular dysfunction.[9,10] Imaging modalities, including echocardiography with myocardial deformation analysis (global longitudinal strain – GLS), can detect subclinical abnormalities and contribute to prognostic stratification, reinforcing the importance of systematic cardiologic evaluation in these patients.[11] Despite recognition of the increased cardiovascular risk, myocardial involvement in MPA remains underdiagnosed and poorly characterized, particularly regarding GLS-detectable deformation patterns and their clinical implications.

Keywords

Microscopic Polyangiitis; Anti-Neutrophil Cytoplasmic Antibody-Associated Vasculitis; Dilated Cardiomyopathy; Echocardiography

Mailing Address: Karoline Gonzaga Costa •
Hospital Universitário de Brasília. Quadra 204, Lt 06, Bl B, Apto 403. Postal code: 71939-540. Águas Claras, Brasília, DF – Brazil
E-mail: kkgcosta@hotmail.com
Manuscript received March 30, 2026, revised manuscript April 6, 2026, accepted April 15, 2026
Editor responsible for the review: Marcelo Tavares

DOI: https://doi.org/10.36660/abcimg.20260038i

In this context, the aim of this report is to describe a case of dilated cardiomyopathy with severe systolic dysfunction in a young patient with MPA, highlighting the finding of an apical sparing GLS pattern and its diagnostic and follow-up implications.

This case report was approved on March 7, 2026, by the Institutional Research Ethics Committee under Opinion No. 8,265,839 and CAAE 94929525.6.0000.5558, with written informed consent obtained from the patient.

Case Report

A 28-year-old male patient, previously healthy, developed an acute respiratory syndrome in June 2024, initially treated in the outpatient setting as community-acquired pneumonia. In the following weeks, he progressed with cough, hemoptysis, worsening dyspnea, exercise intolerance, lower-limb edema, foamy urine, and hematuria.

Upon hospital admission, he presented with severe anemia (hemoglobin 4.4 g/dL) and acute kidney injury requiring renal replacement therapy (creatinine 8.63 mg/dL; urea 244 mg/dL; potassium 7.1 mEq/L), in addition to hematuria and proteinuria. Chest radiography showed diffuse pulmonary infiltrates and cardiomegaly. Hemodialysis was initiated.

Etiologic investigation revealed positive p-ANCA and a renal biopsy consistent with pauci-immune crescentic glomerulonephritis, confirming the diagnosis of MPA (Figure 1). Pulse therapy with methylprednisolone was administered, followed by three cycles of cyclophosphamide, with clinical improvement.

In November 2024, transthoracic echocardiography (TTE) demonstrated dilated cardiomyopathy with diffuse hypokinesia and severe systolic dysfunction (ejection fraction 26%), with no other evident etiologies. In February and April 2025, he continued to present systolic dysfunction during hospitalizations for infection. The electrocardiogram showed left-sided chamber overload (Figure 2). GLS analysis revealed an apical sparing pattern (Figure 3). Additional findings included moderate functional mitral regurgitation and a small pericardial effusion, along with right ventricular dysfunction (Video 1). The patient is currently under outpatient follow-up in the Cardiology Department of the University Hospital of Brasília, receiving optimized treatment for heart failure with reduced ejection fraction, remaining in functional class II (NYHA), with ongoing clinical and serial echocardiographic monitoring. The case timeline is summarized in Table 1.

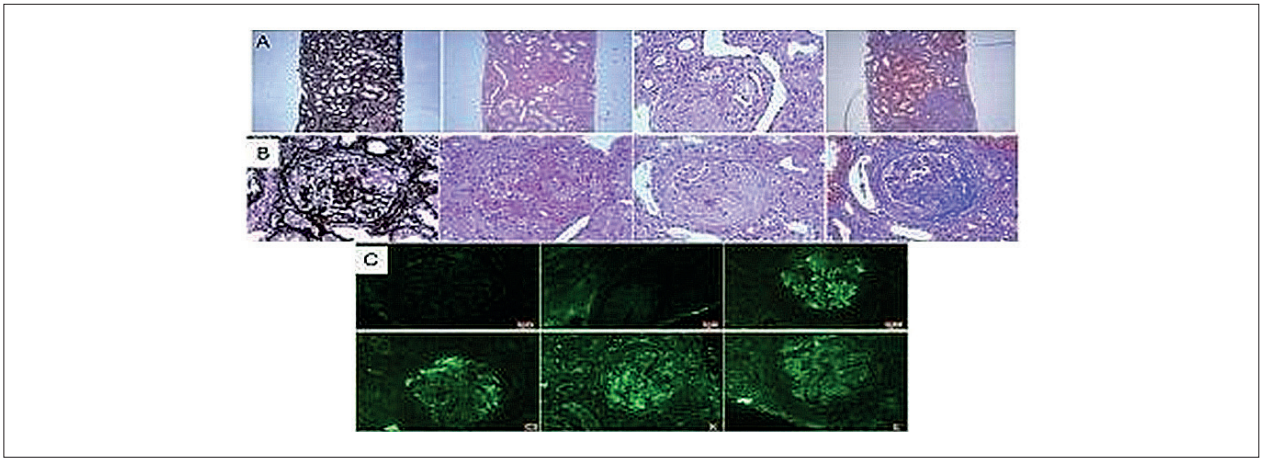

Figure 1 – *Renal biopsy: (A) Tubulointerstitial compartment showing interstitial fibrosis, tubular atrophy, and monocyte infiltration; (B) Sclerotic glomeruli and/or glomeruli with proliferative/necrotizing crescentic lesions; (C) Negative immunofluorescence for light chains and immunoglobulins.*

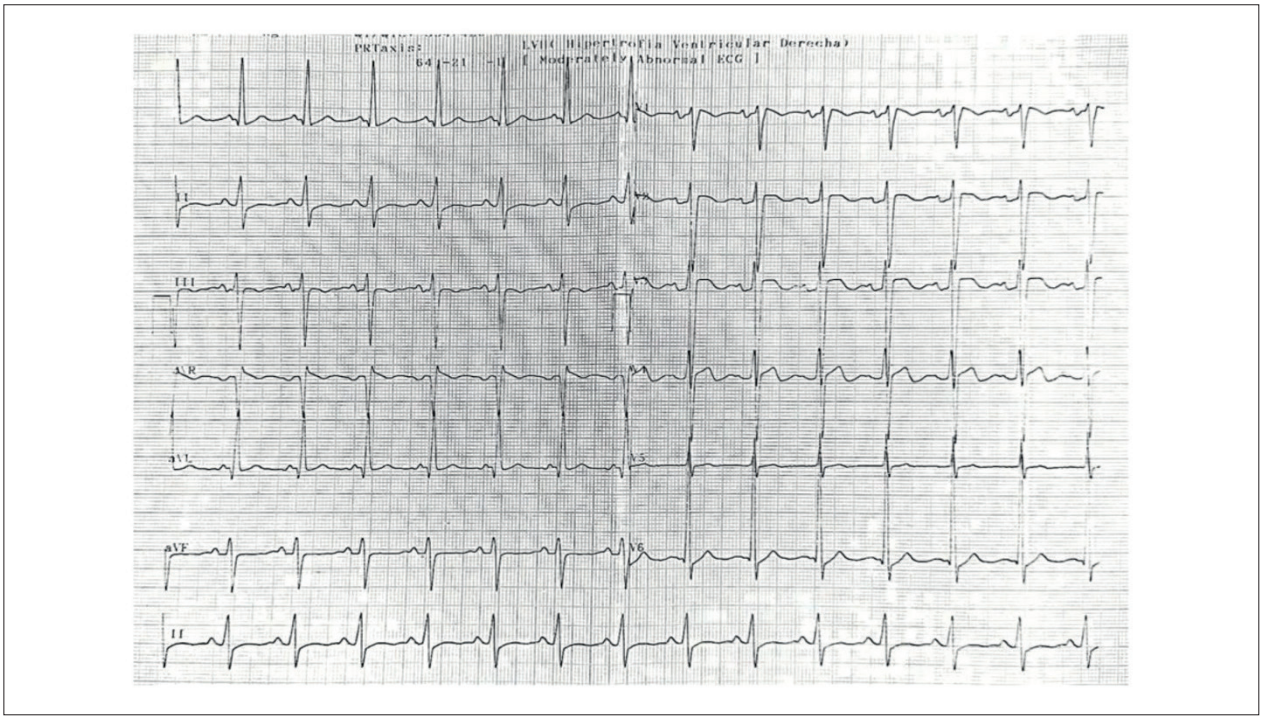

Figure 2 – *Electrocardiogram showing left-sided chamber overload.*

Discussion

Cardiac involvement in ANCA-associated vasculitis is heterogeneous and has historically been more frequently recognized in EGPA, followed by GPA, and considered rare in MPA.[4,9,10] However, its true frequency may be underestimated, as myocardial manifestations can be asymptomatic or attributed to comorbidities, renal dysfunction, or metabolic effects of corticosteroid therapy.[7,8] Recent studies highlight the prognostic impact of cardiovascular involvement and support the need for a proactive approach to screening and follow-up.[5,6]

From a pathophysiological standpoint, ANCA-mediated neutrophil activation promotes diffuse endothelial injury, microvascular inflammation, and possible direct myocardial involvement, favoring functional microvascular ischemia, myocarditis, and progressive ventricular remodeling.[2,12] In MPA, the dilated cardiomyopathy described in case reports and small series has been attributed predominantly to diffuse microvascular inflammation and/or subclinical myocarditis,

which may coexist with hypertension and volume overload in patients with renal dysfunction.[9,11]

In the present case, the identification of severe systolic dysfunction in a young patient, without evidence of coronary artery disease, viral infectious etiology, or drug toxicity, reinforces the plausibility of a causal relationship with MPA.[9] Echocardiography demonstrated not only dilation and diffuse hypokinesia but also a marked reduction in GLS, with an apical sparing pattern characterized by a basal-to-apical deformation gradient, in which the basal segments show greater strain reduction compared with the apical segments, resulting in relative preservation of apical deformation.

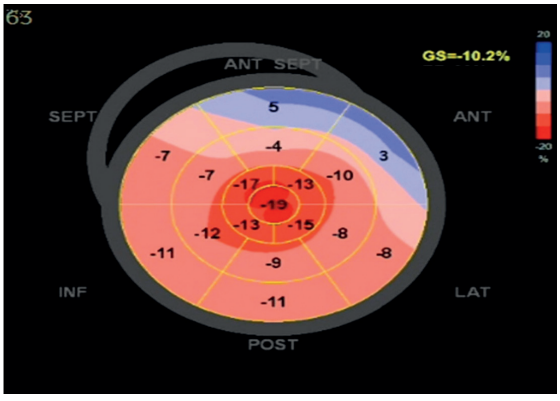

Figure 3 – *Transthoracic echocardiogram: polar map of left ventricular GLS showing reduced strain with an apical sparing pattern.*

The incorporation of GLS as a complementary tool to ejection fraction is supported by the Position Statement of the Department of Cardiovascular Imaging, which recommends its use for early detection of myocardial dysfunction and for serial follow-up, highlighting its incremental value in clinical practice. In alignment with this, international consensus documents also endorse the clinical relevance of GLS. Although this pattern is classically associated with cardiac amyloidosis, it is not pathognomonic and must be interpreted in the context of the clinical presentation and other imaging findings.[11,13-15]

In terms of differential diagnosis, the apical sparing pattern on GLS should be understood as a suggestive but nonspecific sign, most commonly observed in cardiac amyloidosis, but also described in other conditions (e.g., ventricular hypertrophy, pressure-overload cardiomyopathies, chronic kidney disease, and some forms of myocarditis).[11,16] Thus, in the absence of structural findings typical of infiltrative cardiomyopathy, interpretation should integrate conventional echocardiographic parameters (wall thickness, filling pattern, chamber dimensions, right ventricular function, and valvular disease), biomarkers,

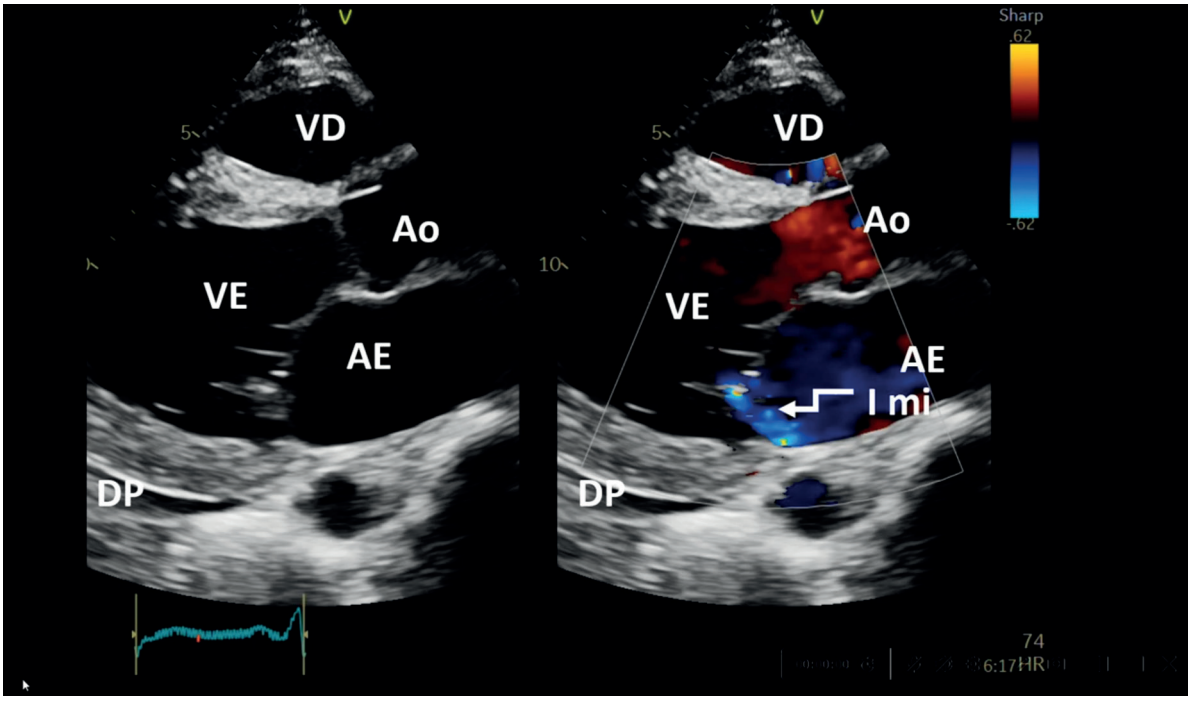

Video 1 – *Transthoracic echocardiogram showing severe left ventricular systolic dysfunction, moderate right ventricular dysfunction, functional mitral regurgitation, and GLS with an apical. View: http://abcimaging.org/supplementary-material/2026/3902/ABCImag-2026-0038_RC_Video_MPA.mp4*

Table 1 – Timeline of clinical events, examinations, and interventions

Date	Main clinical event	Examinations/interventions
Jun/2024	Acute respiratory syndrome	Outpatient treatment for pneumonia
Jul/2024	Pulmonary–renal syndrome and heart failure; dialysis dependent AKI	Hemodialysis initiated on 07/01/2024; chest X ray showing cardiomegaly and diffuse infiltrates
Aug/2024	Diagnostic confirmation	Positive p ANCA; renal biopsy on 08/31/2024 (pauci immune)
Sep/2024	Remission induction	Pulse therapy with methylprednisolone + cyclophosphamide (3 cycles)
Oct/2024	Hospital discharge	Follow up with Nephrology
Nov/2024	Cardiology diagnosis	Echocardiogram: dilated cardiomyopathy
Feb/2025	Hospitalization for infection; start of cardiology follow up	Therapy for HFrEF
Apr/2025	Persistence of dysfunction	Echocardiogram/strain: GLS –10% with apical sparing
Follow up	Clinical stability	Functional class II (NYHA); therapeutic optimization

IAKI: acute kidney injury; ANCA: antineutrophil cytoplasmic antibodies; HFrEF: heart failure with reduced ejection fraction; NYHA: New York Heart Association.

and – when available – cardiac magnetic resonance (CMR) for assessment of edema and fibrosis (LGE/T1/ECV), thereby reducing the risk of false positives and guiding follow-up.[11,17]

The practical message of this case highlights the importance of a cardiovascular imaging–based approach. In the setting of ANCA-associated vasculitis with possible myocardial involvement, TTE is recommended to assess cardiac structure and function, including GLS for detecting subclinical dysfunction and enabling serial comparison. In situations of unexplained decline in left ventricular ejection fraction (LVEF)/GLS, disproportionate symptoms, or discordance between clinical status and echocardiographic findings, CMR should be considered for tissue characterization and evaluation of myocarditis or fibrosis. Additionally, periodic reassessment is advisable at intervals determined by disease activity, functional class, and hemodynamic stability.[8,11]

Thus, this case illustrates two important points: (i) the need for systematic cardiovascular surveillance in ANCA-associated vasculitis — including MPA — with serial TTE and, when available, GLS and/or CMR for more detailed characterization; and (ii) the importance of clinical–imaging correlation when faced with suggestive echocardiographic patterns, avoiding isolated conclusions. Multidisciplinary management involving nephrology, rheumatology, and cardiology remains essential to optimize outcomes and guide timely interventions.[8,11]

One limitation that should be mentioned in this report is the absence of CMR for tissue characterization. The exam was not performed for two reasons: (1) unavailability within the public health system (SUS) during the evaluation period, and (2) the presence of severe renal dysfunction requiring hemodialysis, a situation in which the administration of gadolinium-based contrast may be associated with the risk of nephrogenic systemic fibrosis — a rare but potentially severe and difficult-to-manage event. Thus, interpretation of the imaging findings was based on clinical–echocardiographic correlation, including GLS analysis.

Conclusion

We report a rare cardiac manifestation of MPA in a young patient, presenting with dilated cardiomyopathy and severe systolic dysfunction, associated with an apical sparing pattern on GLS. This case reinforces the importance of systematic and serial cardiovascular evaluation in patients with ANCA-associated vasculitis, aiming for early diagnosis and improved prognostic stratification.

Author Contributions

Conception and design of the research: Costa KG; acquisition of data: Costa KG, Paiva MUB; analysis and interpretation of the data: Costa KG, Otto MEB; writing of the manuscript: Costa KG, Otto MEB, Assunção NM, Paiva MUB; critical revision of the manuscript for intellectual content: Costa KG, Otto MEB, Fernandes AFL, Lima RLR, Dias RMS.

Potential Conflict of Interest

No potential conflict of interest relevant to this article was reported.

Sources of Funding

There were no external funding sources for this study.

Study Association

This article is part of the Medical Residency by Karoline Gonzaga Costa conducted at Hospital Universitário de Brasília.

Ethics Approval and Consent to Participate

This study was approved by the Ethics Committee of the Faculdade de Medicina of Universidade de Brasília (UNB) under the protocol number 94929525.6.0000.5558. All the procedures in this study were in accordance with the 1975 Helsinki Declaration, updated in 2013. Informed consent was obtained from all participants included in the study.

Use of Artificial Intelligence

The authors did not use any artificial intelligence tools in the development of this work.

Availability of Research Data

The underlying content of the research text is contained within the manuscript.

References

1. Nguyen Y, Pagnoux C, Karras A, Quéméneur T, Maurier F, Hamidou M, et al. Microscopic Polyangiitis: Clinical Characteristics and Long-Term Outcomes of 378 Patients from the French Vasculitis Study Group Registry. J Autoimmun. 2020;112:102467. doi: 10.1016/j.jaut.2020.102467.
2. Jennette JC, Falk RJ. Small-Vessel Vasculitis. N Engl J Med. 1997;337(21):1512-23. doi: 10.1056/NEJM199711203372106.
3. Hellmich B, Sanchez-Alamo B, Schirmer JH, Berti A, Blockmans D, Cid MC, et al. EULAR Recommendations for the Management of ANCA-Associated Vasculitis: 2022 Update. Ann Rheum Dis. 2024;83(1):30-47. doi: 10.1136/ard-2022-223764.
4. Yates M, Watts R. ANCA-Associated Vasculitis. Clin Med. 2017;17(1):60-4. doi: 10.7861/clinmedicine.17-1-60.
5. Moiseev S, Bulanov N, Crnogorac M, Direskeneli H, Galesic K, Gazel U, et al. Traditional and Disease Specific Risk Factors for Cardiovascular Events in ANCA-Associated Vasculitis: A Multinational Retrospective Study. J Rheumatol. 2023;50(8):1094. doi: 10.3899/jrheum.220851.C1.
6. Xie W, Xiao S, Li X, Huang J, Zhang Z. Cardiovascular and Cerebrovascular Outcomes in Anti-Neutrophil Cytoplasmic Antibody-Associated Vasculitis: A Systematic Review with Meta-Analysis. Autoimmun Rev. 2024;23(6):103587. doi: 10.1016/j.autrev.2024.103587.
7. Kronbichler A, Leierer J, Gauckler P, Shin JI. Comorbidities in ANCA-Associated Vasculitis. Rheumatology. 2020;59(Suppl 3):iii79-iii83. doi: 10.1093/rheumatology/kez617.
8. Kronbichler A, Bajema IM, Bruchfeld A, Kirsztajn GM, Stone JH. Diagnosis and Management of ANCA-Associated Vasculitis. Lancet. 2024;403(10427):683-98. doi: 10.1016/S0140-6736(23)01736-1.
9. Sarmad A, Ghozloujeh ZG, Hanna PE, Kronbichler A, Geetha D, Heidari-Bateni G, et al. Cardiovascular Involvement in ANCA-Associated Vasculitis. Nephrol Dial Transplant. 2025;40(12):2256-67. doi: 10.1093/ndt/gfaf070.
10. Thompson GE, Bourne MH Jr, Moura MC, Baqir M, Cartin-Ceba R, Makol A, et al. Pleuritis and Pericarditis in Antineutrophil Cytoplasmic Autoantibody-Associated Vasculitis. Chest. 2021;160(2):572-81. doi: 10.1016/j.chest.2021.02.049.
11. Sarmad A, Ghozloujeh ZG, Hanna PE, Kronbichler A, Geetha D, Heidari-Bateni G, et al. Cardiovascular Involvement in ANCA-Associated Vasculitis. Nephrol Dial Transplant. 2025;40(12):2256-67. doi: 10.1093/ndt/gfaf070.
12. Nakazawa D, Masuda S, Tomaru U, Ishizu A. Pathogenesis and Therapeutic Interventions for ANCA-Associated Vasculitis. Nat Rev Rheumatol. 2019;15(2):91-101. doi: 10.1038/s41584-018-0145-y.
13. Almeida ALC, Melo MDT, Bihan DCSL, Vieira MLC, Pena JLB, Del Castillo JM, et al. Position Statement on the Use of Myocardial Strain in Cardiology Routines by the Brazilian Society of Cardiology's Department Of Cardiovascular Imaging - 2023. Arq Bras Cardiol. 2023;120(12):e20230646. doi: 10.36660/abc.20230646.
14. Thomas JD, Edvardsen T, Abraham T, Appadurai V, Badano L, Banchs J, et al. Clinical Applications of Strain Echocardiography: A Clinical Consensus Statement from the American Society of Echocardiography Developed in Collaboration with the European Association of Cardiovascular Imaging of the European Society of Cardiology. J Am Soc Echocardiogr. 2025;38(11):985-1020. doi: 10.1016/j.echo.2025.07.007.
15. Kittleson MM, Ruberg FL, Ambardekar AV, Brannagan TH, Cheng RK, Clarke JO, et al. 2023 ACC Expert Consensus Decision Pathway on Comprehensive Multidisciplinary Care for the Patient with Cardiac Amyloidosis: A Report of the American College of Cardiology Solution Set Oversight Committee. J Am Coll Cardiol. 2023;81(11):1076-126. doi: 10.1016/j.jacc.2022.11.022.
16. Kottam A, Hanneman K, Schenone A, Daubert MA, Sidhu GD, Gropler RJ, et al. State-of-the-Art Imaging of Infiltrative Cardiomyopathies: A Scientific Statement from the American Heart Association. Circ Cardiovasc Imaging. 2023;16(11):e000081. doi: 10.1161/HCI.0000000000000081.
17. Arbelo E, Protonotarios A, Gimeno JR, Arbustini E, Barriales-Villa R, Basso C, et al. 2023 ESC Guidelines for the Management of Cardiomyopathies. Eur Heart J. 2023;44(37):3503-626. doi: 10.1093/eurheartj/ehad194.

TAV-in-TAV for Acute Failure of a Transcatheter Aortic Valve in a High Surgical Risk Octogenarian Patient

Gustavo Carvalho,[1] Maria Fernanda Miranda Carvalho,[2] Enio Eduardo Guérios,[1] Pedro Calegari,[1] Cláudia Biondo Zanlorensi,[1] Fernando Silva Botelho,[1] Bruna O. Erbano,[1] Vinícius D. Vaz[3]

CHC UFPR,[1] Curitiba, PR – Brasil

Universidade Positivo Curso de Medicina,[2] Curitiba, PR – Brazil

Anis Rassi Heart Hospital,[3] Goiânia, GO – Brazil

Abstract

An 82-year-old patient with severe aortic valve stenosis and high risk for conventional surgery due to chronic renal dysfunction and restrictive lung disease underwent transfemoral transcatheter aortic valve implantation (TAVI) using a self-expanding Navitor® prosthesis (Abbott). Immediately after implantation, valve dysfunction was observed, characterized by inversion of the right coronary leaflet, resulting in severe acute prosthetic regurgitation and hemodynamic instability. Therefore, a 21.5 mm balloon-expandable Myval® prosthesis was also implanted (TAV-in-TAV). The critical condition was resolved with immediate hemodynamic recovery. This case demonstrates the efficacy and safety of TAV-in-TAV as a bailout intervention in acute prosthetic failure.

Introduction

Degenerative aortic stenosis is the most prevalent valvular heart disease in older patients and is often associated with high mortality when untreated.[1,2] The standard treatment is valve replacement; however, the surgical risk is elevated in older patients and in those with significant comorbidities.[1,2] Transcatheter aortic valve implantation (TAVI) is a safe and effective alternative in these cases.[1-3] Although immediate mechanical complications (e.g., acute prosthetic dysfunction) are rare, they may be potentially fatal.[1-4] Immediate malfunction of Navitor® prostheses has recently been reported, possibly related to manufacturing defects or adverse anatomical interactions.[5]

This report describes a case of immediate dysfunction of a self-expanding prosthesis (Navitor®), successfully corrected using an emergent transcatheter aortic valve–in–transcatheter aortic valve (TAV-in-TAV) along with a balloon-expandable prosthesis (Myval®).

Keywords

Aortic Valve Stenosis; Prostheses and Implants; Aortic Valve Insufficiency; Heart Valve Prosthesis

Mailing Address: Gustavo Carvalho •
CHC UFPR. Dionira M Klemtz, 201, casa 107. Postal code: 81320-390. Bairro Fazendinha, Curitiba, PR – Brazil
E-mail: gustavocarvalho1975@gmail.com
Manuscript received November 26, 2025, revised manuscript March 1, 2026, accepted March 11, 2026
Editor responsible for the review: Maria Otto

DOI: https://doi.org/10.36660/abcimg.20250111i

Case Report

An 82-year-old female patient presented severe symptomatic aortic stenosis (New York Heart Association [NYHA] functional class III), chronic renal dysfunction (estimated glomerular filtration rate of 28 mL/min/1.73 m²), and chronic restrictive lung disease. The Society of Thoracic Surgeons score indicated a high risk for open valve replacement surgery. After discussion, the team chose to treat using TAVI.

The valve annulus area and perimeter were 325 mm² and 64 mm, respectively (Figure 1). Considering the symmetrical structural pattern and the degree and distribution of calcifications, a self-expanding prosthesis (Navitor®) was chosen.

The procedure was performed under sedation and local anesthesia, with access through the right femoral artery. After valvuloplasty with an 18x40 mm balloon, a 25 mm Navitor® self-expanding prosthesis (Abbott) was implanted. Delivery was uneventful. However, immediately after, angiography showed severe aortic insufficiency. Intraoperative transesophageal echocardiography revealed severe prosthetic insufficiency resulting from the inversion of the right coronary leaflet of the prosthesis (Figure 2). The patient developed significant hemodynamic instability, requiring inotropic support and advanced airway management.

The team attempted to correct the complication using Pigtail and Simon catheters to adjust the inverted leaflet, as well as a post-dilation with a 20 x 40 mm balloon; both attempts were ineffective. Therefore, an emergency TAV-in-TAV implantation was performed. Since the origin of the left coronary artery was relatively low (11 mm) and the sinotubular junction was narrow (24 x 25 mm), the implantation of a new self-expanding prosthesis could potentially cause coronary occlusion or sequestration of the coronary sinus. Therefore, a balloon-expandable prosthesis (Myval® 21.5 mm; Meril) was implanted, along with a drug-eluting stent in the left main coronary artery for protection. The procedure was guided simultaneously by fluoroscopy and transesophageal echocardiography and achieved technical success, with immediate correction of valvular insufficiency, restoration of hemodynamic stability, and absence of limited coronary perfusion (Figure 2). The mean trans prosthetic gradient after the procedure was 6 mmHg, without evidence of paravalvular leak.

The patient remained hemodynamically stable and was discharged after four days. At the 30-, 60-, and 90-day follow-up appointments, she remained in functional class I (NYHA), without additional complaints.

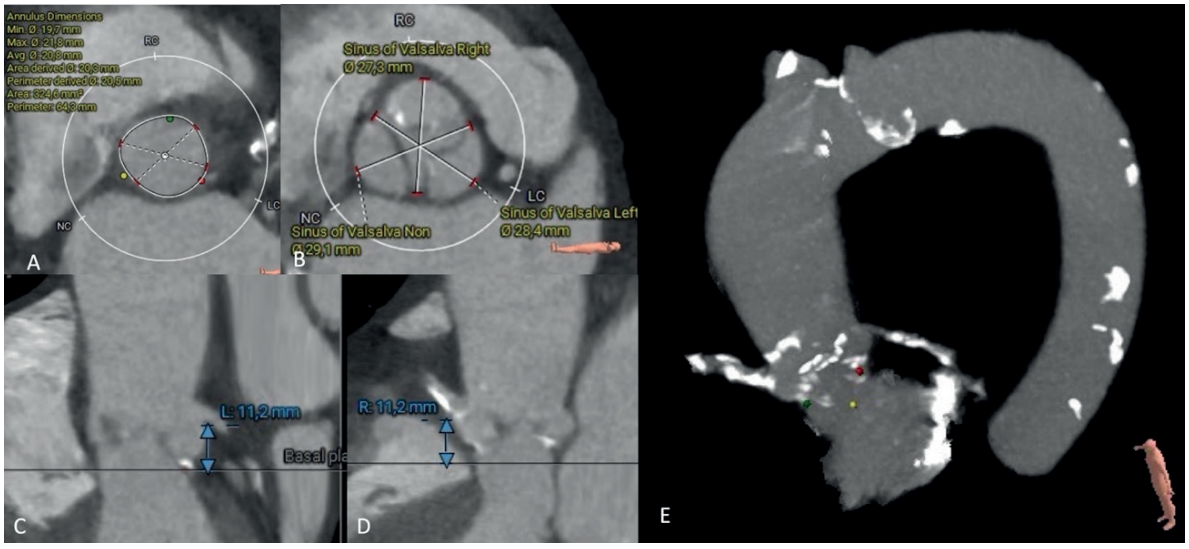

Figure 1 – *Structural characteristics of the aortic valve to be addressed. A – The valve annulus has few irregularities, with symmetrical calcifications of the cusps without extension to the left ventricular outflow tract (area 325 mm² and perimeter 64 mm). B – Wide sinuses of Valsalva with symmetrical points of calcification. C and D – Adequate heights of the left and right coronary arteries, respectively. E – Significant coronary artery calcifications, moderate to significant in the aortic valve, and discrete calcifications in the ascending and descending thoracic aorta.*

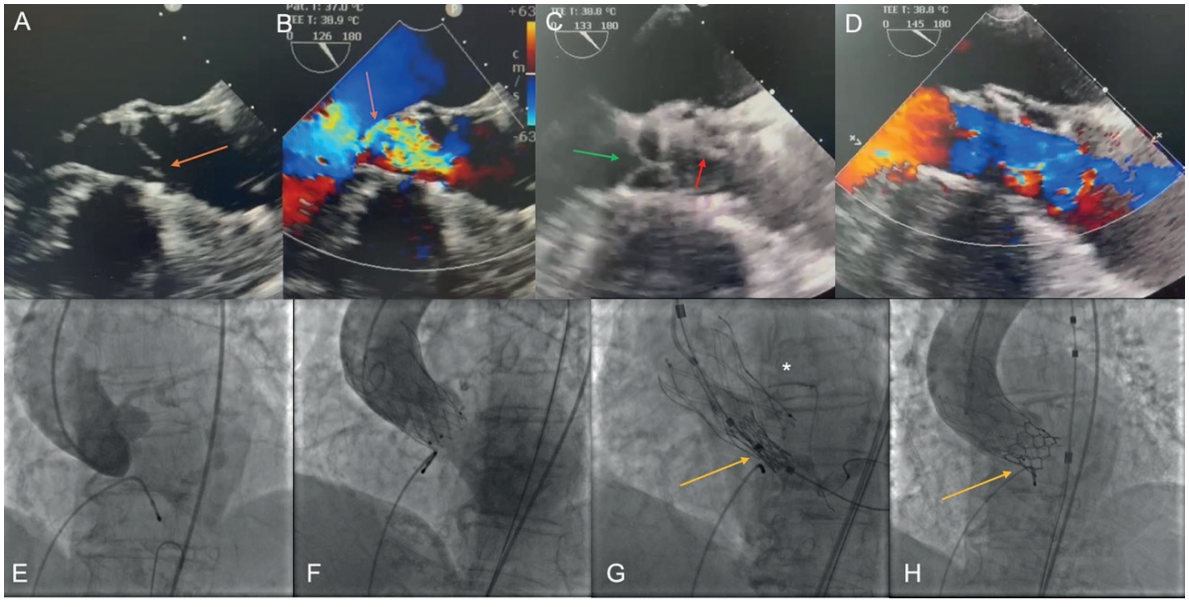

Figure 2 – *Echocardiogram and fluoroscopy images. A and B – Echocardiogram showing the damaged NAVITOR prosthesis leaflet (arrow), with significant regurgitation (arrow). C and D – Myval prosthesis implanted inside the NAVITOR prosthesis, functioning normally on echocardiogram. E – Angiography of the native aortic valve with significant stenosis and slight regurgitation. F – NAVITOR prosthesis implanted with significant regurgitation. G – (*) Stent positioned in the left main coronary artery. G and H - Positioning of the Myval prosthesis (arrow) and after its implantation inside the NAVITOR prosthesis (arrow), functioning normally.*

Discussion

Acute malfunction of a percutaneous aortic prosthesis is a rare complication, usually associated with freezing of one of the prosthesis leaflets, which may be corrected with catheters.[4] In contrast, the prosthetic dysfunction in this case was due to the inversion of one of the leaflets of the newly implanted prosthesis, which did not respond to manipulation. In the literature, only one similar case was found, in which the authors attributed the complication to unfavorable anatomy leading to asymmetrical under-expansion of the prosthesis and leaflet failure, which was also successfully treated by implanting a second balloon-expandable prosthesis within the initial prosthesis.[5]

Acute malfunction of transcatheter prostheses should not be attributed only to device defects or failures in the preparation and handling of the delivery system.[1,5] Anatomy plays a determining role in the immediate performance and adequate expansion and coaptation of the leaflets, especially in self-expanding valves. Elliptical or markedly asymmetrical annuli, intense and heterogeneous calcification, calcium protrusion into the left ventricular outflow tract or into the sinuses of Valsalva, and irregular distribution of radial forces along the annulus may hinder proper prosthesis positioning, potentially causing underexpansion, malposition, structural stent distortion, and immediate valve dysfunction; these features did not occur in this case. These aspects reinforce the importance of a tomographic preprocedural evaluation, with detailed three-dimensional analysis of the ring geometry and calcification pattern, and the need for an individualized implant strategy and selection of the prosthesis type, particularly in challenging anatomies.[1,5] On the other hand, the present case raises discussion about the quality control and traceability of transcatheter prostheses, as subtle manufacturing defects may only be identified at implantation, as also reported in recent studies.[5]

The literature supports that transcatheter reintervention in previously implanted valves is a safe and effective alternative to reoperation, especially in high-risk patients.[6-11] However, this study demonstrates the effectiveness of the TAV-in-TAV in acute cases and reinforces the importance of complete preprocedural planning to guide the emergency selection of a second prosthesis and to determine techniques to avoid additional complications, such as acute coronary occlusion secondary to the second implant.[12]

Coronary occlusion, particularly of the left main coronary artery, is one of the most feared complications during valve-in-valve (ViV) and TAV-in-TAV procedures, especially in anatomies with small sinuses of Valsalva, low coronary ostia height, and prosthetic leaflets at risk of displacement towards the coronary arteries.[12] In this study, a prophylactic strategy was chosen, with a stent prepositioned in the left main coronary artery, ready for immediate release in case of limited coronary flow after ViV prosthesis implantation. Given adequate flow preservation and the absence of angiographic or hemodynamic evidence of coronary obstruction, a "chimney" technique was not required, and the stent was safely removed. This approach illustrates a staged, individualized strategy that mitigates risk in potentially unfavorable anatomies, avoiding unnecessary additional interventions in the absence of actual coronary compromise.[1,12]

Although conventional surgery is viable for treating transcatheter prosthesis failures, this procedure is associated with high perioperative morbidity and mortality, especially in older and high-risk patients.[13-15] In this study, due to the age of the patient and comorbidities, the team chose an emergency transcatheter approach, resulting in an immediate hemodynamic recovery and avoiding a high-risk reoperation.

The literature on transcatheter ViV implantation in dysfunctional bioprostheses mainly describes the use of balloon-expandable prostheses from the Edwards SAPIEN family, particularly in the initial series and multicenter registries that established the feasibility and safety of the technique. However, growing evidence suggests that the TAV-in-TAV may be successfully applied using different transcatheter platforms, provided that anatomical and technical criteria are met.[16] In this study, the immediate availability of a Myval® balloon-expandable prosthesis (Meril) enabled a rescue TAV-in-TAV, with rapid restoration of valve competence and clinical stabilization. This outcome reinforces that, in critical scenarios, prompt therapeutic decision-making and versatility in the use of different transcatheter devices may determine the success of the procedure, increasing the applicability of the ViV beyond the devices most widely described in the literature, particularly when surgery is prohibitive.

Immediate hemodynamic recovery and sustained clinical stability illustrate the importance of advanced training of the multidisciplinary team and the strict application of the techniques described in current guidelines and contemporary TAV-in-TAV series.[1-4,13-15]

Conclusions

This case illustrated a rare yet critical immediate dysfunction of a self-expanding prosthesis during transcatheter aortic valve implantation, which was successfully corrected with TAV-in-TAV using a balloon-expandable prosthesis. This technique may represent an immediate, effective, and potentially lifesaving alternative, especially in patients with high surgical risk; however, its success depends on an experienced team, detailed prior anatomical planning, and multiple device options.

Author Contributions

Conception and design of the research: Carvalho G, Calegari P; acquisition of data: Carvalho G, Carvalho MFM, Guérios EE, Zanlorensi CB, Botelho FS, Erbano BO, Calegari P, Vaz VD; analysis and interpretation of the data: Carvalho G, Carvalho MFM, Guérios EE; obtaining financing: Carvalho G, Carvalho MFM; writing of the manuscript: Carvalho G, Carvalho MFM; critical revision of the manuscript for intellectual content: Carvalho G, Guérios EE; angiography images: Carvalho G; echocardiogram images: Zanlorensi CB, Botelho FS; reference review: Erbano BO, Calegari P, Vaz VD.

Potential Conflict of Interest

No potential conflict of interest relevant to this article was reported.

Sources of Funding

There were no external funding sources for this study.

Study Association

This study is not associated with any thesis or dissertation work.

Ethics Approval and Consent to Participate

This study was approved by the Ethics Committee of the Hospital de Clínicas da Universidade Federal do Paraná under the protocol number 93429725.9.0000.0096. All the procedures in this study were in accordance with the 1975 Helsinki Declaration, updated in 2013. Informed consent was obtained from all participants included in the study.

Use of Artificial Intelligence

The authors did not use any artificial intelligence tools in the development of this work.

Availability of Research Data

The underlying content of the research text is contained within the manuscript.

References

1. Praz F, Borger MA, Lanz J, Marin-Cuartas M, Abreu A, Adamo M, et al. 2025 ESC/EACTS Guidelines for the Management of Valvular Heart Disease. Eur Heart J. 2025;46(44):4635-736. doi: 10.1093/eurheartj/ehaf194.
2. Tarasoutchi F, Montera MW, Ramos AIO, Sampaio RO, Rosa VEE, Accorsi TAD, et al. Update of the Brazilian Guidelines for Valvular Heart Disease - 2020. Arq Bras Cardiol. 2020;115(4):720-75. doi: 10.36660/abc.20201047.
3. Leon MB, Smith CR, Mack M, Miller DC, Moses JW, Svensson LG, et al. Transcatheter Aortic-Valve Implantation for Aortic Stenosis in Patients Who Cannot Undergo Surgery. N Engl J Med. 2010;363(17):1597-607. doi: 10.1056/NEJMoa1008232.
4. Bansal A, Puri R, Yun J, Krishnaswamy A, Jilaihawi H, Makkar R, et al. Management of Complications after Valvular Interventions. EuroIntervention. 2025;21(8):e390-e410. doi: 10.4244/EIJ-D-24-00066.
5. Horita R, Hachinohe D, Otake R, Diaz JA, Shitan H, Fujita T. Acute Leaflet Malfunction of Navitor Valve with Severe Intraprosthetic Aortic Insufficiency Immediately after Implantation. Cardiovasc Interv Ther. 2024;39(3):331-2. doi: 10.1007/s12928-024-00995-6.
6. Eggebrecht H, Schäfer U, Treede H, Boekstegers P, Babin-Ebell J, Ferrari M, et al. Valve-in-Valve Transcatheter Aortic Valve Implantation for Degenerated Bioprosthetic Heart Valves. JACC Cardiovasc Interv. 2011;4(11):1218-27. doi: 10.1016/j.jcin.2011.07.015.
7. Deharo P, Bisson A, Herbert J, Lacour T, Etienne CS, Porto A, et al. Transcatheter Valve-in-Valve Aortic Valve Replacement as an Alternative to Surgical Re-Replacement. J Am Coll Cardiol. 2020;76(5):489-99. doi: 10.1016/j.jacc.2020.06.010.
8. Sá MPBO, Van den Eynde J, Simonato M, Cavalcanti LRP, Doulamis IP, Weixler V, et al. Valve-in-Valve Transcatheter Aortic Valve Replacement versus Redo Surgical Aortic Valve Replacement: An Updated Meta-Analysis. JACC Cardiovasc Interv. 2021;14(2):211-20. doi: 10.1016/j.jcin.2020.10.020.
9. Ktenopoulos N, Apostolos A, Karanasos A, Drakopoulou M, Katsaros O, Simopoulou C, et al. Safety and Efficacy of Transcatheter Aortic Valve Implantation (TAVI) for Pure Aortic Regurgitation; A Systematic Review and Meta-Analysis. Eur Heart J. 2024;45(Suppl 1):ehae666.1905. doi: 10.1093/eurheartj/ehae666.1905.
10. Gallo M, Fovino LN, Blitzer D, Doulamis IP, Guariento A, Salvador L, et al. Transcatheter Aortic Valve Replacement for Structural Degeneration of Previously Implanted Transcatheter Valves (TAVR-in-TAVR): A Systematic Review. Eur J Cardiothorac Surg. 2022;61(5):967-76. doi: 10.1093/ejcts/ezab443.
11. Makkar RR, Kapadia S, Chakravarty T, Cubeddu RJ, Kaneko T, Mahoney P, et al. Outcomes of Repeat Transcatheter Aortic Valve Replacement with Balloon-Expandable Valves: A Registry Study. Lancet. 2023;402(10412):1529-40. doi: 10.1016/S0140-6736(23)01636-7.
12. Tarantini G, Fabris T, Nai Fovino L. TAVR-in-TAVR and Coronary Access: Importance of Preprocedural Planning. EuroIntervention. 2020;16(2):e129-32. doi: 10.4244/EIJ-D-19-01094.
13. Todaro D, Picci A, Tamburino C, Barbanti M. Self-Expanding vs. Balloon-Expandable Devices for Transcatheter Aortic Valve Implantation. In: Giordano A, Biondi-Zoccai G, Frati G, editors. Transcatheter Aortic Valve Implantation: Clinical, Interventional and Surgical Perspectives. Cham: Springer; 2019. p. 305-29.
14. Landes U, Webb JG, De Backer O, Sondergaard L, Abdel-Wahab M, Crusius L, et al. Repeat Transcatheter Aortic Valve Replacement for Transcatheter Prosthesis Dysfunction. J Am Coll Cardiol. 2020;75(16):1882-93. doi: 10.1016/j.jacc.2020.02.051.
15. Hirji SA, Percy ED, McGurk S, Malarczyk A, Harloff MT, Yazdchi F, et al. Incidence, Characteristics, Predictors, and Outcomes of Surgical Explantation after Transcatheter Aortic Valve Replacement. J Am Coll Cardiol. 2020;76(16):1848-59. doi: 10.1016/j.jacc.2020.08.048.
16. Hahn RT, Webb J, Pibarot P, Ternacle J, Herrmann HC, Suri RM, et al. 5-Year Follow-Up from the PARTNER 2 Aortic Valve-in-Valve Registry for Degenerated Aortic Surgical Bioprostheses. JACC Cardiovasc Interv. 2022;15(7):698-708. doi: 10.1016/j.jcin.2022.02.014.

Echocardiographic Assessment During Treatment of Acquired Pulmonary Artery Stenosis Due to Mediastinal Mass Compression: A Case Report

Carolynne Ferreira Machado,[1] *Patrick Ventorim Costa,*[1] *Ana Carolina Main Lucas,*[1] *Fernando Luiz Torres Gomes,*[1] *Fabricio Thebit Bortolon,*[1] *Laira Bernabe Mota,*[1] *Karllayno Camatta Milleri*[1]

Hospital Universitário Cassiano Antonio Moraes,[1] *Vitória, ES – Brazil*

Introduction

Acquired pulmonary artery stenosis is a rare entity that has scarcely been described in the literature, and it is mainly associated with compression of the pulmonary artery trunk and its branches by mediastinal tumors (teratomas and lymphomas).[1] We report the case of a young patient with non-Hodgkin lymphoma in the anterior mediastinum that led to extrinsic compression and local luminal invasion of the pulmonary artery trunk, causing significant impact on the right heart chambers, with subsequent improvement after chemotherapy.

Case report

A 33-year-old male patient, without prior comorbidities, presented with cough, dyspnea, and the appearance of a nodular lesion in the anterior cervical region, which progressively enlarged, accompanied by hyperemia and a 15-kg weight loss over 1 year. Physical examination revealed a palpable, painless, and immobile mass approximately 4.5 cm above the suprasternal notch. Cardiac auscultation identified a systolic ejection murmur (3+/6+), audible in all areas and radiating to the suprasternal notch. Chest computed tomography angiography showed a mediastinal mass measuring 11.5 × 9.5 cm, compressing the pulmonary arterial trunk, supra-aortic arterial trunks, superior vena cava, left brachiocephalic vein, and right brachiocephalic vein, with signs suggestive of tumor thrombosis (Figure 1). Transthoracic echocardiography showed right ventricular enlargement and thickening with impaired contractile function, turbulent flow in the pulmonary artery trunk, and bifurcation of the pulmonary arteries, likely due to extrinsic compression or invasion by a mass originating from the anterior mediastinum. The peak right ventricle to pulmonary artery gradient was 79 mmHg, with a peak velocity of 4.4 m/s, and the pulmonary valve remained intact (Figure 2). Biopsy of the cervical mass identified an undifferentiated malignant neoplasm, and immunohistochemistry confirmed diffuse large B-cell non-Hodgkin lymphoma.

Chemotherapy was initiated, with clinical follow-up and transthoracic echocardiography every 3 months, showing progressive reduction of the mediastinal mass (Figure 3). After 9 months of treatment, the patient exhibited complete normalization of right ventricular function and gradients (Figure 4).

At the end of treatment, the patient developed severe febrile neutropenia, which was difficult to manage, and ultimately died of probable septic shock.

Discussion

Mediastinal lymphomas can involve large vessels, with significant hemodynamic obstructions capable of generating murmurs or symptoms, depending on the location of maximal tumor growth. In cases with cardiac involvement, the most common symptoms are chest pain, dyspnea, and cough, with an audible murmur observed in 81% of patients. Acquired pulmonary arterial stenosis is rare and strongly associated with mediastinal tumors, frequently Hodgkin lymphoma, with uncertain prognosis.[2] Chronic obstructions may increase pressures in the right chambers and cause tricuspid regurgitation, ventricular dysfunction, and, in cases with patent foramen ovale, a right-to-left shunt with cyanosis and increased risk of paradoxical embolism.[3] Transthoracic echocardiography plays a key role in defining the etiology of pulmonary stenosis.[3] In the reported case, the mediastinal mass and its lateral compressive effect were clearly visible in short-axis view, with significant acceleration of flow in the pulmonary artery and normal valve opening, suggesting an external cause of the flow turbulence. Moreover, normalization of pulmonary artery flow and right ventricular function occurred after mass reduction with chemotherapy.

Conclusion

Early identification of this pathology, combined with timely initiation of therapy, can directly influence prognosis.[4] Reduction of the mediastinal mass through chemotherapy, radiation therapy, or surgery can relieve compression of the pulmonary artery, leading to normalization of blood flow and improvement in right heart chamber function.[5]

Author Contributions

Conception and design of the research and writing of the manuscript: Machado CF, Costa PV; acquisition of data:

Keywords

Pulmonary Artery Stenosis; Lymphoma; Dyspnea

Mailling Address: Carolynne Ferreira Machado •
Hospital Universitário Cassiano Antonio Moraes. Avenida Marechal campos, n 1355. Postal code: 29043-260. Bairro Santa Cecília, Vitória, ES – Brazil
E-mail: carolynne-95@hotmail.com
Manuscript received November 6, 2025, revised manuscript January 13, 2026, accepted March 16, 2026
Editor responsible for the review: Andrea Vilela

DOI: https://doi.org/10.36660/abcimg.20250091i

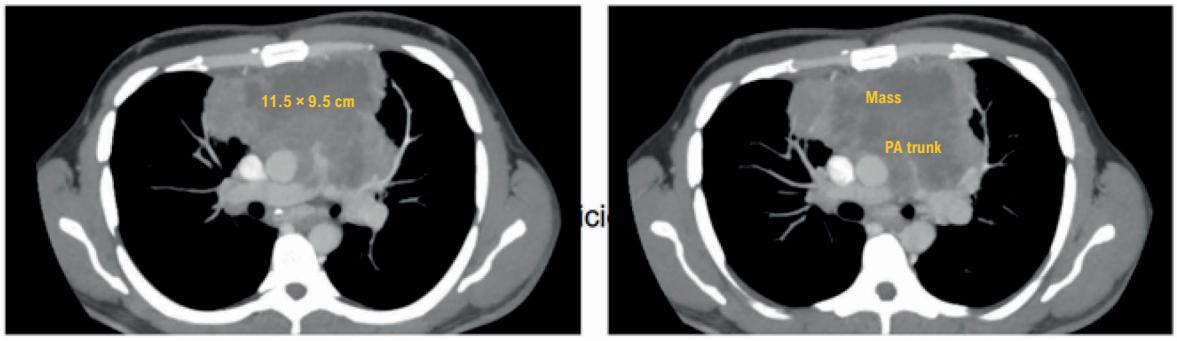

Figure 1 – *Chest computed tomography angiography showing the mediastinal mass. PA: pulmonary artery.*

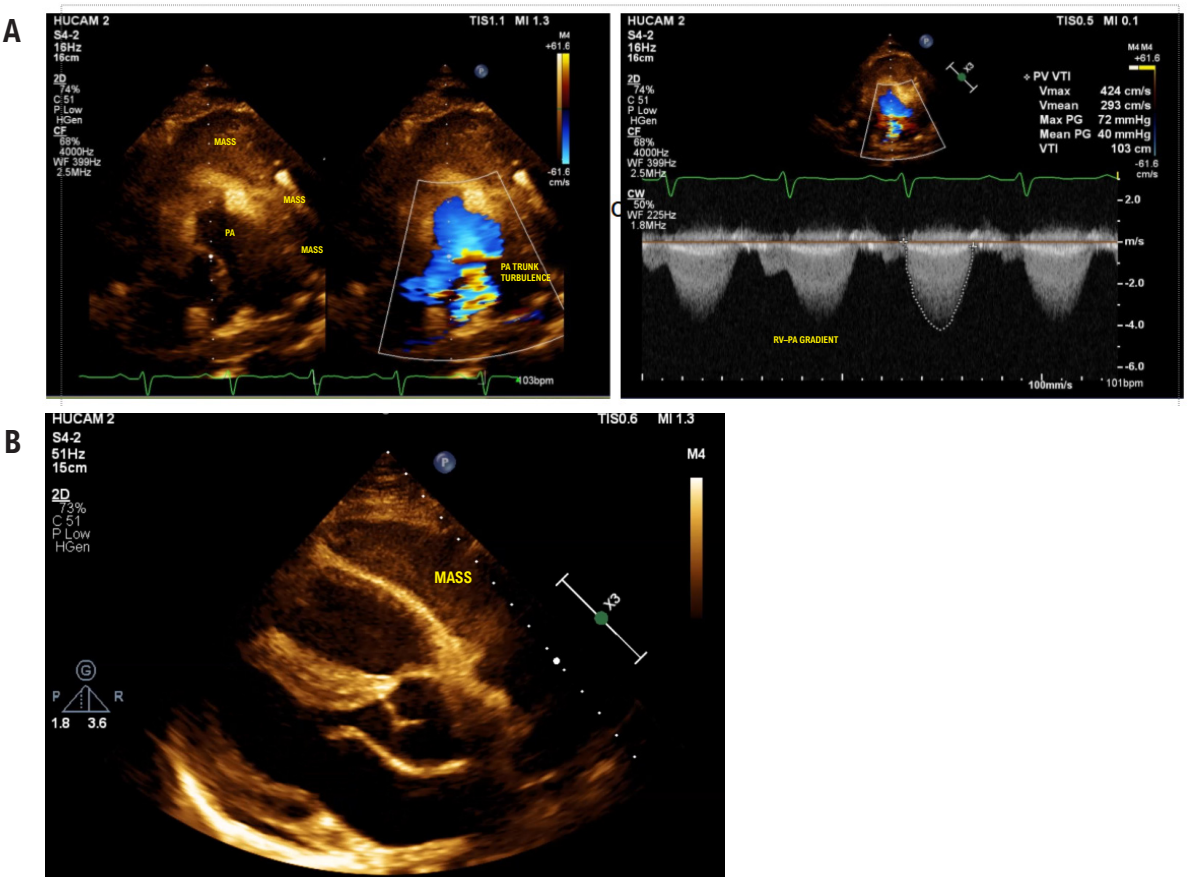

Figure 2 – *A) Parasternal short-axis view, showing the mass causing pulmonary stenosis. B) Parasternal long-axis view, showing the presence of a mass compressing the right ventricle. PA: pulmonary artery; RV: right ventricle.*

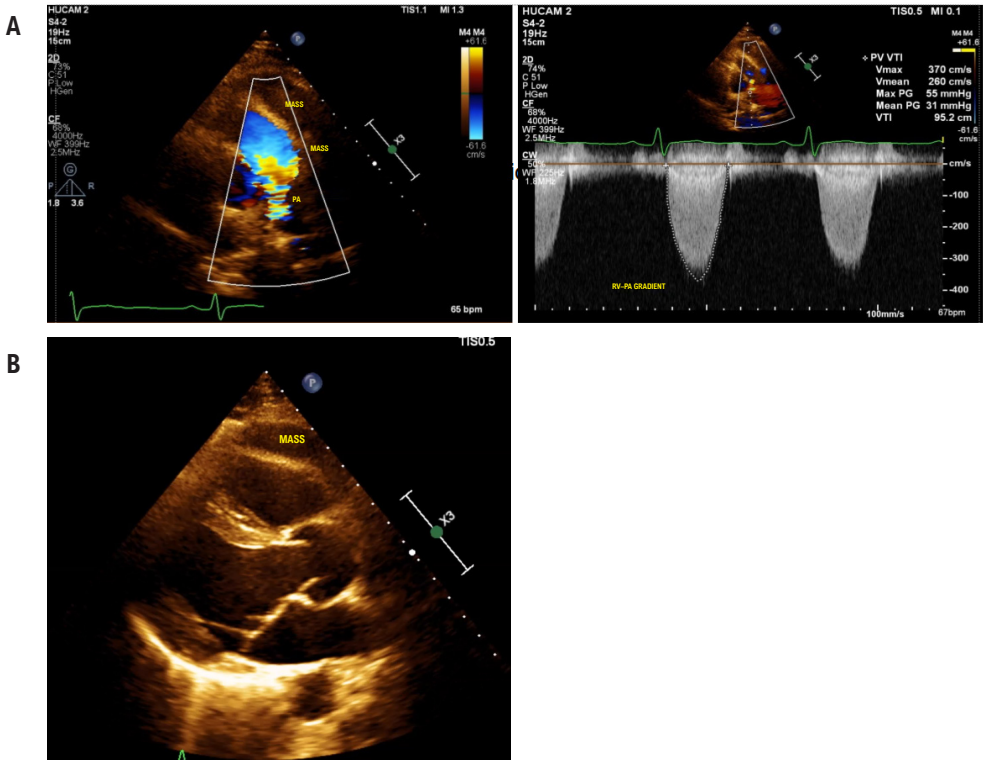

Figure 3 – *A) Mediastinal mass and pulmonary valve gradients showing reduction. B) Parasternal long-axis view, showing reduction of the mass in the mediastinum. PA: pulmonary artery; RV: right ventricle.*

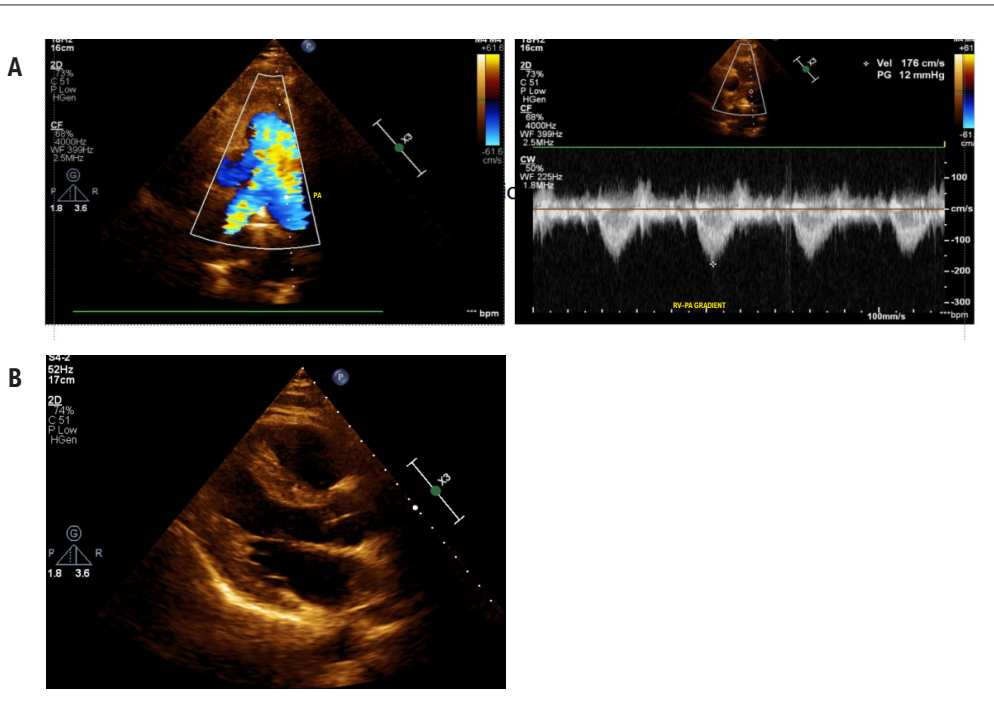

Figure 4 – *A) Maximum pulmonary valve gradient of 12 mmHg. B) Parasternal long-axis view, showing absence of the mass after treatment. PA: pulmonary artery; RV: right ventricle.*

Machado CF, Costa PV, Lucas ACM, Mota LB, Milleri CK, Bortolon FT; analysis and interpretation of the data: Machado CF, Costa PV, Lucas ACM; critical revision of the manuscript for important intellectual content: Machado CF, Costa PV, Lucas ACM, Gomes FLT.

Potential Conflict of Interest

No potential conflict of interest relevant to this article was reported.

Sources of Funding

There were no external funding sources for this study.

Study Association

This article is part of the habilitation thesis of Carolynne Ferreira Machado; Patrick Ventorim Costa, Ana Carolina Main Lucas; Laira Bernabe Mota; Karllayno Camatta Milleri; Fabrício Thebit Bortolon; and Fernando Luiz Torres Gomes at the Cassiano Antônio de Moraes University Hospital (HUCAM/UFES).

Ethics Approval and Consent to Participate

This study was approved by the Ethics Committee of the Hospital Universitário Cassiano Antônio de Moraes - HUCAM/UFES under the protocol number 88256725.1.0000.5071. All the procedures in this study were in accordance with the 1975 Helsinki Declaration, updated in 2013. Informed consent was obtained from all participants included in the study.

Use of Artificial Intelligence

The authors did not use any artificial intelligence tools in the development of this work.

Availability of Research Data

The underlying content of the research text is contained within the manuscript.

References

1. Robinson T, Lynch J, Grech E. Non-Hodgkin's Lymphoma Causing Extrinsic Pulmonary Artery Compression. Eur J Echocardiogr. 2008;9(4):577-8. doi: 10.1093/ejechocard/jen069.
2. Marshall ME, Trump DL. Acquired Extrinsic Pulmonic Stenosis Caused by Mediastinal Tumors. Cancer. 1982;49(7):1496-9. doi: 10.1002/1097-0142(19820401)49:7<1496::aid-cncr2820490731>3.0.co;2-3.
3. Voss TH, Arantes FBB. Acquired Pulmonary Stenosis in an Adolescent with Lymphoma. Arq Bras Cardiol: Imagem Cardiovasc. 2022;35(3):eabc294. doi: 10.47593/2675-312X/20223503eabc294.
4. Ozer N, Deveci OS, Kaya EB, Demircin M. Mediastinal Lymphoma Causing Extrinsic Pulmonary Stenosis. Turk Kardiyol Dern Ars. 2009;37(6):421-4.
5. Pugliatti P, Donato R, Grimaldi P, Nunnari F, Gregorio C, Zito C, et al. Extrinsic Pulmonary Stenosis in Primary Mediastinal B-Cellular Lymphoma. J Clin Ultrasound. 2015;43(1):68-70. doi: 10.1002/jcu.22133.

Visualization of the Ascending Aorta by Transthoracic Echocardiography: Could a Modified Parasternal Long-Axis View Provide Additional Imaging of a Longer Aortic Segment?

Heba Farouk,[1,2] *Karim El-Chilali,*[3] *Axel Kloppe*[2,4]

Cardiovascular Medicine Department, Faculty of Medicine, Cairo University,[1] *Cairo – Egypt*
Marienhospital Gelsenkirchen GmbH,[2] *Gelsenkirchen – Germany*
Prosper-Hospital gGmbH,[3] *Recklinghausen, NRW – Germany*
Department of Cardiology and Angiology, University Hospital Bergmannsheil Bochum, Ruhr-University Bochum,[4] *Bochum – Germany*

Introduction

Assessment of the ascending aorta is an essential component of standard transthoracic echocardiography (TTE).[1] While visualization of the aortic root and proximal ascending aorta is routinely achieved using the standard parasternal long-axis view (PLAX), imaging of the mid and distal ascending aorta remains technically challenging.[2-6] Current recommendations suggest moving the transducer to upper left intercostal spaces or alternatively using right parasternal windows to improve visualization of these segments in patients with adequate acoustic windows.[3]

In clinical practice, experienced echocardiographers often obtain satisfactory visualization of the tubular ascending aorta using individualized modifications of conventional views. However, less experienced operators and general cardiologists may fail to consistently image these segments because the upper left parasternal long-axis view (uPLAX) is poorly described in the literature, whereas acquisition of the right parasternal view is more technically demanding and time-consuming.

In the current study, we describe a modified parasternal long-axis view (mPLAX) designed to facilitate visualization of the mid and distal ascending aorta without changing the patient's position or intercostal space. We also evaluated the non-inferiority of this modified approach compared with the conventional uPLAX view for imaging a longer segment of the tubular ascending aorta.

Methods

Study population

A total of 169 consecutive patients referred for TTE were prospectively included in this study, of whom 35% were women. Patients with poor TTE windows, severe congestive symptoms, tachycardia, inability to maintain the left lateral decubitus position, or unsuccessful acquisition of the uPLAX view were excluded.

Echocardiographic acquisition

The mPLAX view was obtained from the standard PLAX position. After acquisition of the conventional PLAX image, the transducer was translated approximately 2-3 cm medially toward the sternum using a rightward sliding movement. This maneuver was followed by a 20°-30° clockwise rotation of the probe. In some patients, slight caudal angulation was additionally required to maintain alignment of the ascending aortic long axis within the imaging plane.

Importantly, all maneuvers were performed without changing the intercostal space, patient position, or transducer-skin contact.

Measurements

The length of the visualized ascending aortic segment was measured from the aortic annulus to the distal limit of the visible aortic segment in the PLAX, uPLAX, and mPLAX views. Ascending aortic diameter was measured at end-diastole using the leading-edge-to-leading-edge method in each view.

Statistical analysis

The mPLAX view was considered non-inferior to the uPLAX view if the lower boundary of the 95% confidence interval (CI) for the difference in visualized ascending aortic length exceeded the predefined non-inferiority margin of 3 mm.

Table 1 summarizes the baseline clinical and echocardiographic characteristics. Figure 1 shows representative examples of imaging the ascending aorta using different TTE views.

Results

Visualization of the ascending aorta

The visualized ascending aortic segment was significantly longer using the mPLAX view than using the uPLAX view (60.6 ± 9.3 mm vs 44.3 ± 8.2 mm, respectively). The mean difference (MD) between both techniques was 16.4 mm (95% CI, 15.1-17.6 mm; $p < 0.001$).

Keywords

Ascending aorta; Echocardiography; Aortic imaging

Mailing Address: Heba Farouk •
Cardiovascular Medicine Department, Faculty of Medicine, Cairo University. Kasr Alainy. CEP: 11593. Cairo – Egypt
Email: heba.farouk@outlook.de
Manuscript received May 1, 2026, revised manuscript May 4, 2026, accepted May 4, 2026
Editor responsible for the review: Marcelo Tavares

DOI: https://doi.org/10.36660/abcimg.20260068i

Table 1 – Baseline and echocardiographic characteristics

Variable	All patients (n = 169)	Male (n = 110)	Female (n = 59)	p-value
Age, years	67 ± 15	66 ± 14	69 ± 16	0.084
Height, cm	171 ± 10	175 ± 9	163 ± 5	< 0.001
Weight, kg	84 ± 17	89 ± 17	76 ± 13	< 0.001
BMI, kg/m^2	28.1 ± 5.6	29.3 ± 6.1	28.3 ± 4.7	0.139
BSA, m^2	1.95 ± 0.23	2.04 ± 0.22	1.79 ± 0.16	< 0.001
Hypertension	135 (80%)	89 (81%)	46 (78%)	0.649
Diabetes mellitus	53 (31%)	37 (34%)	16 (27%)	0.384
Dyslipidemia	114 (68%)	76 (69%)	38 (64%)	0.536
Atrial fibrillation	49 (29%)	32 (29%)	17 (29%)	0.970
CAD	70 (41%)	55 (50%)	15 (25%)	0.002
Aorta segment length in PLAX, mm	31.4 ± 5.9	31.7 ± 6.1	30.8 ± 5.6	0.323
Aorta diameter in PLAX, mm	31.9 ± 5.1	33.3 ± 4.3	29.3 ± 5.5	< 0.001
Aorta segment length in uPLAX, mm	44.3 ± 8.2	45.7 ± 8.0	41.5 ± 7.8	0.001
Aorta diameter in uPLAX, mm	33.2 ± 5.3	33.9 ± 4.8	31.8 ± 6.0	0.015
Aorta segment length in mPLAX, mm	60.6 ± 9.3	62.1 ± 8.8	57.9 ± 9.7	0.006
Aorta diameter in mPLAX, mm	34.9 ± 5.7	35.7 ± 5.3	33.5 ± 6.2	0.020

BMI: body mass index; BSA: body surface area; CAD: coronary artery disease; mPLAX: modified parasternal long-axis view; PLAX: parasternal long-axis view; uPLAX: upper left parasternal long-axis view.

Ascending aortic diameter

The ascending aortic diameter measured in the mPLAX view was significantly greater than that obtained in the uPLAX view (34.9 ± 5.7 mm vs 33.2 ± 5.3 mm, respectively), with a MD of 1.7 mm (95% CI, 1.2-2.3 mm; p < 0.001).

This difference was primarily observed among individuals with hypertension (n = 135). In this subgroup, ascending aortic diameter measured 35.6 ± 5.7 mm in the mPLAX view compared with 33.5 ± 5.4 mm in the uPLAX view, corresponding to a MD of 2.1 mm (95% CI, 1.5-2.7 mm; p < 0.001).

In contrast, among individuals without hypertension (n = 34), ascending aortic diameter was comparable between the two views (32.4 ± 5.0 mm in mPLAX vs 32.1 ± 5.2 mm in uPLAX), with no statistically significant difference (MD, 0.3 mm; 95% CI, −1.3 to 1.9 mm; p = 0.709).

Non-inferiority analysis

The predefined criterion for non-inferiority of the mPLAX view relative to the uPLAX view for visualization of a longer ascending aortic segment was met.

Sex-based analysis

Ascending aortic length and diameter were greater in men than in women using both imaging approaches. However, the incremental gain in visualized aortic length achieved with the mPLAX view compared with the uPLAX view was similar between sexes (16.3 mm [95% CI, 14.8-17.9 mm] in men vs 16.4 mm [95% CI, 14.3-18.5 mm] in women).

Study limitations

This study has several limitations. First, it represents a single-center experience and therefore requires external validation before widespread adoption. Nevertheless, given the simplicity and rapid acquisition of the mPLAX view, we believe that this approach is readily applicable in routine clinical practice.

Second, ascending aortic measurements obtained using the mPLAX view were not compared with reference imaging modalities such as computed tomography. However, in individuals without hypertension, aortic diameters measured using the mPLAX and uPLAX views were highly consistent.

Conclusions

In this study, we proposed a mPLAX focused on optimizing visualization of the ascending aorta. The rightward transducer translation partially removes the left ventricle from the imaging plane, whereas the simultaneous clockwise rotation and slight caudal angulation improve alignment with the ascending aortic long axis by correcting the heart-aorta angle.[7]

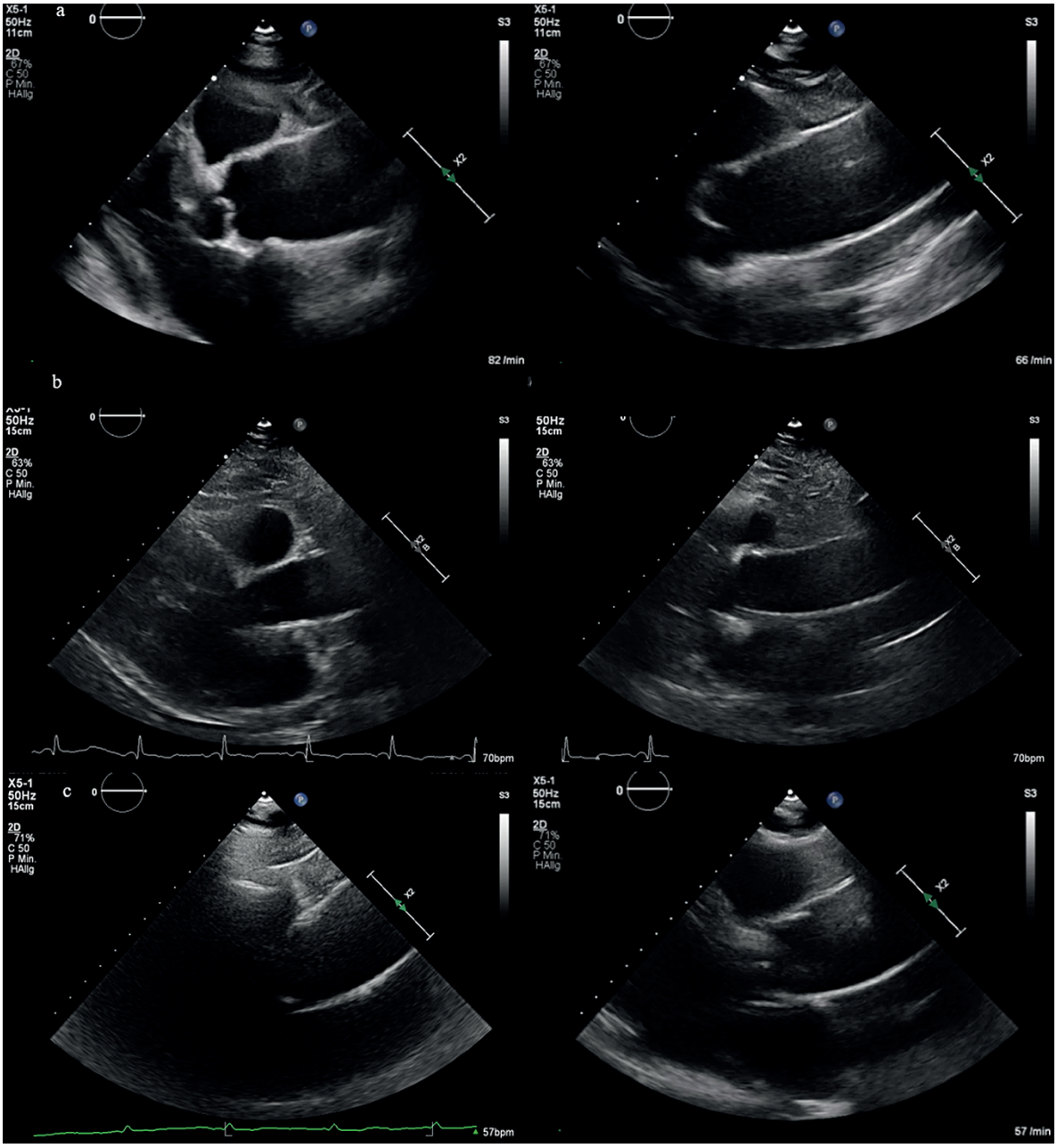

Figure 1 – *Visualization of the ascending aorta in three patients (A, B, and C) using the uPLAX view (left panels) and the mPLAX (right panels).*

We believe that the mPLAX view may serve as an additional non-inferior TTE window for visualization of a longer segment of the tubular ascending aorta during routine TTE examinations. Because this view can be obtained without changing the patient's position or intercostal space, it is easier and faster to acquire, particularly for general cardiologists and less experienced echocardiographers performing high-volume daily studies.

This approach may be especially useful during routine TTE follow-up of patients with previously documented mid-distal ascending aortic aneurysms identified by computed tomography and adequate parasternal acoustic windows.

Author Contributions

Conception and design of the research and critical revision of the manuscript for intellectual content: Farouk H, El-Chilali K,

Kloppe A; acquisition of data and writing of the manuscript: Farouk H; analysis and interpretation of the data and statistical analysis: El-Chilali K; supervision: Kloppe A.

Potential Conflict of Interest

No potential conflict of interest relevant to this article was reported.

Sources of Funding

There were no external funding sources for this study.

Study Association

This study is not associated with any thesis or dissertation work.

Ethics Approval and Consent to Participate

This retrospective study analyzed fully anonymized echocardiographic data. No interventions were performed, and ethics committee approval was not required under local regulations.

Use of Artificial Intelligence

The authors did not use any artificial intelligence tools in the development of this work.

Availability of Research Data

All datasets supporting the results of this study are available upon request from the corresponding author, subject to ethical and confidentiality considerations.

References

1. Hartnell GG. Imaging of Aortic Aneurysms and Dissection: CT and MRI. J Thorac Imaging. 2001;16(1):35-46. doi: 10.1097/00005382-200101000-00006.
2. Elefteriades JA, Farkas EA. Thoracic Aortic Aneurysm Clinically Pertinent Controversies and Uncertainties. J Am Coll Cardiol. 2010;55(9):841-57. doi: 10.1016/j.jacc.2009.08.084.
3. Evangelista A, Sitges M, Jondeau G, Nijveldt R, Pepi M, Cuellar H, et al. Multimodality Imaging in Thoracic Aortic Diseases: A Clinical Consensus Statement from the European Association of Cardiovascular Imaging and the European Society of Cardiology Working Group on Aorta and Peripheral Vascular Diseases. Eur Heart J Cardiovasc Imaging. 2023;24(5):e65-e85. doi: 10.1093/ehjci/jead024.
4. Evangelista A, Flachskampf FA, Erbel R, Antonini-Canterin F, Vlachopoulos C, Rocchi G, et al. Echocardiography in Aortic Diseases: EAE Recommendations for Clinical Practice. Eur J Echocardiogr. 2010;11(8):645-58. doi: 10.1093/ejechocard/jeq056.
5. Upadhyaya K, Ugonabo I, Satam K, Hull SC. Echocardiographic Evaluation of the Thoracic Aorta: Tips and Pitfalls. Aorta. 2021;9(1):1-8. doi: 10.1055/s-0041-1724005.
6. Goldstein SA, Evangelista A, Abbara S, Arai A, Asch FM, Badano LP, et al. Multimodality Imaging of Diseases of the Thoracic Aorta in Adults: From the American Society of Echocardiography and the European Association of Cardiovascular Imaging: Endorsed by the Society of Cardiovascular Computed Tomography and Society for Cardiovascular Magnetic Resonance. J Am Soc Echocardiogr. 2015;28(2):119-82. doi: 10.1016/j.echo.2014.11.015.